5. SITE 547[1]

Shipboard Scientific Party[2, 3]

HOLE 547

Date occupied: 3 May 1981

Date departed: 4 May 1981

Time on hole: 8 hr., 36 min.

Position: 33°46.84′N; 09°20.98′W

Water depth (sea level; corrected m, echo-sounding): 3938

Water depth (rig floor; corrected m, echo-sounding): 3948

Bottom felt (m, drill pipe): 3950.5 (beneath rig floor)

Penetration (m): 32.0

Number of cores: 1

Total length of cored section (m): 3.5

Total core recovered (m): 3.5

Core recovery (%): 100

Oldest sediment cored:
Depth sub-bottom (m): 3.5
Nature: Nannofossil ooze
Age: late Pleistocene–Recent

Basement: Not reached

HOLE 547A

Date occupied: 4 May 1981

Date departed: 10 May 1981

Time on hole: 6 days, 50 min.

Position: 33°46.84′N; 09°20.98′W

Water depth (sea level; corrected m, echo-sounding): 3938

Water depth (rig floor; corrected m, echo-sounding): 3948

Bottom felt (m, drill pipe): 3950.5 (beneath rig floor)

Penetration (m): 744.5

Number of cores: 73

Total length of cored section (m): 674.5

Total core recovered (m): 333.5

Core recovery (%): 49.4

Oldest sediment cored:
Depth sub-bottom (m): 583
Nature: Claystone and calcareous claystone
Age: Albian
Measured velocity (km/s): 2.0–2.2

Basement: Not reached

HOLE 547B

Date occupied: 10 May 1981

Date departed: 22 May 1981

Time on hole: 12 days, 13 hr., 34 min.

Position: 33°46.84′N; 09°20.98′W

Water depth (sea level; corrected m, echo-sounding): 3938

Water depth (rig floor; corrected m, echo-sounding): 3948

Bottom felt (m, drill pipe): 3951.0 (beneath rig floor)

Penetration (m): 1030.0

Number of cores: 36

Total length of cored section (m): 305.5

Total core recovered (m): 154.8

Core recovery (%): 50.6

Oldest sediment cored:
Depth sub-bottom (m): 932.5
Nature: Grayish red and gray sandy mudstone
Age: Rhaetian–Hettangian
Measured velocity (km/s): 2.0–2.5

Basement: Not reached

Principal results: At Site 547, located near the faulted northeastern flank of the sialic block drilled at Site 544 (Fig. 1), three holes were drilled. A summary log is shown in Figure 2.

Hole 547

This was a pilot hole to test conditions for casing a reentry hole; total depth (T.D.) was 32.5 m.

Hole 547A

0–141.1 m: Unit I pale yellowish brown foraminiferal nannofossil ooze and nannofossil ooze, Quaternary to late Miocene (N23–N17). Rests unconformably on

141.1–204.3 m: Unit IIA, greenish gray nannofossil ooze; middle to early Miocene (N15–N4).

---

[1] Hinz, K., Winterer, E. L., et al., *Init. Repts. DSDP*, 79: Washington (U.S. Govt. Printing Office).

[2] Karl Hinz (Co-Chief Scientist), Bundesanstalt für Geowissenschaften und Rohstoffe, 3 Hannover, Postfache 510153, Federal Republic of Germany; E. L. Winterer (Co-Chief Scientist), Geological Research Division, Scripps Institution of Oceanography, La Jolla, CA 92093; Peter O. Baumgartner, Geological Research Division, Scripps Institution of Oceanography, La Jolla, CA 92093 (present address: Escuela Centroamericana de Geologia, Apartado 35, Ciudad Universitaria Rodrigo Facio, San José, Costa Rica); Martin J. Bradshaw, Department of Geological Sciences, University of Aston, Birmingham B4 7ET, United Kingdom (present address: Shell International Petroleum Company, The Hague, The Netherlands); James E. T. Channell, Lamont-Doherty Geological Observatory, Columbia University, Palisades, New York (present address: Department of Geology, 1112 GPA Building, University of Florida, Gainesville, Florida 39611); Michel Jaffrezo, Département de Géotectonique, Université Pierre et Marie Curie, 4 place Jussieu, 75230 Paris Cedex 05, France; Lubomir F. Jansa, Geological Survey of Canada, Bedford Institute of Oceanography, Dartmouth, Nova Scotia, Canada; Robert Mark Leckie, Department of Geological Sciences, University of Colorado, Boulder, Colorado 80309 (present address: Department of Geology and Geography, University of Massachusetts, Amherst, Massachusetts 01003); Johnnie N. Moore, Department of Geology, University of Montana, Missoula, Montana 59812; Jürgen Rullkötter, Institut für Erdöl und Organische Geochemie, ICH-5, KFA Jülich, Postfach 1913, D-517 Jülich, Federal Republic of Germany; Carl H. Schaftenaar, Department of Geophysics, Texas A&M University, College Station, Texas 77843 (present address: Chevron, U.S.A., 700 S. Colorado Blvd., Denver, Colorado 80222); Torsten H. Steiger, Institut für Paläontologie und Historische Geologie, Universität München, Richard-Wagner-Strasse 10, D-800 Munchen 2, Federal Republic of Germany; Vassil T. Vuchev, Kansas Geological Survey, University of Kansas, Lawrence, Kansas 66044 (present address: Geological Institute, Bulgarian Academy of Sciences, UL. Academy G. Bonchev, Block 2, 1113 Sofia, Bulgaria); and George E. Wiegand, Department of Geology, Florida State University, Tallahassee, Florida 32306.

[3] The descriptions of sites, cores, and data included in these site reports were completed within one year of the cruise, but many of the topical chapters that follow were completed at a later date. More data were acquired and authors' interpretations matured during this interval, so readers may find some discrepancies between site reports and topical papers. This is particularly true of biostratigraphic age assignments. The timely publication of the *Initial Reports* series, which is intended to report the early results of each leg, precludes incurring the delays that would allow the site reports to be revised at a later stage of production.

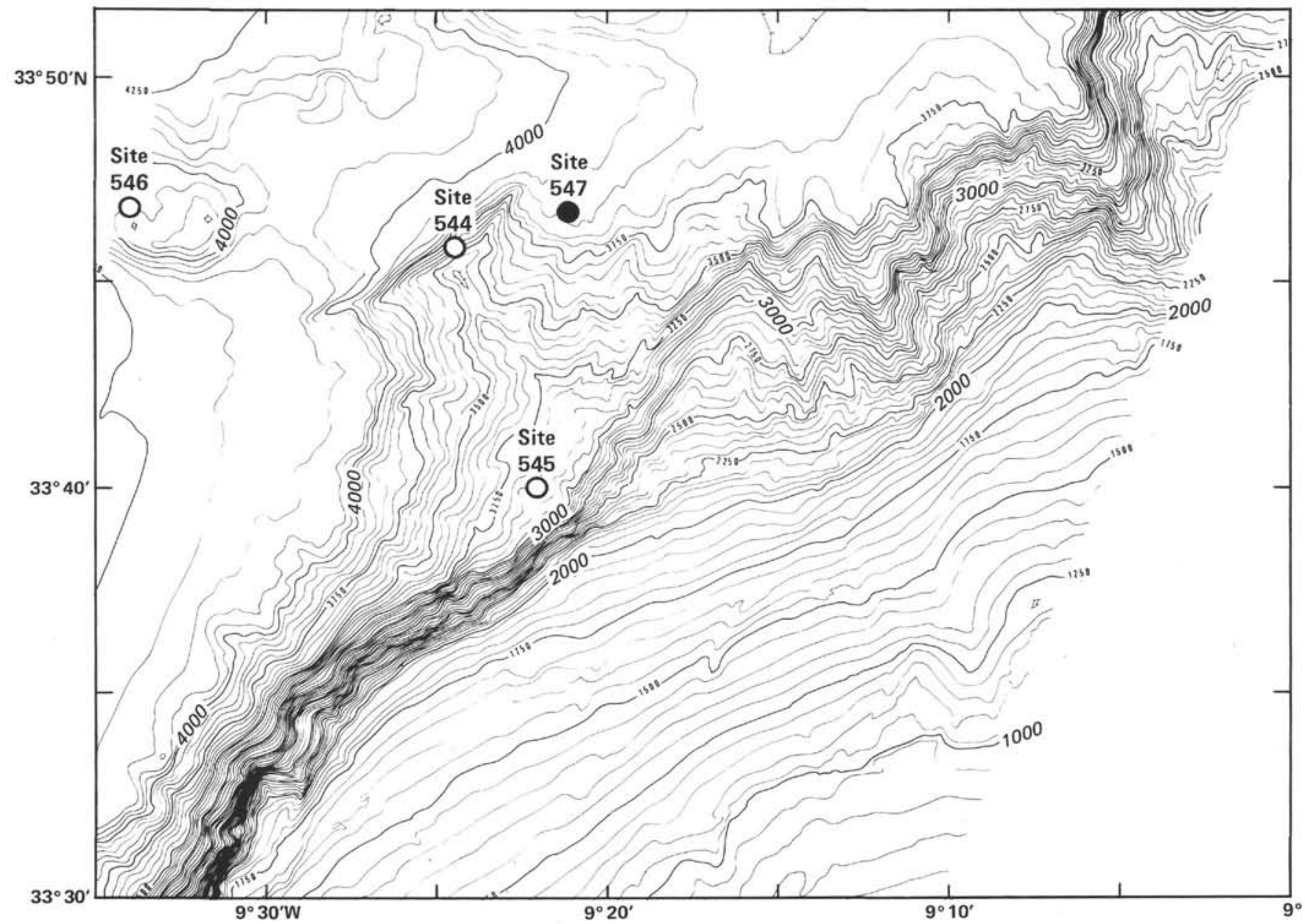

Figure 1. Bathymetry around Site 547 based on SEAZAGAN Seabeam map (Auzende et al., this volume). Depths in m.

204.3–225.7 m: Unit IIB, greenish gray, slightly clayey nannofossil ooze to chalk; late Eocene. Rests unconformably on

225.7–279.0 m: Unit III, greenish gray, siliceous, clayey nannofossil chalk; porcellanite nodules; sheared and contorted bedding and intraformational breccia layers common. Resedimented Eocene, Paleocene, and common Cretaceous fossils. Probably late Eocene in age.

279.0–364.5 m: Subunit IVA, greenish gray, clayey nannofossil chalk, siliceous and cherty; early Eocene (P7) to early Paleocene (P1).

364.5–422.6 m: Subunit IVB, mainly debris flows of greenish gray nannofossil chalk, early Paleocene (P1) to middle Campanian in age. Rests unconformably (at Red reflector) on

422.6–744.5 m (T.D.): Unit V, grayish green nannofossil-bearing claystone and mudstone, with layers of flat pebble mudstone conglomerate. Middle to late Cenomanian at the top, late Albian at T.D.

Hole 547B (reentry hole)

773 m: Unit V, dark grayish green mudstone with intraformational mudstone conglomerate layers; late Albian. Clasts of micrite and packstone occur in the lower 60 cm. Valanginian to late Albian.

773–838.9 m: Subunit VIA, red and green nodular and aptychus limestone and limestone pebble and breccia beds; Pliensbachian–Berriasian.

838.9–932.5 m: Subunit VIB, dark gray shale with clasts of micritic limestone grading downward into pale brown to grayish red calcareous claystone with nodules of dense micrite. Lower part highly fractured. Grayish black silty shale alternating with beds of light olive gray micritic limestone, pebbly limestone beds, dolomitic silty shale, and microcrystalline dolomite beds. Limestone breccia, conglomerates, and nodular limestone overlie a stromatolitic(?) bed near the base. Late Hettangian–early Sinemurian to Pliensbachian.

932.5–1030 m (T.D.): Unit VII, grayish red and gray sandy mudstone with dominantly sandier intervals, 2–5 cm thick. Minor granules of composite quartz and feldspar and small gypsum veins occur locally. Clasts of sandy mudstone and muddy dolomite are present. Dolomite, dolomitic limestone, and sandy granules and pebbles are very abundant at the base. Unit VII is interpreted as a nonmarine deposit and correlated with the red beds at Site 544. Rhaetian–Hettangian (or older).

BACKGROUND AND OBJECTIVES

Objectives at Site 547 (planning Site MAZ-9)

The original objective at Site MAZ-9, which is only about 1 km north of Site 547, was to penetrate a complete section of the Cenozoic and Mesozoic to basement, at a place where the seismic profiler records (Fig. 3) showed a much thicker development of the acoustic stratigraphy than at Site 544 and where all units might be expected to be present in a more distal or seaward facies than at Site 545. The Blue reflector, believed to mark the top of the Jurassic carbonate platform sequence, is traceable to MAZ-9, and we therefore expected to find the platform rocks here and perhaps to pin down the date of drowning of the platform and something of its earlier subsidence history. The thick Cenozoic and Cretaceous

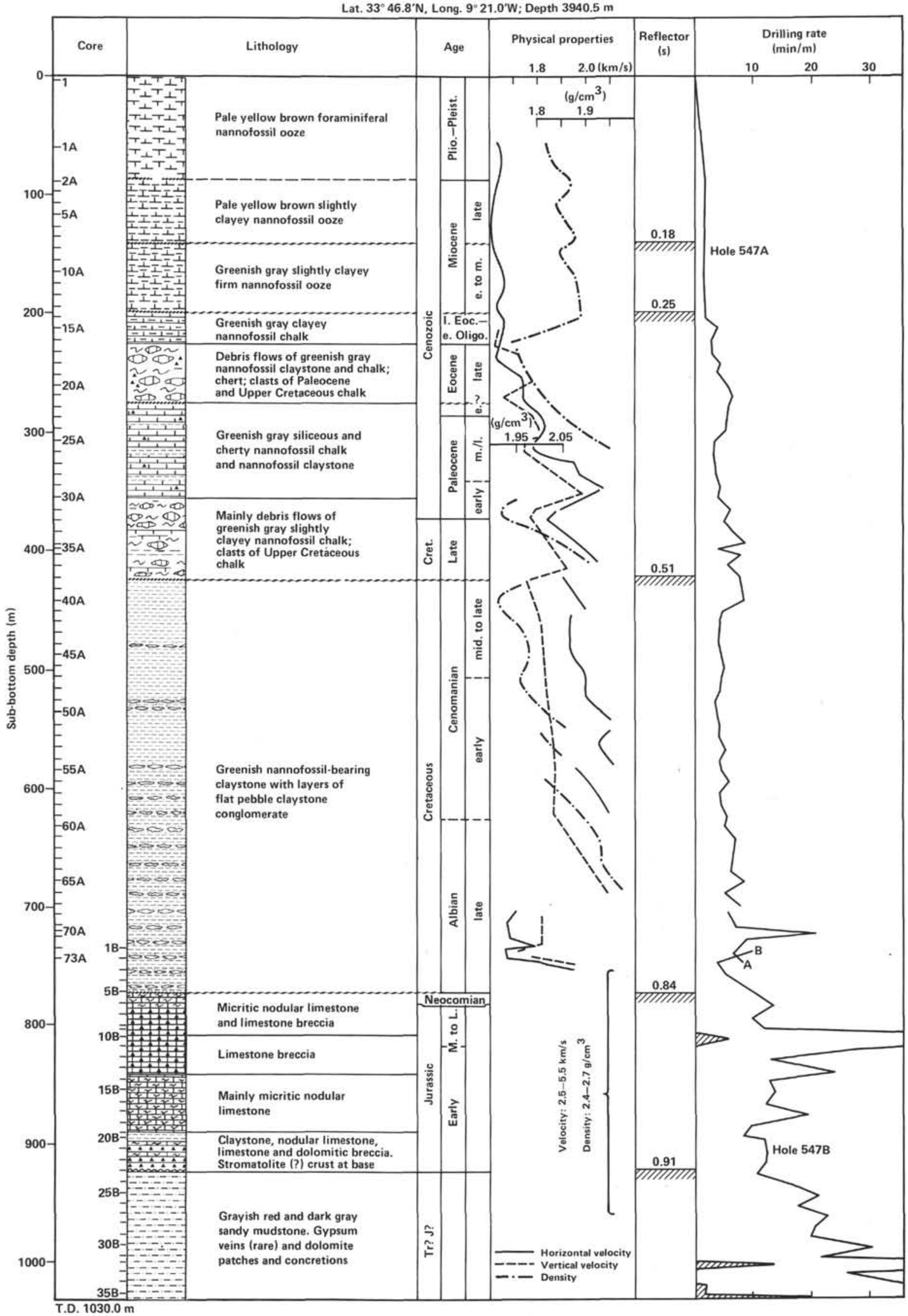

Figure 2. Summary graphic log of drilling results, Holes 547A and 547B.

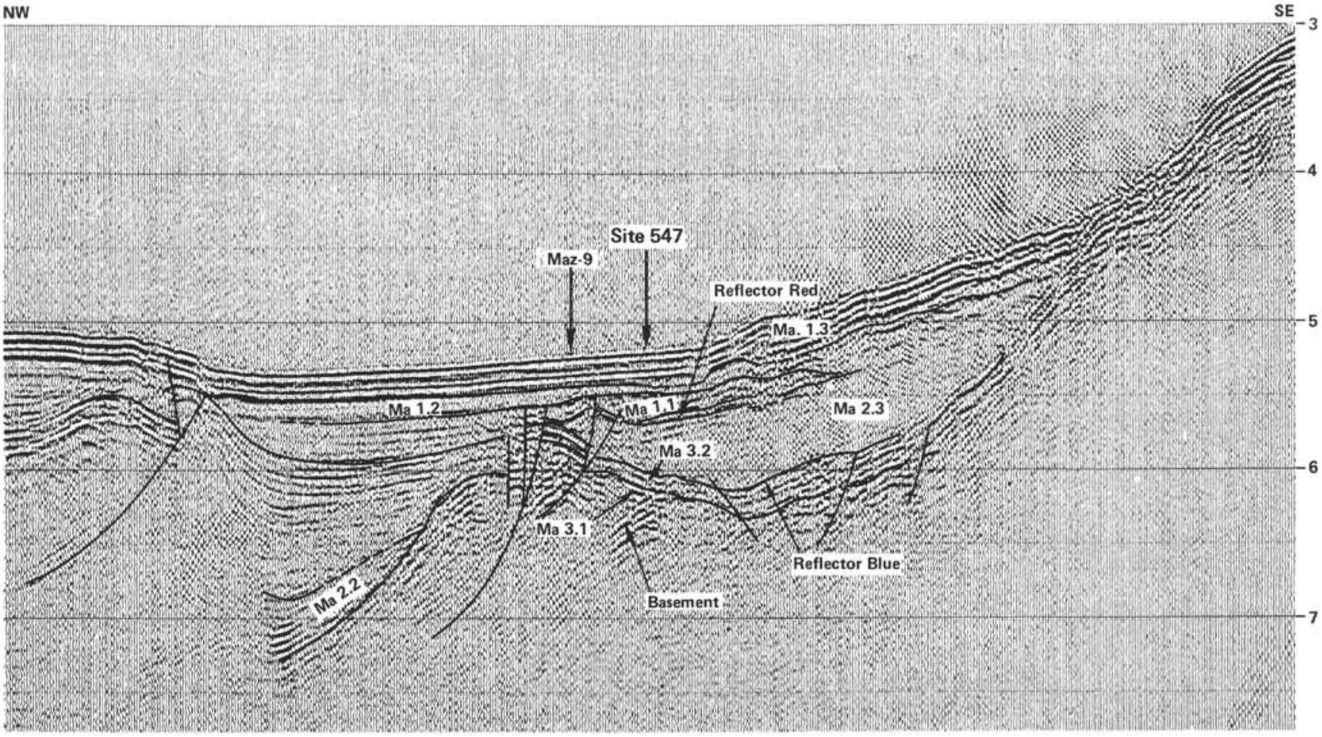

Figure 3. Seismic record of multichannel seismic line *M* 53-07, shotpoints 330–850, with interpreted seismic sequences. For a discussion of the seismic units, see the regional synthesis chapter by Winterer and Hinz, this volume.

section believed to be present at MAZ-9 offered the opportunity not only to obtain a record of the succession of oceanic environments, but to bracket more precisely some of the unconformities that were so uncertainly dated in the Morocco Basin during Leg 50.

The drilling results at Sites 544, 545, and 546 had reconfirmed for us the need for drilling at MAZ-9. Beside the problem of the hiatus in the Tortonian part of the Miocene, we could see from the seismic records that Cenozoic beds older than those cored at Site 545 were present at MAZ-9, and we thought that these would most likely be Paleogene in age. A record of the stratigraphy of these rocks was required to document this interval of history, which had so far been unavailable to us. There was also the possibility of finding Upper Cretaceous rocks on the slope at MAZ-9. Upper Cretaceous beds younger than Cenomanian are unknown on the Northwest African margin seaward of the edge of the continental shelf.

The results at Sites 544 and 545 showed that the Jurassic carbonate stratigraphy in the Mazagan area is complex and includes strong facies differences over short distances. We therefore wanted to core a complete section of these strata at MAZ-9 to try to rationalize and to anchor more firmly the rather loosely constrained Jurassic stratigraphy inferred from Sites 544 and 545.

Finally, we reasoned that the salt facies at Site 546 might find landward expression at MAZ-9 in some related facies, perhaps a sabkha; we would thus be better able to date the salt and place it in the context of the succession on the Northwest African continental margin.

The relations of the four drilling sites of Leg 79 to the Mazagan escarpment and slope and to the salt diapirs are shown in Figure 4.

OPERATIONS

Operations at Site 547 lasted for 19 days, beginning at 1323 GMT on 3 May, when a double-life beacon was dropped, until 1434 hr. on 22 May, when the ship got under way for Lisbon. During the 19 days we drilled three holes: 547, a hole to test near-surface conditions for washing-in 16 in. casing for a planned reentry, which we washed to a depth of 32 m before the sediments became too stiff to penetrate without rotating the bit; 547A, a hole 744.5 m deep, cored continuously from 79.5 m to the total depth; and 547B, a reentry hole which was cored continuously from 724.5 to the total depth of 1030 m and which required three reentries to complete. We abandoned this hole before reaching basement because we ran out of time.

The approach to Site 547 (Fig. 5) was planned so that *Glomar Challenger* would pass directly over Site 544 on a course from Site 546, turn at Site 544, and run directly to the plotted location of MAZ-9, on *Meteor* seismic line 53-10. By a piece of good luck, the acoustic beacon at Site 544, which had been dropped 16 days earlier, was still functioning when we passed by, and this gave us a good fix to begin the run over MAZ-9. The *Challenger* seismic profile across MAZ-9 (Fig. 6) looked reasonably like *Meteor* profile M 53-10, a line very nearly parallel to the *Challenger* track. We steamed about 3 mi. farther to see how the seismic picture developed and then, having satisfied ourselves that the east-dipping reflectors, at

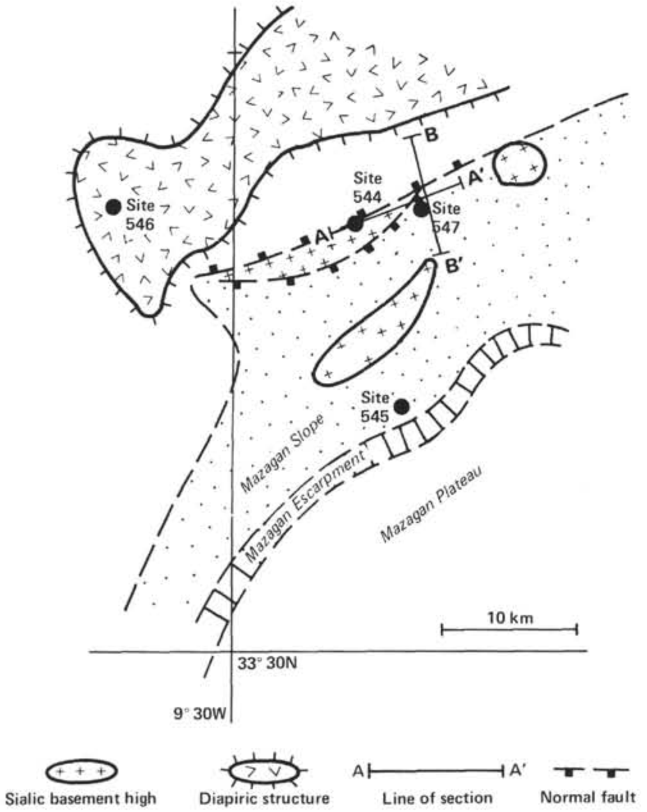

Figure 4. Map of Mazagan Escarpment area, showing Leg 79 sites and major geologic features. Line A-A′ is line of seismic reflection profile *M* 53-10; B-B′ is profile *M* 53-07.

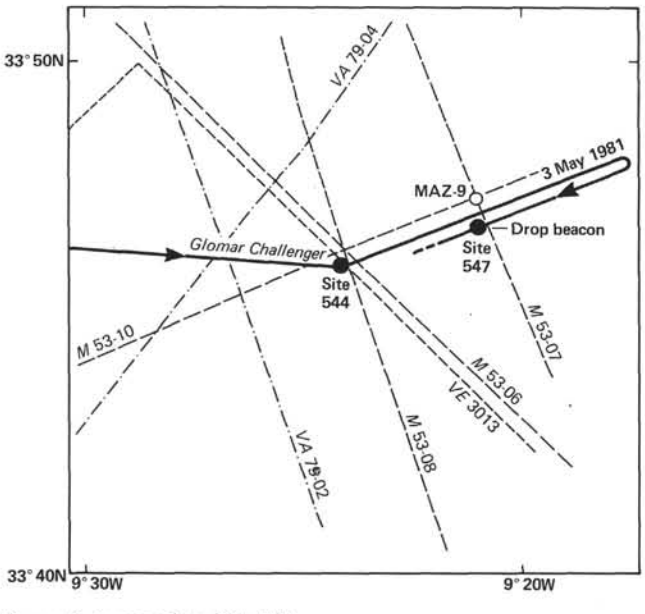

Figure 5. Approach to Site 547.

least the Red reflector, were conforming to the general picture for MAZ-9, we turned back on a reciprocal course and dropped the beacon at 1423 hr. on 3 May. The subsequent series of satellite fixes indicated that Site 547 is about 1 km due south of MAZ-9, and within half a kilometer of the *Meteor* 53-07 seismic line. When due account of the structural grain of the area is made, Site 547 projects onto *M* 53-07 at about Shot Point 566 (see Fig. 30, later).

Before arriving at Site 547, we had decided to make this a reentry site. The experience at Site 545 showed us that the Jurassic limestones might be several hundred meters thick, and the seismic records near MAZ-9 showed that the top of the limestones was probably at a depth greater than that at Site 545. Any hope of reaching basement with a single bit thus seemed overoptimistic.

The first business, after establishing the depth of the seafloor, was to test the induration of the upper part of the sediment column to determine how much 16-in. casing would be needed or could be washed in. The first core taken from Hole 547, in the interval 3944.5 to 3954.0 m below the derrick floor, recovered 3.5 m of material, and we therefore established the seafloor depth as 3950.5 m below the derrick floor (3940.5 m below sea level). We then washed ahead to a depth of 32 m, where the bit would not penetrate farther without being rotated. This was established as the depth to which the 16-in. casing could be washed.

We lifted the bit above the seafloor and began operations in Hole 547A, a pilot hole to explore as deeply as possible, perhaps event to basement. Because we planned to take a series of hydraulic piston cores after completing Hole 547A, a bit-release mechanism was deployed with the bit. We chose a short-tooth bit in the belief that it would be more effective than a long-tooth bit if we were able to reach the Jurassic limestone. We washed ahead to a depth of 51 m, where we cut Core 547A-1 to a depth of 60.5 m, and then washed ahead again to take Core 547A-2 from 79.5–89 m. We believed that the HPC would carry us no farther than 79.5 m, so we commenced continuous coring at this depth.

Coring proceeded without interruption or unusual incident for the next 5 days. The rate of penetration gradually decreased from about 1.5 min./m in the Pleistocene, Pliocene, and Miocene (0–205 m) to about 5 min./m in the Paleogene and Upper Cretaceous (205–422 m) (although with considerable variation) and from about 4 to 7 min./m in the Lower Cretaceous (422–744.5 m).

We ran an Eastman Survey device at 488 m, and found the hole to be inclined more than 6°. At 507 m, the Survey showed 9.5°; and at 650 m, the reading was greater than 12° (we had no device aboard for values greater than 12°).

After Core 73 was cut at a depth of 744.5 m, the drilling engineers advised us to cease coring, because the bit, which had now rotated in all for about 54 hr., was behaving as if a cone might be loose. We were still in Cretaceous claystone and, although we thought that the top of the Jurassic limestone was not far below, we could not believe this bit would last all the way to basement. We therefore decided to pull out of the hole to change bits.

By this time, we had also decided that any effort to take HPC cores in the Pleistocene section had a lower priority than obtaining cores of the Jurassic and reach-

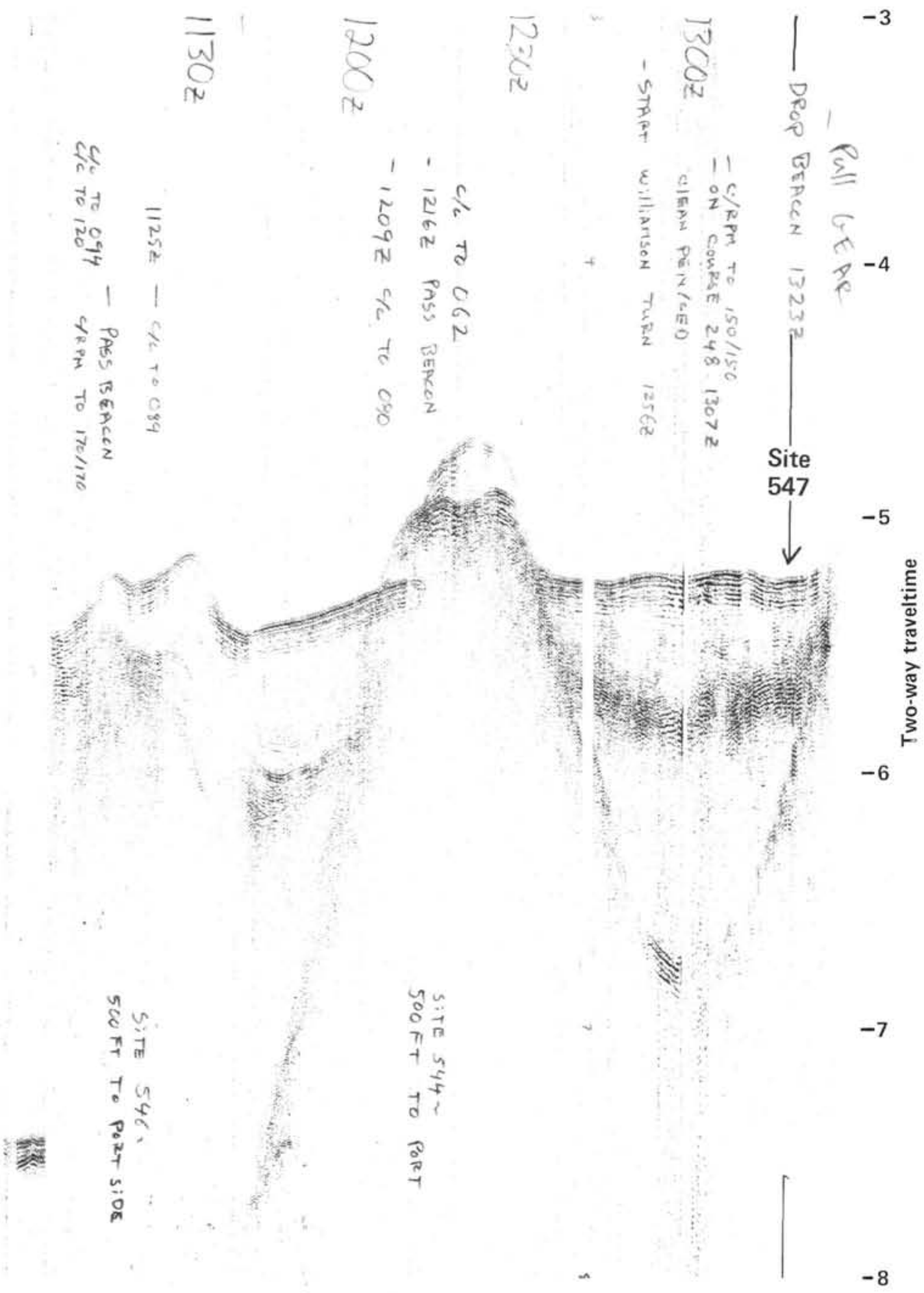

Figure 6. Reflection profiler record made from *Glomar Challenger.*

ing basement, so we began preparations for reentry Hole 547B. The reentry cone and the 16-in. casing were lowered to the seafloor and washed in on the morning of May 12 with a 14-in. bit (experience at Site 416 during Leg 50 indicated that washing the 16-in. casing through the upper clayey oozes might go very slowly with only a 10-in. bit.) Another round trip was made to change again to a 10-in. long-tooth bit, chosen to speed up cutting through the Cretaceous claystone.

We lowered the pipe to a point a few meters above the reentry cone, then lowered the sonar search device to seek the cone. After three failures of the device and about 17 hr. of time the tool worked and we began maneuvering the ship over the cone. It took another 2 hr. to reenter.

After the pipe was washed in to a depth of 211.5 m, the overshot device was sent down to retrieve the core barrel, but it could not do so, even after five tries. Thus we were forced to make yet another round trip to remove the core barrel, at a cost of 17 hr. for the round trip and another 6 hr. to lower the sonar tool, maneuver over the cone, and reenter (Reentry 2).

From 211.5 to 724.5 m, using a long-tooth bit, we drilled very quickly: 500 m in one day. At 724.5 m, continuous coring was resumed, in the belief that the steep inclination of Hole 547A (more than 12°, with apparent dips in cores of 23°), meant that the hole had terminated at a somewhat shallower depth beneath the seafloor than its length indicated. In fact, correlation of distinctive lithologic features shows that Core 1 of Hole 547B (724.5–734.0 m) correlates with Core 73 of Hole 547A (735.0–744.5 m) and confirms that Hole 547A is inclined strongly from the vertical in its lower part.

Coring with this bit proceeded to Core 547B-9, at a depth of 803.5 m. At 773 m, we cored the top of the Jurassic limestone. Drilling was very slow and the engineers advised retrieving the bit, even though it had rotated only about 30 hr. We therefore pulled out of the hole, changed bits and reentered the hole for the third time. The used bit showed loose bearings and a cracked cone.

We cored ahead using a button or short-tooth bit in limestone breccia and claystone to 925 m, where the lithology changed to red sandy mudstone. Coring rates in the limestone were about 12 min./m, except in some of the breccia intervals, but in the red mudstone the rate slowed progressively from about 12 min./m at the top to more than 50 min./m in the last core.

At a depth of 1030 m, the bit would not rotate when over 20,000 lbs. of weight was applied, and the engineers advised us that further progress was impossible. There was no time for another reentry, and we did not want to risk leaving pieces of the bit in the hole, because we hoped that it could be completed to basement and logged on a future leg. Thus we abandoned the hole.

By 1030 hr. on 22 May, the bit was on deck (with all bearings completely destroyed, but with all four cones still present), and we prepared to depart for Lisbon. Because the transit was judged to take only 40 hr., we made a seismic reflection survey in the Leg 79 area, linking Sites 544, 545 and 547, and running a tie line between *Meteor* profiles. This took about 8 hr.. The "single-life" beacon at Site 545, dropped on 23 April, was still chirping when we crossed it on 22 May. A calendar of operations at Site 547 is shown in Figure 7, and the coring operations are summarized in Table 1.

SEDIMENT LITHOLOGY

A detailed log of the lithology and biostratigraphy of the three holes drilled at Site 547 is shown at the end of this chapter, as Figure 35.

Hole 547

A total of 32 m of sediment was penetrated in Hole 547, but only the top 3.5 meters were cored.

Unit I (0–3.5 m; Core 1)

The top 3.5 m of the sedimentary pile at Site 547 consist of a highly disturbed clayey or slightly clayey nannofossil ooze of late Pleistocene–Recent age, dominantly pale yellowish brown (10YR 6/2) in color, but with occasional gray olive green (5GY 3/2) and moderate olive brown (5Y 4/4) layers. Foraminiferal content averages about 2% but rare patches of foraminiferal ooze (e.g., 547-1-3, 16–20 cm) may originally have been winnowed concentrations. Smear slides show a trace of quartz and feldspar silt, also silt-sized dolomite rhombs. Carbonate bomb estimations of total carbonate were not made.

The upper 75 cm of the core is oxidized to moderate brown (5YR 4/4); below this, occasional layers and burrow fills enriched in ferrous sulfides occur.

Discussion: Unit I is pelagic sediment deposited above the foraminiferal lysocline with a contribution of terrigenous clay and silt from the shelf (?coast).

A lamina of formainifer sand suggests an increase of bottom current activity that reworked sediment. The pale yellowish brown color of the unit as a whole reflects a thick surface layer of oxygenated sediment during deposition; the present zone of active seawater diffusion and high oxygen content is probably expressed by the transition to a moderate brown colored sediment in the top 75 cm of the core. Below this level, occasional ferrous sulfide concentrations along layers and in burrow fills reflect local reducing microenvironments around relatively high concentrations of organic matter.

Hole 547A

Drilling at Hole 547A penetrated to 744.5 m and achieved core recovery of 49%. One spot core was taken at 5–60.5 m (Core 1) and continuous coring started at 79.5 m (Cores 2 to 73). Five units are recognized. Unit I consists of 141.1 m of pale yellowish brown, slightly clayey nannofossil ooze deposited from the early Pleistocene to late Miocene. Unconformably beneath Unit I, Unit II is composed of 84.6 m of greenish gray to grayish green clayey nannofossil ooze, which encompasses two unconformities and ranges from the middle Miocene to Late Eocene. Unit III contains 53.3 m of olive gray to brown pebbly-cobbly clayey nannofossil chalk deposited during the Late Eocene. Unit IV consists of 143.6 m of siliceous chalk, porcellanite, and chert overlying pebbly-bouldery clayey chalks, which range from Eocene to Late Cretaceous (Campanian) in age. The mid-Cretaceous is represented by Unit V, 318.8 m of dark greenish gray nannofossil-bearing claystone.

Unit I (0–141.1 m; mud line to 547A-8-4, 7 cm)

Unit I, of late Pleistocene–Recent to late Miocene age, consists of 141.1 m of mainly pale yellowish brown (10YR 5/2), commonly highly disturbed clayey nannofossil and foraminiferal nannofossil ooze. The age of the top of the unit is assumed from the results of Hole 547; a thin layer of glauconite-bearing foraminiferal ooze marks the lower boundary, which adjoins greenish gray (5G 6/1) slightly clayey nannofossil ooze of Unit II.

Within the interval from 0 to 79.5 m., only one core, between 51 and 60.5 m, was taken. This consists of pale yellowish brown clayey foraminiferal nannofossil ooze (63% $CaCO_3$ from carbonate bomb analysis) with some light olive gray (5Y 6/1) and pale brown (10YR 5/2) bands. A similar lithology was encountered when coring recommenced at 79.5 m.

Foraminiferal content in Unit I decreases downward. The foraminifer:nannofossil ratio, about 1:7 in Cores 1, 2, and 3, falls to about 1:10 in Core 4, and foraminifers were absent from many smear slides of the nannofossil

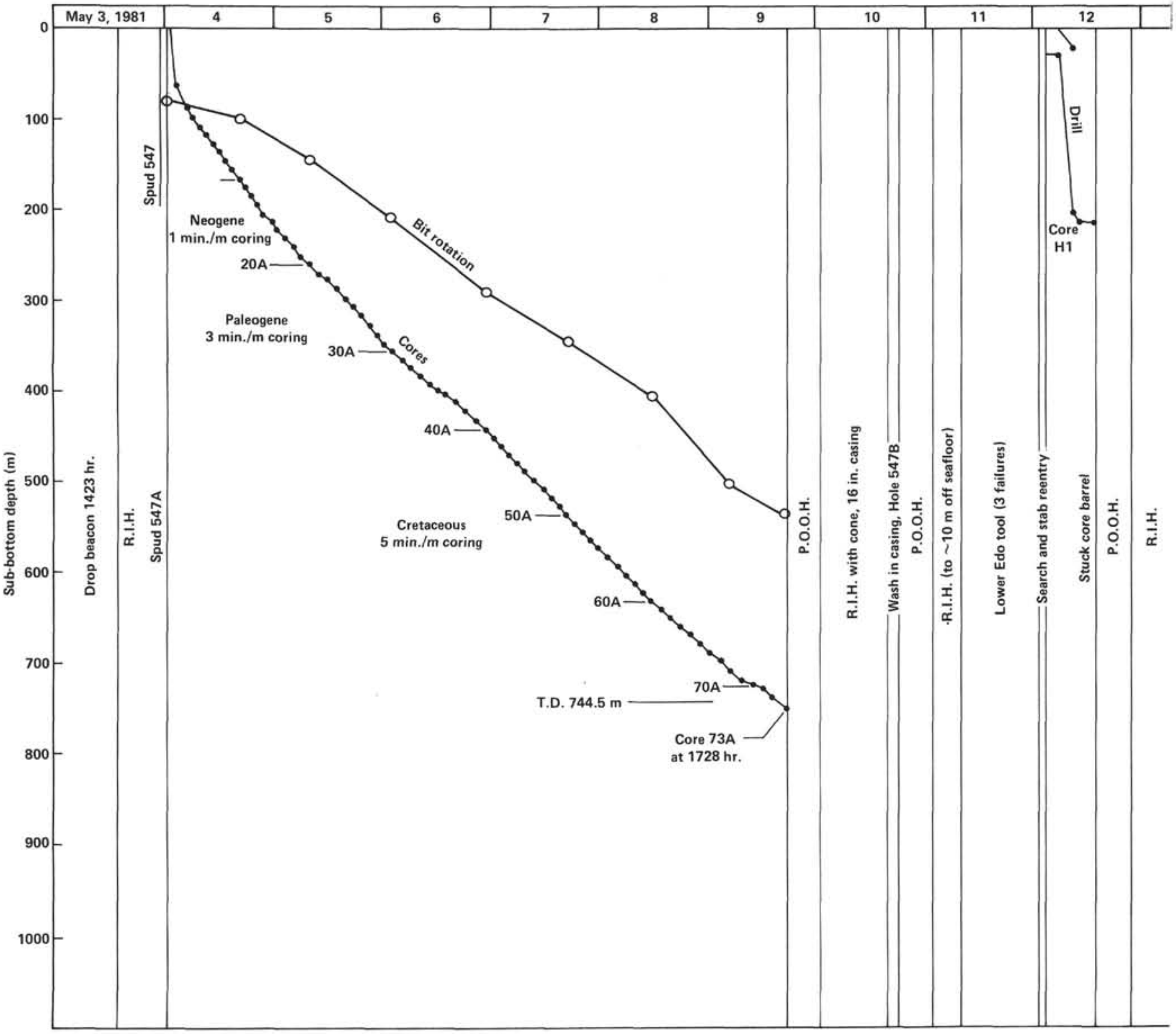

Figure 7. Calendar of operations, Holes 547, 547A, and 547B.

oozes encountered below this level. Thin layers of foraminiferal ooze in Cores 1 and 2 reflect the higher proportion of foraminifers higher in the unit and presumably indicate rare phases of current reworking; siliceous biogenic debris is extremely rare throughout.

Carbonate bomb data indicate a terrigenous component of between 37 and 45% through most of the unit, decreasing below Core 3 (98.5 m) to around 25%; however, slit-sized quartz and corroded feldspar rarely total more than 1% of the sediment. Present throughout Unit I are silt-sized dolomite rhombs in amounts normally around 2%.

The pale yellowish brown color of most of the unit is replaced by grayish orange pink (5YR 5/2) in Cores 3 and 4. Lighter and darker color alternations were detected in Core 4 and color interlayering of pale yellowish brown and yellowish gray (5Y 7/2) on a 2-3 cm scale was detected in Section 547A-6-3, but generally disturbance was too great to discern such subtleties. Thin layers and burrow fills of gray or black pyritic sediment are ubiquitous in Unit I but certainly less common than in equivalent strata at Site 545.

Discussion: Unit I represents pelagic deposition above the foraminiferal lysocline with terrigenous sediment from the nearby coast. The pale yellowish brown and gray orange pink colors suggest a well-oxygenated bottom sediment profile, whereas local laminae and burrow fills of ferrous-sulfide-rich ooze represent reducing microenvironments around concentrations of organic detritus. These features are less abundant than at Site 545 but their density is comparable to Site 544, reflecting the greater distance of Sites 544 and 547 from sites of higher organic productivity over the shelf, as well as slower sedimentation rates that permit more oxidation by fungi

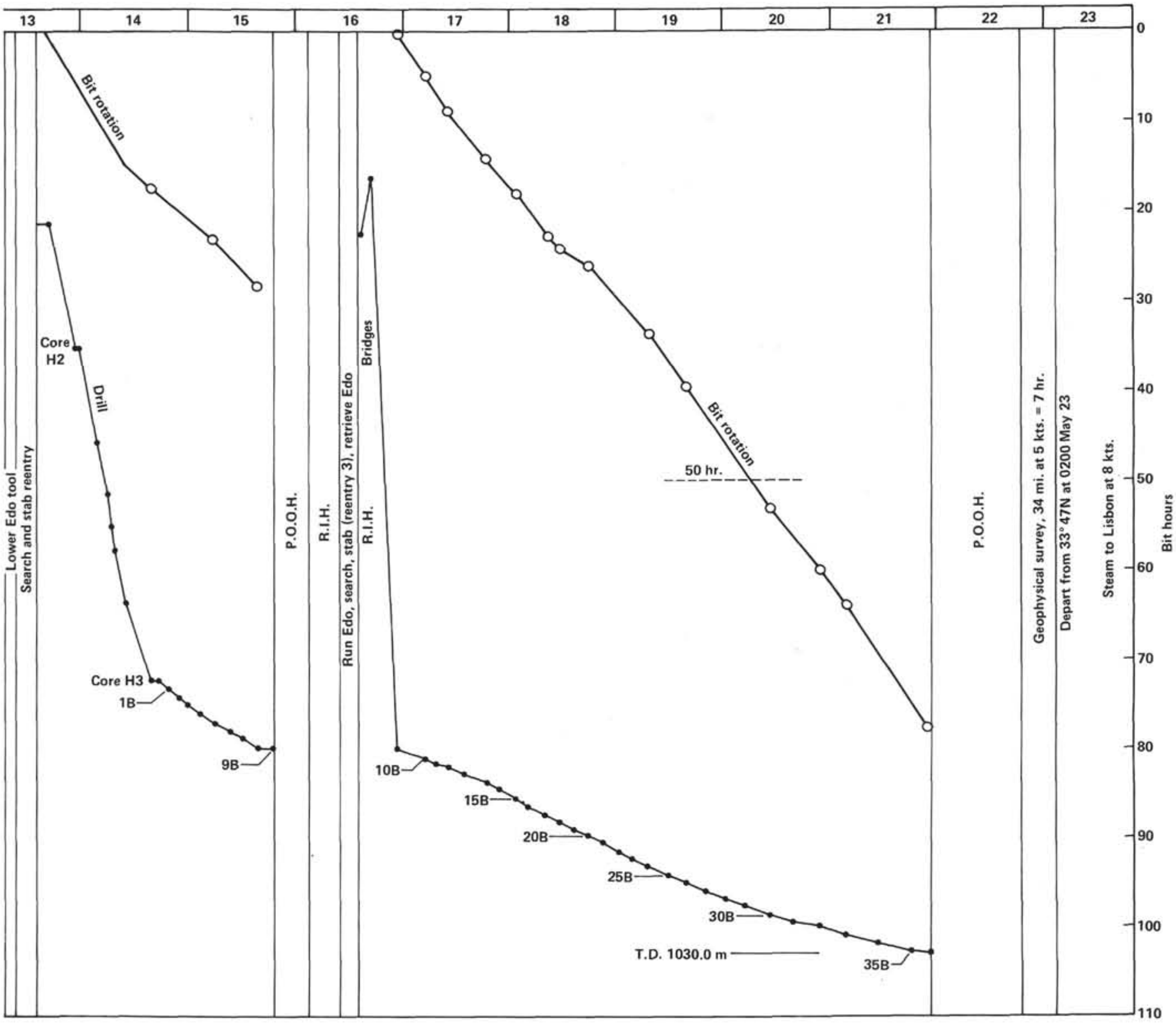

Figure 7. (Continued).

and heterotrophic bacteria within the surface sediments. The terrigenous fractions of the late Miocene to Pleistocene section at Sites 544 and 547 are comparable.

The lowest 7 cm of Unit I is well-sorted, medium sand composed mainly of foraminifers, but medium-sand-sized glauconite also occurs; in the lowermost centimeter it increases in abundance to form 50% of the sediment. This basal deposit clearly reflects a phase of increased bottom current activity and, judging from the glauconite abundance, slow sedimentation.

Unit II (141.1–225.7 m; 547A-8-4, 7 cm to 547A-17-3, 73 cm)

The 84.6 m of green gray variable clayey nannofossil ooze and nannofossil claystone which constitute Unit II span the late Eocene–early Oligocene to middle or early late Miocene in age. two hiatuses have been biostratigraphically detected; the lower, which occurs at 547A-15-1, 130 cm, is also marked by a short sedimentological change which enables division of Unit II into two subunits.

Definition of the top of Unit II has been discussed above; the base is drawn at 547A-17-3, 71 cm, where grayish green (10GY 5/2) to greenish gray (5G 6/1) nannofossil claystone sharply overlies a thick conglomeratic Eocene debris flow.

Subunit IIA (early Miocene to middle or early late Miocene; 141.1–204.3 m; 547A-8-4, 7 cm to 547A-15-1, 130 cm)

Greenish gray (5G 6/1) and light greenish gray (5GY 8/1) slightly clayey nannofossil ooze dominates Subunit IIA, becoming firmer downward. Drilling distortion (with the formation of "drilling cakes"; see report for Site 545) is moderate to severe below Core 8. Color interlayering of greenish gray (5G 6/1) and light olive gray (5Y

Table 1. Coring summary, Site 547.

Core no.	Date (May 1981)	Time	Depth from drill floor (m) Top Bottom	Depth below seafloor (m) Top Bottom	Length cored (m)	Length recovered (m)	Percentage recovered
Hole 547							
1	3	2334	3950.5-3954.0	0.0-3.5	3.5	3.5	100
Wash			3954.0-3982.5	3.5-32.0			
					3.5	3.5	100
Hole 547A							
Wash	4		3950.5-4001.5	0.0-51.0			
1	4	0248	4001.5-4011.0	51.0-60.5	9.5	5.2	55
Wash	4		4011.0-4030.0	60.5-79.5			
2	4	0517	4030.0-4039.5	79.5-89.0	9.5	5.3	56
3	4	0639	4039.5-4049.0	89.0-98.5	9.5	0.7	7
4	4	0757	4049.0-4058.5	98.5-108.0	9.5	1.6	17
5	4	0922	4058.5-4068.0	108.0-117.5	9.5	7.4	78
6	4	1044	4068.0-4077.5	117.5-127.0	9.5	4.1	43
7	4	1205	4077.5-4087.0	127.0-136.5	9.5	1.9	20
8	4	1331	4087.0-4096.5	136.5-146.0	9.5	6.9	73
9	4	1457	4096.5-4106.0	146.0-155.5	9.5	5.6	59
10	4	1617	4106.0-4115.5	155.5-165.0	9.5	3.1	33
11	4	1744	4115.5-4125.0	165.0-174.5	9.5	5.8	61
12	4	1904	4125.0-4134.5	174.5-184.0	9.5	5.3	56
13	4	2025	4134.5-4144.0	184.0-193.5	9.5	2.7	28
14	4	2145	4144.0-4153.5	193.5-203.0	9.5	5.8	61
15	4	2322	4153.5-4163.0	203.0-212.5	9.5	2.5	26
16	5	0055	4163.0-4172.5	212.5-222.0	9.5	7.7	81
17	5	0229	4172.5-4182.0	222.0-231.5	9.5	6.5	68
18	5	0416	4182.0-4191.5	231.5-241.0	9.5	2.4	25
19	5	0556	4191.5-4201.0	241.0-250.5	9.5	2.3	24
20	5	0759	4201.0-4210.5	250.5-260.0	9.5	9.7	102
21	5	1014	4210.5-4220.0	260.0-269.5	9.5	8.9	94
22	5	1218	4220.0-4229.5	269.5-279.0	9.5	2.7	28
23	5	1423	4229.5-4239.0	279.0-288.5	9.5	5.9	62
24	5	1619	4239.0-4248.5	288.5-298.0	9.5	2.2	23
25	5	1752	4248.5-4258.0	298.0-307.5	9.5	5.4	57
26	5	1928	4258.0-4267.5	307.5-317.0	9.5	0.9	9
27	5	2108	4267.5-4277.0	317.0-326.5	9.5	3.2	34
28	5	2244	4277.0-4286.5	326.5-336.0	9.5	3.0	34
29	6	0028	4286.5-4296.0	336.0-345.5	9.5	2.7	28
30	6	0212	4296.0-4305.5	345.5-355.0	9.5	5.4	57
31	6	0417	4305.5-4315.0	355.0-364.5	9.5	0.6	6
32	6	0619	4315.0-4324.5	364.5-374.0	9.5	5.5	58
33	6	0827	4324.5-4334.0	374.0-383.5	9.5	9.0	95
34	6	1051	4334.0-4343.5	383.5-393.0	9.5	9.4	99
35	6	1228	4343.5-4348.0	393.0-397.5	4.5	2.9	64
36	6	1412	4348.0-4353.0	397.5-402.5	5.0	3.2	64
37	6	1610	4353.0-4362.5	402.5-412.0	9.5	5.5	58
38	6	1826	4362.5-4372.0	412.0-421.5	9.5	4.5	47
39	6	2041	4372.0-4381.5	421.5-431.0	9.5	1.2	13
40	6	2240	4381.5-4391.0	431.0-440.5	9.5	2.9	31
41	7	0027	4391.0-4400.5	440.5-450.0	9.5	2.4	25
42	7	0216	4400.5-4410.0	450.0-459.5	9.5	5.5	58
43	7	0407	4410.0-4419.5	459.5-469.0	9.5	4.2	44
44	7	0600	4419.5-4429.0	469.0-478.5	9.5	6.8	72
45	7	0752	4429.0-4438.5	478.5-488.0	9.5	3.2	34
46	7	0949	4438.5-4448.0	488.0-497.5	9.5	4.9	52
47	7	1138	4448.0-4457.5	497.5-507.0	9.5	4.7	49
48	7	1331	4457.5-4467.0	507.0-516.5	9.5	2.6	27
49	7	1515	4467.0-4476.5	516.5-526.0	9.5	3.5	37
50	7	1654	4476.5-4486.0	526.0-535.5	9.5	4.8	51
51	7	1841	4486.0-4495.5	535.5-545.0	9.5	6.0	63
52	7	2027	4495.5-4505.0	545.0-554.5	9.5	3.9	41
53	7	2220	4505.0-4514.5	554.5-564.0	9.5	3.4	36
54	8	0009	4514.5-4524.0	564.0-573.5	9.5	2.6	27
55	8	0203	4524.0-4533.5	573.5-583.0	9.5	4.3	45
56	8	0408	4533.5-4543.0	583.0-592.5	9.5	6.0	63
57	8	0603	4543.0-4552.5	592.5-602.5	9.5	8.2	86
58	8	0757	4552.5-4562.0	602.0-611.5	9.5	7.5	79
59	8	0955	4562.0-4571.5	611.5-621.0	9.5	7.6	80
60	8	1148	4571.5-4581.0	621.0-630.5	9.5	6.8	72
61	8	1404	4581.0-4590.5	630.5-640.0	9.5	5.8	61
62	8	1555	4590.5-4600.0	640.0-649.5	9.5	4.3	45
63	8	1813	4600.0-4609.5	649.5-659.0	9.5	5.1	54
64	8	2015	4609.5-4619.0	659.0-668.5	9.5	5.1	54
65	8	2244	4619.0-4628.5	668.5-678.0	9.5	0.4	4
66	9	0043	4628.5-4638.0	678.0-687.5	9.5	3.3	35
67	9	0303	4638.0-4647.5	687.5-697.0	9.5	3.3	35
68	9	0519	4647.5-4657.0	697.0-706.5	9.5	6.1	64
69	9	0732	4657.0-4666.5	706.5-716.0	9.5	4.9	52
70	9	1016	4666.5-4671.0	716.0-720.5	4.5	4.4	98
71	9	1223	4671.0-4676.0	720.5-725.5	5.0	2.4	48
72	9	1448	4676.0-4685.5	725.5-735.0	9.5	6.3	66
73	9	1728	4685.5-4695.0	735.0-744.5	9.5	5.7	60
					674.5	333.5	49
Hole 547B							
H1	12	2215	3979.0-4162.5	28.0-211.5		0.01	
H2	13	2331	4162.5-4305.0	211.5-354.0		0.1	
H3	14	1700	4305.0-4675.5	354.0-724.4		6.9	
1	14	1956	4675.5-4685.0	724.5-734.0	9.5	0.1	1
2	14	2204	4685.0-4694.5	734.0-743.5	9.5	7.7	81
3	15	0013	4694.5-4704.0	743.5-753.0	9.5	7.5	79
4	15	0257	4704.0-4713.5	753.0-762.5	9.5	7.0	74
5	15	0604	4713.0-4723.0	762.5-772.0	9.5	9.5	100
6	15	0936	4723.0-4732.5	772.0-781.5	9.5	6.1	64
Hole 547B (Cont.)							
7	15	1232	4732.5-4742.0	781.5-791.0	9.5	5.5	58
8	15	1538	4742.0-4751.5	791.0-800.5	9.5	6.0	63
9	15	1912	4751.5-4754.5	800.5-803.5	3.0	2.7	90
H4	16	1653	3951.0-4112.5	0.0-160.5		1.5	
H5	16	2308	4112.5-4754.5	160.5-803.5		0.3	
10	17	0515	4754.5-4761.0	803.5-810.0	6.5	5.5	85
11	17	1033	4761.0-4770.0	810.0-819.0	9.0	6.0	67
12	17	1357	4770.0-4779.0	819.0-828.0	9.0	2.9	32
13	17	1848	4779.0-4788.0	828.0-837.0	9.0	2.8	31
14	17	2157	4788.0-4797.0	837.0-846.0	9.0	2.7	30
15	18	0112	4797.0-4806.0	846.0-855.0	9.0	2.7	30
16	18	0426	4806.0-4815.0	855.0-864.0	9.0	3.1	34
17	18	0835	4815.0-4824.0	864.0-873.0	9.0	1.9	21
18	18	1118	4824.0-4833.0	873.0-882.0	9.0	2.4	27
19	18	1400	4833.0-4842.0	882.0-891.0	9.0	2.3	26
20	18	1743	4842.0-4846.5	891.0-895.5	4.5	3.1	69
21	18	2054	4846.5-4856.0	895.5-905.0	9.5	2.4	25
22	19	0018	4856.0-4865.5	905.0-914.5	9.5	3.5	37
23	19	0316	4865.5-4874.5	914.5-923.5	9.0	2.3	26
24	19	0712	4874.5-4883.5	923.5-932.5	9.0	1.7	19
25	19	1145	4883.5-4892.5	932.5-941.5	9.0	6.2	69
26	19	1549	4892.5-4901.5	941.5-950.5	9.0	5.8	64
27	19	2022	4901.5-4910.5	950.5-959.5	9.0	6.1	68
28	20	0048	4910.5-4919.5	959.5-968.5	9.0	7.8	87
29	20	0501	4919.5-4928.5	968.5-977.5	9.0	3.6	40
30	20	1040	4928.5-4937.5	977.5-986.5	9.0	5.4	60
31	20	1520	4937.5-4946.5	986.5-995.5	9.0	5.7	63
32	20	2156	4946.5-4951.0	995.5-1000.0	4.5	3.4	76
33	21	0345	4951.0-4960.5	1000.0-1009.5	9.5	4.6	48
34	21	1102	4960.5-4969.5	1009.5-1018.5	9.0	3.3	37
35	21	1841	4969.5-4978.5	1018.5-1027.5	9.0	4.0	44
36	21	2244	4978.5-4981.0	1027.5-1030.0	2.5	1.5	60
					305.5	163.61	54

6/1) with grayish yellow green (5GY 7/2) occurs on a 6–15 cm scale in Core 10; alternations of light greenish gray (5GY 8/1) and greenish gray, 10 to 40 cm thick, occur in Cores 12 and 13. Although bioturbation is common throughout and is expressed by light olive gray (5Y 6/1) mottling and mm-scale pyritic burrow fills, identifiable ichnofossils are lacking.

The ooze becomes less clayey downward; carbonate bomb analysis indicates that the terrigenous component in Core 8 is about 35%, decreasing to between 25 and 30% in Core 9 and below. Terrigenous quartz-feldspar content occurs in only a few smear slides in more than trace quantities, but the glauconite component, though small (about 1%), is nevertheless significantly higher than in Unit I. Foraminifers are rare down to Core 13, except for two layers of foraminiferal nannofossil ooze in Section 547A-11-3 (78–81 cm, and 116–120 cm), which are both rich in glauconite sand at the base. Within Core 13, the foraminifer:nannofossil ratio rises to about 1:20. Siliceous biogenic debris (radiolarians and sponge spicules) was recognized only in Core 14. Silt-sized dolomite rhombs form about 1% of the sediment throughout the subunit.

A hiatus between the early and middle Miocene has been recognized within Core 14, using foraminifer biostratigraphy. This break may be in Section 4 of that core, at 14 cm, where a slight color change from light greenish gray (5GY 8/1) to greenish gray (5GY 6/1) and light olive gray (5Y 5/2) ooze was detected. Although the latter darker colors (accompanied by moderate green gray, 5GY 4/1, and dark green gray, 5GY 4/1, dominate the lower part of the subunit, light greenish gray (5GY 8/1) reappears locally.

Subunit IIB (late Eocene to middle Oligocene; 204.3–225.7 m, 547A-15-1, 130 cm to 547A-17-3, 73 cm)

The sharp contact between Subunits IIA and IIB marks a downward change from greenish gray (5GY 6/1) and light olive gray (5Y 5/2), slightly clayey nannofossil ooze to less bioturbated and firmer grayish green (10GY 5/2) nannofossil clay. Burrow fills of Subunit IIA sediment occur within the top centimeters of Subunit IIB; the contact represents a hiatus embracing much of the Oligocene.

Grayish green (10GY 5/2) and greenish gray (5G 6/1) colors dominate Subunit IIB (21.4 m), with poorly defined color interlayering of lighter and darker shades. The degree of consolidation increases downward, so that the sediments of Core 16 and below are claystones. Terrigenous clay content of Subunit IIB varies between 47 and 56% (carbonate bomb analysis); quartz and feldspar occur only in trace quantities throughout. Foraminifers are also rare and siliceous biogenic debris was only locally recorded.

Bioturbation increases in intensity downward. Planolites, characterized by darker greenish gray shades, is common and is accompanied by a dense network of smaller-diameter burrows; true Chondrites and Zoophycos occur in Cores 16 and 17 and pyritic "tubes" are ubiquitous.

Discussion: As in Unit I, the hemipelagic sediments of Unit II were deposited above the foraminiferal lysocline; the presence of Seilacher's (1967) Nereites ichnofacies reflects their deep bathymetric position but mainly indicates a low-energy environment. Despite their separation by a considerable unconformity, Subunits IIA and IIB differ significantly only in their clay content, their degree of consolidation, and the higher glauconite content of IIA.

The significance of the upper boundary of Unit II has been discussed under Unit I. (Further consideration of this topic is found in the lithologic section of the Site 545 site report.) At Sites 544 and 545, the lower Miocene rests on the Upper Jurassic and Cenomanian, respectively, but at Site 547 a thick Paleogene sequence has been preserved.

Unit III (225.7–279.0 m; 547A-17-3, 73 cm to base of Core 22)

The grayish green and green gray nannofossil claystone on Subunit IIB sharply overlies a 53.3-m-thick conglomeratic unit of late Eocene age (Fig. 8). The base is placed below the last occurrence of highly disturbed layers in Core 22 and above the yellow gray (5Y 7/2) and light olive gray (5Y 6/1) clayey nannofossil chalk of Core 23.

In terms of sediment grade, Unit III varies from a clayey gravel (Fig. 9) through gravelly clay to occasional, unbroken clay intervals; the largest gravel clast is 4.2 m thick (− 12 ϕ), penetrated in the lower sections of Core 21. Cores 19 through 21 display a matrix of light olive gray (5Y 5/2), olive gray (5Y 3/2), and moderate olive brown (5Y 4/4) clayey or slightly clayey nannofossil ooze–chalk containing about 56% carbonate (carbonate bomb data). Core 22 displays a matrix of light olive gray and yellowish gray clayey nannofossil chalk more similar to Subunit IVA. Terrigenous quartz-feldspar content is also low (about 1%) and forminifers form less than

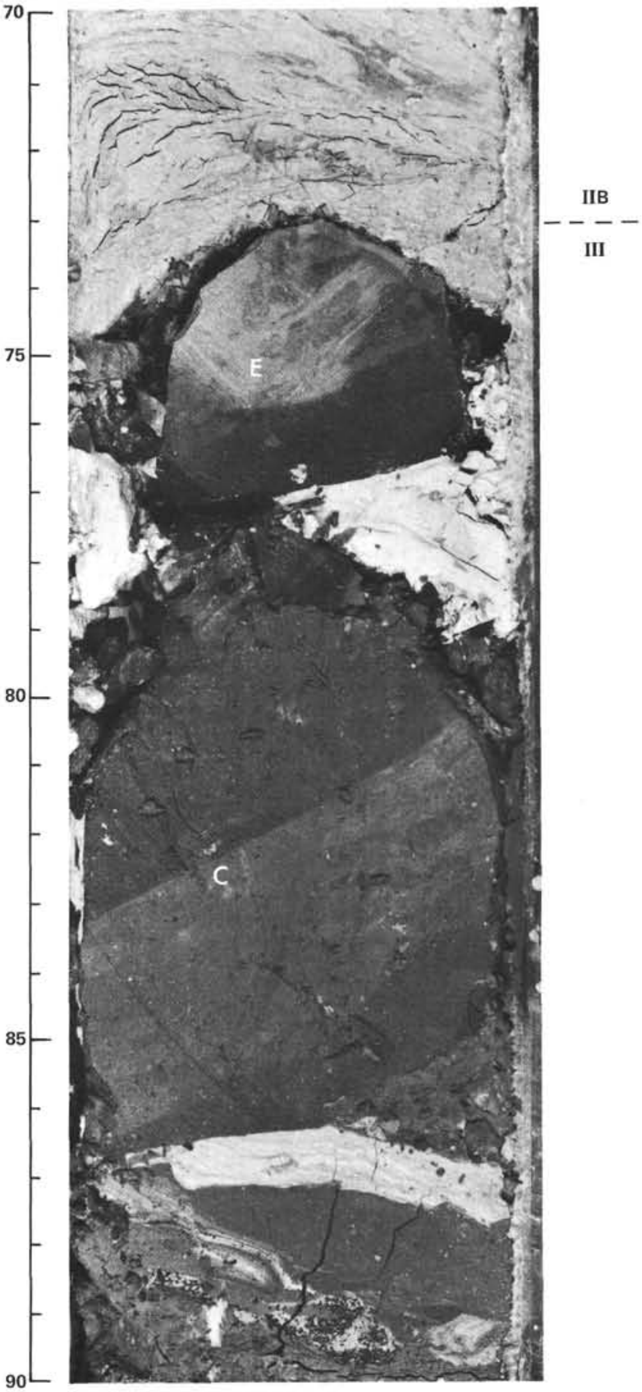

Figure 8. Contact between Units II and III (547A-17-3, 73 cm). Note clast types C (olive gray nannofossil claystone) and E (porcellanite) within uppermost part of conglomerate. Sample 547A-17-3, 70–90 cm.

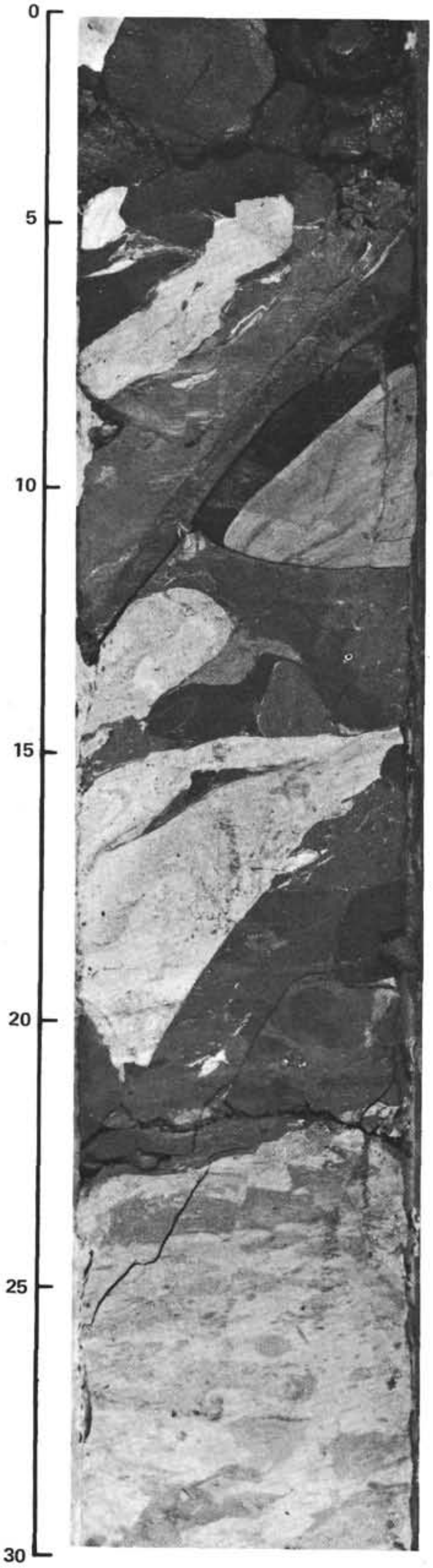

Figure 9. Typical view of clast-rich upper part of conglomeratic Unit III. Note especially clast of light greenish gray clayey nannofossil chalk in lower part of section, which displays Zoophycos and Planolites burrows. Sample 547A-18-1, 0–30 cm.

5% of the sediment. Floating within this matrix are clasts, originally rounded to subangular but compacted after deposition, of the following varieties:

A. Dusky yellow green (5GY 5/2) or grayish olive green (5GY 3/2) nannofossil claystone and nannofossil-bearing claystone (11–17% $CaCO_3$);

B. Grayish yellow green (5GY 7/2) bioturbated clayey nannofossil chalk;

C. Olive gray (5Y 3/2) nannofossil claystone;

D. Light greenish gray (5GY 8/1) clayey nannofossil and foraminiferal-nannofossil chalk;

E. Olive gray (5Y 4/1) medium light gray (N6) and dusky yellowish brown (10YR 2/2) porcellanite, displaying traces of bioturbation.

Of these, clast type D is the most abundant numerically, with an average diameter of 5 cm; apart from type E, it is also the least compacted. Clast types B and E are the least common. Clast type A bears a remarkable similarity to the Cenomanian claystones of Unit V at this site (and also of Subunit IIIA at Site 545). A 4.2-m-thick clast of this lithology forms the base of the unit. In both clasts and matrix there has been some recrystallization of what was probably nannofossil carbonate to calcite microspar.

Packing of clasts varies widely throughout Cores 19 to 22 and the matrix shows slump and convolution structures indicative of submarine mud flow and slide deposits. Thick clast-free intervals occur in 547A-21-1, 547A-21-2, 0–30 cm, 547A-21-2, 77 cm through 547A-21-6, 40 cm, 547A-20-3, 30–100 cm, 547A-20-4, and 547A-20-5, 0–45 cm and 90-150 cm. Bioturbation, picked out by darker brown shades, is common within these intervals and includes Planolites burrows.

The upper part of Unit III is similar to the lower, but clast-free intervals are fewer and thinner and clast density within the conglomerates is higher; deformation and compaction of soft sediments has thus distorted textures to extreme proportions. Nevertheless, where matrix can be clearly differentiated, it appears to be dusky yellow brown (10YR 2/2), olive brown (5Y/YR 3/2), or light olive gray (5Y 5/2) clayey or slightly clayey nannofossil ooze–chalk.

Clast variety essentially continues as in the lower unit. Clast type B contains concentrations of glauconite sand and an ichnofauna of Planolites, Zoophycos, and Chondrites picked out by olive brown shades; some examples of clast type D also display intense bioturbation. Some type C clasts tend toward olive brown (5Y/YR 3/2) shades, and porcellanite clasts (type E) increase in abundance upward in the unit.

Discussion: The sediments of Unit III fit comfortably into a mud-supported debris-flow model. We conclude that the clast-free intervals in cores 20 and 21 are either *in situ* pelagic deposits or the accumulations of clast-free mud flows; we favor the former explanation owing to their common ichnofauna. This conclusion implies that Unit III is an accumulation of discrete flow bodies rather than the deposits of a single event.

Preliminary compositional and paleontological studies on the clasts suggest that most are of Eocene and Paleocene age, also with a Late Cretaceous component.

Unit IV (279.0–422.6 m; 547A-23 to 547A-39-1, 105 cm)

Unit IV consists essentially of bioturbated greenish gray (5GY 6/1) and grayish green (10GY 5/2) variably clayey nannofossil chalk of middle Campanian to late Paleocene or early Eocene age. The upper boundary of the unit is formed by the base of the conglomeratic Unit III and Unit IV sharply overlies grayish olive green nannofossil claystones of middle Cretaceous (Cenomanian) age. The occurrence of gravelly intervals in the lower half of the unit enables a two-fold division.

Subunit IVA (early Paleocene to late Paleocene or early Eocene; 279.0–364.5 m; 547A-23 to 547A-31,CC

The conglomeratic Unit III overlies a sequence of bioturbated greenish gray (5GY 6/1), light greenish gray (5GY 8/1), and very light gray (N8) variably clayey nannofossil chalk and subordinate nannofossil claystone. Total carbonate content (determined by bomb analysis) decreases downward from about 71% (slightly clayey nannofossil chalk) in Cores 22 and 23, through about 60% (clayey nannofossil chalk) in Cores 24 and 25, to about 35% (nannofossil claystone) in Cores 26 and 27; carbonate content then increases to about 60% for the remainder of the subunit.

Amongst the biogenic fraction of Subunit IVA, foraminifers are normally present only in trace quantities and nowhere exceed 3% of the total sediment. Siliceous biogenic debris markedly increases from a trace to in excess of 5% (locally 20%) in the core catcher of Cores 30 and 31; most of this component consists of radolarians. Recrystallization of some nannoplankton to calcite microspar is common throughout the unit, and a small proportion (about 1%) of silt-sized dolomite rhombs was detected in most smear slides.

The higher siliceous content of Subunit IVA relative to the rest of the Tertiary sequence presumably explains the abundance of chertification in the cores. All stages appear to be present, from incipient porcellanite through to olive gray (5Y 4/1) and olive black (5Y 2/1) chert; the sediment surrounding the 5–15-cm-diameter nodules changes color from typical greenish gray (5GY 6/1) to dark greenish gray (5GY 4/1) and is relatively enriched in silica, low in carbonate (about 30%). Cherts and porcellanites occur through the subunit and the lack of biogenic siliceous debris in smear slides from the higher cores presumably reflects mobilization and concentration of silica in local centers.

The quartz-feldspar fraction does not exceed 2% except in Cores 30 to 31, where up to 10% was recorded. This abundance is associated with an influx of silt-sized volcanic glass and needs further study.

Bioturbation in Subunit IVA is profuse and picked out by olive gray (5Y 6/1) colors; Planolites, Chondrites-like burrows, and Zoophycos abound. A progressive decrease in the clarity of these structures occurs downward through Core 30.

Subunit IVB (middle Campanian to early Paleocene; 364.5–422.6 m Core 547A-32 to Sample 547A-39-1, 105 cm)

Subunit IVB differs from IVA in that conglomeratic layers occur. The matrix of these conglomerates and the intervening sediments is essentially similar to those of IVA: greenish gray (5GY 6/1) and grayish green (10GY-5/2) variably clayey nannofossil or foraminiferal nannofossil chalk. Terrigenous content increases slightly downward from about 28% in Core 33 to 40% near the base; the quartz-feldspar component nowhere exceeds 3% of the total sediment. The foraminiferal:nannofossil ratio falls slightly throughout the subunit (1:8 to 1:11) but is nevertheless higher than for many of the other Cenozoic units at Site 547. Small quantities of radiolarians and sponge spicules were detected in smear slides, but much original siliceous biogenic debris has probably been mobilized to form the porcellanite nodules encountered at a few places in the section. As in most of the other Cenozoic units, silt-sized dolomite rhombs form about 2% of the sediment.

The conglomeratic units within Subunit IVB display clear upward trends in thickness, clast sorting, and clast matrix ratio, although the clast composition changes little. Four clast types are recognized:

A. Dusky yellow green (5GY 5/2) to dark greenish gray (5GY 4/1) nannofossil-bearing claystone or (rarely) nannofossil claystone, containing about 16% $CaCO_3$ (carbonate bomb analysis) and closely resembling clast type A of Unit III;

B. Greenish gray (5GY 6/1) to grayish green (10GY 5/2) slightly clayey nannofossil chalk commonly displaying bioturbation (Zoophycos, etc.); this clast type is similar to the conglomerate matrix;

C. Light olive gray (5Y 6/1) to olive gray (5Y 4/1) nannofossil claystone or (rarely) clayey nannofossil chalk;

D. Gray porcellanite.

Of these four types, B is by far the most common, whereas D is rare. Clasts are rounded to subangular and many are extremely deformed by postdepositional compaction (Fig. 10).

The conglomeratic intervals in the lower half of Subunit IVB have a low clast-to-matrix ratio, the latter commonly forming 95% of intervals which may be several meters thick. Thin clast-free intervals show some slumping and bioturbation, with Zoophycos, Planolites, and the like. In the upper half of Subunit IVB, the conglomeratic intervals become more discrete, thinner (average of 50 cm, with a maximum of 1.8 m) and sharp-based and show distinct fining-upward trends. The clasts in the lower conglomerates are poorly sorted, and some approach 50 cm in diameter; sorting is better in the higher intervals, and the clasts are smaller (normally less than 10 cm in diameter). The upper intervals have a high clast-to-matrix ratio (about 3:2) and are separated by 1–2-m-thick, clast-free, bioturbated intervals displaying exquisite Zoophycos (Fig. 11). Frequently the upper conglomerates contain abundant glauconite sand in their matrix.

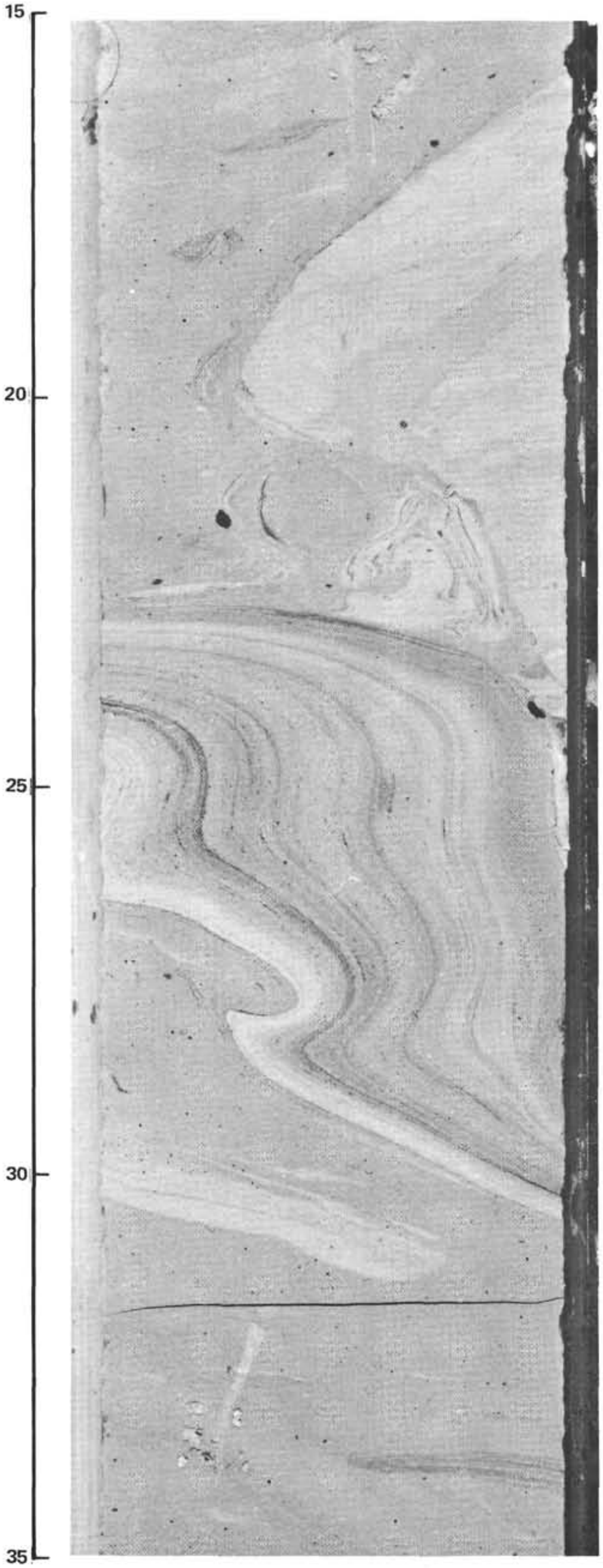

Figure 10. Postdepositional deformation of clasts in clast-poor gravelly interval toward the base of Subunit IVB. Sample 547A-37-1, 15–35 cm.

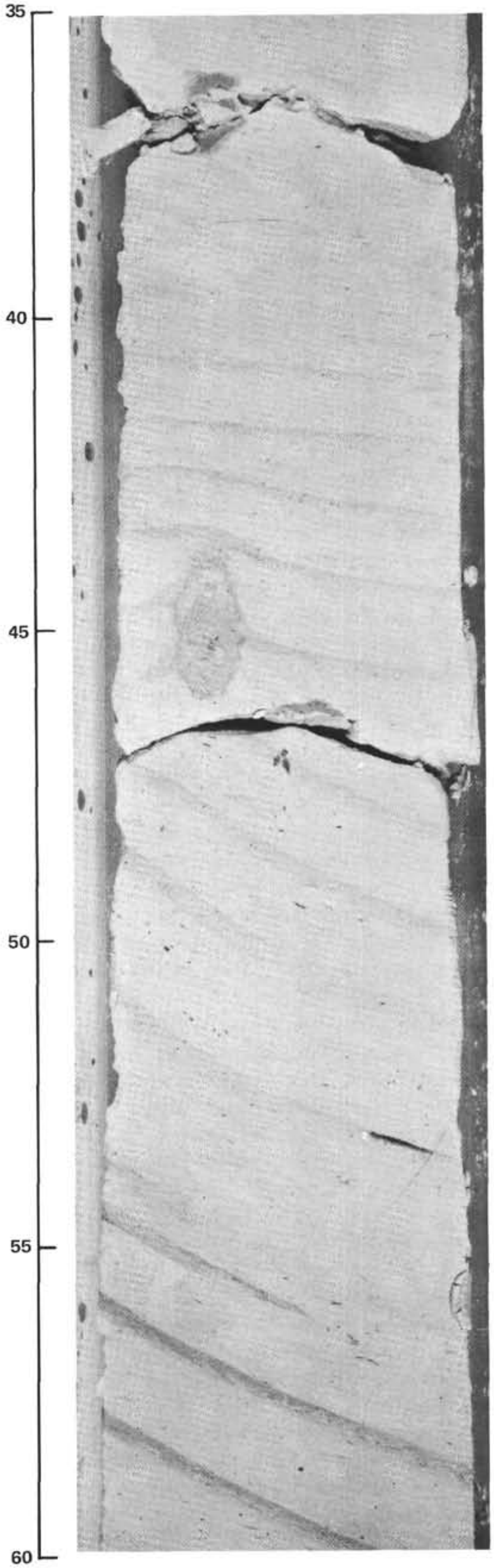

Figure 11. Superb example of Zoophycos with central vertical burrow in a bioturbated clast-free interval near the top of Subunit IVB. Sample 547A-33-2, 35–60 cm.

Discussion: Unit IV consists largely of pelagic sediment deposited above the foraminifer lysocline, and the Nereites ichnofacies of the clast-free intervals attests to a normally low-energy environment (Seilacher, 1967). The distribution and fabric of the gravelly intervals, within thick, clast-poor lower intervals with great variation in clast size, suggest deposition by proximal submarine mud flows which must have moved downslope as a thick "slurry." The upward trend to better-sorted, clast-rich, graded layers indicates more distal gravity flows whose activity ceased at the boundary between Subunits IVA and IVB.

Unit V (422.6–744.5 m; 547A-39-1, 105 cm to Core 73, bottom)

Unit V encompasses 318.8 m of Cretaceous (late Albian to middle–late Cenomanian age) claystone and calcareous claystone with subordinate amounts of pebbly-cobbly claystone and mudstone. The dominant lithology is dark greenish gray (5GY 4/1), grayish olive green (5GY 3/2), and grayish green (10G 4/2) nannofossil claystone. Laminae of olive gray (5Y 4/1), greenish black (5Y 2/1), and olive black (5Y 2/1) result from flattened and stretched burrows lying parallel to bedding. Laminae are wispy and discontinuous, range from 0.5 to 4 mm in thickness, and are generally indistinct.

Intervals of planar laminated claystone to mudstone occur in the lower part of the unit (Cores 58, 59, 69, 71, and 73) and form a very minor lithology (less than 1%). These laminated intervals range from 5 to 30 cm in thickness, they are generally darker in color and contain shell fragments and more quartz silt than the dominant lithology. At the base of the unit (547A-73-4, 0–95 cm), planar laminated claystone of this type is olive black with brownish black (5YR 3/1) laminae, the darkest sediment within the entire unit.

The other minor lithology of this unit is pebbly-cobbly claystone–mudstone and mudstone conglomerate. It occurs mostly in the lower part of the unit (Fig. 12). Pebbly intervals consist of both matrix-dominated and clast-dominated claystone; they are from 5 cm to 2 m thick and form 18% of the unit. The thicker intervals are generally clast dominated and contain the largest clasts, up to 17 cm although dominantly from 2 mm to 6 cm. Most pebbles are flattened, stretched, and deformed around others (Fig. 12). Some, however, are relatively undeformed. Contorted bedding, small slump folds, and load features are commonly associated with the pebbly intervals (Fig. 13).

Clasts in thicker pebbly intervals (those greater than 20 cm) in some beds show a poor development of normal grading; generally, however, they are not graded or show a complex mixture of normal and reverse grading. Colors of the clasts are mostly shades of green and gray—medium gray (N4), light olive gray (5Y 5/2), grayish olive (10Y 4/2), very pale green (10G 3/2)—and contain the same textures and structures as the matrix and dominant lithology (nannofossil-bearing claystone); these clasts show the most deformation and flattening. There are small numbers of olive gray (5Y 3/2) clasts that

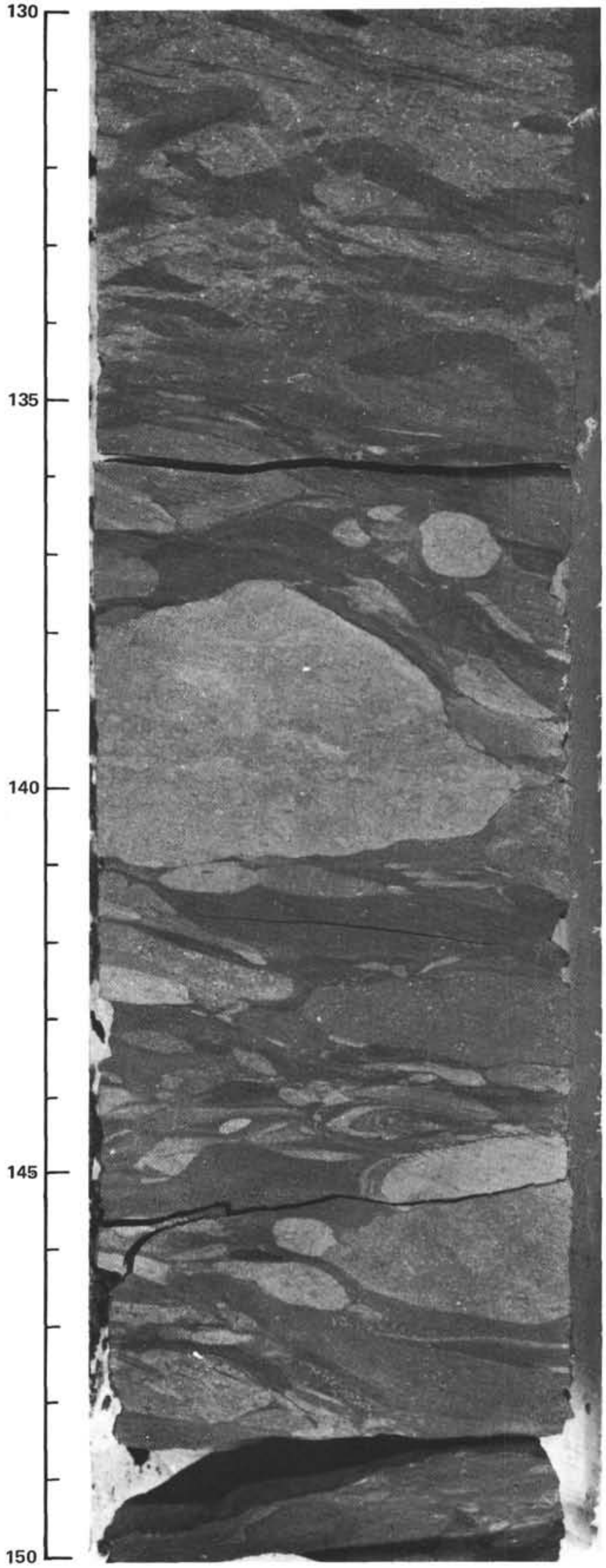

Figure 12. Flattened and deformed clasts in conglomeratic intervals of Unit V. Sample 547A-69-2, 130–150 cm.

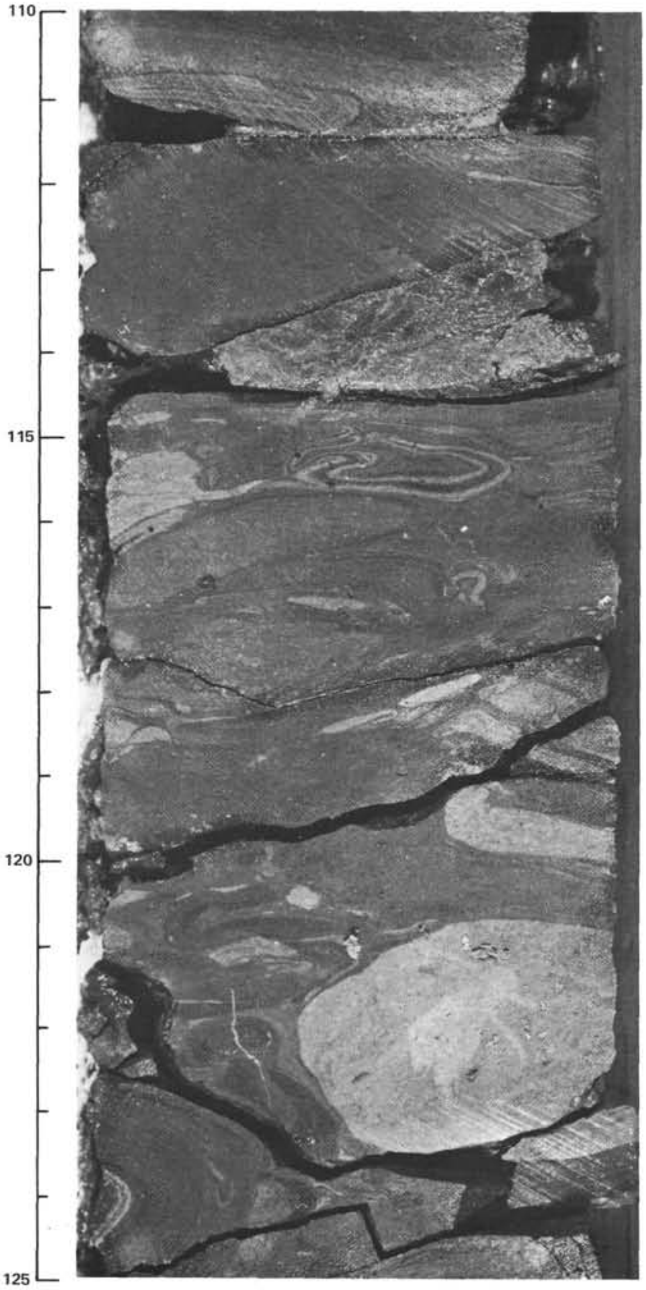

Figure 13. Slump folding and contorted bedding associated with conglomeratic intervals of Unit V. Sample 547A-68-1, 110–125 cm.

show very little deformation; other clasts and laminae are deformed around them.

The pebbly intervals are in sharp contact with sediment below and locally have diffusely laminated and burrowed intervals above them. Some distinct sedimentation units contain a lower pebble-rich bed overlain by a planar laminated interval which grades into burrowed claystone above.

Pebbly-cobbly layers compose from 2.2 to 72.4% of any core (Table 2) and average 18% of total recovered sediment. The thickness of layers ranges from 5 to 140 cm and averages 20 cm. Thickness of individual layers increases downward in the unit.

Table 2. Pebble layers in mid-Cretaceous rocks at Site 547 (Cores 39–73).

Core	Recovery (cm)	Total pebble layer thickness (cm)	% Pebbly layers	Individual layer thickness (cm)	Average thickness (cm)
39	45	0			
40	285	0			
41	245	0			
42	550	0			
43	420	0			
44	680	70	10.3	10, 10, 25, 5, 20	14
45	318	0			
46	490	0			
47	465	0			
48	300	0			
49	345	0			
50	480	0			
51	595	85	14.3	15, 10, 15, 10, 10, 10, 15	12
52	390	0			
53	341	10	2.9	10	10
54	255	0			
55	425	0			
56	600	55	9.2	10, 10, 20, 10, 5	11
57	780	70	9.0	30, 15, 5, 5, 10, 5	12
58	760	50	6.6	15, 10, 5, 20	13
59	760	65	8.6	5, 15, 5, 25, 10, 5	11
60	670	15	2.2	5, 10	8
61	580	70	12.1	15, 15, 10, 20, 10	14
62	440	20	4.5	5, 15	10
63	510	265	52.6	40, 85, 90, 5, 20, 20, 5	38
64	515	105	20.4	10, 15, 5, 75	26
65	40	0			
66	335	20	6.0	5, 15	10
67	325	0			
68	615	445	72.4	5, 80, 10, 80, 20, 40, 20, 50, 140	49
69	480	95	19.8	10, 25, 15, 10, 35	19
70	470	0			
71	240	80	33.3	40, 40	40
72	630	120	19.0	5, 35, 35, 45	30
73	575	120	20.9	50, 40, 30	40
Average			18		30

Nannofossil claystone and calcareous claystone form 82% of the recovered sediment of Unit V. The upper 37 m (Cores 39–42) are characterized by swelling claystone. (As soon as the core was split, the claystone swelled and pushed out of the liner.) The 128 m below the swelling clays (Cores 43–56) are composed of a mixture of waxy and swelling claystone. The lower interval (Cores 56-73) is dominated by waxy claystone only. XRD analysis (aboard ship) shows that 1Md illite, kaolinite, and mixed-layer smectite-illite(?) are present in the swelling claystone (Fig. 14). The waxy claystone contains only 1Md illite and kaolinite. The presence of smectite accounts for the swelling characteristics of the claystone.

Burrows within the unit are generally flattened and deformed beyond recognition. They generally cover less than 30% of the surface area of a split core and range from 1 mm to 4 cm in "diameter." Mostly simple tubes are present; minor Chondrites, Nereites, and Zoophycos are recognizable. Pyrite commonly is concentrated in burrows but also occurs as spherules and small nodules up to 5 mm across. Barite and calcite veins occur rarely throughout the section.

The percentage of carbonate in the claystone ranges from 13 to 49%, but dominantly lies between 20 and 30%. The main carbonate constituent is nannofossils with subordinate foraminifers and dolomite rhombs. In

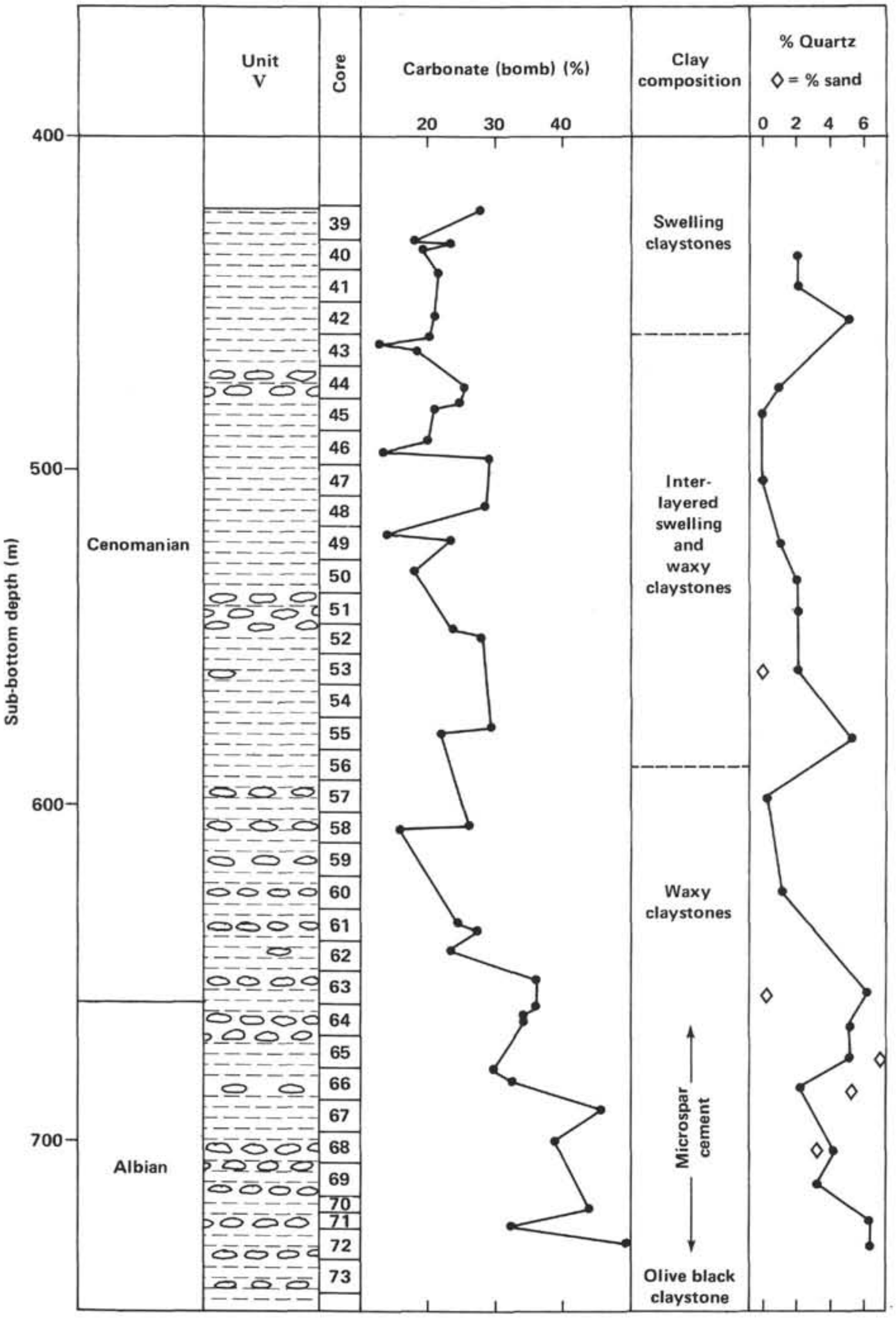

Figure 14. Components of sediments in Unit V, Hole 547A.

the lower part of the unit, carbonate is dominated by a fine microspar that formed well-indurated, calcareous, cemented claystone. In this interval the nannofossil constituent is quite variable, depending, presumably, on the state of recrystallization into microspar. In this lower interval, carbonate content increases, as does the percentage of quartz and sand. This increase in coarser clastics may have increased the permeability of the claystone and aided carbonate cementation.

Discussion: Unit V consists of terrigenous clays and subordinate pelagic biogenic particles deposited by suspension on a slope above the foraminiferal and nannofossil CCD. Abundant burrowing indicates that bottom waters were well oxygenated and supported a diverse benthic fauna. Resedimentation was common: most of the material originated from contemporaneous, partially lithified sediment, and large amounts of soft-sediment deformation resulted. A minor amount of slightly older, more lithified material was also reworked into Unit V. The abundant pebble and cobble layers with assocated slump fold indicate significant debris-flow-like deposition, with much mixing and slumping. The planar, more silty and sandy (shell fragments) layers above some pebble beds resulted from upper flow regime deposition by turbibidity currents. The dominance of clast-rich layers and the paucity of these "fine-grained" turbidite tails indicate at least two sources. The greater amount of quartz silt and sand and shell debris in the "fine-grained" turbidites suggests that they originated from higher up the continental slope where quartz was available. The pebble-cobbly layers originated from local areas, probably the slope of the basement high to the southwest (Site 544). If this is the case, the decrease in abundance and thickness of conglomeratic intervals upward in the unit suggests that the depositional slope generally decreased through time. Because the intervals are discrete and are separated by significant thicknesses of suspension sediment, initiation of the debris flows was episodic. This catastrophic resedimentation was mixed with normal sedimentation from suspension and distal turbidites from the continental slope to the east.

At Site 545, Cretaceous claystones of a similar age (Unit III) were drilled as 253 to 341 m. Although the two sites have considerably different thicknesses of strata (about 90 m for Site 545; about 320 m for Site 547), they are approximately comparable in age. Late Albian to late Cenomanian foraminifer and nannofossil assemblages were found in both sections, but because the upper contact in both units is unconformable, their differing thicknesses may be the result of either disparate sedimentation rates or erosion to different levels. Although farther seaward, Site 547 Unit V claystones contain considerably more and thicker conglomeratic intervals than Site 545 Unit III claystones.

Hole 547B

Hole 547B penetrated to 1030 m sub-bottom and achieved a core recovery of 50.6%. Wash cores were taken at depths of 211.5, 354.0, and 724.5 m sub-bottom and then, after the third reentry, at 160.5 and 803.5 m sub-bottom. At Hole 547B, continuous coring started at 724.5 m. Three units are recognized. The first overlaps with and is a continuation of Unit V of Hole 547A; it is therefore designated V. It consists of dark green calcareous claystone of Early Cretaceous age.

Unit VI is composed of a complex assemblage of limestone breccia, nodular limestone, and mudstone. Underlying this resedimented carbonate and terrigenous sequence is red and gray sandy mudstone of Unit VII.

Because the hole at 547A had a fairly large inclination (more than 12° from vertical by the downhole tool, and apparent dips in cores up to 25°), a direct correlation by depth alone is unwise. However, lithologic comparisons between holes allow a correlation that departs only slightly from the correlation by depth alone.

The last section (547A-73-4, 0–95 cm) taken in 547A contained the first occurrence of olive gray and olive black claystone. Core 1 of Hole 547B contained greenish gray claystone typical of the interval above the base of Core 547A-73. Core 547B-2 contained a 1.5 + m sequence of mudstone conglomerate in an olive gray mudstone matrix. Because conglomeratic intervals of this thickness were not present in 547A and olive gray claystone occurred only in Core 73, it seems likely that Section 547B-2-1 correlates with a interval just below Section 547A-73-4. Because Hole 547B was drilled closer to the vertical, the sub-bottom depth of 735 m is used to mark the beginning of the continuation of Unit V at the top of Core 2. The remainder of Unit V in 547B is 28.5 m thick, and the entire unit is 350.4 m thick.

Unit V (735.0–773.0 m; Core 1, top to 547B-6-1, 105 cm)

The basal 28.5 m of Unit V consists of olive gray, slightly calcareous mudstone–claystone with subordinate conglomeratic intervals like that in 547A. Mudstone is indistinctly laminated with flattened burrows. Pyrite is very common in burrows and as disseminate spherules. Downward the mudstone becomes slightly greener (grayish olive green). Nannofossils constitute from 1 to 25% but commonly less than 10%, foraminifers a trace to 1%, and total carbonate from 13 to 61%.

The conglomeratic intervals contain highly flattened and stretched clasts of mudstone–claystone identical to those of 547A. The clasts are mostly pebble- to cobble-sized. Locally (Section 547B-2-1), slump folds are associated with conglomeratic intervals. Three clasts that were not mudstone were found in Hole 547B: one was a "granite" cobble in Wash Core H3,CC and the other two were pebbles of very altered granite and calcareous feldspathic sandstone in Section 547B-2-3. The "granite" cobble is very similar to the granitic gneiss of Site 544; it contains mylonitic grain boundaries, but no obvious foliation. The altered granite clast has a major mineralogy identical to that of the granite but contains abundant calcite veins and chlorite. The third clast is a calcareous feldspathic sandstone with composite grains of feldspar and quartz and with mylonitic quartz and feldspar grains like those in the granite and altered granite.

The base of Unit V is defined at the lowest occurrence of dark greenish gray and grayish olive mudstone (547B-6-1, 105 cm). Clasts of micrite and packstone identical to those found in Unit VI occur in the lower 60 cm of the unit. The clasts range from pebble-sized to boulder-sized and are angular.

Discussion: The basal interval of Unit V contains textures and structures like those in Hole 547A (see Hole 547A report), indicating hemipelagic deposition on a slope with abundant resedimentation. The presence of the "granite" and sandstone clasts indicates some influence from outside the site of deposition. The clasts probably originated from the granitic gneiss of Site 544 or a nearby high of similar terrane. The large size of the clasts suggests that basement, weathered basement, and sandstones derived from the basement were quite close to Site 547. For such clasts to be deposited in deep marine environments so close to the source, significant relief is necessary. The basement block which was the source must have been exposed to erosion during this time and was perhaps periodically uplifted. This suggests a fault between Sites 547 and 544, forming a steep escarpment down which granitic debris was transported into a deep slope environment and mixed with hemipelagic muds and resedimented conglomerates.

Unit VI 773.0–932.5 m; (547B-6-1, 107 cm to base of Core 547B-24)

The greenish gray nannofossil-bearing claystone of the Albian Unit V is unconformably underlain by a limestone and claystone sequence 159.5 m thick (Unit VI).

The lithologic composition of the unit is highly variable, consisting of alternating beds of light gray micritic limestone, reddish and greenish nodular limestone, limestone breccia, conglomerate, calcareous shale, dark gray shale, rich in organic matter, minor quartz-sandy limestone, and microcrystalline dolomite.

We have subdivided the limestone sequence into two subunits: the upper subunit is mainly well-cemented limestone, in contrast to the lower subunit, which has intercalated calcareous shale, quartz, and sandstone intraclasts and shale rich in organic matter. The lithologic variability reflects the complex development of the limestone, which is due to its location on the flank of the outer basement high, in the front of the Mazagan Escarpment. Thus mixing because of downhill transport from both the Mazagan Plateau and the outer basement high influenced deposition at this location.

Subunit VIA (773.0–838.9 m; 547B-6-1, 107 cm to 547B-14-2, 37 cm)

Subunit VIA is a light gray micritic limestone with incipient nodular texture in the upper part and well-developed nodular texture and multiple limestone breccias in the lower part. Nodular limestone in Core 8 is reddish brown and greenish gray, with micritic nodules that are up to 3 cm in size and are enveloped by an argillaceous micritic matrix. Both limestones contain well-developed stylolites.

Three types of allochthonous carbonates occur within the micritic limestone: (1) limestone breccia, (2) limestone conglomerate, and (3) skeletal grainstone. The limestone breccia forms 20–30-cm-thick beds composed of limestone clasts several millimeters to 15 cm in size. Clasts are mostly unsorted, except in one bed (547B-7-2, 110–125 cm), which shows grading. The breccia is both clast- and micritic-matrix-supported. The conglomeratic beds are composed of reddish and greenish biomicrite and peloid grainstone, cemented by sparry calcite. The grainstone beds are least common and are composed of sand-sized microclasts of micrite, peloid grainstone, coated grains, oolites, and skeletal debris, all cemented by sparry calcite.

The faunal remains in the micritic limestone and possibly in the matrix of the breccia beds are ammonities, aptychi, *Saccocoma*, calpionellids, radiolarians, short filaments, and foraminifers. Fauna in the clasts are calpionellids, *Tubiphytes,* with shells of *Bositra*, which is also concentrated on several bands of lumachella in Section 547B-8-3. The micritic limestone is locally bioturbated and partially dolomitized near the upper boundary of the subunit. A bed of greenish calcareous claystone is present in the first core near the top of the subunit.

Below the nodular limestone, multiple limestone breccia beds and minor beds of reddish brown and pale green (10G 6/2) nodular limestone are present. (A crinkle-laminated crust occurs at 547B-8-3, 145 cm.)

The breccia beds, which are 20–40 m thick, are composed of mainly greenish limestone clasts deposited in a light brownish micrite matrix. The breccia is clast-supported, with clasts angular and subangular in shape. Three clast sizes can be recognized: (1) 10 to 18 cm, (2) 2 to 4 cm, and (3) sand-sized particles. The clasts are composed of a light gray grainstone with coated grains, oncolites, ooids, coated *Bositra* fragments, crinoids, sponge spicules, crust fragments, thick-walled mollusk fragments, ammonites, and annelids. The matrix of the breccia is pale yellowish brown micrite and silt-sized, pelleted packstone, with minor fossil debris, composed, for instance, of pentacrinoids, *Tubiphytes*, and foraminifers. The breccia beds are separated from each other by layers of micritic crust, 1–4 cm thick.

Geopetal fabric in the breccia beds, with several stages of void filling, is quite common. Commonly, voids geopetally filled with multilayered internal sediment separate the crust from the underlying limestone intraclasts (Fig. 15). Thus, the micritic crusts separate individual breccia beds.

A 2-m thickness of greenish and reddish brown nodular limestone occurs in Sections 547B-10-3 and 547B-10-4. The nodules of dense biomicrite and micrite are 1 cm across and scattered throughout highly calcareous claystone matrix. Slightly nodular bands up to 4 cm in thickness enclose smaller nodules. Some nodules may be reworked, but mostly the nodular limestone in *in situ*.

Clastic influence increases downward from Section 547B-10-1 as the amount of quartz silt and sand, silty calcareous claystone, reddish-colored, quartz-silty, calcareous shale, and coarse-grained fragments of grayish red feldspathic sandstone increase. From Core 11 downward, the breccia clasts become coarser and more angular. Pink micrite, pelleted packstone, and skeletal wackestone for the majority of the clasts, which have an average size of 4 cm. Pyrite and stylolites are common, as is microfracturing.

The lower boundary of Subunit VIB is placed at the top of a layer of dark gray calcareous shale.

Subunit VIB (838.9 to 932.5 m; 547B-14-2, 37 cm to 547B-24, base)

More than half (13.6 m; 52.2%) of the recovered section (26.1 m; 30.2%) from the more argillaceous lower division of Unit VI consists of nodular and incipiently nodular micrite in a clay–claystone or mud–mudstone matrix. A further quarter (25.6%) of the division consists of oligomictic gravel conglomerate in which micrite is by far the dominant phenoclast type. Thinly laminated and variably calcareous claystone is medially common; peloid boundstones and dark-colored, organic-matter-rich shales, though subordinate, are important for interpretation of the unit.

Pale red (10R 6/2) or pale yellowish brown (10YR 6/2) micrite in a darker yellowish brown (about 10YR 4/2) matrix forms nearly 75% of the major facies. Pale red nodules in a pale brown (5YR 5/2) or moderate brown (5YR 4/4) matrix are also common, whereas light olive gray (5Y 5/2) or even grayish olive (10Y 4/2) matrices are rare. The nodules vary between 0.1 and 2 cm in diameter (measured normal to bedding), averaging 0.6 cm; they have a compact to platy form. In thin section they commonly display a relict peloidal texture. All gradations occur, from massive micrite, through micrite with clay wisps or seams which fail to delimit separate nod-

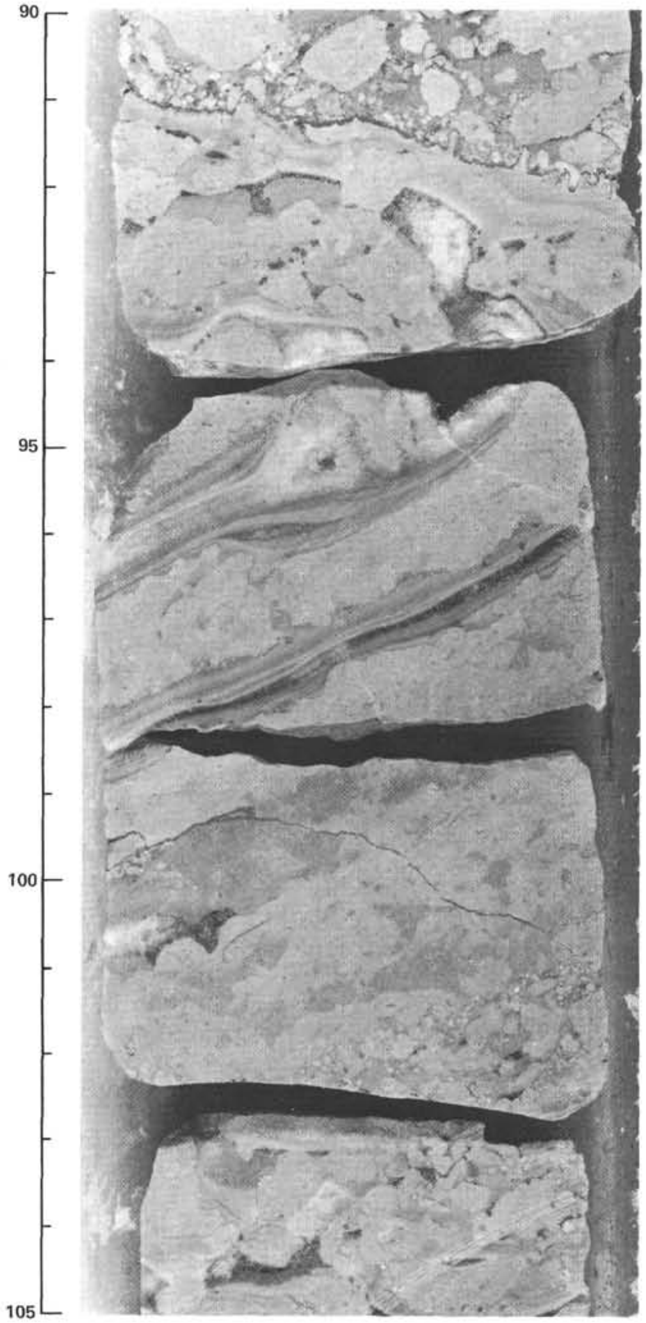

Figure 15. Void-filling interval sediment between breccia layers. Sample 547B-11-1, 90–105 cm.

ules, to micrite nodules "floating" in a clay or mud matrix (Fig. 16). Two phases of nodule formation can in places be recognized: several sharply defined nodules, the size of small pebbles, are enveloped within larger, clayey micrite "nodules" which have a more gradational boundary with the surrounding matrix. Discrete nodules can locally be demonstrated *in situ* by dark-colored burrows which pass from matrix through nodule, but in some sections the *in situ* fabric has clearly been disrupted. Though the nodules appear to have undergone sedimentary reworking into monomictic conglomerates, and some disturbance may have been by bioturbation, the

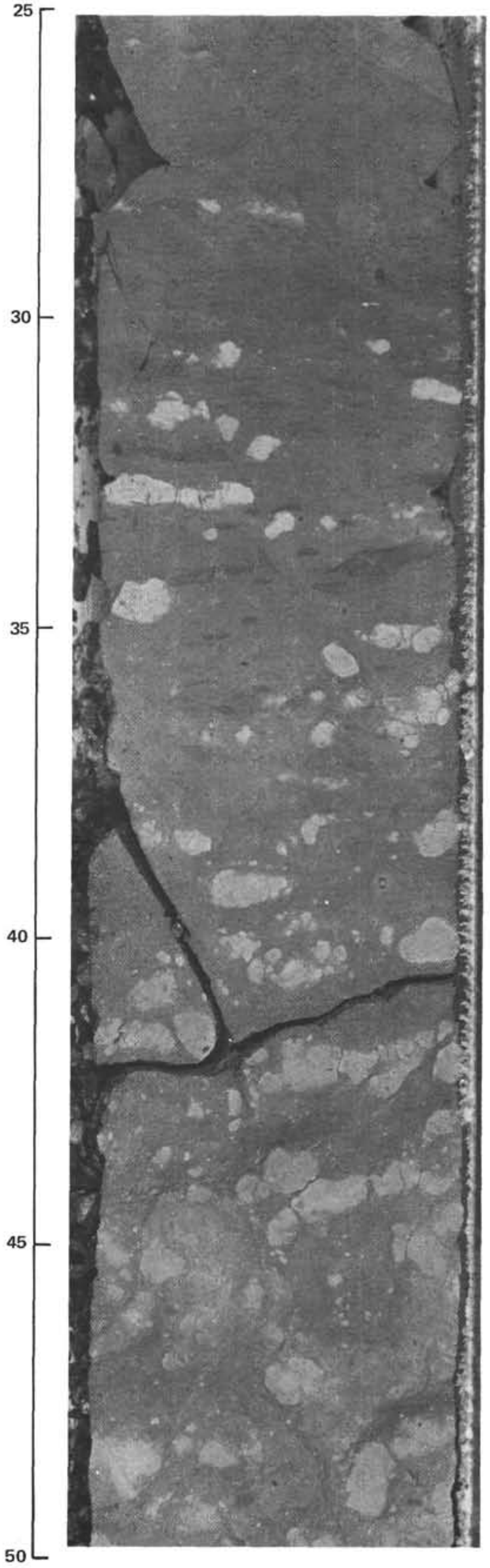

Figure 16. Micritic nodules floating in mud matrix. Sample 547B-15-2, 25-50 cm.

major causes of the disruption are probably compaction and possibly tectonism (Fig. 17). The entire subunit exhibits intense microfaulting and parts are strongly deformed. Many clay seams in the micrite-dominated intervals are stylolitic.

Some 65% of the oligomicitic gravel conglomerate facies has a dark greenish-gray (5GY 4/1) clay or mud matrix; olive gray (5Y 4/1) or light olive gray (5Y 6/1) matrices are also common; grayish olive green (5GY 3/2), grayish green (10G 4/2), and yellow brown colors are rare. Light olive gray and medium gray (N5) calcite-cemented lithologies occur in Cores 21 and 24. Most of this facies is phenoclast-supported, though matrix-supported intervals occur; the gravel is granule-sized to large-pebble-sized, with an estimated mean diameter in the small-pebble category (about -3 ϕ). Compact to platy, subangular to well-rounded micrite phenoclasts are overwhelmingly dominant, some have a relict peloidal texture—undoubtedly derived from the nodular micrite and clay facies. Platy clasts of a variety of laminites also occur in the lower part of the subunit; an olive brown or dark yellowish brown (10YR 4/2) microsparite laminite containing quartz sand layers is conspicuous. Olive gray (5Y 3/2) mudstone pebbles are common in the higher part of Subunit VIB and single phenoclasts encountered include a peloid grainstone containing a chert rich in bivalves and a grayish red (5R 4/2) sandy mudstone (in Core 14) resembling that of Unit VII.

Discussion: The repetition of breccia intervals and micrite crusts has a definite cyclicity. The poor sorting and open framework of the breccia beds resulted from deposition by debris flows containing very little fine-grained sediment. Possibly the fine sediments were transported farther toward the basin. The fine-grained limestone turbidite sequences occurring in the basin farther from the Moroccan coast (Leg 50, Site 416) may be the distal counterparts of the coarse, proximal debris flows of Site 547. Limestones at Site 544, which was drilled on the top of the structural block which extends through Site 547, are very similar to clasts in Subunit VIA, indicating that some of Subunit VIA is younger than or about the same age as the limestones at Site 544. Unfortunately, the limestones at Site 544 are also not reliably dated. In contrast to Site 544, the limestones which overlie the red beds (Unit VII) at Site 547 are low-energy carbonates, mainly micrites, with a stromatolitic(?) bed near the base, which is overlain by limestone breccias, conglomerates, and nodular limestones. The presence of breccia beds near the base of the limestone sequence suggests that the basement subsided very rapidly. The occurrence of radiolarians down almost to the contact with the red beds is also best explained by such subsidence, associated with the rapid establishment of "deep" water conditions. The organic-matter-rich shales present in the lower half of the sequence may represent periods of restriction or slower circulation in a localized depression. The increase in clastics in the upper part of the unit suggests a terrigenous source (red beds and basement). The dominance of micritic clasts in the breccia beds indicates that the clasts were derived from erosion of the deeper part of the carbonate slope or reworked from the *in situ* nodular limestone.

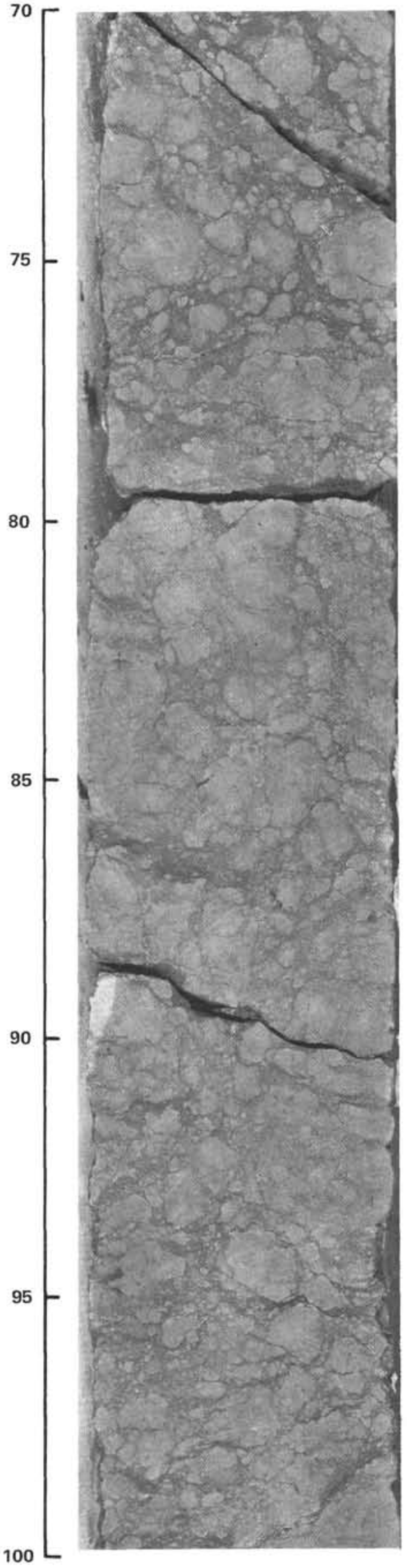

Figure 17. Disrupted nodules. Sample 547B-17-1, 70–100 cm.

The depositional conditions became pelagic during the sedimentation of Subunit VIA, when micritic limestones with calpionellids were deposited. The occurrence of intraclasts with calpionellids and high-energy, shallow-water, carbonate grains in turbidites indicates that depositional conditions were pelagic (nodular limestone and claystone), and that sedimentation was modified by transport of carbonates by turbidity currents and debris flows from the shallow, high-energy Mazagan Plateau shelf area and local highs. Some clasts were probably derived from the slope and top of the basement high at Site 544.

Unit VII (923.5–1030.0 m; Cores 25 to 36)

Beneath the complex lithologies of Unit VI lie 97.5 m of grayish red and gray gypsum-bearing calcareous sandy mudstones to calcareous sandy mudstone. Alternating intervals of red and gray, from 10 cm to 2 m thick, are separated by and contain mottled zones in the upper part of the unit (above Section 547B-31-2). Patches of color mottling occur throughout these major color alternations. Below, the unit is dominantly grayish red. The gray coloration probably results from reduction of hematite-stained mudstone during diagenesis because of the percentage of organic matter. It is common along microfractures and veins of dolomite and gypsum.

Very fine to very coarse sand is scattered throughout the mudstone and also concentrated in irregular patches and stringers with diffuse laminae and in layers 2–4 cm thick. Sand content is dominantly 5–10%, except in sandier intervals where it ranges up to 40%. Quartz and feldspar dominate the sand fraction; mica and heavy minerals are subordinate. Minor granules of composite quartz and feldspar occur locally. Sand is angular to subrounded.

Granules are more common downward in the unit, as in the presence of sandier intervals that range from 1 to 25 cm thick but are dominantly 2–5 cm thick. Coarse to granule-sized grains are concentrated in these intervals and are only rarely scattered throughout the mudstone. In Core 36, however, abundant dolomite, dolomitic limestone, and sandstone granules and pebbles are very abundant. Below Core 25, "clasts" of gypsiferous mudstone and muddy dolomite are present. These range from 2 mm to 3 cm across, generally increase in size downward, are rounded to subrounded, and are identical to the surrounding rock. Most are compact and irregularly shaped, showing little evidence of transport. A small number have been flattened and elongated during compaction. All these characteristics suggest that these "clasts" are nodules formed in the surrounding mudstone. Some clast-bearing intervals also contain minor contorted layers.

The sandy mudstone is almost completely structureless. Local indistinct mottling and irregular stringers of sand may have resulted from bioturbation and/or water escape during compaction. Sand-free mudstone does occur in the unit but forms less than 1% of the entire section. Sand content generally increases from the top downward; variation in the amount of coarse grains is common.

Spongy, webby masses of dolomite are common throughout the sandy mudstone. These masses are concentrated in zones from 2 to 20 cm thick, where they form a gray mottling. Small gypsum veins 2 mm to 2 cm thick and patches and isolated crystals of gypsum are common within the dolomite masses, especially in sandier intervals.

The lower contact of Unit VII was not reached at Site 547. The base is placed at the lowest recovered interval of sandy mudstone at 1030.0 m. The top of the unit is placed below the last occurrence of limestone breccia of Unit VI (top of Core 25). Above this a minor amount of red and gray sandy mudstone is interlayered with gray claystone and dolomite breccia.

Discussion: The sandy mudstone of Unit VII was deposited in a continental environment dominated by a granitic source terrane. Deposition was very rapid, resulting in poor sorting, massive structure, and very little concentration of sand in distinct layers. Gypsum and carbonate precipitated in the sand muds as they lithified, suggesting that somewhat arid conditions existed. The large percentage of fresh feldspar and granite clasts suggests that weathering of the source rock was minimal.

Deposition was probably dominated by mud flow and high-gradient, braided-flow complexes—essentially distal fan deltas or alluvial fans. Mud clasts were commonly ripped up and redeposited by fairly strong currents. At least one channel drained a complex source terrane, leading to the formation of the granule intervals found in Core 36.

BIOSTRATIGRAPHY

Biostratigraphic Summary

Neogene

Foraminifers and calcareous nannofossils are abundant and well preserved in the 204-m-thick Neogene section of Hole 547A (Unit I and Subunit IIA). Radiolarians are rare in the uppermost 141 m of the sequence. The Neogene extends from Core 1 through 547A-15-1, 130 cm.

Nearly 90 m of Pleistocene-age sediment were drilled at Hole 547A (Cores 1 and 2). The Pliocene section, however, is less than 20 m thick. A late Pliocene age was determined for the upper part of Core 3 using nannofossils. In Sample 547A-3,CC an early to middle Pliocene age is indicated by foraminiferal and nannofossil evidence. Core 4 is also of early to middle Pliocene age according to the foraminiferal evidence, but nannofossils suggest a latest Miocene age.

Cores 5 through 8 represent the late Miocene. A lithologic boundary between Unit I and Subunit IIA at 547A-8-4, 7 cm corresponds to a short diastem in the early late Miocene (N16) that is inferred from nannofossil and foraminiferal evidence. Middle Miocene sediments extend down to 547A-14-4, 14 cm, where there is an obvious hiatus between the foraminiferal middle Miocene (N9–N11) and the early Miocene (N4–N6). The nannofossils do not indicate such a break.

Paleogene and Late Cretaceous

The Paleogene and Late Cretaceous sequence of Hole 547A is characterized by periods of episodic debris flows and hemipelagic deposition which correspond with Units IIB, III, IVA, and IVB. The biostratigraphy of these lithologic units is here discussed in stratigraphic order.

Subunit IVB extends from 547A-39-1, 105 cm to the base of Core 31. This interval is characterized by common debris flows. The microfauna and flora indicate a Late Cretaecous age for most of the succession; the Cretaceous/Tertiary boundary occurs in the lower sediments of Core 32. Cores 33 and 34 are late to middle Maestrichtian in age, Cores 35 through 38 are early Maestrichtian to middle Campanian.

Subunit IVA lacks the debris flows of IVB. It also lacks any significant amount of reworked microfossils. In Cores 31 through 23, the progressive deposition of hemipelagic lower Paleocene (P1) through lower Eocene-upper Paleocene (P5-P6) sediments is indicated by foraminifers and nannofossils and supported by radiolarian evidence. The lithologic boundary between Units III and IVA is placed between Cores 22 and 23. Microfossil evidence yields a late Eocene age for Core 22, suggesting that this interval is in fact reworked sediments from Unit IVA incorporated into the base of debris-flow Unit III.

A late Eocene age is assigned to the sediments of Unit III (Core 22 through 547A-17-3, 71 cm). This sequence contains an array of redeposited clast types ranging in age from middle Cretaceous through Eocene. Reworked foraminifers, nannofossils, and radiolarians are common in the matrix also.

Subunit IIB (547A-17-3, 71 cm through 547A-15-1, 130 cm) is again a hemipelagic deposit containing little to no reworked older microfossils. A middle Oligocene-late Eocene age is indicated.

Middle Cretaceous

A thick succession of Cenomanian and upper Albian sediments was cored at Site 547 (Unit V). The 350-m-thick sequence extends from 547A-39-1, 105 cm through 547B-6-1, 53 cm. Foraminifers are abundant and well preserved. Four zones are represented: middle to late Cenomanian *Rotalipora cushmani* Zone, early Cenomanian *R. gandolfii* Zone, and late Albian *Planomalina buxtorfi* and *Ticinella breggiensis* zones. The boundaries of these zones, including the Cenomanian/Albian boundary, are not clearly defined. There may be repeated assemblages near zonal transitions. There is much redeposition within the section, which probably accounts for its great thickness. Nannofossils and radiolarians found throughout the section also support the Cenomanian and late Albian age assignment.

Dark olive-colored clasts contained within a breccia at the base of Unit V (Sample 547B-6-1, 53-84 cm) yielded an early to middle Albian age based on foraminifer and nannofossil evidence. Below this (near the base of Section 547B-6-1) is a claystone for which foraminifers and nannofossils indicate a Valanginian-middle Hauterivian age.

Neocomian and Jurassic

Limestones with clay interbeds extend from 547B-6-1, 107 cm through 547B-24. Calpionellids in the limestones of Sections 547B-6-2 through 547B-6-4 indicate an early Berriasian-late Tithonian age. Punctaptychus punctatus, an aptychus from Sample 547B-6-3, 142-143 cm, suggests a Tithonian age (Renz, this volume). Lamellaptychus sparcilamellosus, an aptychus found in Sample 547B-7-3, 69 cm, is typical for a Kimmeridgian age. Also sporadically occurring in the limestones of Cores 6 through 10 are *Saccocoma*, protoglobigerinids, pelagic bivalves, ammonite fragments, and other aptychi. These fossils are generally long-ranging and suggestive of a middle to Late Jurassic age.

The claystone interbeds contain sparse foraminifer, ostracode, and nannofossil assemblages. In 547B-6-2 through 547B-14-2, 37 cm (Subunit VIA), the sediments are generally barren of calcareous nannofossils, or where they are present they are heavily overgrown. Rare to few benthic foraminifers in the lower clays of Core 7 suggest a Kimmeridgian age; those from Core 10 indicate a Bajocian to Callovian age. Late Pliensbachian-(?early Toarcian) foraminifers in 547B-11,CC are associated with limestone breccias and thus may be reworked. Nannofossils and foraminifers support a Pliensbachian age for Cores 12 through 18; Cores 18-20 may be early Pliensbachian or late Sinemurian in age. Cores 21-23 are Sinemurian and Core 24 late Hettangian or early Sinemurian. Palynomorphs recovered from the underlying beds indicate an early Sinemurian-late Hettangian age for the lower part of Core 24 and a Hettangian-?Rhaetian age for Core 25 (Fenton, this volume).

Nannofossils

At Site 547, Hole 547 consists of one core from the upper sediment. Hole 547A has discontinuous coring for the first 79.5 m: Core 1 was obtained from a depth of 51.0 to 60.5 m, Core 2 at 79.5 m, where continuous coring was resumed. Hole 547B is a reentry hole with continuous coring. Most cores are described from core-catcher (CC) samples unless the catcher was believed to be contaminated or obvious age breaks are noted from the core-catcher sample; in these cases, samples were taken from within the core in addition to the core catcher.

The sediments of Hole 547-1,CC are of Pleistocene age. Further investigation by scanning electron microscope is needed to accurately determine the late Pleistocene marker *Emiliania huxleyi*. A representative assemblage is *Calcidiscus macintyrei, Gephyrocapsa oceanica, G. caribbeanica, G.* spp., and *Discolithina viginitiforata; C. macintyrei* is considered reworked from early Pleistocene sediments.

Hole 547A

The nannofossils of Core 1 are late Pleistocene in age and are placed within the *Emiliania huxleyi* Zone (NN21) (Gartner, 1977). A characteristic assemblage of Core 1 is *Calcidiscus macintyrei* (considered reworked), *Pseudoemiliania lacunosa, Disolithina viginitiforata, Gephyrocapsa oceanica*, and *G. caribbeanica*. In Core 2, of

Pleistocene age, further investigation by scanning electron microscope is necessary to determine the presence or absence of *E. huxleyi*. Nannofossils in all the Pleistocene cores are common in abundance and show moderate to good preservation.

Section 547A-3-1, 0 to 20 cm is placed within the *Discoaster brouweri* Zone, *D. tamalis* Subzone (bottom half of NN16) (Okada and Bukry, 1980); this is of late Pliocene age. The interval from 547A-3-1, 55 cm to 547A-3,CC is of mid to early Pliocene age; this interval cannot be zoned. A typical assemblage of the Pliocene includes *D. broweri, D surculus, D. tamalis, D. variabilis, and C. macintyrei*. Nannofossils are few to common in abundance and preservation is moderate to good in Core 3. The latest Pliocene is missing in core 3; this may be due to poor recovery between Cores 2 and 3 or to a hiatus.

The calcareous nannofossils of Core 4 are placed within the *Amaurolithus tricorniculatus* Zone, *Triquetrorhabdulus rugosus* Subzone of latest Miocene age. The interval from Core 5 through 547A-8-2, 24 cm is of late Miocene age; the *D. quinqueramus* Zone (NN11) (Okada and Bukry, 1980) is the only zone resolvable. Nannofossils are few to common in abundance and preservation is moderate to good. A representative assemblage of these intervals contains *A. primus, T. rugosus, D. brouweri, D. variabilis, C. macintyrei*, and *Reticulofenestra pseuodoumbilica*.

The interval from 547A-8-4, 129–130 cm through 547A-9-3, 120–121 cm is placed within the *D. hamatus* Zone (NN9) (Okada and Bukry, 1980) of early late to late middle Miocene age. *D. hamatus, C. macintyrei, R. pseudoumbilica, T. rugosus*, and *D. variabilis* are representative of this assemblage; preservation is moderate to good, nannofossils are common in abundance.

The interval from 547A-9,CC through 547A-11,CC contains nannofossils of middle Miocene age (NN7–NN8) but cannot be zoned more precisely because marker fossils are missing. A common assemblage contains *T. rugosus, C. macintyrei, Coccosphaera leptopora, R. pseudoumbilica*, and *D. variabilis*; nannofossils are common and preservation is moderate to good.

The nannofossil assemblage of 547A-12,CC through 547A-14,CC is of early middle Miocene age but cannot be placed within a specific zone. *Calcidiscus macintyrei, Cyclicargolithus floridanus, D. deflandrei*, and *R. pseudoumbilica* are typical of this interval; nannofossils are common and preservation is poor to moderate.

The interval from 547A-15-1, 60–61 cm through 547A-15-1, 110–111 cm is early Miocene in age, though no zones can be resolved. Sample 547A-15-2, 60–61 cm is of middle Oligocene age (top half of NP23–NP24), as defined by the presence of *Sphenolithus distentus. Calcidiscus macintyrei, Cyclicargolithus abisectus, Dictyococcites bisectus, C. floridanus, Discoaster deflandrei*, and *S. predistentus* are representative of the "Oligocene" assemblages. Sample 547A-15,CC cannot be placed within a zone, but appears to be Oligocene in age. The assemblage is similar to that above; preservation is moderate to good and nannofossils are common in abundance.

The interval from 547A-16-1, 50–51 cm through 547A-17-1, 50–51 cm is tentatively placed within the *Helicosphaera reticulata* Zone (NP21–NP22) (Okada and Bukry, 1980) of early Oligocene age. The assemblage contains, among others, *Reticulofenestra umbilica, Isthmolithus recurvus, C. floridanus, Coccolithus formosus, D. tani nodifier*, and *S. predistentus*. Nannofossils are few to common and preservation is moderate to good.

The interval from 547A-17-2, 50–51 cm through 547A-17-3, 64–65 cm appears to be latest Eocene or earliest Oligocene. The assemblage in 547A-17-4, 100 cm through 547A-22-2, 90–91 cm is placed within either the *D. barbadiensis* Zone (NP18–NP20) or *R. umbilica* Zone (NP16–NP17) (Okada and Bukry, 1980) of late Eocene age. This interval is deposited in a debris flow; the youngest of the nannofossils are *R. umbilica, Dictyococcites bisectus, C. formosus*, and *Cyclicargolithus floridanus*, and from these the age was determined. There is much reworking: nannofossils of the early mid-Eocene, Paleocene, and Late Cretaceous are found within the assemblage. Preservation is poor to moderate with this interval.

The interval from 547A-23-1, 19–20 cm through 547A-25-3, 49–50 cm does not appear to be in a debris flow, and the amount of reworking is small. The interval consists of a good Paleocene assemblage with *Discoaster multiradiatus, D. mohleri, Fasciculithus tympaniformis*, and *Heliolithus kleinpellii*. However, *C. formosus*, an Eocene form, appears in Cores 23 and 25, thus this interval cannot be excluded. Nannofossils are common and preservation is moderate to good.

Sample 547A-26-1, 4 cm is placed within the *Discoaster mohleri* Zone (NP7–NP8) (Okada and Bukry, 1980) of late Paleocene age; Sample 547A-26-1, 40 cm is assigned to the *H. kleinpellii* Zone (NP6) (Okada and Bukry, 1980). *F. tympaniformis, Cruciplacolithus tenuis, Prinsius bisulcus*, and *Heliorthus concinnus* are common to both assemblages, though *D. mohleri* is included within the upper interval. The age boundary corresponds with a lithology break.

The interval from 547A-27-1, 60 cm through 547A-30-3, 69 cm is of middle Paleocene age, with an assemblage containing *F. tympaniformis, Chiasmolithus bidens, C. danicus, Cruciplacolithus tenuis*, and *C. primus*. Dissolution appears to be prevalent in this assemblage.

The interval from 547A-31-1, 46 cm through 547A-32-4, 30 cm is tentatively placed in the *Zygodiscus sigmoides* Zone, *C. tenuis* Subzone (NP2) (Okada and Bukry, 1980); because nannofossils are poorly preserved and rare to few in abundance, there is some question about the exact age. The assemblage within this interval is *C. tenuis, C. primus, Markalius astroporus*, and *Chiasmolithus* spp. (Sample 547A-33-1, 86–87 cm is placed in the *Micula mura* biohorizon of latest Maestrichtian age [Thierstein, 1976].)

The interval from 547A-33-4, 86–87 cm through 547A-34-6, 69–68 cm is dated by the *Lithraphidites quadratus* biohorizon of Thierstein (1976), which is of mid to late Maestrichtian age. A representative sample of the assemblage is *L. quadratus, Tetralithus aculeus, Eiffellithus eximus, E. turriseiffeli*, and *M. staurophora*; preservation is moderate and nannofossils are common.

The interval from 547A-35-1, 67–68 cm through 547A-36-3, 67–68 cm is placed within the *Tetralithus trifidus* total range Zone of Thierstein (1976); it is of mid-Campanian to early Maestrichtian age. The assemblage is essentially the same as above, with the exclusion of *L. quadratus* and the inclusion of *T. trifidus* and *T. gothicus*.

The interval from 547A-37-1, 65–66 cm through 547A-39-1, 10–11 cm is placed within the *T. aculeus* biohorizon (Thierstein, 1976); it is mid-Campanian to early Maestrichtian in age. *T. aculeus, T. gothicus, M. staurophora, E. eximus, E. turriseiffeli*, and *Microrhabdulus decoratus* are typical of the assemblage in this interval; nannofossils are common in abundance and preservation is moderate to good.

The interval from 547A-40-1, 70–71 cm through 547A-62,CC contains a nannofossil assemblage placed within the *Lithraphidites alatus* biohorizon (Thierstein, 1976) of Cenomanian age. The assemblage is similar to the one above except for the addition of *L. alatus*.

The biohorizon defined by the base of *Eiffellithus turriseiffeli* (Thierstein, 1976) is that which is used in 547A-63,CC through 547B-6-1, 39–40 cm to date the interval. The assemblage is of late Albian age and includes such forms as *E. turriseiffelli, stephanolithion laffittei, Vagalapilla stradneri, Cretarhabdus angustiforatus, Parhabdolithus asper*, and *Transolithus orionatus*. Preservation ranges from poor to good; nannofossils are few to common in abundance. Cores 547A-72 and 547A-73 overlap with Section 547B-1-3; all are late Albian in age.

Hole 547B

Within Section 547B-6-1 there are some apparent clasts of early to middle Albian age; these clasts contain essentially the same forms as do upper Albian sediments except for *E. turriseiffeli*.

The interval from 547B-6-1, 106 cm to 547B-6-1, 139–140 cm, considered *in situ* between limestone beds, appears to be Valanginian to mid-Hauterivian in age. This age range is defined by the top of *Cruciellipsis cuvillieri* and the bottom of *Calcicalathina oblongata* (Thierstein. 1976).

As limestone beds became prominent, only bands of claystone and clay were sampled. The nannofossils in the interval from 547B-6-4, 47–48 cm to 547B-7-3, 135–137 cm are Tithonian to Kimmeridgian in age. A representative assemblage consist of *Watznaueria* spp., *Cyclagelosphaera deflandrei*, and *C. margareli*; nannofossils are few and preservation is moderate.

The interval from 547B-15-1, 2–4 cm through 547B-18-1, 103–104 cm is early Pliensbachian in age (Hamilton, 1979). A typical sample consists of *Calyculus* spp., *Tubirhabtus patulus, Crepidolithus crucifer, C.* spp., *Parhabdolithus liasicus, Schizosphaerella punctulata, Zygodiscus erectus, Staurorhabdus quadriarculla*, and *Crucirhabdus primulus*; nannofossils are common to few in abundance, and preservation is moderate to good. Abundance in 547B-19-1, 71–72 cm is low and the age of the sample is therefore indeterminate; the sample is no younger than early Pliensbachian.

The interval from 547B-20-1, 126–127 cm through 547B-22-1, 33–36 cm is Sinemurian in age (Hamilton, 1979). The assemblage is similar to the cores above except for the inclusion of *P. marthae*; nannofossils are few to common in abundance and preservation is moderate.

All samples taken below 547B-22-1, 33–36 cm are barren of nannofossils.

Cenozoic and Mesozoic Foraminifers

Hole 547A

Neogene

Abundant and well-preserved foraminifers were recovered from the 204-m-thick Neogene section at Hole 547A (Units I and IIA). Two diastems are recognized within the sequence, one within the early late Miocene and the other between the middle and early Miocene. Foraminiferal zonations for the Cenozoic are after Stainforth et al., (1975).

Core-catcher samples from Cores 547A-1 and 547A-2 comprise the Pleistocene (N22–N23) *Globorotalia truncatulinoides* Zone. Characteristic planktonic species include *Globorotalia truncatulinoides, G. crassiformis, G. inflata, G. scitula, Globigerina bulloides, G. quinqueloba, G. glutinata, G. falconensis, Globigerinoides ruber, G. conglobatus, G. trilobus, Orbulina universa*, and *Neogloboquadrina pachyderma*. The Quaternary section is roughly 90 m thick at this site.

Cores 547A-3 and 547A-4 represent the early to middle Pliocene (N18–N19) *Globorotalia margaritae* Zone, characterized by the presence of *G. margaritae, G. plesiotumida, G. acostaensis, Globigerina nepenthes, Globoquadrina altispira, Globigerinoides trilobus, O. universa*, and *Sphaeroidinellopsis paenedehiscens*.

The late Miocene (N17) *Globorotalia acostaensis* Zone extends from Core 5 through 547A-7,CC. Common planktonics include *G. acostaensis, G. juanai, G. plesiotumida, Globigerinoides trilobus, Globigerina nepenthes, Globoquadrina altispira, S. subdehiscens*, and *O. universa*.

The specimens of *Globorotalia acostaensis* are dominantly sinistrally coiled in Sample 547A-7,CC, implying a pre-Messinian age (probably late Tortonian). A late Miocene–middle Miocene age (N15) is represented by the *Globorotalia menardii* Zone in Sample 547A-8,CC. A short hiatus is inferred for the early late Miocene (N16). Common foraminifers in 547A-8,CC include *G. menardii, G.* cf. *praemenardii, G. lenguaensis, Globigerinoides trilobus, Globigerina nepenthes, S. seminulina*, and *O. universa*.

The middle Miocene (N9–N15) is represented by the *Globorotalia siakensis* Zone and a series of short-duration zones of the *G. fohsi* group. Characteristic species include *G. siakensis, G. praemenardii, G. fohsi* group, *Globigerinoides trilobus, Globoquadrina dehiscens, G. altispira, S. seminulina*, and *O. universa*.

A color change in Sample 547A-14-4, 14 cm may represent the hiatus between the middle Miocene (N9–N11) and early Miocene (N4–N6). Common planktonics in 547A-14,CC include *Catapsydrax unicavus, C. dissimilis, Globigerina venezuelana, Globigerinoides trilobus*, and *Globoquadrina dehiscens*. A lithology break at 547A-15-1, 130 cm represents the Neogene/Paleogene boundary.

Paleogene

At least 151 m of Paleogene sediments were cored in Hole 547A. The interval from Core 15 through 547A-17-3, 71 cm is assigned a middle Oligocene–late Eocene age (Unit IIB). Foraminiferal assemblages are moderately to well preserved and few to common in abundance, but have a low diversity. Characteristic planktonic species encountered include *Catapsydrax dissimilis, C. unicavus, Globorotalia opima nana, Globigerina venezuelana*, and *G. angiporoides*.

Unit III extends to the base of Core 22. It is a complicated slope deposit containing an array of redeposited clast types ranging in age from middle Cretaceous through Eocene. The matrix, too, contains abundant reworked Late Cretaceous, Paleocene, and Eocene foraminifers. This unit is tentatively assigned an early Oligocene–late Eocene age, based on the following recurrent planktonic species: *C. unicavus, C. dissimilis, Globigerinatheka* cf. *index, Globorotalia increbescens, G.* cf. *pentacamerata, Globigerina linaperta, G. venezuelana, G. ampliapertura, G.* cf. *eocaena, G. angiporoides, Pseudohastigerina micra*, and *Chiloguembelina cubensis*.

Older Paleogene planktonics mixed with the "autochthonous" assemblages include *Globorotalia subbotinae, G.* cf. *aragonensis, G.* cf. *angulata, G.* cf. *conicotruncana, Globigerina primitiva*, and *G. soldadoensis*. Late Cretaceous species present include *Globotruncana angusticarinata, G. primitiva, G. renzi, G. coronata, G. fornicata, G. arca, G. sigali, G. stuartiformis, G. mayaroensis, Rugoglobigerina rugosa, R. scotti*, and *Heterohelix* spp. These represent a wide range in ages from the Maestrichtian to Coniacian. Rare specimens of *Rotalipora appenninica* and *R. greenhornensis* of Cenomanian age are also present. Reworked specimens of all ages are generally well preserved.

Unit IVA, which comprises Cores 23 through 31 and which ranges in age from earliest Eocene to early Paleocene and is characterized by *in situ* assemblages containing few or no reworked older foraminifers. Faunas range from few to abundant with moderate to good preservation.

Core-catcher samples from Cores 23 and 24 yield an earliest Eocene–late Paleocene age (P5–P6). Characteristic species include *Globorotalia aequa-subbotinae, G. acuta, G.* cf. *occlusa, G.* cf. *velascoensis, Globigerina mckannai, G. linaperta, G. primitiva*, and *G. soldadoensis*.

A late Paleocene age (P3–P5) is indicated for 547A-25,CC. Typical planktonics are *Globorotalia acuta, G. occlusa, G.* cf. *angulata, G. conicotruncana, G.* cf. *pusilla, Globigerina triloculinoides*, and *G. mckannai*.

Cores 27 through 29 are assigned a middle to early Paleocene age (P2–P3); *Globigerina triloculinoides, Globorotalia pseudobulloides, G.* cf. *pusilla*, and *G.* cf. *angulata* are commonly present.

Cores 30 and 31 are early Paleocene (P1) in age. Characteristic planktonics include *Globigerina triloculinoides* and *Globorotalia pseudobulloides*, with rare *Globigerina daubjergensis*.

Early Paleocene–Late Cretaceous

Unit IVB is represented by Core 547A-32 through 547A-39-1, 105 cm; it is similar to Unit IVA but is characterized by numerous debris flows. The foraminiferal assemblages consist of few to abundant, moderately to well-preserved earliest Tertiary and Late Cretaceous species. Faunas from Section 547A-32-2 belong to the early Paleocene (P1) *Globigerina daubjergensis* Zone, characterized by *G. daubjergensis, G. triloculinoides*, and *Globorotalia pseudobulloides*. The core-catcher sample from Core 32 yielded an earliest Paleocene assemblage of the *Globigerina eugubina* Zone, including *Eoglobigerina* cf. *danica, G. fringa, Globigerina* sp., and *Guembelitria* sp.

The late to middle Maestrichtian encompasses Cores 33 and 34. Characteristic taxa are *Abathomphalus mayaroensis, Globotruncana contusa, G. stuarti, G. falsostuarti, G. arca, Rugoglobigerina* spp., and *Heterohelix* spp. Cores 35 through 38 are early Maestrichtian–middle Campanian in age. Typical species of Globotruncana include *G. fornicata, G. stuartiformis, G. obliqua, G. lapparenti, G. arca*, and G. cf. *rosetta*.

Holes 547A and 547B

Middle Cretaceous

The lithologic boundary at 547A-39-1, 1–5 cm marks the top of the 350-m-thick succession of Cenomanian and upper Albian sediments. Foraminiferal assemblages are abundant and well preserved. The Cenomanian extends from Cores 547A-39 through 547A-60. Common planktonic species include *Rotalipora appenninica, R. cushmani, R. greenhornensis, R. brotzeni, R. gandolfii, Praeglobotruncana* spp., *Hedbergella delrioensis, H. planispira, H. amabilis, Calvihedbergella simplex, Globigerinelloides bentonensis, G. caseyi, Schackoina cenomana*, and *S. multispinata*. Cores 547A-39 through 547A-46 are tentatively assigned to the middle to late Cenomanian *R. cushmani* Zone. The early Cenomanian *R. gandolfii* Zone is suggested for Cores 47 through 60. Cretaceous zones are after van Hinte (1976).

The upper Albian extends from Core 547A-61 through 547B-6-1, 53 cm. The *Planomalina buxtorfi* Zone is characterized by *P. buxtorfi, R. appenninica, R. ticinensis, S. cenomana*, and *Praeglobotruncana delrioensis*. Typical representatives of the *Ticinella breggiensis* Zone include *T. breggiensis, T. raynaudi, T. primula, R. ticinensis*, and *R. subticinensis*. An early to middle Albian age is assigned to the interval from 547B-6-1, 53–84 cm.

Hole 547B

Early Cretaceous and Jurassic

The first limestone conglomerates occur at 547B-6-1, 107 cm. Foraminifers indicating a Valanginian–middle Hauterivian age are present in Sample 547B-6-1, 140–144 cm. A hiatus is suspected in the upper part of Section 547B-6-2, where limestone contains calpionellids of early Berriasian–late Tithonian age. Clay interbeds are generally rare between Section 547B-6-2 and 547B-14-2, 37 cm (Subunit VIA). Benthic foraminifers are rare to few in abundance with poor to moderate preservation. They are commonly iron-stained. A Kimmeridgian age is suggested for benthic foraminifers from clays in Core 547B-7, Oxfordian for those in Sample 547B-8-4, 4–8 cm, and a Bajocian to Callovian age for those in Sample 547B-10-3, 125 cm. Liassic (late Pliensbachian-?earliest Toarcian) foraminifers are present in 547B-11,CC but are associated with limestone breccias and hence may be redeposited.

In Subunit (VIB 547B-14-2, 37 cm through Core 547B-24), clay interbeds become more common. Moderately to well-preserved Jurassic benthic foraminifers, predominantly nodosariids, have been recovered from these sediments. Abundance is rare to common. An early Pliensbachian age is assigned to Cores 14 to 20, late Sinemurian to Core 22, and (?)Hettangian to (?)Sinemurian to the upper part of Core 24. No foraminifers are recorded below Core 24.

Thin-Section Biostratigraphy of the Jurassic Limestones

Calpionellids are found only in Core 6, both in pebbles (547B-6-2, 97–100 cm) and in apparently *in situ* sediments which occur both above (547B-6-2, 40–44 cm) and below (547B-6-2, 142–148 cm; 547B-6-3, 45–49 cm and 105–109 cm, and 547B-6-4, 108–112 cm) the level of the pebbles. In the pebbles, as in the *in situ* sediments, the genera *Calpionella, Tintinnopsella*, and *Crassicolithina* are represented. The top of the Jurassic limestones would be dated as Zone B (or from Zone C) of Remane (in Jansa et al., 1980), that is, top of the Tithonian or early Berriasian.

Saccocoma occurs, in some places abundantly, in Cores 547B-6 and 547B-7. Ophinoid fragments, somewhat resembling *Saccocoma*, occur down to Core 547B-10 and perhaps also in Core 547B-12.

Protoglobigerina are certainly present in Core 547B-7 and doubtfully present in Core 547B-8.

Pelagic bivalves (?*Bositra*) or "filaments" occur in Core 8 and form coquina layers in Section 547B-8-3 (Fig. 18).

From Cores 547B-6 to 547B-16 radiolarians are associated with the fossils just listed, but from Cores 547B-17 to 547B-24 they constitute the only fossils present, aside from ostracodes and a variety of debris. All radiolarians are calcitized.

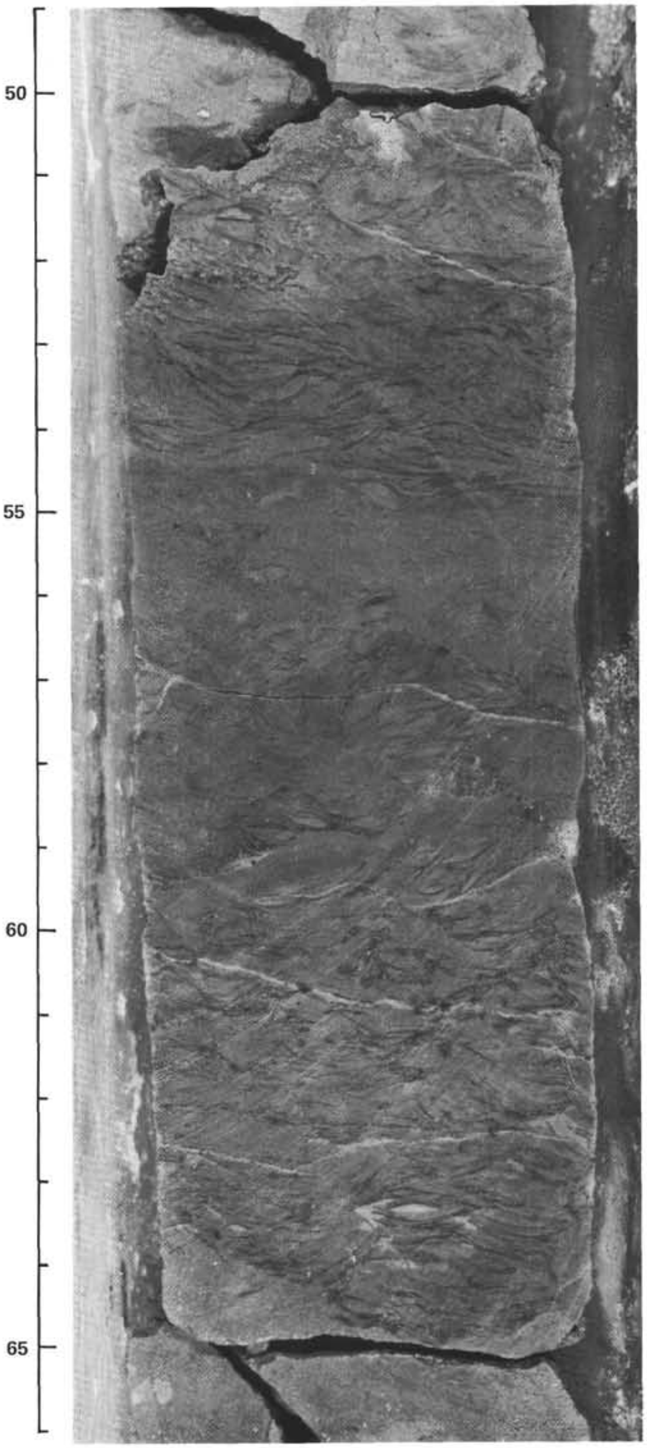

Figure 18. Concentrated pelagic bivalve (?*Bositra*) shells. Sample 547B-8-3, 50–65 cm.

Benthic organisms are not frequent in thin sections except in the upper part of the Jurassic limestone (Cores 547B-6 to 547B-12). These include miliolids, nodosariids, lagenids, and lenticulinids, among others. In Hole 547B *Trocholina* occurs in Cores 6 and 8 and serpulids in Cores 10 and 12.

For biostratigraphy, only the calpionellids provide a relatively precise date for the uppermost Jurassic limestones.

The other organisms identified (*Saccocoma*, protoglobigerines, pelagic bivalves, etc.) are generally distributed in Tethyan Middle and Upper Jurassic pelagic facies, but have poorly defined and especially long ranges.

Radiolarians and Other Siliceous Fossils

Throughout almost all the Cenozoic and Cretaceous sequence drilled at Site 547, pyrite is abundant in the acid residues prepared for radiolarians and other siliceous fossils. Most of the recovered radiolarian assemblages are indeed pyritized. However, some Cenozoic samples show well-preserved siliceous assemblages, most probably still consisting of opal-A, along with partly or totally pyritized specimens that are in an excellent state of preservation.

Cenozoic

No radiolarians and only traces of sponge spicules have been recovered from the uppermost 140 m (Core 547A-1 through 547A-8-3, 90–94 cm) of Pleistocene–Recent to late Miocene age. Pyrite is generally rare and the yellow brown colors indicate a well-oxygenated bottom sediment.

Sample 547A-8,CC, middle Miocene in age, contains abundant pyritized burrow fillings, pyritized sponge spicules, and pyrite inner casts of foraminifers as well as glauconite. Cores 547A-9 through 547A-11, all of middle Miocene age, contain abundant pyritized, partly pyritized, and siliceous radiolarians as well as few to common pyritized diatoms and siliceous and pyritized sponge spicules.

The interval from 547A-14-3, 84–88 cm through 547A-15-1, 30–33 cm contains abundant and reasonably well preserved assemblages characteristic of the upper part of the early Miocene *Calocycletta virginis* Zone.

Samples 547A-16,CC and 547A-17-1, 40–42 cm contain rare, poorly preserved radiolarians assignable to the late Eocene *Thyrsocyrtis bromia* Zone. However, species known to be restricted to the middle Eocene, such as *T. hirsuta hirsuta*, may indicate some reworking.

The interval from Section 547A-17-3 through 547A-17,CC contains the topmost part of a conglomeratic unit including various radiolarian-bearing lithologies, as noted here.

Sample 547A-17-3, 135–137 cm (olive brown [5YR 3/2] nannofossil claystone) contains a partly siliceous fauna assignable to the late Paleocene–early Eocene *Bekoma bidartensis* Zone.

Sample 547A-17-4, 129–132 (greenish gray [5GY 8/1] clayey nannofossil chalk) contains species such as *Stylosphaera goruna* and *Buryella pentadica*, indicating an early to middle Paleocene age, below the *Bekoma bidartensis* Zone.

In Sample 547A-18,CC the depositional age of this conglomeratic unit is probably indicated by a middle Eocene assemblage assignable to the *Phormocyrtis striata striata* or the *Theocotyle cryptocephala cryptocephala* Zones. In the interval from 547A-19,CC through 547A-23,CC so far only rare and poorly preserved assemblages have been found.

Sample 547A-24,CC contains common, moderately preserved siliceous and pyritized radiolarians assignable to the late Paleocene to early Eocene *B. bidartensis* Zone.

The interval from Sample 547A-25,CC through 547A-29,CC shows often abundant and well-preserved siliceous and pyritized assemblages of an unzoned early to middle Paleocene age, below the *B. bidartensis* Zone. A typical assemblage includes *Stylosphaera goruna, Dorcadospyris platyacantha, Buryella tetradica, B. pentadica, Pterocodon lex, Bekoma campechensis*, and many others.

In Samples 547A-31,CC and 547A-32-1, 85–88 cm, abundant but poorly preserved assemblages contain Paleocene forms.

In the interval from 547A-32-2, 56–60 cm through 547A-37,CC all samples were barren.

Cretaceous

From Cores 547A-43 to 547A-73, the bottom of Hole 547A, an acid residue of nearly every core-catcher sample was prepared. All residues contain abundant pyrite as burrow fillings and as inner casts of benthic and planktonic foraminifers, juvenile bivalves, and ammonites; occasionally there are pyritized radiolarians, which are in most of the samples not determinable.

However, the interval from 547A-44,CC through 547A-45,CC shows, in several samples, an abundant pyritized assemblage, excellently preserved. It is assignable to the late early to late Cenomanian *Rotaforma hessi* Zone (Pessagno, 1976).

In Hole 547B, so far only 547B-3,CC contains common, poorly preserved, pyritized radiolarians giving a vague indication of an Albian to Cenomanian age.

AGE-VERSUS-DEPTH CURVE

The age-versus-depth diagram for Site 547 is shown in Figure 19. A minor hiatus may exist at the Miocene/Pliocene boundary. The average sedimentation rate for the late Miocene was between 9 and 22 m/m.y.

An unconformity separates the upper Miocene from the middle Miocene sediments, which consist of greenish gray clayey nannofossil ooze and nannofossil claystone (Unit IIA), as at the other sites of Leg 79. The sedimentation rate during the middle Miocene was about 10 m/m.y.

A distinct hiatus with a time value of 10–15 m.y. separates the Miocene sediments from the underlying lower Oligocene to upper Eocene sediments, consisting, from the top to the bottom, of pelagic nannofossil ooze, debris flows, and siliceous nannofossil chalk (Units IIB and III). The rate of sedimentation of these strata was about 14 m/m.y.

Beneath another unconformity are lower Eocene, Paleocene, and Upper Cretaceous sediments, consisting mainly of greenish gray clayey nannofossil chalk, subordinate nannofossil claystone, and debris flows (Unit IV). The sedimentation rate during deposition of these beds was about 7 m/m.y.

Beneath a distinct regional unconformity with a time value of about 18 m.y. there occurs a 350-m-thick se-

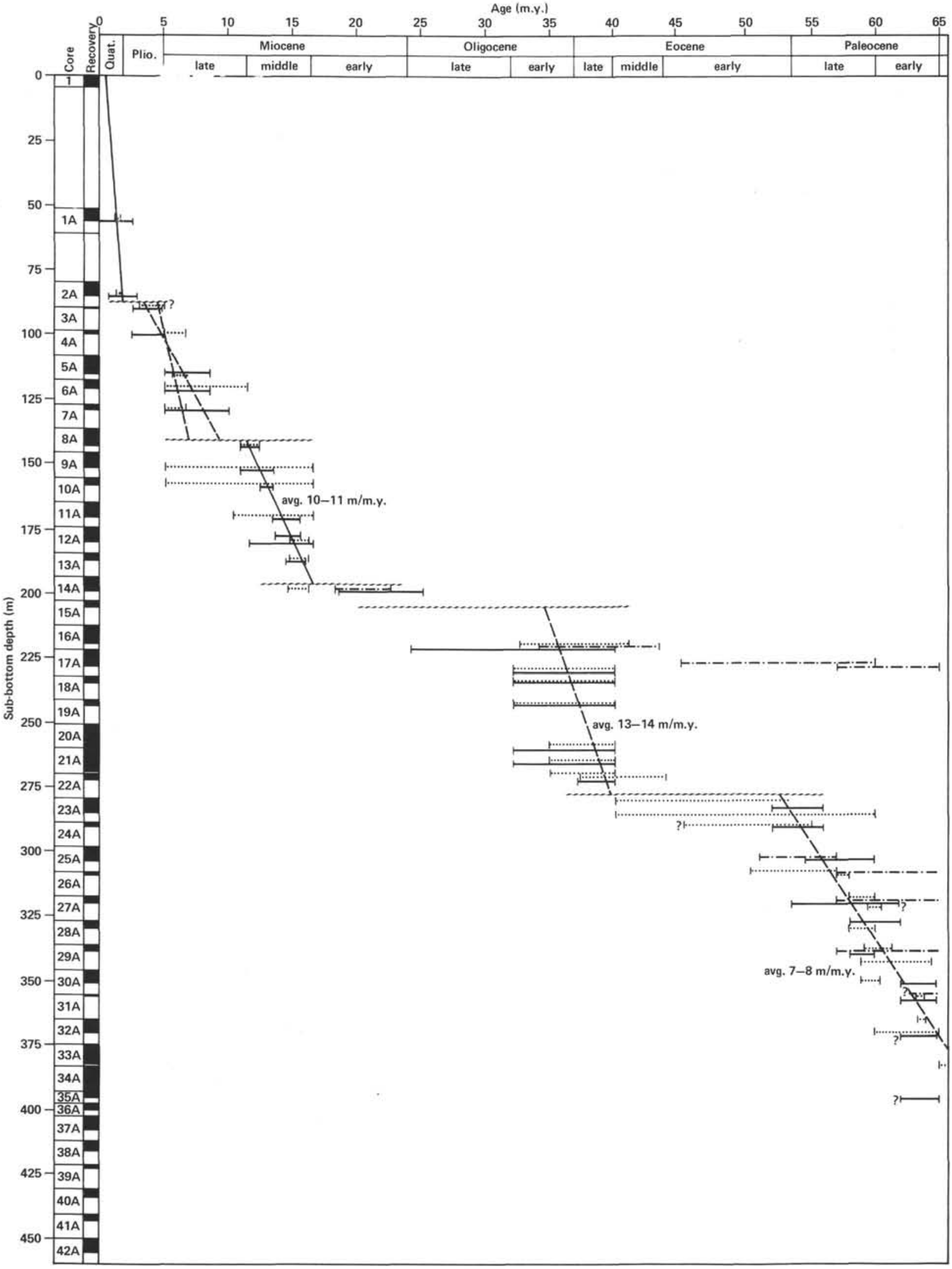

Figure 19. Depth vs. age, Site 547.

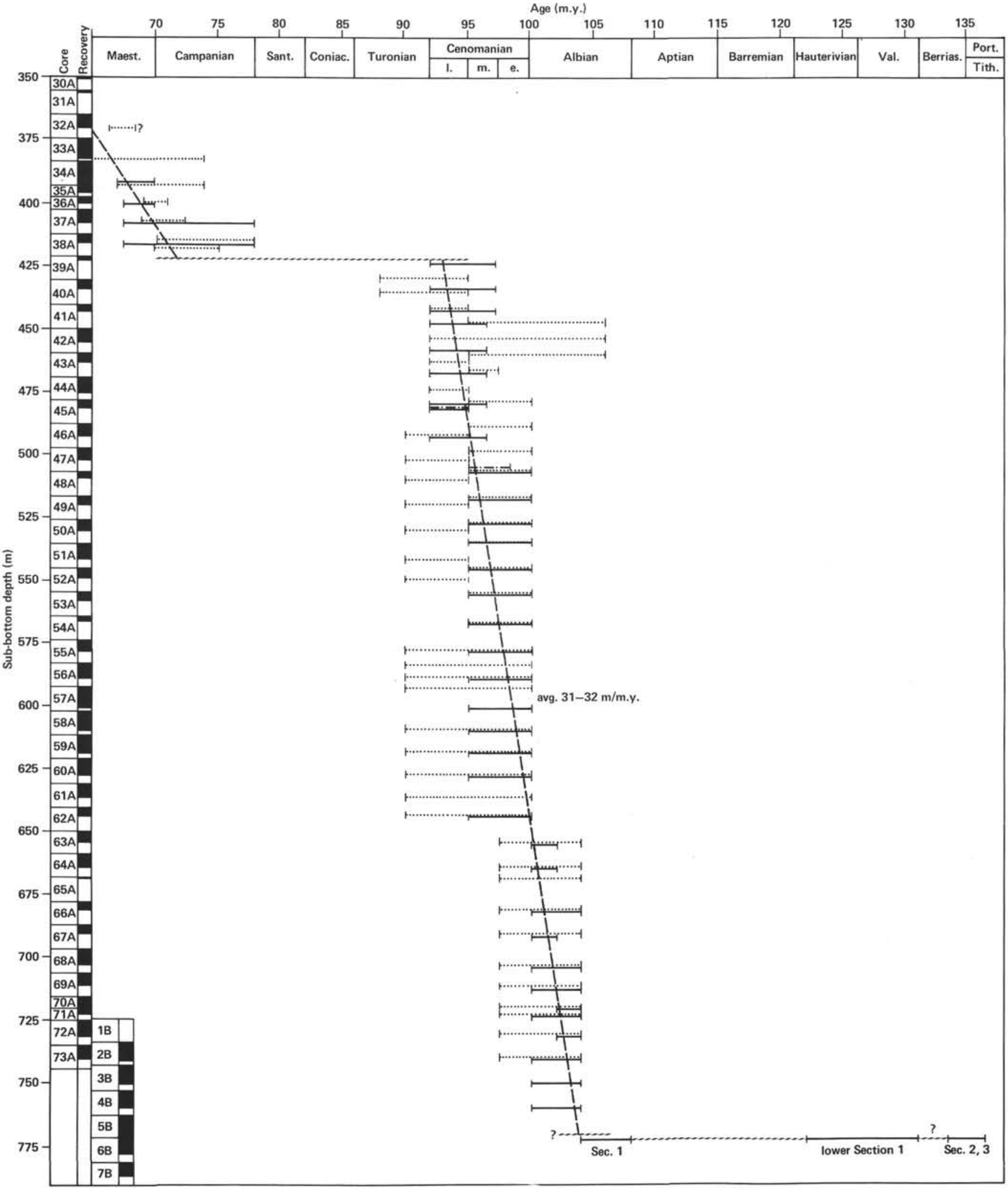

Figure 19. (Continued).

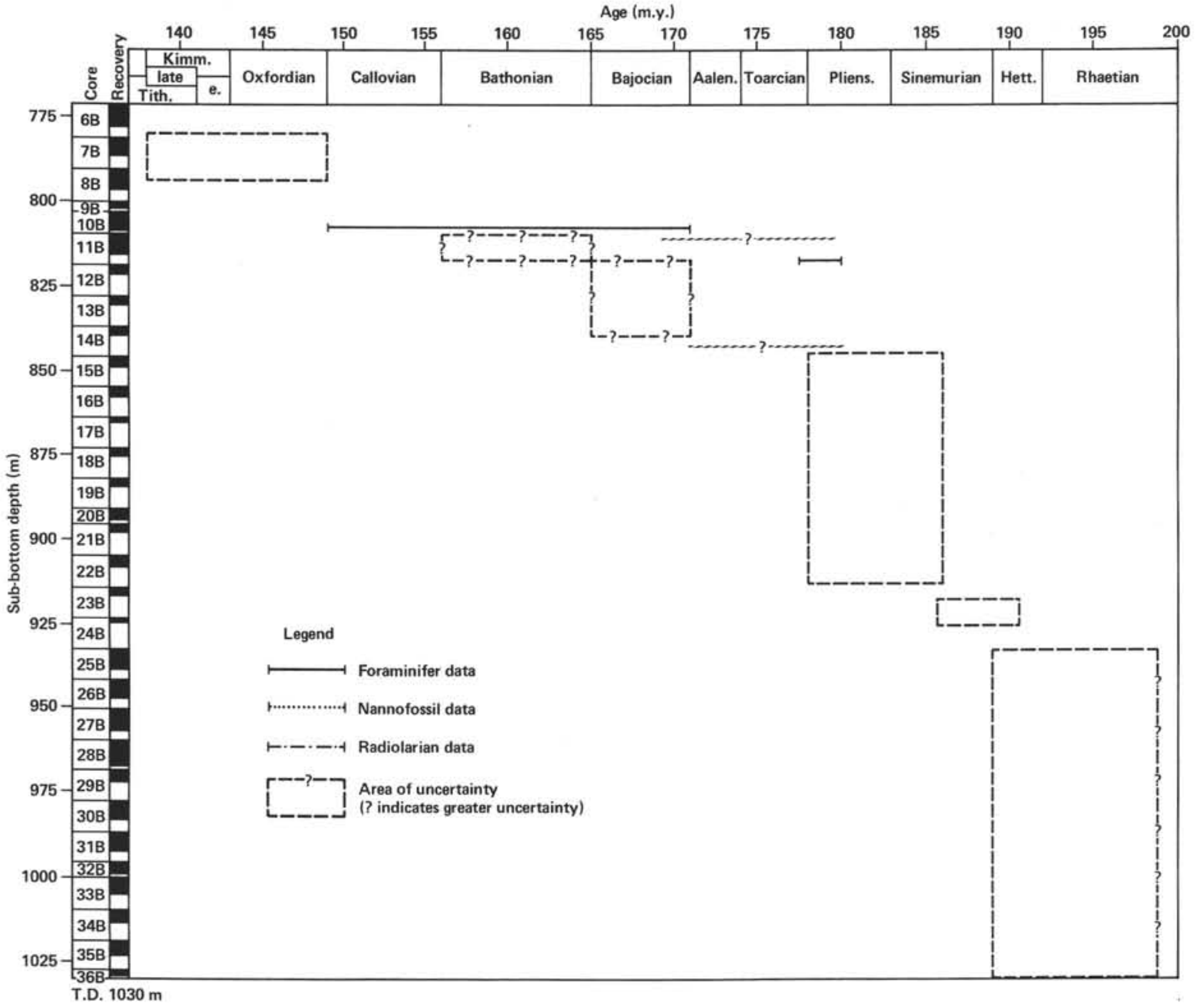

Figure 19. (Continued).

quence of greenish nannofossil claystone interbedded with layers of intraformational conglomerate consisting of flat claystone pebbles and ranging in age from late Cenomanian at the top to late Albian at the base (Unit V). The rate of accumulation of this Cretaceous unit was about 31 m/m.y.

Below the Albian sediments, the Lower Cretaceous and Jurrasic strata have too few reliable zonal fossils to permit good estimates of rates of sedimentation, except in the qualitative sense that the Lower Jurassic beds accumulated more rapidly than the Upper Jurassic beds.

ORGANIC GEOCHEMISTRY

Carbon and Nitrogen Contents

Table 3 summarizes the analytical results for organic carbon, carbonate, and organic nitrogen contents. The amount of organic matter in the sediments above the early Miocene/Oligocene unconformity (Lithologic Units I and IIA) is as low as in the equivalent sections at the other sites occupied during Leg 79. A sudden increase in organic matter appears in the upper Eocene slump sequence of Unit III (Fig. 20). Low C_{org} values are again encountered in the underlying Unit IV (lower Eocene-upper Cretaceous). Lithologic Unit V appears to be subdivided according to organic carbon contents. The values are fairly constant around 0.7% C_{org} in the Cenomanian but increase to slightly above 1% in the Albian, with an exceptional value of 3.2% C_{org} in a slump at the base of this section. The distribution of organic matter is dependent upon lithology in Unit VI (Lower Cretaceous-Jurassic). The limestones are very lean in organic carbon, whereas higher values were observed in the claystones containing calcareous nodules. Very high organic carbon contents were found in the thin organic-matter-rich claystone layers ("black shales") in Cores 547B-15 through 547B-22 of Subunit VIB (Fig. 20). Low and uniform organic matter values characterize the sandy mudstones of Unit VII. Similar variations, although at a correspondingly lower level, were observed for the organic nitrogen contents (Table 3). The statistical evaluation of organic carbon and nitrogen data is summarized in Table 4.

The carbonate contents are generally high in Lithologic Units I through IV, although there is a drop to about 45% $CaCO_3$ in Subunit IIB after a gradual increase in Units I and IIA. A remarkable decrease occurs in the claystones of Unit V to an average value of 22%

Table 3. Carbon and nitrogen contents and pyrolysis data, Site 547.

							Rock-Eval pyrolysis					
Sample (interval in cm)	Sub-bottom depth (m)	Litho-logic unit	Age	C_{org} (%)	$CaCO_3$ (%)	N_{org} (%)	S_1	S_2 (mg/g rock)	S_3	Hydrogen index (mg HC/g C_{org})	Oxygen index (mg CO_2/g C_{org})	T_{max} (°C)
Hole 547A												
1-2, 144-150[a]	54.0	I	Pleistocene	0.21	50.9	0.04						
1-3, 118-120	55.2			0.25	49.4	0.05						
1-4, 0-2	55.5			0.25	49.4	0.05	—	0.05	1.05	20	420	383
2-3, 118-120	83.7			0.21	52.9	0.04						
2-4, 0-2	84.0			0.20	55.0	0.04	—	0.03	1.19	14	595	377
5-3, 118-120	112.2		Miocene	0.13	61.6	0.03						
5-4, 0-2	112.5			0.11	65.7	0.03	—	0.01	0.84	5	726	396
5-4, 144-150[a]	114.0			0.10	63.1	0.03						
8-3, 118-120	140.7			0.11	56.0	0.03						
8-4, 0-2	141.0			0.11	78.4	0.02	—	—	0.59	—	537	—
9-3, 144-150[a]	150.5	IIA		0.07	78.4	0.02						
11-3, 118-120	169.2			0.14	74.8	0.02						
11-4, 0-2	169.5			0.16	67.2	0.03	—	0.03	0.52	21	322	405
14-2, 144-150[a]	196.5			0.10	67.2	0.02						
14-3, 118-120	197.7			0.10	69.2	0.02						
14-4, 0-2	198.0			0.12	67.2	0.02	—	0.02	0.65	13	538	407
17-1, 118-120	223.2	IIB	Oligocene	0.30	45.8	0.04						
17-2, 0-2	223.5			0.30	44.3	0.04	—	0.07	1.28	22	427	419
17-3, 137-139	226.4	III	late Eocene	3.45	66.7	0.16	—	12.68	3.36	368	97	429
18-1, 99-100	232.5			5.22	64.6	0.23	—	33.21	1.98	636	38	412
20-4, 118-120	256.2			3.06	57.5	0.11						
20-5, 0-2	256.5			2.59	53.4	0.11	—	13.65	2.51	527	97	428
20-5, 140-150[a]	258.0			1.54	59.0	0.07						
21-5, 10-11	266.1			0.62	10.6	0.05	—	0.15	0.82	25	132	423
22-1, 149-150	271.0			0.35	70.8	0.04	—	0.14	0.90	40	258	418
23-3, 118-120	283.2	IVA	early Eocene-late Paleocene	0.21	73.8	0.03						
23-4, 0-2	283.5			0.25	57.5	0.03	—	0.02	1.00	6	401	443
25-3, 140-150[a]	302.5		Paleocene	0.33	59.5	0.04						
27-1, 118-120	318.2			0.37	48.3	0.05						
27-2, 0-2	318.5			0.33	51.9	0.04	—	0.26	1.40	78	424	429
30-3, 110-120[a]	349.7			0.10	66.2	0.02						
30-3, 118-120	349.7			0.11	64.6	0.02						
30-4, 0-2	350.0			0.09	67.7	0.02	—	0.02	0.83	23	918	429
33-4, 118-120	379.7	IVB	Maestrichtian Campanian	0.13	53.9	0.02						
33-5, 0-2	380.0			0.09	73.3	0.02	—	0.07	1.73	80	1921	492
35-1, 140-150[a]	394.5			0.08	62.6	0.02						
37-2, 118-120	405.2			0.10	61.1	0.02						
37-3, 0-2	405.5			0.10	56.5	0.02	—	0.10	1.34	102	1336	405
40-1, 110-120[a]	432.2	V	Cenomanian Albian	0.59	17.8	0.05						
40-1, 118-120	432.2			0.61	23.9	0.05						
40-2, 0-2	432.5			0.53	20.3	0.05	—	0.24	2.00	45	377	427
41-1, 149-150	442.0			0.62	22.3	0.05	—	0.30	1.83	49	294	417
43-2, 118-120	462.2			0.43	13.7	0.04						
43-3, 0-2	462.5			0.51	18.3	0.05	—	0.08	1.80	15	353	422
45-2, 140-150[a]	481.5			0.70	22.3	0.06						
46-2, 118-120	490.7			0.55	13.7	0.05						
46-3, 0-2	491.0			0.56	29.0	0.05	—	0.39	1.51	70	271	430
49-2, 118-120	519.2			0.76	14.2	0.05						
49-3, 0-2	519.5			0.72	24.4	0.05	—	0.35	1.61	49	224	420
50-2, 140-150[a]	529.0			0.61	18.3	0.07						
52-2, 118-120	547.7			0.78	23.9	0.05						
52-3, 0-2	548.0			0.68	27.9	0.05	—	0.36	1.84	53	271	419
55-1, 140-150[a]	575.0			0.77	20.8	0.06						
55-2, 118-120	576.2			0.62	29.5	0.05						
55-3, 0-2	576.5			0.65	21.8	0.05	—	0.39	2.37	60	364	422
58-4, 118-120	607.7			1.06	25.9	0.07						
58-8, 0-2	608.0			0.93	15.7	0.11	—	0.55	2.02	59	217	422
60-4, 140-150[a]	627.0			0.59	25.9	0.05						
61-3, 118-120	634.7			0.66	24.9	0.06						
61-4, 0-2	635.0			0.68	27.4	0.06	—	0.32	2.11	48	310	426
64-2, 118-120	661.7			0.71	34.1	0.05						
64-3, 0-2	662.0			0.69	34.1	0.05	—	0.32	1.79	46	260	429
66-2, 140-150[a]	681.0			1.06	48.8	0.07						
67-2, 118-120	690.2			1.14	49.9	0.08						
67-3, 0-2	690.5			1.11	41.2	0.08	—	2.26	1.70	204	153	431
70-2, 104-106	718.6			1.01	54.5	0.06						
70-2, 136-150[a]	718.9			0.90	39.7	0.07						
70-3, 0-2	719.0			1.11	39.3	0.08	—	2.21	2.15	199	194	430
73-3, 118-120	739.0			1.21	33.6	0.08						
73-4, 0-2	739.5			1.18	34.6	0.08	—	2.59	1.87	219	159	434
Hole 547B												
2-4, 118-120	739.7			1.47	18.2	0.10						
2-5, 0-2	740.0			1.64	20.6	0.09	—	1.30	1.47	79	90	433
5-6, 111-113	771.1			1.60	33.7	0.09						
5-7, 0-2	771.4			1.48	39.1	0.08	—	2.39	1.90	162	128	427
6-1, 77-78	772.8			3.24	25.0	0.16	—	15.40	2.03	475	63	428
6-1, 136-138	773.5	VIA	Haut.-Val.	0.45	11.9	0.07	—	0.10	0.20	23	43	507
6-3, 54-55	775.5		Berr.-Tith.	0.06	58.5	0.02						
6-3, 55-56	775.5			0.03	87.6	0.01						
8-3, 118-120	795.2		Jurassic	0.12	78.9	0.01						
10-3, 19-20	806.7			0.10	48.8	0.02						
10-3, 51-52	807.0			0.12	41.5	0.02						
14-1, 126-127	838.3			0.11	74.0	0.01						
14-2, 56-57	839.1	VIB		0.63	9.0	0.06	—	—	0.43	—	68	—
15-2, 16-18	847.7			2.26	8.0	0.08	—	2.93	1.64	130	73	429
18-1, 119-121	874.2			0.99	37.1	0.08	—	0.29	0.94	29	95	434
20-1, 13-15	891.1			6.76	9.5	0.14	—	41.83	1.16	612	17	417
22-1, 13-14	903.2			1.29	8.0	0.07	—	0.92	1.26	71	98	433
25-1, 0-10	932.5	VII	Early Jurassic - Triassic	0.26	8.5	0.08						
25-3, 148-150	937.0			0.49	7.5	0.06	—	0.16	0.63	33	127	465
25-4, 30-32	937.3			0.23	10.9	0.04						
26-3, 135-150[a]	946.0			0.22	8.5	0.05						
3-4, 35-37	982.4			0.20	26.9	0.04						
34-1, 118-120	1010.7			0.12	10.0	0.05						
34-2, 0-2	1011.0			0.10	13.4	0.04						

Note: — = not detected.

[a] Residues from interstitial water analysis.

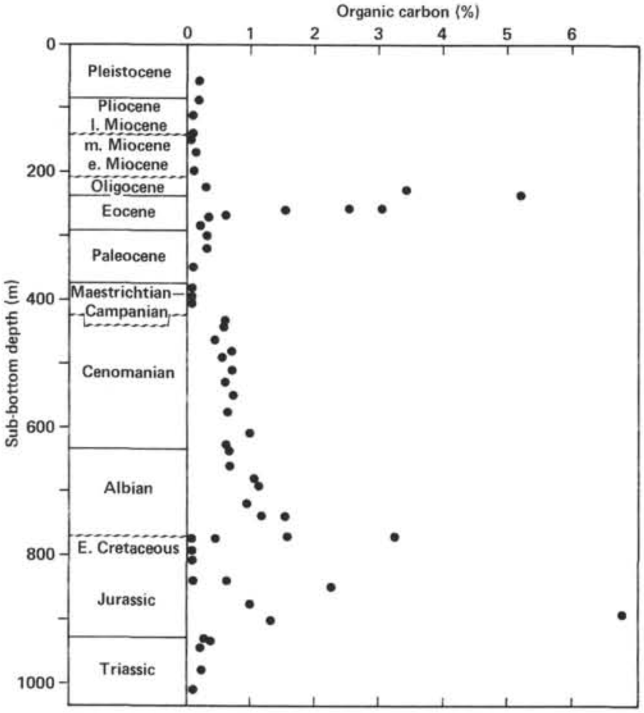

Figure 20. Organic carbon content versus depth for sediments from Holes 547A and 547B.

$CaCO_3$. The organic carbon content indicates that there is a subdivision in this unit by increasing to more than 30% $CaCO_3$ in the Albian section of Unit V. Within Unit VI, the carbonate content varies significantly, being statistically different for the claystones and the nodular limestones in this rhythmic sequence. Finally, the carbonate content remains low, with a mean of 12%, in the sandy mudstones of the deepest Unit VII (Table 4). Again, as at Site 544, there is a strong increase of carbonate content with depth within the Pleistocene–Miocene interval, Units I and IIA ($r = 0.75$; $r_{05;6} = 0.47$) (Table 5).

In all, of 10 units (including subunits) tested for possible correlation between noncarbonate material and organic carbon contents in the sediments from Site 547 (only sets of samples with N more than 5 are considered), seven do not show any significant correlation (Table 5). Among them is the largest and most homogeneous sample set of the Cenomanian section of Unit V (N = 22). There is a weak but significant correlation between the two attributes in the Albian part of Unit V and a strongly positive and significant correlation in Units I and IVA (Table 5).

Rock-Eval Pyrolysis

The results of Rock-Eval pyrolysis (summarized in Table 3) indicate that the kerogens in the Cenozoic

Table 4. Statistical characteristics of $CaCO_3$, C_{org}, and N_{org} contents in sediments from Site 547.

Lithologic unit (thickness in m)	Age	N	$CaCO_3$ (%)				C_{org} (%)				N_{org} (%)			
			Range	Mean	Variance	S.D.	Range	Mean	Variance	S.D.	Range	Mean	Variance	S.D.
I (140)	Pleistocene-late Miocene	10	49.4–78.4	58.2	75.1	9.1	0.10–0.25	0.17	3×10^{-3}	0.06	0.02–0.05	0.04	8×10^{-5}	0.010
IIA (63)	Miocene	6	67.2–78.4	70.7	19.2	4.8	0.07–0.16	0.12	9×10^{-4}	0.03	0.02–0.03	0.02	1×10^{-5}	0.24
IIB (21)	Oligocene	2	44.3–45.8	45.1	0.6	1.1	0.30–0.30	0.30	0.00	0.00	0.04–0.04	0.04	0.0	0.0
III (53)	late Eocene Nannofossil clayey chalk	5	53.4–66.7	60.2	23.3	5.4	1.54–5.22	3.2	1.45	1.35	0.07–0.23	0.14	3×10^{-3}	0.06
	Nannofossil silty claystone	1		10.6				0.62				0.05		
	Nannofossil chalk	1		70.8				0.35				0.04		
IVA (71)	early Eocene–Paleocene	8	48.3 73.8	61.2	63.4	8.5	0.09–0.37	0.22	0.01	0.11	0.02–0.05	0.03	1×10^{-4}	0.01
IVB (70)	Maestrichtian–Campanian	5	53.9–73.3	61.5	44.7	7.5	0.08–0.13	0.10	3×10^{-4}	0.02	0.02–0.02	0.02	0.0	0.0
V (230)	Cenomanian	22	13.7–29.5	21.9	23.1	4.9	0.43–1.06	0.66	0.02	0.14	0.04–0.11	0.06	2×10^{-4}	0.01
(120)	Albian	15	18.2–54.5	36.4	96.9	10.2	0.69 3.24	1.30	0.34	0.61	0.05–0.16	0.08	6×10^{-4}	0.03
VI	Hauterivian–Jurassic													
(160)	Calcareous claystones	5	8.0–11.9	9.3	2.1	1.6	0.45–6.76	2.28	5.42	2.60	0.06–0.14	0.08	9×10^{-4}	0.03
	Nodular limestones	6	41.5–87.6	64.9	237.6	18.1	0.03–0.12	0.09	1×10^{-3}	0.04	0.01–0.02	0.02	3×10^{-5}	8×10^{-3}
	Clayey silty limestone	1		37.1				0.99				0.05		
VII (100)	Early Jurassic–Triassic	7	7.5–26.9	12.2	39.1	6.8	0.10–0.49	0.23	0.01	0.13	0.04–0.06	0.05	5×10^{-5}	8×10^{-3}
	Total	94												

Note: Mean $(\bar{y}) = \frac{1}{N}\sum_{i=1}^{N} y_i$; Variance $= \frac{1}{N}\sum_{i=1}^{N} y_i^2 - \left(\frac{1}{N}\sum_{i=1}^{N} y_i\right)^2$; S.D. $= \sqrt{\text{var}\frac{N}{N-1}}$

Table 5. Correlations between noncarbonate material and C_{org} (in total sediment) in the different lithologic units at Site 547.

Lithologic unit	Age	N	r	$r_{05;N}$	Correlation
I	Pleistocene–late Miocene	10	0.79	0.56	Yes
IIA	Miocene	6	0.45	0.83	No
III	late Eocene	5	−0.58	0.90	No
IVA	early Eocene–Paleocene	8	0.77	0.63	Yes
IVB	Maestrichtian–Campanian	5	0.66	0.90	No
V	Cenomanian	22	−0.16	0.36	No
	Albian	15	0.47	0.44	Yes
VI	Haut.-Jurassic Calcareous claystones	5	0.12	0.90	No
	Nodular limestones	6	0.47	0.83	No
VII	Early Jurassic–Triassic	7	0.32	0.71	No

Note: r = correlation coefficient; $r_{05;N}$ = 95% critical value of the correlation coefficient; the correlation is significant when 1 r 1 ≥ $r_{05;N}$.

and Mesozoic sediments at Site 547 form four different groups (Fig. 21).

1. The organic matter in the Cenozoic and in some of the Cretaceous and Jurassic sediments is severely degraded (e.g., oxidized), and pyrolysis yields low hydrogen index (IH) and in most cases extremely high oxygen index (IO) values (data points outside the encircled clusters). Included in this group are two sediments from Lithologic Unit IVB (Upper Cretaceous), because they yield large amounts of carbon dioxide upon pyrolysis, although their hydrogen content is slightly elevated. Most of the samples in this group plot outside the IH/IO diagram in Figure 21. The organic matter seems to be of a residual terrestrial nature, similar to that in most of the Cenozoic sediments at the other sites drilled during Leg 79. This general characteristic is in accordance with microscopic and organic geochemical evidence for organic matter in hemipelagic Tertiary sediments in other areas of the Northwest African continental margin, for example, at DSDP Sites 397 and 415 (Rullkötter et al., 1982), although Boutefeu (1980) reports higher hydrogen index values. The hydrocarbon potential of the organic matter in these sediments is nil.

2. The second organofacies comprises the kerogens in most of the Cenomanian sediments and an Eocene sediment from Lithologic Unit III, namely Sample 547A-22-1, 149–150 cm. The organic matter in these sediments is still hydrogen-deficient and oxygen-rich. The samples plot just below the kerogen type III trend line (Fig. 21); thus the organic matter is of terrigenous origin and partly oxidized during transport, which reduces the hydrocarbon potential to a negligible or at best low level, for gas generation only. A similar kerogen type was encountered in the late Cenomanian and Albian sediments at DSDP Site 415 in the Agadir Canyon off Morocco (Boutefeu, 1980).

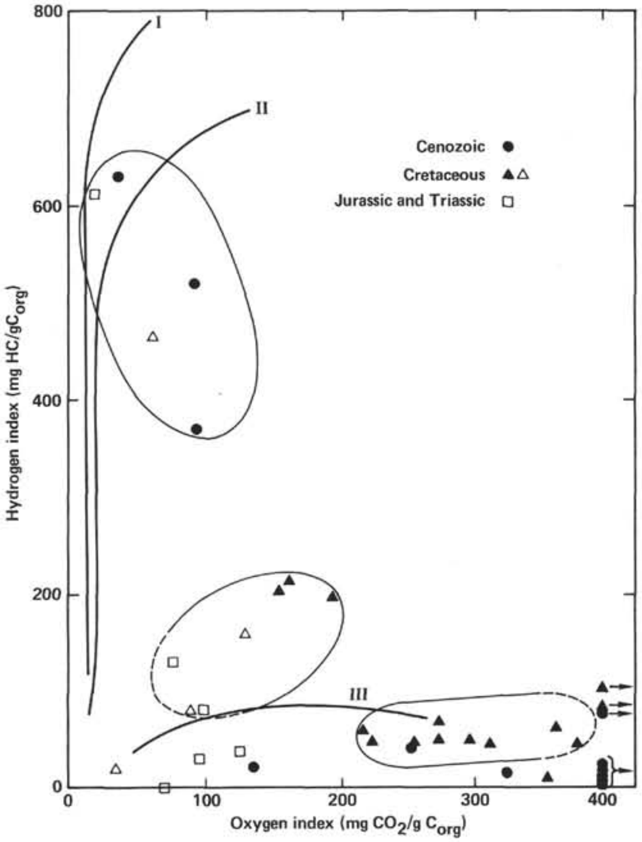

Figure 21. Results of Rock-Eval pyrolysis displayed as hydrogen index versus oxygen index diagram for Cenozoic and Mesozoic sediments from Holes 547A (closed symbols) and 547B (open symbols). Encircled clusters mark different organofacies types.

3. The Albian sediments from Site 547 contain a mixture of terrigenous and marine organic matter, with the former predominating. The relatively low oxygen contents indicate environmental conditions during deposition that were favorable for the preservation of organic matter, possibly mainly because sedimentation rates were high and thus the organic matter was rapidly buried. Hydrogen and oxygen index values are both moderate (Fig. 21), similar to the values found for the Albian sediments at Site 545, resulting in a good hydrocarbon generation potential of these kerogens, mainly for gas. Two Jurassic sediments from Sections 547B-15-2 and 547B-22-1 are similar in kerogen type to the Albian samples.

4. Finally, there is a group of sediments with hydrogen-rich organic matter characterized by high hydrogen index and low oxygen index values in Figure 21. Three of the samples are from the Eocene slump sequence of Lithologic Unit III. Their kerogen appears to be marine planktonic in origin, with very low to moderate admixtures of terrigenous organic matter. Kerogens of this type are not normally deposited under deep-water conditions, unless the whole water column is anoxic. Thus, it is most likely that these sediments from Lithologic Unit III are allochthonous, and that primary deposition occurred in an oxygen-minimum layer impinging on the

outer shelf–upper slope of the Mazagan Plateau. Later, downslope transport led to final deposition at the present setting, and rapid burial preserved the high amounts of easily degradable organic matter in the deep oxic waters. A high potential for liquid hydrocarbon generation can be ascribed to these kerogens. Similar organic-carbon-rich sediments with hydrogen-rich kerogens of dominantly marine algal provenance were found in a lower Miocene slump sequence at the continental rise off Northwest Africa, DSDP Site 397, south of the Canary Islands (Cornford et al., 1979).

An Albian clast found at the base of Lithologic Unit V (Section 547B-6-1) and a Jurassic claystone from Section 547B-20-1 appear to have an origin similar to the Unit III Eocene sediments just described. The Jurassic claystone represents one of several thin "black shale" layers observed in Cores 547B-15 through 547B-22. Very fine lamination was seen occasionally, but most of these layers are much disturbed by drilling. When less disturbed, the "black shales" graded into lighter, gray brown claystones with increasing bioturbation down the cores. Samples from Sections 547B-15-2 and 547B-22-1 represent what may be considered intermediate levels (Fig. 21). They have been described as moderately hydrogen and oxygen rich, like the Albian sediments.

The temperatures of maximum pyrolysis yield (used to indicate the maturity of the organic matter; Espitalie et al., 1977) exhibit the usual rapid increase in the most immature sediments (Fig. 22). A value of about 410°C is reached at about 200 m sub-bottom depth. Below this depth, the underlying Cenozoic sediments in places yielded T_{max} values higher than the values that would correspond to their present burial depth, and those values show considerable scatter. It seems possible that this phenomenon can be attributed to the redeposited nature of most of the sediments in the Eocene and Paleocene sections, and that at least some of these sediments underwent permaturation at their primary sites of deposition.

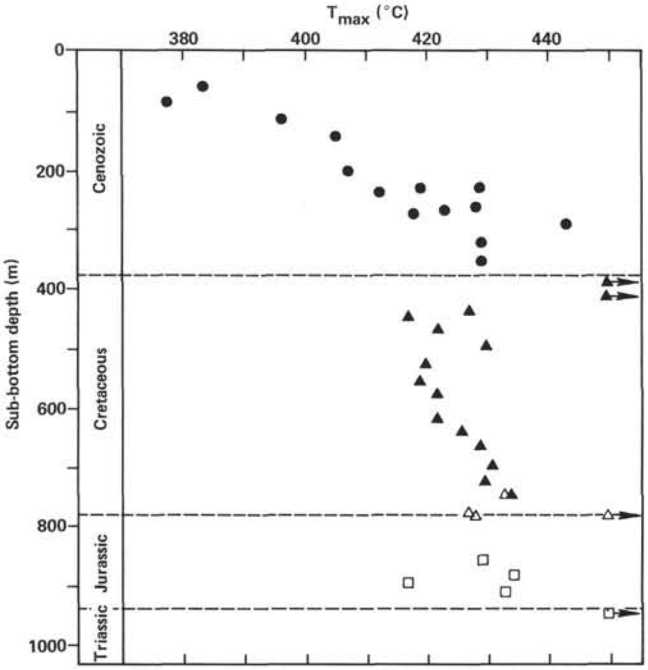

Figure 22. Temperature of maximum pyrolysis yield (T_{max}) versus depth profile for sediments from Holes 547A (closed symbols) and 547B (open symbols).

The T_{max} values of the Cretaceous sediments remain near 425°C between 425 and 650 m sub-bottom depth but show a distinct increase in the Albian sediments. If this increase is real and not caused by reworked material or the low level of accuracy in T_{max} determination, then the upper Albian sediments at Site 547 approach marginal maturity, corresponding to about 0.5% vitrinite reflectance, at the relatively shallow depth of 750 m. This fact suggests erosion of a considerable pile of sediment during formation of the unconformity between middle and Upper Cretaceous beds at this site, assuming heat flow and maturation conditions similar to those found already on the Northwest African continental margin (Rullkötter et al., 1982). Apart from some scatter, the temperatures stay at a level of about 433°C within the upper ~ 100 m of the Jurassic section.

Gas Chromatography of Light Hydrocarbons

No gas pockets were encountered in the sediments at Site 547. Thus, hydrocarbon analysis was based solely on carrier gas stripping gas chromatography of fresh sediment samples (Table 6). Absolute total C_2 through C_6 hydrocarbon concentrations (in nl/g dry sediment) over the entire depth interval ranged between less than 1 and 79. Low absolute concentrations were found in the Cenozoic sediments (0.8 to 3.8), with an exceptional higher value in Sample 547A-23-4, 0–2 cm (12.0). In contrast to this, the total C_2 through C_6 hydrocarbon concentrations were higher throughout the Cretaceous sediment sequence (13.0 to 79.0), with only one exception (Sample 547B-6-1, 136–138 cm; 4.0).

Normalized to organic carbon content, however, this difference between Cenozoic and Cretaceous sediments largely disappears. In most sample, the hydrocarbon concentrations reach values of several thousand nl/g C_{org}, indicating a relationship between organic carbon content and total C_2–C_6 hydrocarbon concentration. An exception is the kerogens of three Eocene samples (547A-17-3, 137–139 cm; 547A-18-1, 99–100 cm; 547A-20-5, 0–2 cm) with extremely low hydrocarbon concentrations (42 to 61 nl/g C_{org}) from olive brown clayey nannofossil chalks from the slump sequence within Lithologic Unit III (Eocene). In contrast to all other Site 547 sediments, which contain more or less oxidized terrigenous organic matter, these three seem to be of a predominantly marine algal origin (cf. discussion of Rock-Eval pyrolysis).

In conclusion, the bulk of the hydrocarbons observed are a product of early diagenetic transformation of terrigenous organic matter. The correlation between hydrocarbon concentrations and organic matter contents suggests indigenous hydrocarbon formation. This is easily comprehensible for the Albian and Cenomanian sediments containing unoxidized or only slightly oxidized terrigenous organic matter, but it is not straightforward

Table 6. Light hydrocarbon (C_2–C_6) values (in nl/g sediment) detected in sediments from Site 547 by carrier gas stripping gas chromatography.

Sample (interval in cm)	Sub-bottom depth (m)	Litho-logic unit	C_2	C_3	i-C_4	n-C_4	neo-C_5	i-C_5	n-C_5	cy-C_5	i-C_6 + ai-C_6	n-C_6 + Me-cy-C_5	cy-C_6	Total HC	Total HC (nl/g C_{org})
Hole 547A															
11-4, 0–2	169.5	IIA	1.0	1.6	0.8	0.4	—	tr	tr	—	tr	tr	—	3.8	2,375
14-4, 0–2	198.0		1.2	1.1	0.6	0.4	tr	0.2	0.2	—	tr	tr	—	3.7	3,083
17-2, 0–2	223.5	IIB	0.4	0.2	0.2	—	—	—	—	—	—	—	—	0.8	267
17-3, 137–139	226.4		1.4	0.6	tr	tr	—	0.1	tr	—	—	—	—	2.1	61
18-1, 99–100	232.5	III	1.1	0.9	0.4	0.3	—	0.3	0.2	—	tr	tr	—	3.2	61
20-5, 0–2	256.5		0.6	0.4	0.1	tr	—	tr	tr	—	—	—	—	1.1	42
23-4, 0–2	283.5		2.4	5.0	1.2	1.4	—	0.6	0.3	0.3	0.3	0.5	—	12.0	4,800
27-2, 0–2	318.5	IVA	0.7	0.8	0.1	0.2	—	0.1	0.1	tr	tr	0.1	tr	2.1	636
30-4, 0–2	350.0		0.9	0.3	tr	tr	—	tr	tr	—	—	—	—	1.2	1,333
33-5, 0–2	380.0	IVB	0.6	1.1	0.7	0.2	—	tr	tr	—	—	—	—	2.6	2,889
37-2, 118–120	405.2		0.7	0.3	0.1	tr	—	—	—	—	—	—	—	1.1	1,100
41-1, 149–150	442.0		3.9	5.1	2.0	1.5	tr	1.3	1.5	tr	0.7	1.6	0.1	17.7	2,855
43-3, 0–2	462.5		3.7	3.1	0.7	1.1	tr	1.1	1.1	0.2	0.6	1.4	tr	13.0	2,549
46-2, 118–120	490.7		5.8	5.4	1.5	2.2	tr	2.0	1.8	0.3	1.0	2.4	tr	22.4	4,073
49-2, 118–120	519.2		4.6	8.6	3.5	4.0	tr	5.2	3.7	0.9	1.9	4.8	tr	37.2	4,895
52-3, 0–2	548.0		4.3	5.3	1.9	2.0	tr	2.7	1.7	0.4	0.8	2.3	tr	21.4	3,147
55-2, 118–120	576.2		8.4	13.0	5.0	5.4	tr	6.7	3.8	1.3	1.8	5.1	tr	50.5	8,145
58-4, 118–120	607.7	V	7.8	10.6	4.2	4.1	tr	7.9	3.0	1.3	1.1	3.7	tr	43.7	4,123
61-4, 0–2	635.0		7.3	10.2	3.8	3.6	tr	4.5	2.4	0.8	0.7	3.0	tr	36.3	5,338
64-5, 0–2	665.0		7.0	8.8	3.1	3.0	0.1	3.2	1.9	0.8	0.9	2.8	tr	31.6	4,580
67-2, 118–120	690.2		15.0	21.0	7.0	7.1	tr	6.8	4.3	1.6	1.8	5.9	tr	70.5	6,184
70-3, 0–2	719.0		9.1	11.4	4.0	3.9	tr	3.2	2.8	1.2	1.8	7.8	tr	45.2	4,072
73-3, 118–120	739.2		2.7	6.5	3.5	3.7	0.1	4.2	3.4	0.7	1.8	4.9	tr	31.5	2,603
Hole 547B															
2-4, 118–120	736.7		6.1	18.7	10.2	9.0	0.1	9.2	7.3	2.3	4.4	11.7	tr	79.0	5,374
5-6, 111–113	771.7		8.6	12.4	5.7	5.5	0.2	5.9	4.6	1.2	2.5	6.7	tr	53.3	3,626
6-1, 136–138	773.4	VIA	0.8	0.9	1.1	0.2	—	0.2	0.2	—	0.2	0.2	—	4.0	889

Note: Compounds are listed in order of retention times; tr = trace; — = not detected.

for the Cenozoic samples, with their more strongly oxidized organic matter. An alternative explanation for the Cenozoic figures is upward diffusion–migration from the Cretaceous strata. The concentration gradient, together with the low organic carbon contents in the Cenozoic sediments, would, in that case, have accidentally led to concentration values (nl/g C_{org}) similar to those in the Cretaceous sediments.

A comparison of the compositional features of the light hydrocarbons supports the assumption that the hydrocarbons originated from predominantly terrigenous kerogens. The light hydrocarbon gas chromatograms of Samples 547A-67-2, 118–120 cm (Albian) and 547A-49-2, 118–120 cm (Cenomanian) (Fig. 23) exhibit striking compositional similarities. In addition, the isobutane/*n*-butane and isopentane/*n*-pentane ratios (isoalkanes predominating) may be taken as an indication of the immaturity or marginal maturity of the source organic matter. The hydrocarbon composition of most of the Cenozoic sediment samples is very similar to those shown in Figure 23.

In contrast to this, the hydrocarbons stripped from the three Eocene sediment samples probably containing marine algal kerogens have a different composition, indicated by the presence of additional compounds eluting just before *n*-propane and *n*-butane (Fig. 23). Although definitive identification was impossible because there are no reference standards, these compounds, which appear exclusively in the three Eocene samples from Lithologic Unit III were tentatively assumed to be the olefinic hydrocarbons propene and isobutene, on the basis of their relative retention times.

The relatively high isobutane/*n*-butane ratio in the Lower Cretaceous calcareous claystone (547B-6-1, 136–138 cm), compared to all other sediments investigated (Table 6), can only be interpreted as reflecting slightly different source organic matter in this sample.

INORGANIC GEOCHEMISTRY

A summary of the inorganic geochemical data for Site 547 is given in Table 7 and in Figure 24.

PHYSICAL PROPERTIES

Measurements of compressional-wave velocity, wet-bulk density, porosity, water content, and shear strength were made at Site 547.

The properties measured in Hole 547A are summarized in Tables 8 and 9. Figure 25 shows their variation with depth.

Unit I (0–141.1 m) consists of clayey nannofossil ooze and clayey foraminiferal–nannofossil ooze characterized by velocities near 1.6 km/s, densities near 1.85 g/cm^3, and porosities of about 52%.

Velocity and density in the variably clayey nannofossil ooze and claystone of Unit II (141.1-225.7 m) both show slight increases to about 1.65 km/s and 1.89 g/cm^3, respectively.

The shear strengths measured in Units I and II (Table 9), although quite variable, increase to approximately 200 kPa at a sub-bottom depth of about 200 m.

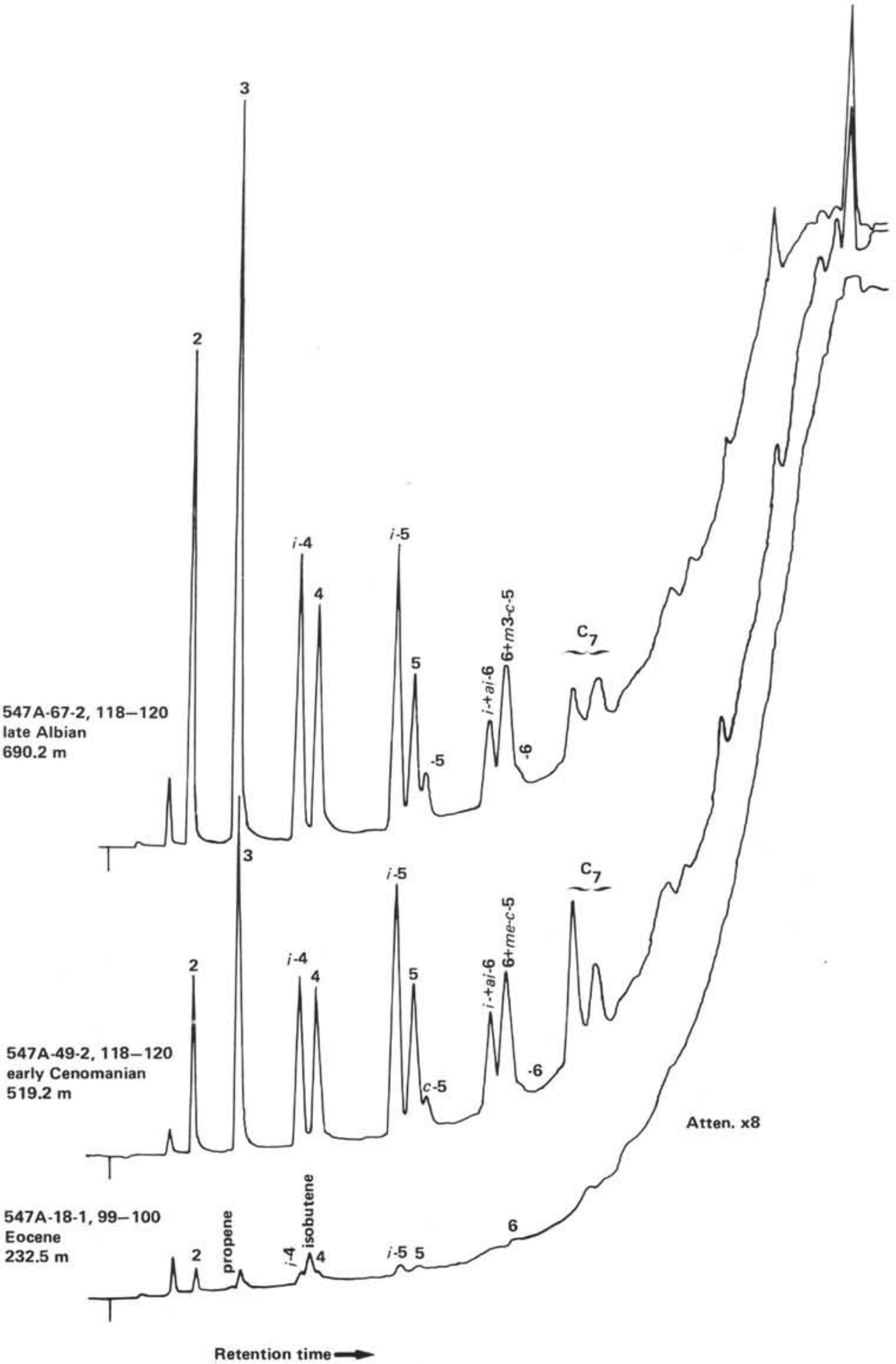

Figure 23. Gas chromatograms of light hydrocarbons obtained from fresh sediment samples by carrier gas stripping. The Albian and Cenomanian samples show a strong compositional similarity, whereas the sample from the Eocene slump sequence has a markedly different light hydrocarbon distribution.

In the conglomeratic clayey gravel and gravelly clay (Unit III, 225.7–279.0 m), velocities are variable but show an increase with depth to over 1.9 km/s. In this unit density increases to 1.95 g/cm^3 whereas porosity decreases to about 45%.

At the top of Subunit IVA (279.0–364.5 m) velocities are initially near 1.7 km/s, but increase relatively rapidly to over 2.0 km/s. Near the base of the subunit horizontal velocities are about 0.10 km/s higher than vertical velocities. Subunit IVB (364.5–422.5 m) exhibits a trend similar to Subunit IVA. Velocities at the top of this subunit are near 1.8 km/s and increase to approximately 2.0 km/s at the bottom. Horizontal velocities are up to 0.12 km/s higher than vertical velocities. Density,

Table 7. Summary of shipboard inorganic geochemical data, Holes 547A and 547B.

Sample (interval in cm)	Sub-bottom depth (m)	pH	Alkalinity (meq/l)	Salinity (‰)	Calcium (mmoles/l)	Magnesium (mmoles/l)	Chlorinity (‰)
IAPSO standard seawater		7.66	2.44	35.2	10.55	64.54	19.378
Surface seawater		8.10	2.43	36.6	11.05	56.73	20.27
Hole 547A							
1-2, 144–150	53.96–54.00	7.41	7.10	35.2	5.44	50.34	19.65
5-4, 144–150	113.96–114.00	7.23	4.99	35.2	9.89	45.89	19.79
9-3, 144–150	150.44–150.50	7.28	3.76	35.2	14.79	42.79	20.00
14-2, 140–150	196.40–196.50	7.20	2.81	35.5	17.90	40.58	20.20
20-5, 140–150	257.90–258.00	7.05	2.70	35.2	20.56	40.26	19.76
25-3, 140–150	302.40–302.50	7.20	2.47	36.3	21.14	40.22	20.62
30-3, 140–150	349.90–350.00	7.13	2.29	36.8	24.43	36.75	21.44
35-1, 140–150	394.40–394.50	—	—	36.3	25.30	35.52	21.44
40-1, 110–120	432.10–432.20	7.46	1.49	35.8	26.63	35.87	20.41
45-2, 140–150	481.40–481.50	7.35	1.44	36.6	28.77	33.85	21.41
50-2, 140–150	528.90–529.00	7.65	1.19	37.4	31.07	32.87	21.65
55-1, 140–150	574.90–575.00	—	—	37.3	31.40	30.38	21.48
60-4, 140–150	626.90–627.00	—	—	38.4	33.36	29.86	21.85
66-2, 140–150	680.90–681.00	—	—	40.8	—	—	—
70-2, 136–150	718.86–719.00	—	—	41.2	37.18	29.28	23.74
Hole 547B[a]							
2-3, 140–150	738.45–738.55			40.7	37.80	29.97	23.21
5-6, 140–150	771.45–771.55			41.2	40.17	30.96	23.63
11,CC (7–14)	819.00–819.07			42.9	48.77	34.69	23.69
25-1, 0–10	932.55–932.65			44.0			
26-3, 135–150	945.92–946.07			44.3	58.49	29.64	23.04
27-1, 140–150	951.95–952.05			45.1			
28-3, 140–150	963.95–964.05			46.8			24.82
30-3, 0–10	980.45–980.55			44.7	57.91	32.79	22.94

Note: Dash indicates an insufficient quantity of water for analyses.

[a] Not enough water available to test for pH and alkalinity in Hole 547B samples.

porosity, and water content also show this repeating trend in Subunits IVA and IVB.

Unit V (422.5-773.0 m) consists of claystone and calcareous claystone characterized by slowly, nearly uniformly increasing vertical velocities above about 660 m sub-bottom depth. However, in this interval the difference between horizontal velocities and vertical velocities is large, and two clearly defined cycles occur (Fig. 26). Below 660 m velocities become quite variable, and horizontal velocities remain considerably higher than vertical velocities. In Unit V density increases from about 1.9 to approximately 2.2 g/cm^3, and porosity steadily decreases from nearly 50 to about 30% at 745 m subbottom depth.

Most interesting is the cyclic behavior of the physical properties in Unit III and Subunit IVB and the associated velocity, density, and porosity inversion at the bases of these units. On the whole, these properties correlate very well with the lithologic units.

The physical properties measured at Hole 547B are summarized in Table 8; Figure 27 shows their variation with depth.

The horizontal velocities in Unit V are near 2.3 km/s except in the lowest several meters, where two samples indicate horizontal velocities near 2.0 km/s. Vertical velocities are 0.15 to 0.39 km/s less than the measured horizontal velocities in this claystone.

Unit VI (773–932.5 m) is a compositionally highly variable unit composed of alternating beds of micritic limestone, nodular limestone, limestone breccia, conglomerates, calcareous shale, sandy limestone, and microcrystalline dolomite. This variable composition is reflected in the variability of the physical properties measured. Velocities range from about 2.0 to 5.7 km/s, densities vary from 2.2 to 2.7 g/cm^3, and porosities between 2 and 29% were measured.

At the top of the sandy mudstone (Unit VII, 932.5–1030 m), velocities drop from the generally higher values in Unit VI to about 2.0 km/s. Velocities near 3.0 km/s were measured in the interval between 960 and 980 m sub-bottom depth, however. Velocities and densities below this depth remain slightly higher than those in the upper 30 m of this unit.

SEISMIC STRATIGRAPHY

Site 547 is located on the northeastern flank of a northwest-trending spur in front of the Mazagan Plateau. This structural high, having an area of about 150 km^2 at 3200 to 3900 m water depth (Figs. 1 and 28), is a subsided continental basement block. Gneissic basement, overlain by pre-Oxfordian reddish brown calcareous and sandy mudstone and muddy sandstone, 58 m thick, was drilled at Site 544.

Site 547 was selected to sample a Jurassic sequence more complete than those at Sites 544 and 545.

The seismic coverage near Site 547 (Fig. 29) includes single trace lines of *Vema* cruise 30-13, *Glomar Challenger* Leg 41 and multichannel seismic lines of *Meteor* cruise *M* 53. From the results at Site 544, we had reason to suppose that the Jurassic sediments at the proposed Site MAZ-9 on shotpoint 596 of line *M* 53-07 (Fig. 30) might have a thickness similar to that at Site 544. Therefore we moved the site location about 1000 m downslope to the northeast.

Site 547 lies in 3940.5 m water depth about 350 m west of *Meteor* line M5307. The seismic record of this line (Figs. 30 and 31) has been used for the seismostratigraphic analysis that follows, and that is summarized in

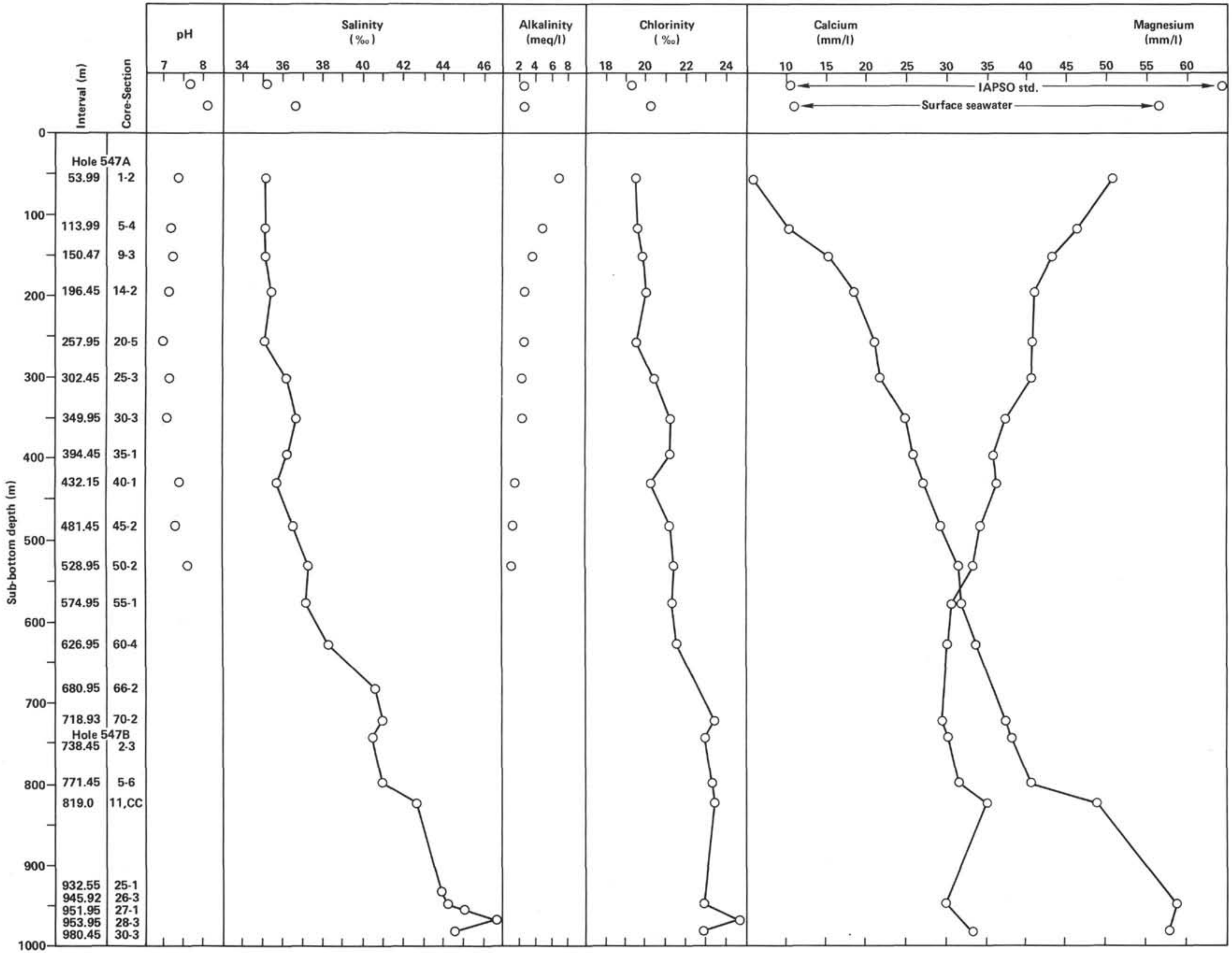

Figure 24. Inorganic geochemistry, Site 547.

Table 8. Summary of physical properties for Holes 547A and 547B.

Sample (interval in cm)	Sub-bottom depth (m)	Velocity		GRAPE		Density (g/cm^3)	Porosity (%)	Water content (%)	Acoustic impedance (10^5 $g/cm^{-2} \cdot s^{-1}$)
		Horizontal (km/s)	Vertical (km/s)	Density (g/cm^3)	Porosity (%)				
Hole 547A									
1-2, 128–130	53.8	1.60				1.80	54.5	30.3	2.89[a]
1-4, 35–37	55.9	1.62				1.83	53.5	29.2	2.96[a]
2-2, 114–116	82.2	1.63				1.83	52.9	28.9	2.98[a]
3-1, 13–15	89.1	1.62				1.87	51.1	27.3	3.02[a]
4-1, 82–84	99.3	1.60				1.87	50.6	27.1	3.00[a]
5-3, 83–85	111.8	1.57				1.84	52.1	28.3	2.88[a]
6-3, 87–89	121.4	1.59				1.85	51 2	27.6	2.93[a]
7-1, 131–133	128.3	1.58				1.85	52.0	28.1	2.92[a]
8-4, 118–120	142.2	1.60				1.88	49.9	26.6	3.00[a]
9-3, 107–109	150.1	1.59				1.84	52.0	28.3	2.92[a]
10-2, 106–108	158.1	1.60				1.85	50.5	27.4	2.96[a]
11-3, 99–101	169.0	1.65				1.88	49.3	26.2	3.10[a]
12-3, 134–136	178.9	1.65				1.88	49.6	26.3	3.10[a]
13-2, 88–90	186.4	1.64				1.88	49.6	26.4	3.09[a]
14-3, 104–106	197.6	1.61				1.89	48.8	25.8	3.04[a]
15-1, 113–115	204.1	1.65				1.89	48.0	25.3	3.12[a]
16-4, 117–119	218.2	1.65	1.64	1.84	51.9	1.83	52.7	28.8	3.00
17-4, 72–74	227.2	1.60	1.59	1.76	56.6	1.74	55.1	31.7	2.76
18-1, 75–77	232.3	1.72	1.71	1.69	60.4	1.69	56.1	33.2	2.88
19-1, 94–96	242.0	1.61	1.61	1.76	56.4	1.72	55.7	32.4	2.78
20-5, 9–11	256.6	1.73	1.77	1.81	53.1	1.80	52.0	29.0	3.18
21-1, 55–57	260.6	2.00	1.91	1.94	45.7	1.95	45.2	23.2	3.72
22-2, 66–68	271.7	1.64	1.62	1.81	53.4	1.77	55.2	31.2	2.87
23-4, 67–69	284.2	1.72	1.68	1.87	50.1	1.82	50.8	27.8	3.05
24-1, 31–33	288.8	1.80	1.77	1.95	45.4	1.94	43.4	22.4	3.44
25-3, 6–8	301.1	1.82	1.79	1.87	50.5	1.87	47.3	25.4	3.35
26-1, 19–21	307.7	1.80	1.72	1.80	54.1	1.77	52.4	29.5	3.05
27-1, 37–39	317.4	1.77	1.72	1.94	45.5	1.92	45.8	23.9	3.31
28-2, 65–67	328.7	1.94	1.85	1.98	42.9	1.99	40.9	20.5	3.68
29-1, 69–71	336.7	1.96	1.87	2.01	41.2	2.00	40.4	20.2	3.74
30-1, 66–68	346.2	2.24	2.15			2.13	32.5	15.3	4.57
30-4, 34–36	350.4	2.06	1.96	2.04	39.7	2.02	40.1	19.9	3.96
32-3, 97–99	368.5	1.87	1.77	1.98	43.1	1.95	44.8	23.0	3.45
33-3, 112–114	378.1	1.83	1.74	1.93	46.2	1.91	48.1	25.2	3.33
34-5, 59–61	390.1	1.95	1.85	1.98	43.3	1.99	43.0	21.6	3.69
35-2, 36–38	394.9	1.88	1.86	2.04	39.4	2.03	41.4	20.4	3.77
36-2, 130–132	400.3	2.04	2.00	2.19	30.9	2.18	32.2	14.8	4.36
37-3, 139–141	406.9	2.02	1.91	2.09	36.6	2.10	37.5	17.9	4.00
38-1, 95–97	413.0	2.04	1.92	2.13	34.0	2.11	36.7	17.4	4.06
39-1, 48–50	422.0	2.13	2.12	2.26	26.5	2.17	33.0	15.2	4.61
40-2, 82–84	433.3	1.92	1.72	1.98	42.9				
41-2, 87–89	442.9	1.96		1.90	47.8	1.92	47.7	24.8	3.76[a]
42-3, 35–37	453.4	2.00	1.78			1.92	49.5	25.8	3.43
43-1, 15–17	459.7	1.93	1.80	1.98	43.0	1.94	47.0	24.2	3.49
44-3, 114–116	473.2	1.82	1.74	1.98	43.2	1.95	47.5	24.3	3.40
45-2, 11–13	480.1	1.92	1.82	2.00	42.2	1.98	45.2	22.9	3.61
46-3, 50–52	491.5	1.92	1.80	1.98	43.0	1.98	45.4	23.0	3.57
47-2, 106–108	500.1	1.95	1.81	2.01	41.6	1.98	44.9	22.7	3.58
48-1, 134–136	508.4	1.83	1.81	1.98	43.3	1.98	45.0	22.7	3.58
49-1, 7–9	516.6	2.00	1.82	1.94	45.3	1.96	46.6	23.8	3.56
50-3, 22–24	529.2	2.00	1.82	2.01	41.4	1.99	44.5	22.3	3.62
51-3, 26–28	538.8	2.05	1.84	2.01	41.5	2.02	42.3	20.9	3.71
52-3, 21–23	548.2	2.11	1.87	2.06	38.2	2.04	42.2	20.7	3.82
53-3, 23–25	557.7	2.09	1.84	2.03	40.0	2.01	42.6	21.2	3.69
54-2, 79–81	566.3	2.05	1.84	2.07	37.7	2.02	42.3	21.0	3.72
55-2, 77–79	575.8	2.08	1.86	2.04	39.5	2.04	42.5	20.8	3.80
56-3, 112–114	587.1	2.12	1.95	2.14	33.9	2.11	37.7	17.9	4.11
57-2, 46–48	594.5	1.99	1.87	2.04	39.4				
58-4, 88–90	607.4	2.02	1.82	2.04	39.7				
59-5, 4–6	617.6	2.08	1.88	2.07	37.7				
60-4, 31–33	625.8	2.10	1.83	2.03	40.4				
61-2, 101–103	633.0	2.13	1.85	2.09	36.5				
62-3, 82–84	643.8	2.21	1.94	2.13	34.1				
63-3, 48–50	653.0	2.27	1.96	2.13	34.3				
64-3, 11–13	662.1	2.28	1.90	2.08	37.1				
64-4, 44–46	664.0	2.51	2.38	2.29	24.7				
65-1, 30–32	668.8	2.19	2.06	2.13	34.5				
66-1, 6–8	678.1	2.32	2.00	2.16	32.6				
66-2, 110–112	680.6	2.39	2.23	2.25	26.8				
67-2, 102–104	690.0	2.20	1.94	2.10	35.8				
68-4, 134–136	702.9	2.12	2.07	2.16	32.0	2.17	32.8	15.2	4.49
69-2, 121–123	709.2	2.41	2.25	2.29	24.5	2.28	26.8	11.7	5.14
70-2, 33–35	717.8	2.32	2.10	2.22	29.2	2.21	30.9	14.0	4.64
71-1, 43–45	725.9	2.37	2.20	2.25	27.1	2.24	28.5	12.7	4.93
72-3, 11–13	738.1	2.04	1.97	2.23	28.1	2.21	32.0	14.5	4.35
73-1, 38–40	744.9	2.21	2.01	2.15	33.1	2.15	34.5	16.0	4.31
Hole 547B									
2-1, 91–93	734.9	2.33	2.01	2.06	38.1	2.07	38.2	18.5	4.15
3-1, 21–23	743.7	2.32	1.93	2.11	35.4	2.09	37.9	18.1	4.03
4-1, 54–56	753.6	2.32	1.98	2.15	33.1	2.11	35.9	17.0	4.17
4-4, 24–26	757.8	2.36	2.17	2.22	28.9	2.23	29.2	13.1	4.84
5-2, 59–61	764.6	1.97	1.82						
6-1, 16–18	772.2	2.10	1.91	2.07	37.6	2.06	39.2	19.1	3.93
6-2, 21–23	773.7	3.18	3.22	2.38	19.7	2.40	19.7	8.2	7.73
6-3, 64–66	775.7	3.56	3.33						
6-4, 122–124	777.7	5.73	5.51	2.68	1.5	2.71	2.4	0.9	14.92
7-2, 2–4	783.0	3.38	3.14			2.49	14.0	5.6	7.82
8-1, 92–94	791.9	3.88	3.47			2.52	12.2	4.8	8.74
8-4, 69–71	796.2	5.28	5.08			2.63	5.0	1.9	13.37
9-2, 79–81	802.8	4.46	4.45			2.61	7.4	2.8	11.61
10-1, 80–82	804.3	5.03	5.00	2.64	3.8	2.63	5.1	1.9	13.14
10-4, 53–55	808.5	2.94	2.68	2.42	17.2	2.42	18.3	7.6	6.48

Table 8. (Continued).

Sample (interval in cm)	Sub-bottom depth (m)	Velocity Horizontal (km/s)	Velocity Vertical (km/s)	GRAPE Density (g/cm^3)	GRAPE Porosity (%)	Density (g/cm^3)	Porosity (%)	Water content (%)	Acoustic impedance (10^5 g/cm^{-2}·s^{-1})
Hole 547B (Cont.)									
11-2, 19-21	811.7	5.39	5.48	2.65	3.2	2.66	4.2	1.6	14.57
11-4, 36-38	814.9	4.01	3.99	2.59	6.6	2.59	8.7	3.4	10.34
12-1, 84-86	819.9	5.41	5.32	2.69	1.0	2.67	2.9	1.1	14.22
13-2, 78-80	830.3	5.68	5.66	2.69	0.8	2.70	2.4	0.9	15.28
14-1, 109-111	838.1	4.31	4.12	2.52	10.6	2.56	9.2	3.6	10.55
15-2, 78-80	848.3	3.00	3.10	2.44	15.5	2.45	16.1	6.5	7.59
16-1, 51-53	855.5			2.51	11.7	2.49	13.9	5.6	
17-1, 94-96	865.0	4.50		2.55	9.3	2.56	10.0	3.9	11.51[a]
18-1, 42-44	873.4	2.03	2.00	2.22	28.9				
19-1, 31-33	882.3	4.85	4.59	2.53	10.1	2.57	8.5	3.3	11.80
20,CC 25-27	894.1	3.41	3.19	2.46	14.7	2.48	14.8	6.0	7.91
21-1, 108-110	896.6	3.59	3.61	2.58	7.3	2.59	14.1	5.5	9.36
22-2, 84-86	907.4	4.10	4.18	2.61	5.8	2.59	9.4	3.6	10.82
23-1, 25-27	914.8	4.61	4.81	2.65	3.3	2.62	7.5	2.9	12.59
24-1, 18-20	923.7	4.79	4.53	2.60	5.9	2.60	9.4	3.6	11.79
25-2, 123-125	935.2	1.98	1.97	2.30	24.1	2.27	28.7	12.6	4.46
26-1, 62-64	942.1	1.98	1.91	2.23	28.5	2.21	32.0	14.5	4.22
27-3, 22-24	953.7	2.06	1.98	2.27	26.0	2.24	31.3	13.9	4.44
28-2, 129-131	962.3	3.20	3.27	2.37	20.1	2.42	18.5	7.6	7.90
30-2, 87-89	979.9	2.88	2.68	2.38	19.5	2.37	23.3	9.8	6.35
31-2, 30-32	988.3	2.58	2.25	2.33	22.3	2.33	24.6	10.5	5.24
32-2, 89-91	997.9	2.35	2.31	2.35	20.9	2.35	25.3	10.8	5.43
33-3, 111-113	1004.1	2.06	2.06	2.31	23.5			11.9	
34-1, 96-98	1010.5	2.47	2.44	2.38	19.3	2.37	24.1	10.2	5.79
35-1, 23-25	1018.7			2.31	23.3			11.3	
36-1, 100-102	1028.5							10.2	

[a] Value computed using horizontal velocity.

Table 9. Shear strength of sediments for Hole 547A.

Core-Section (interval in cm)	Sub-bottom depth (m)	Shear strength (kPa)
1-2, 132-134	53.8	55
1-4, 38-40	55.9	52
2-2, 118-120	82.2	50
3-1, 17-19	89.2	88
4-1, 85-87	99.4	50
5-3, 89-91	111.9	47
6-3, 93-95	121.4	57
7-1, 135-137	128.4	72
8-2, 68-70	138.7	118
8-3, 6-8	139.6	33
8-4, 123-125	142.2	98
9-3, 113-115	150.1	145
10-2, 100-102	158.0	118
11-3, 108-110	169.1	132
12-3, 139-141	178.9	105
13-2, 96-98	186.5	189
14-3, 94-96	197.5	184
15-1, 116-118	204.2	177
16-4, 122-124	218.2	238
17-4, 74-76	227.3	167

Table 10. (For a general description of seismic sequences in the Mazagan region, see the regional synthesis chapter by Winterer and Hinz, this volume.)

Immediately beneath the seafloor is Sequence Ma 1.3, which is 0.18 s (2-way traveltime) thick, characterized by a subparallel reflection pattern. Ma 1.3 unconformably overlies the seismically more or less transparent Sequence Ma 1.2. Seismic Sequence Ma 1.3 correlates well with Unit I, 141 m thick, which consists of pale yellowish brown foraminiferal nannofossil ooze of late Miocene to Quaternary age. The calculated interval velocity is 1.57 km/s. Sequence Ma 1.2 is correlated with the 63 m of middle to lower Miocene greenish gray nannofossil ooze (Unit IIA).

Beneath the Neogene sequences lies Sequence Ma 1.1, which shows a gently dipping, discontinuous subparallel reflection pattern. The lower boundary of this sequence is defined by an unconformity which, from extrapolation of DSDP Sites 415 and 416 (Lancelot and Winterer, 1980), corresponds with reflector Red (Horizon R in Figs. 30 and 31). Sequence Ma 1.1 represents the 219 m of mainly greenish gray clayey nannofossil chalk and claystone of Late Cretaceous to early Oligocene age (Lithologic Units IIB, III, IVA, and IVB). The calculated interval velocity for Sequences Ma 1.1 and Ma 1.2, about 1.7 km/s, is somewhat lower than the measured sonic velocities, which scatter between 1.59 and 2.15 km/s.

A notable feature of the measured vertical and horizontal sonic velocities, in the depth interval 141 to 423 m (seismic Sequences Ma 1.1 and Ma 1.2) is that these can be grouped into three cycles (Fig. 32). Each cycle is characterized by an increase of the sonic velocities with depth. The sonic velocity cycles are not unequivocally defined in the seismic records although there is apparently a correlation between the sonic velocity cycles and the identified sedimentological units.

Sequence Ma 2.3 forms a nearly transparent wedge with indications of landward onlap onto the sloping surface of Sequence Ma 3, represented by the Blue reflector (horizon B). Seaward, Sequence Ma 2.3 terminates against the domed Blue reflector, which indicates that the structural high drilled at Site 544 already existed during deposition of Sequence Ma 2.3 and probably acted as a barrier to sediment transport.

At Site 547, Sequence Ma 2.3 is 0.33 s thick. It correlates well with Cretaceous Unit V, consisting mainly of 350 m of grayish green nannofossil-bearing claystone and

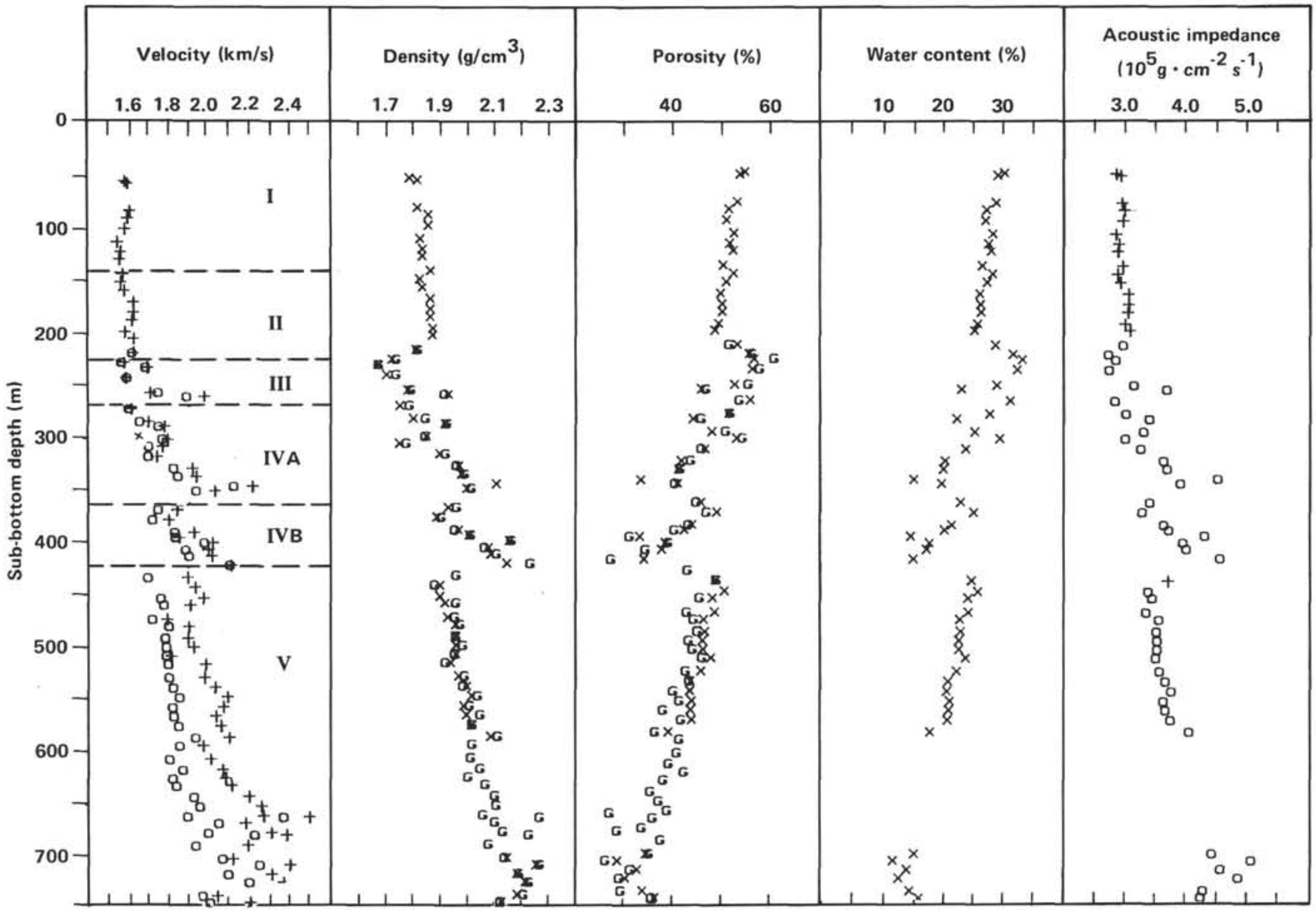

Figure 25. Physical properties versus depth, Hole 547A. +, o represent horizontal and vertical values, respectively. X, G represent gravimetric (immersion) and GRAPE values, respectively.

mudstone. The distribution of the measured vertical and horizontal sonic velocities is very interesting. Within the depth interval from 422 to 660 m, there is linear increase of the vertical sonic velocities with depth, which can be roughly approximated by

$$V_Z = 1510 (V_0) + 0.59(g) Z,$$

where V_0(m/s) is the velocity at seafloor, V_Z(m/s) is the velocity at a depth Z (meters) and $g(s^{-1})$ is the velocity gradient. In contrast to the more or less uniform increase of the vertical sonic velocities, the horizontal sonic velocities show a cyclic grouping. Four cycles are recognizable in the depth interval from 423 to about 660 m (Fig. 32). Within each cycle, the horizontal velocities increase with depth but with a higher gradient than the corresponding vertical sonic velocities. This strange difference in the distribution of the vertical and horizontal sonic velocities might indicate that this Cretaceous interval consists of lithologically similar flow units deposited on a slope in such a manner that the supply and texture of the sediments change systematically from the bottom to the top of the cycle. It is assumed that the horizontal sonic velocities reflect such change, whereas the vertical velocities reflect the overall compaction. Farther away from the basement block, Sequence Ma 2.3 is characterized by a subparallel reflection pattern. The underlying Sequence Ma 2.2, not drilled at Site 547, thins toward the steep flanks of the basement high, indicating that the steeply down-dipping and fault-controlled flanks already existed before the deposition of Sequence Ma 2.2, which is interpreted as Lower Cretaceous pelagic marl and limestone.

At Site 547, the Cretaceous Sequence Ma 2.3 unconformably overlies the Blue reflector, which forms the upper boundary of Sequence Ma 3.2 and represents the top of the drilled Jurassic limestones (Units VIA and VIB). Near Site 547, Sequence Ma 3.2 is distinguished by two parallel, high-amplitude reflectors. Whether each of these amplitude peaks represents a petrophysical boundary cannot be decided without downhole logging. Under the assumption that the lower peak of reflection horizon Blue at Site 547 represents the base of the 159.5 m thickness of Jurassic strata, one calculates an interval velocity of about 4.15 km/s. This value seems reasonable because interval velocities of 4.1 to 4.3 km/s have been derived from stacking velocities at shotpoints 505–513 and 666–673 of *Meteor* line M 53-07. Most of the measured vertical sonic velocities in this interval lie between 3 and 5.6 km/s. Seismic Sequence Ma 3.2 includes Jurassic Lithologic Units VIA and VIB.

Seismic Sequence Ma 3.2 overlies Unit VII, which consists of 97.5 m of grayish red and sandy mudstone and is represented by seismic Sequence Ma 3.1. The bulk of

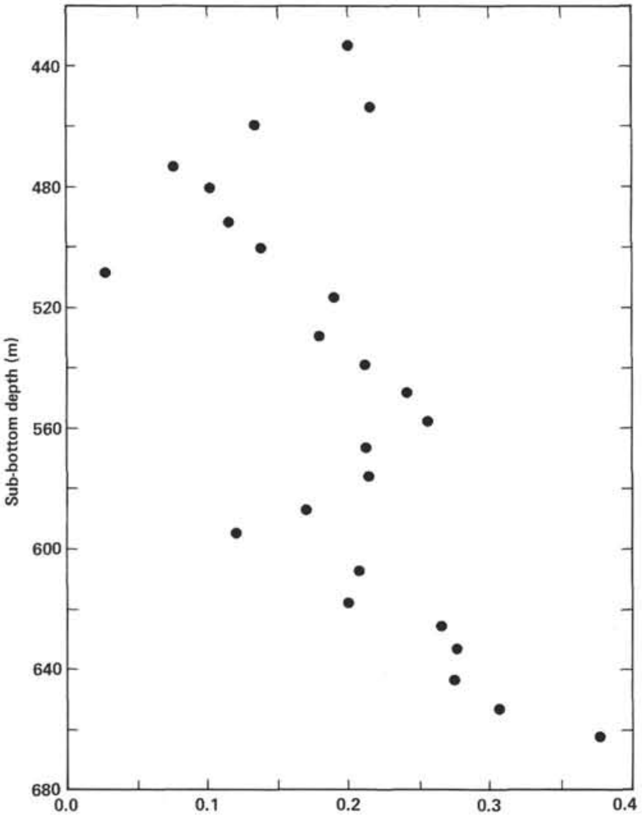

Figure 26. Difference between horizontal and vertical velocities versus depth, Unit V, Hole 547A.

the sonic velocities from Sequence Ma 3.1 lie between 1.9 and 2.7 km/s. In the seismic records at Site 547, a diffraction-like pattern occurs in a depth interval of 1 to 1.05 s beneath the seafloor; this could represent the igneous basement. Assuming an interval velocity of 2.25 km/s, this depth interval would result in a basement depth of 1030 to 1090 m beneath the seafloor. After 1030 m were drilled, Site 547 had to be abandoned because the bit was abrading rapidly and we had run out of time for drilling.

The seismic data indicate that the enormous subsidence of the basin seaward of the continental basement block drilled at Site 544 occurred at least partly after deposition of the Jurassic limestones drilled at Site 544 and before or at the beginning of deposition of Sequence Ma 2.2, consisting of Lower Cretaceous pelagic marl and limestone. The rapid subsidence may have been associated with movements along listric faults and with halokinesis, which together lead to the development of the complex seismic structures so widespread within the deep-water area off Morocco. Smaller-scale normal faulting and tilting probably occurred in the Mazagan slope area at the same time.

SUMMARY AND CONCLUSIONS

Despite the failure to reach crystalline basement, the drilling at Site 547 must be judged highly successful. We obtained a set of continuous cores extending from the Pleistocene to the lowest Jurassic, or perhaps even the Upper Triassic. The Paleogene and Upper Cretaceous sections are remarkable for the presence of debris flows that reworked blocks of older pelagic sediments, and the Middle Cretaceous claystone sequence confirms and extends the findings at Site 545, that these rocks were deposited on a continental slope and almost continuously eroded and redeposited farther downslope as intraformational conglomerates. The Jurassic sediments include micritic nodular limestone, probably deposited at moderate depth and intercalated with breccia containing shallower-water limestone clasts. Claystone beds and dolomitic breccia occur near the base of the marine Jurassic sequence, which overlies a section of red beds at least 98 m thick. The major features of the section are displayed in Figures 33–35.

Neogene Sediments

Neogene sediments at Site 547 are very like those at Site 545, without the limestone gravel beds at the latter site. Down through the late Miocene (N17), the sediments are well-oxidized foraminiferal nannofossil ooze, generally slightly clayey. A small hiatus may have cut out much of the Pliocene. Terrigenous detritus is abundant in these sediments: about 40% in the Pleistocene and about 25% below that level. We interpret these sediments as being deposited above the foraminiferal lysocline at an accumulation rate of ~22 m/m.y. (about 2 g/cm^2 per 10^3 yr.).

The ubiquitous regional unconformity between upper Miocene and middle Miocene sediments occurs at Site 547, here with a time value of about 3–4 m.y.

The beds beneath the unconformity, as at the other sites drilled on Leg 79, are greenish gray clayey nannofossil ooze and nannofossil claystone. The clay content decreases from about 35% at the top of the unit to about 25% at the base. Sediments with siliceous fossils occur only in Core 14, in the lower Miocene. Fossils show the age span of this unit, which is about 63 m thick, to be late middle Miocene (N15) to early Miocene (N4–N6). The lowest beds may be a rather condensed section or even include a hiatus, since the age of the material changes from early middle Miocene (N9–N11) to a level well down in the early Miocene in just one core. The rate of accumulation was only about 7 m/m.y. (about 0.7 g/cm^2 per 10^3 yr.). We interpret this unit to represent pelagic deposition above the CCD but probably a bit below the foraminiferal lysocline.

Paleogene and Upper Cretaceous Sediments

A hiatus separates the lower Miocene sediments from underlying lower Oligocene to upper Eocene beds. This hiatus is doubtless related to the well-known Oligocene erosional "event" recorded at many places around the margins of the Atlantic, but the data from drilling at Site 547 shed no new light on either its precise timing or its causes.

The Paleogene and Upper Cretaceous sequence comprises four units: an upper pelagic nannofossil ooze, a

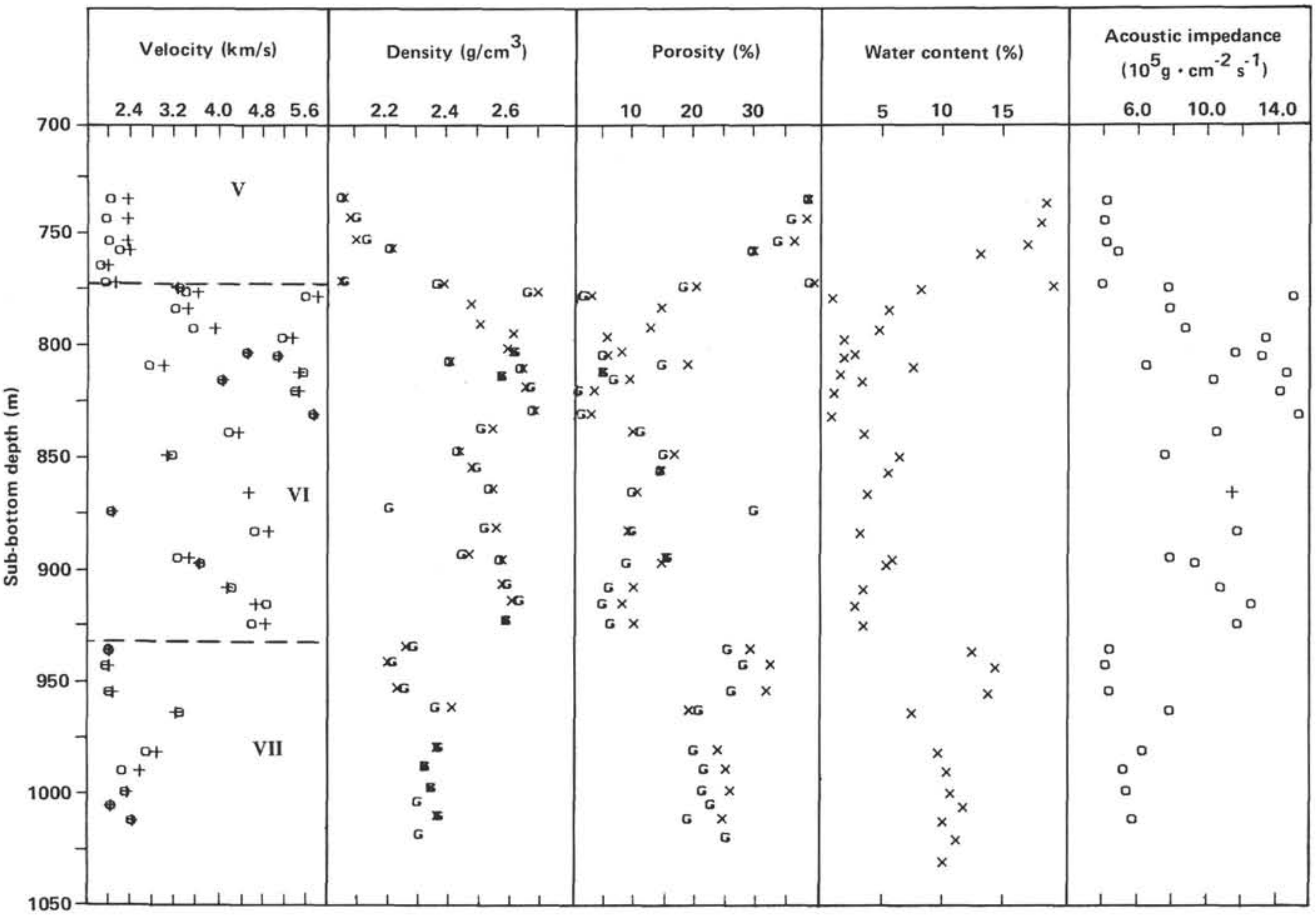

Figure 27. Physical properties versus depth, Hole 547B. + ,o represent horizontal and vertical values, respectively. X,G represent gravimetric (immersion) and GRAPE values.

unit of debris flows, a lower pelagic siliceous nannofossil chalk, and a lower unit of debris flows.

The upper unit, about 21 m thick, consists of greenish clayey nannofossil ooze very like that in the overlying Miocene. Fossils, including radiolarians, indicate a late Eocene to early or middle Oligocene age. The rate of accumulation is not possible to estimate with the paleontological data at hand, but the similarity in lithology with the Miocene suggests a similar rate (about 7 m/m.y., or 0.7 g/cm^2 per 10^3 yr.).

Next below is a unit about 53 m thick consisting largely of conglomerate beds, made of clasts mainly of claystone, nannofossil claystone, clayey chalk, nannofossil chalk, and chert; one is as large as 4.2 m, but most are about 5 cm in diameter. The clasts float in a nannofossil chalk matrix and are somewhat flattened by compaction. A few *in situ* nannofossil chalk beds occur. Terrigenous debris constitutes only 1-5%. Fossils in the clasts and in the matrix represent a broad range of ages, from various parts of the Paleogene and the Late Cretaceous. The youngest fossils are late Eocene in age, and we therefore regard the whole sequence as being of that age. We interpret this unit as debris flows that carried material eroded—probably in parts by slumps and slides—from the upper part of the continental slope, where Upper Cretaceous chalks are still preserved today near the edge of the Mazagan Plateau (see Fig. 23 of Site 545 report).

Below the debris flows, the lower pelagic unit, which is about 86 m thick, consists of greenish gray clayey nannofossil chalk and subordinate nannofossil claystone. Siliceous fossil remains are common, especially in the lower half of the unit, and porcellanite nodules are also common. The age of this unit ranges from earliest Eocene at the top to early Paleocene at the base, and the rate of accumulation was about 6 m/m.y. (0.7 g/cm^2 per 10^3 yr.), about the same as for the pelagic middle Miocene.

The lowest unit in this sequence, of early Paleocene and Late Cretaceous age, is another pile of debris flows, totaling about 58 m in thickness. The clasts in the debris flows are varieties of greenish nannofossil claystone and clayey nannofossil chalk, plus a few pieces of porcellanite. The clasts contain Late Cretaceous (Maestrichtian and Campanian) microfossils.

Middle Cretaceous Rocks

Middle Cretaceous sediments are about 350 m thick at Site 547, and range in age from late Cenomanian at the top to late Albian at the base. Lithologically, these rocks are very like those cored at Site 545, and comprise

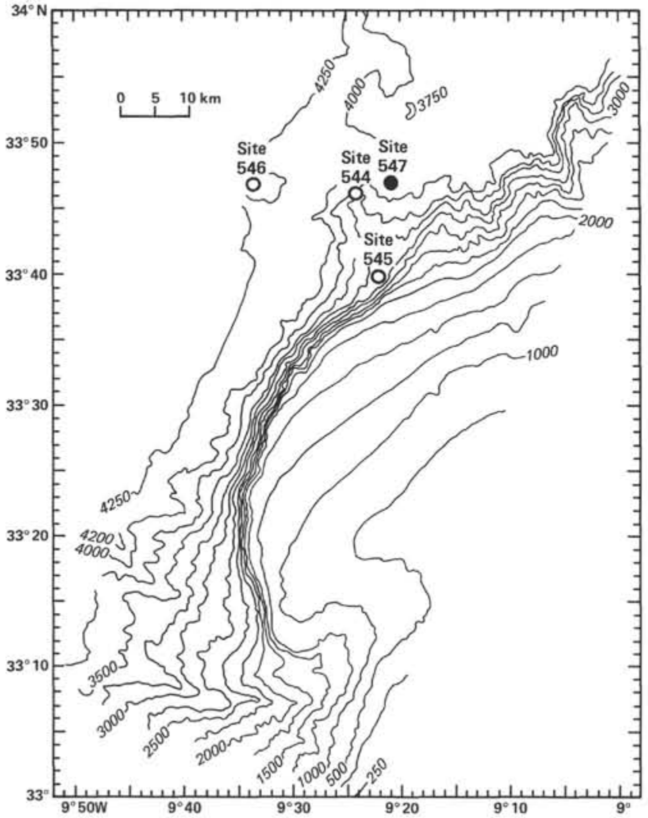

Figure 28. Bathymetric map of the Mazagan continental margin segment, from echo soundings of *Meteor* cruises 9/1967, 39/1975, 53/1980, the *Valdivia* West Africa cruise 1979, and the SEAZAGAN Seabeam survey of *Jean Charcot* (Auzende et al., this volume). Depths in m.

greenish nannofossil claystone and nannofossil-bearing claystone interbedded with layers of intraformational conglomerate consisting of flat claystone pebbles. Burrows are ubiquitous. Planar laminated mudstone, with molluscan shell fragments, occurs as a minor lithology in the lower part of the unit. The clay mineralogy is dominated by swelling clays and waxy claystone, and the lower 157 m by waxy clays alone. The waxy clay gives XRD patterns of kaolinite and illite, whereas the swelling clay also contains mixed-layer smectite–illite. The carbonate content (mainly nannofossils) of the claystone averages about 25%. The rate of accumulation of the Cretaceous claystone was about 35 m/m.y. (about 4.5 g/cm^2 per 10^3 yr.).

We interpret the middle Cretaceous beds as representing deposition on the continental slope above the CCD, in well-oxygenated waters. Downslope resedimentation was common, and minor slumps were frequent. Erosion, perhaps by mass wasting, supplied clasts of recently deposited and hence only weakly consolidated claystone to mud flows. Because certain of its faunal zones are thicker than might be expected, we suggest that the Cretaceous may be sliced internally by low-angle slide surfaces that repeat the section. In sum, gravity-driven resedimentation processes were active at almost all scales, from grain-by-grain resuspension through debris flows to large more or less intact slide sheets.

Jurassic Rocks

Upper Albian sediments at 773 m rest on a very condensed (about 1 m) Neocomian section, which in turn rests on lowermost Cretaceous–uppermost Jurassic limestone. The Neocomian beds include graded layers and the fossils (Valanginian–Hauterivian) may be resedimented.

The Jurassic marine strata comprise three stratigraphic units, overlying red beds.

1. Upper and middle Jurassic, pale reddish and greenish micritic and nodular limestone, interbedded with resedimented limestone breccia (from 547B-6-2, 8 cm through Core 547B-10; about 36 m thick). Bajocian–Callovian to Berriasian.
2. Lower Jurassic limestone breccia, with a few layers of laminated micrite. Breccia layers are commonly separated by crusts and include cavities filled by internal sediments (Cores 11 through 14; about 36 m thick). Upper Pliensbachian.
3. Lower Jurassic pale yellowish brown brecciated nodular limestone and limestone breccia, with occasional layers of gray micrite and mudstone. A stromatolitic(?) layer occurs at the base (Cores 547B-15 to 547B-24-1, 73 cm; about 79 m thick). Hettangian(?) to lower Pliensbachian.

The highest *in situ* sediments below the Cretaceous are micritic nodular limestone with abundant calpionellids indicating an early Berriasian–latest Tithonian age. Alternating pale greenish and reddish brown nodular limestone comprises about 80% and clearly resedimented limestone breccia about 20% of the section down to about 795 m, where the breccia becomes the main lithology.

The nodular limestone strongly resembles the Upper Jurassic nodular limestone units in Tethys. Some layers are only vaguely nodular and resemble the Rosso ad Aptici; other beds, particularly the reddish ones, have isolated nodules that resemble those in parts of the Rosso Ammonitico Superiore (Winterer and Bosellini, 1981). Aptychi and *Saccocoma* occur in these *in situ* beds, along with ammonites, radiolarians, and tiny pelagic mollusks.

The breccia layers are generally 10–30 cm thick and contain unsorted clasts from a few millimeters to 15 cm in size. The breccias are both mud- and grain-supported and the matrix is micritic. The clasts comprise reddish and greenish biomicrite and peloidal grainstone. A few grainstone beds contain clasts that include coated grains, oolites, and skeletal debris. Current-sorted large *Bositra* occur in Core 8 (Fig. 18). Detrital quartz appears at about 805 m and increases in abundance downward.

The next unit below consists mainly of limestone breccia. The breccia beds, 20–40 cm thick, are clast supported, with clasts ranging from sand-sized to 18 cm. The clasts consist of light gray limestone with oncolites, ooids, coated thin-shelled mollusk fragments, sponge spicules, thick-shelled mollusk fragments, and ammonites. The breccia beds are commonly separated by *in situ* crusts a few millimeters thick. Internal sediment and geopetal fabrics are common. Detrital quartz continues to in-

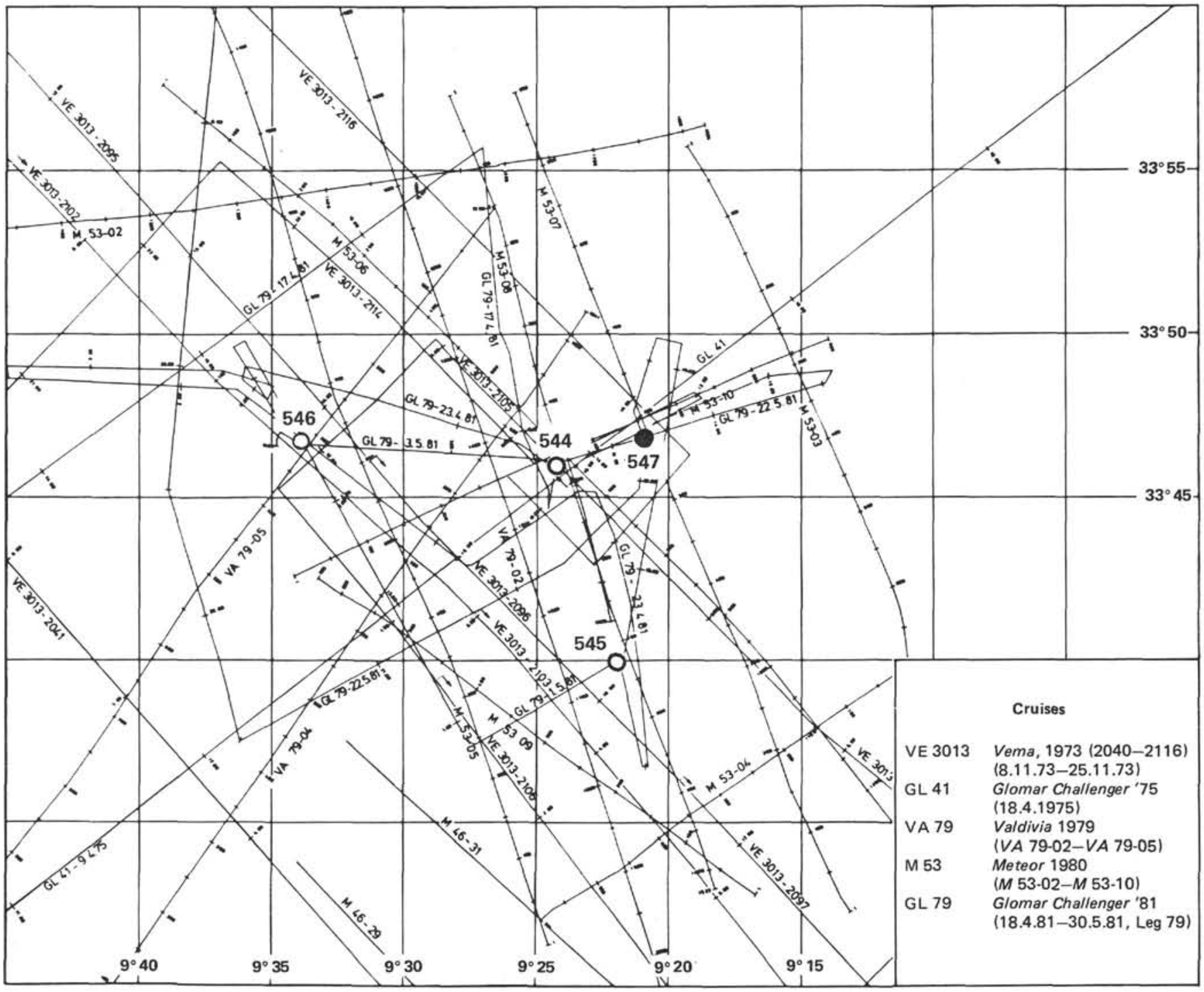

Figure 29. Location of seismic profiles around Site 547.

crease in abundance downward, accompanied by clasts of feldspathic sandstone.

A large hiatus or time of very slow accumulation, possibly extending through much of the Middle Jurassic, separates the upper two units. Pliensbachian-earliest Toarcian foraminifers and nannofossils occur in 547B-11,CC and Bajocian-Callovian foraminifers are identified from 547B-10-3, 125 cm. No age-diagnostic fossils were identified between. The many crusts between breccia layers in Core 11 suggests many small hiatuses.

Beneath the breccia unit is a thickness of about 87 m of mainly yellowish brown brecciated nodular limestone and limestone breccia, commonly with nodules floating in a darker brown clay matrix. A layer of dark organic matter-rich claystone of Pliensbachian age occurs at about 848 m, near the top of the nodular limestone unit.

Beginning at 891 m, for the next 33 m, the stratigraphic succession cored is complex. At the top are a few meters of olive black mudstone that yielded a well-preserved benthic foraminiferal assemblage of early Pliensbachian age. Next below are beds of dolomitic limestone-mudstone breccia, with many color varieties of micritic clasts in a mudstone matrix. Near the base is a layer of laminated micrite with fenestral fabric, resembling stromatolites. At the very base of the unit above the red beds is a dolomitized limestone breccia.

We interpret the succession from 773 to 890 m as representing deposition of more-or-less pelagic limestone at a moderate depth, below the aragonite compensation depth. A depth of a few hundred meters would probably be appropriate for nodular limestone of the type cored here (Winterer and Bosellini, 1981). Limestone clasts from a nearby environment of much shallower water were carried into the nodular limestone milieu as mass movements, perhaps down a fairly steep slope. Many of the limestone breccia fragments are virtually identical with the reddish limestone cored at Site 544, on the nearby gneissic ridge. Site 547 lies downslope from the summit of that ridge, with perhaps one or two treads of a fault-controlled staircase between. The ridge is therefore a plausible source for the breccia clasts. The lime-

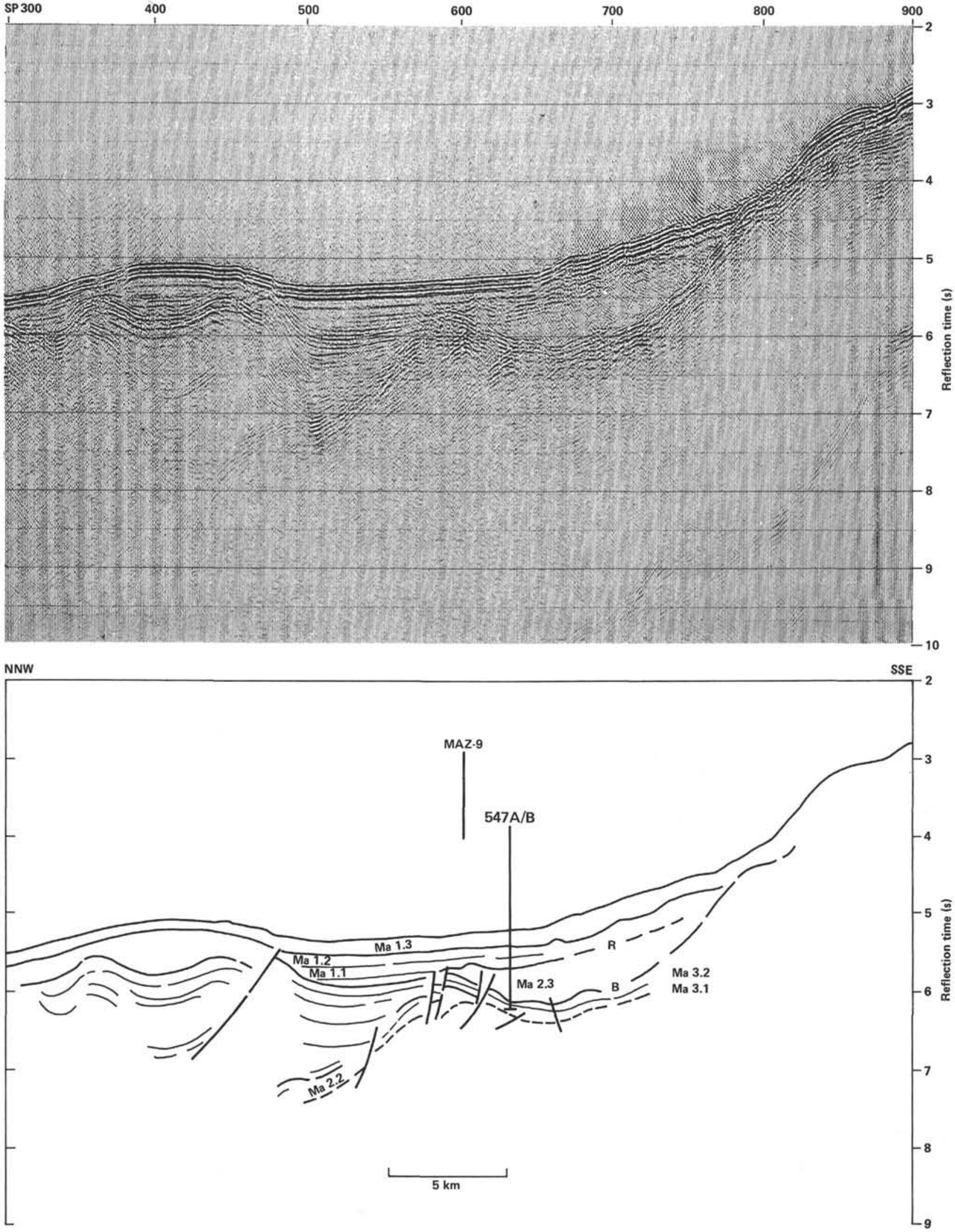

Figure 30. Seismic record of *Meteor* line *M* 53-07 and line drawing with identified seismic sequences and reflectors near Site 547. Location of the profile is indicated in Figure 29.

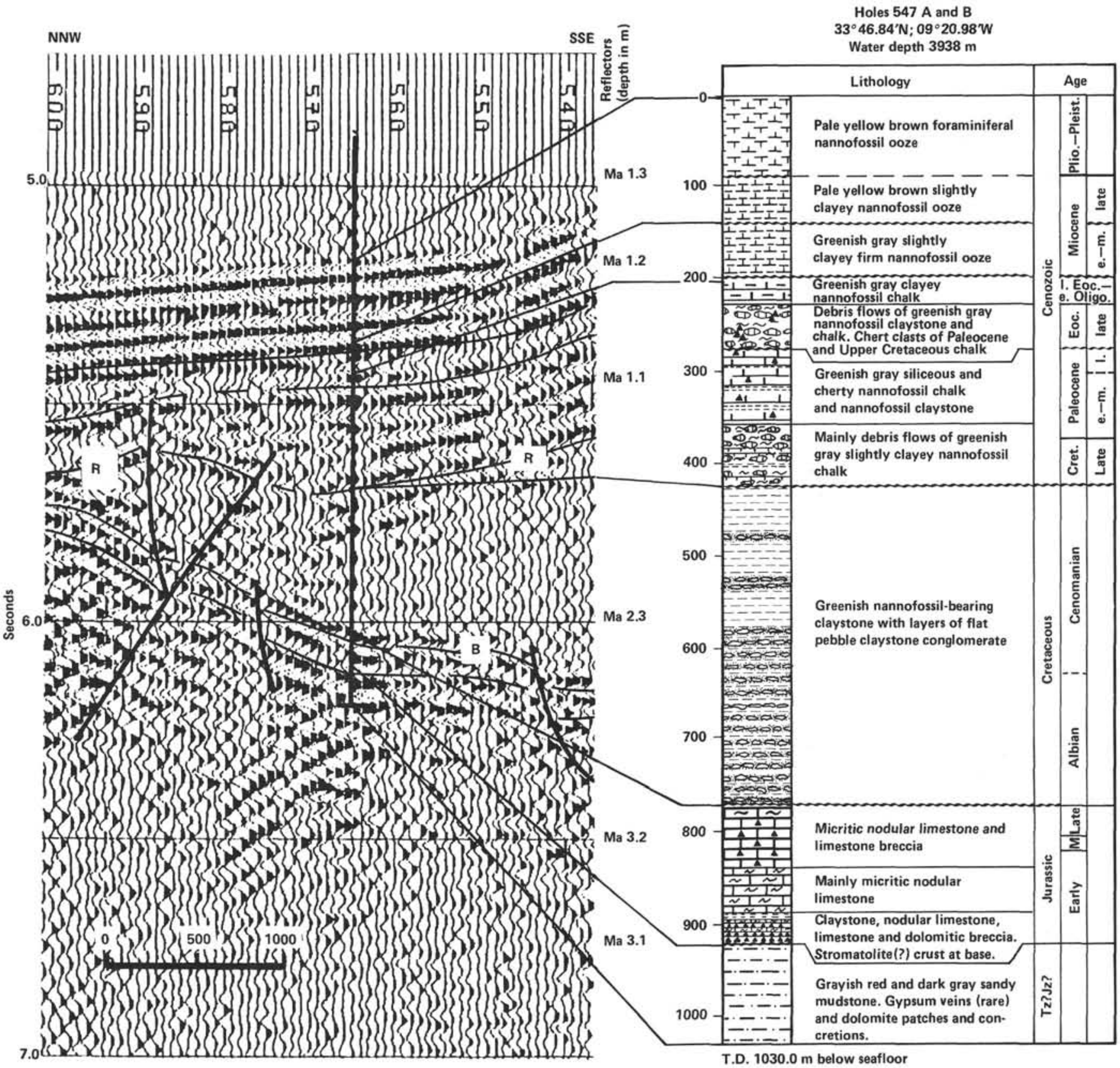

Figure 31. Correlation of seismic sequences and reflectors with drilling results at Site 547. B, blue reflector; R, red reflector.

stone at Site 544 included a somewhat open water facies at the top, containing *Protoglobigerina* and *Bositra*. That facies is poorly represented in the Site 547 breccias.

The claystone at about 891 m suggests more terrigenous influence, and the benthic foraminiferal faunas may indicate shallower water than for the overlying rocks. Although the dolomitic breccia and the stromatolites(?) at the base suggest very shallow water environments, radiolarians occur as low as Core 547B-23, only about 15 m from the base of the marine Jurassic succession.

The lowest lithologic unit at Site 547, at least 106 m thick, consists of grayish red sandy mudstone, interbedded in the upper part of the unit with dark gray sandy mudstone. Bedding is obscure, and sand grains and granules of quartz and feldspar occur as floating grains and as pods and ill-defined laminae, constituting from about 5 to 20% of the rock. A few veins of gypsum were cored, and dolomitic concretions and patches occur. Brecciated intervals were puzzling, because we could not consistently distinguish between original claystone breccia and rocks brecciated during the coring process.

At the very base of the section cored, from 1027.5 to 1030 m, are abundant, loose, poorly rounded pebbles of dolomite.

We interpret this red-bed sequence as a nonmarine deposit, and correlate it with the red beds at Site 544. Its age, as indicated by palynomorphs, is Rhaetian(?) to Hettangian (Fenton, this volume).

The cross sections (Figs. 33 and 34) shows the relations of Site 547 to the basement high drilled at Site 544.

Table 10. Reflection times to key reflectors and interval velocities between reflectors at Site 547.

Seismic sequences	Reflection time beneath seafloor (s)	Sub-bottom depth (m)	Calculated interval velocity (km/s)	Measured sonic velocity (km/s)	Calculated average velocity from seafloor (km/s)	Stratigraphy/Lithology
Ma 1.3			1.57	1.5–1.65		Nannofossil ooze of late Miocene to early Pleistocene age; Unit I
	0.18	141.1			1.57	
Ma 1.2			1.83	1.55–1.65		Nannofossil ooze and claystone of early to middle Miocene age; Unit IIA
	0.25	204.0	1.7		1.64	
Ma 1.1			1.67	1.6–2.05		Clayey nannofossil chalk and claystone of Late Cretaceous to early Oligocene age; Units IIB, III, and IV
Red Reflector	0.51	422.6			1.66	
Ma 2.3			2.12	1.7–2.5		Albian and Cenomanian claystone and calcareous claystone; Unit V
	0.84	772.0			1.84	
Ma 3.2			4.3	2.7–5.5		Jurassic limestone; Unit VI
	0.91	924.0			2.03	
Ma 3.1		not drilled		1.8–3.5		Grayish red to dark gray sandy claystone and red sandy mudstone; Unit VII
	1.0					
Acoustic basement						

REFERENCES

Boutefeu, A., 1980. Pyrolysis study of organic matter from deep Sea Drilling Project Sites 370 (Leg 41), 415, 416 (Leg 50). *In* Lancelot, Y., Winterer, W. L., et al., *Init. Repts. DSDP*, 50: Washington (U.S. Govt. Printing Office), 555–566.

Cornford, C., Rullkötter, J., and Welte, D. H., 1979. Organic geochemistry of DSDP Leg 47A, Site 397 eastern North Atlantic: organic petrography and extractable hydrocarbons. *In* von Rad, U., Ryan, W.B.F., et al., *Init. Repts. DSDP*, 47, Pt. 1: Washington (U.S. Govt. Printing Office), 511–522.

Espitalié, J., Laporte, J. L., Madec, M., Marquis, F., Leplat, P., Paulet, J., and Boutefeu, A., 1977. Méthode rapide de caractérisation des roches-mères, de leur potentiel pétrolier et de leur degré dévolution. *Rev. Inst. Fr. Pet.*, 32:23–42.

Gartner, S., 1977. Calcareous nannofossil biostratigraphy and revised zonation of the Pleistocene. *Mar. Micropal.*, 2:1–25.

Hamilton, G., 1979. Lower and Middle Jurassic calcareous nannofossils from Portugal. *Eclog. Geol. Helv.*, 72(1):1–17.

Jansa, L. F., Remane, J., and Ascoli, P., 1980. Calpionellid and foraminiferal-ostracod biostratigraphy at the Jurassic-Cretaceous boundary, offshore eastern Canada. *Riv. Ital. Paleontol.*, 86:67–126.

Okada, H., and Bukry, D., 1980. Supplementary modification and introduction of code numbers to the low-latitude coccolith biostratigraphic zonation (Bukry, 1973; 1975). *Mar. Micropal.*, 5:321–325.

Pessagno, E. A., Jr., 1976. Radiolarian zonation and stratigraphy of the Upper Cretaceous portion of the Great Valley Sequence, California Coast Ranges. *Micropaleontol. Press Spec. Publ. 2:*1–95.

Rullkötter, J., Cornford, C., and Welte, D. H., 1982. Geochemistry and petrography of organic matter in Northwest African continental margin sediments: Quantity, provenance, depositional environment, and temperature history. *In* von Rad, U. et al. (Eds.), *Geology of the Northwest African Continental Margin:* Berlin (Springer Verlag), pp. 686–703.

Seilacher, A., 1967. Bathymetry of trace fossils. *Mar. Geol.*, 5: 413–428.

Stainforth, R. M., Lamb, J. L., Luterbacher, H., Beard, J. H., and Jeffords, R. M., 1975. *Cenozoic Planktonic Foraminiferal Zonation and Characteristics of Index Forms.* Univ. Kansas Paleontol. Contrib., 62.

Thierstein, H. R., 1976. Mesozoic calcareous nannoplankton biostratigraphy of marine sediments. *Mar. Micropal.*, 1:325–362.

van Hinte, J. E., 1976. A Cretaceous time scale. *Am. Assoc. Pet. Geol. Bull.*, 60:498–516.

Winterer, E. L., and Bosellini, A., 1981. Subsidence and sedimentation on a Juraissic passive continental margin, Southern Alps, Italy. *Am. Assoc. Pet. Geol. Bull.*, 65:394–421.

Date of Acceptance: November 7, 1983

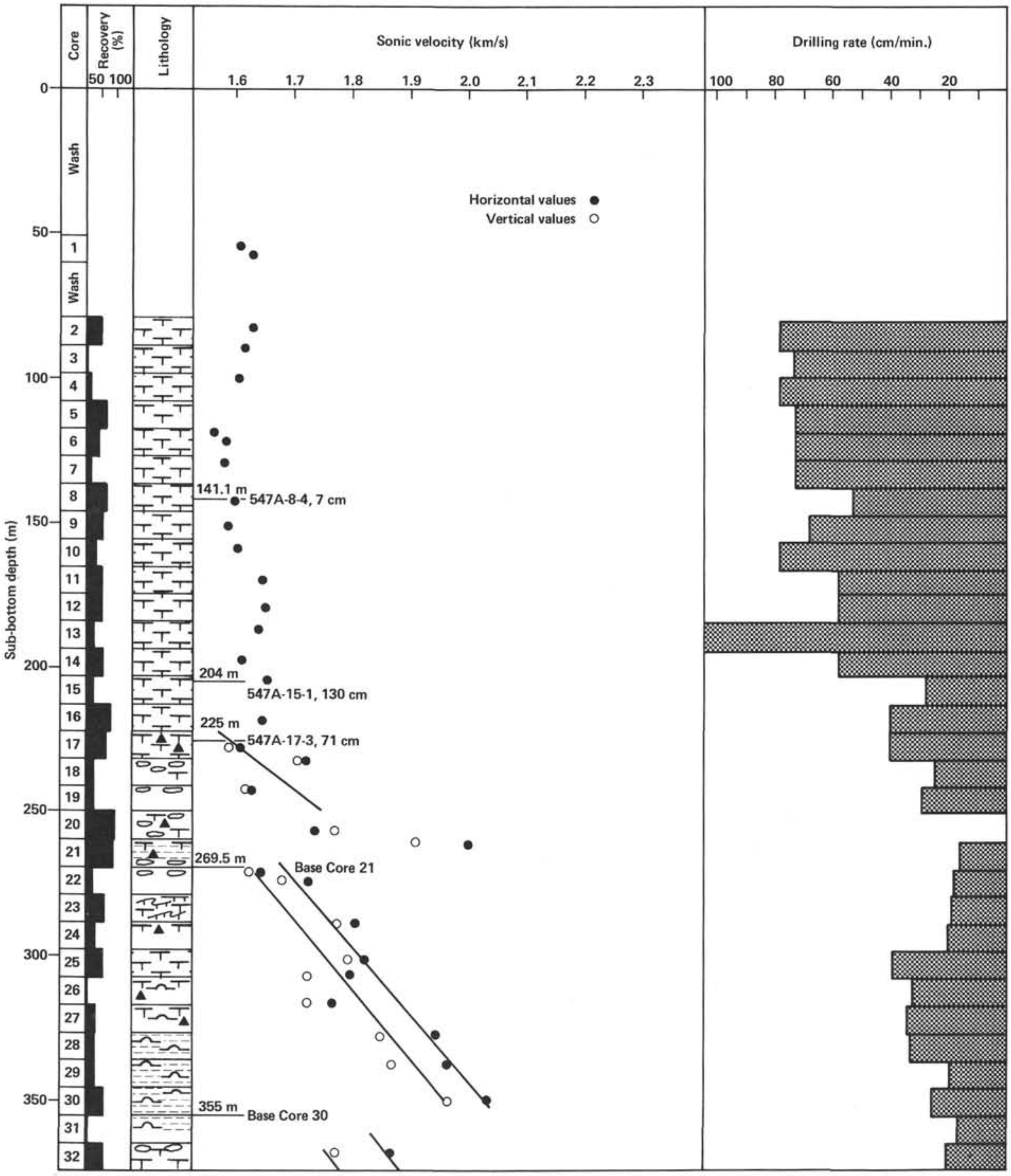

Figure 32. Vertical distribution of horizontal and vertical sonic velocities correlated with drilling and recovery rates.

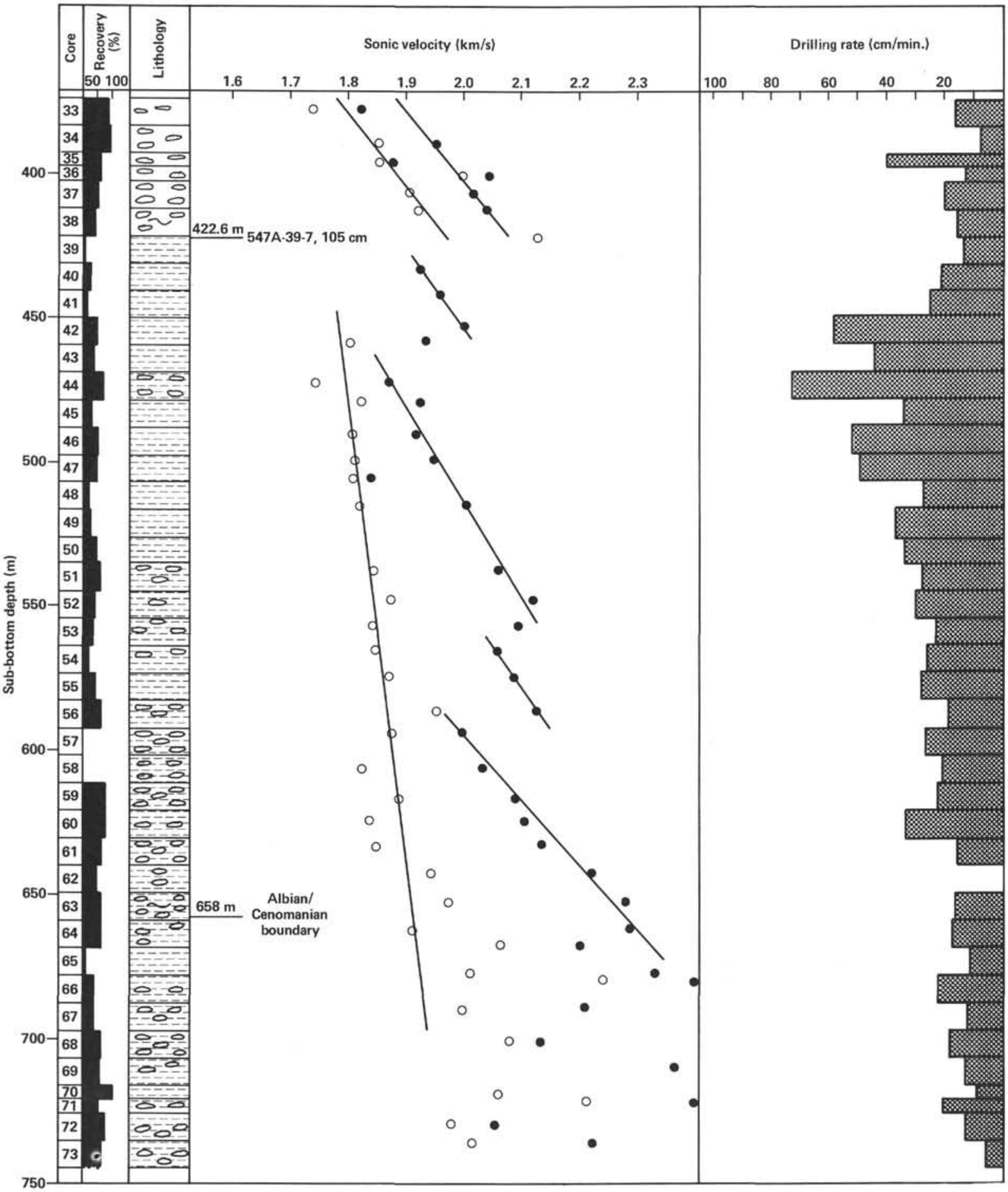

Figure 32. (Continued).

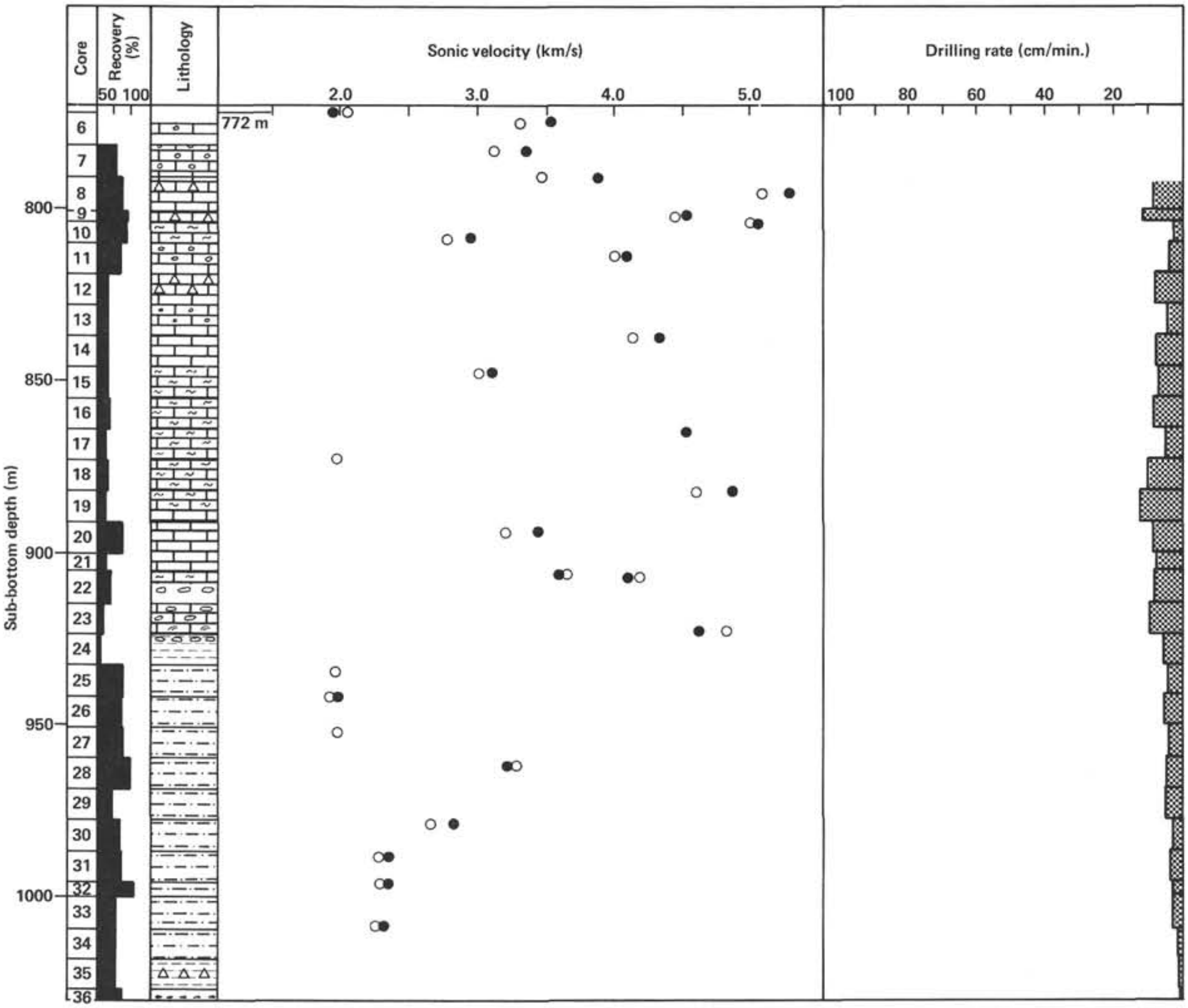

Figure 32. (Continued).

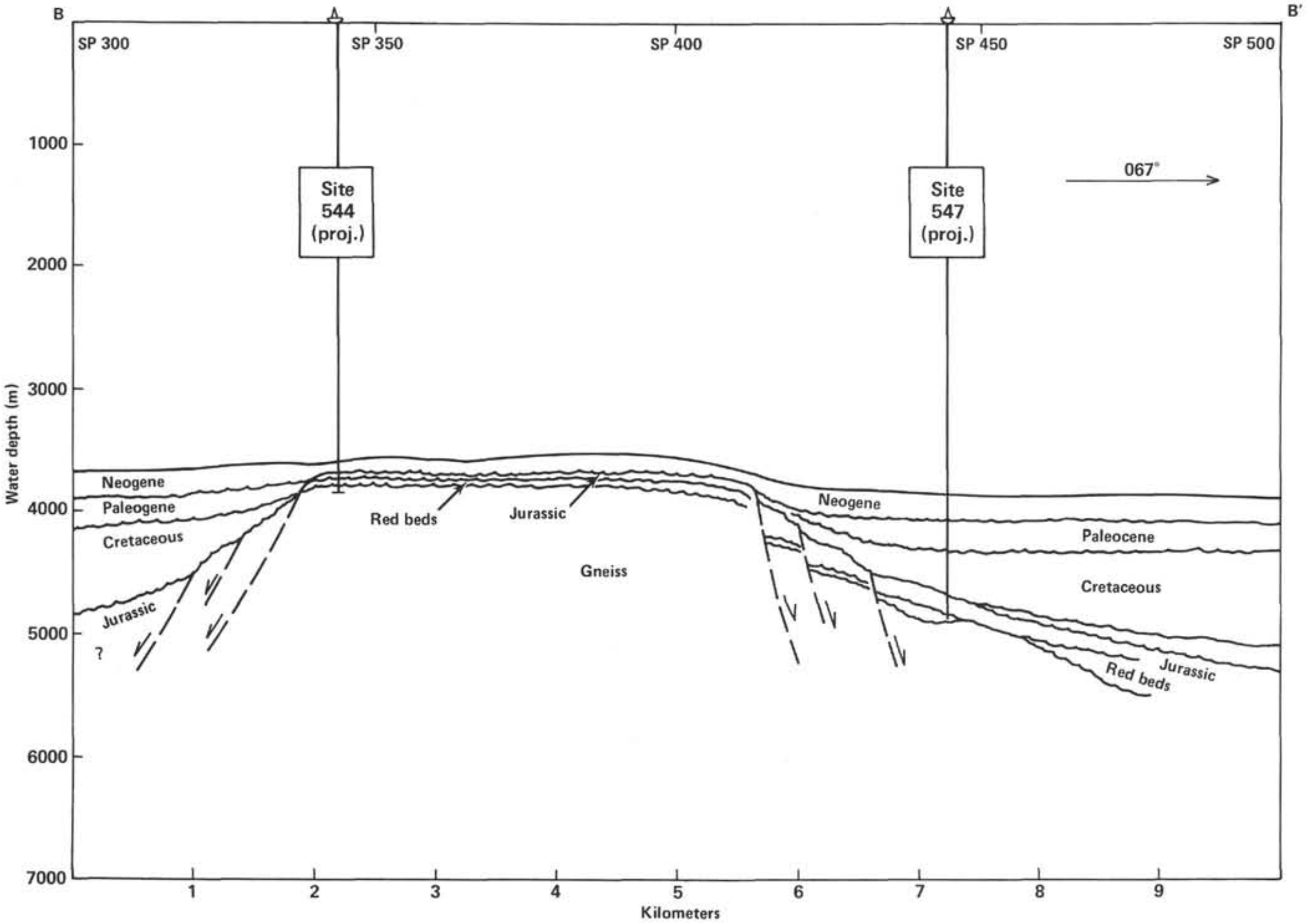

Figure 33. Geologic cross section along *Meteor* seismic profile 53-10, through Sites 544 and 547 (projected into line). SP = shotpoint (line A-A on Fig. 4).

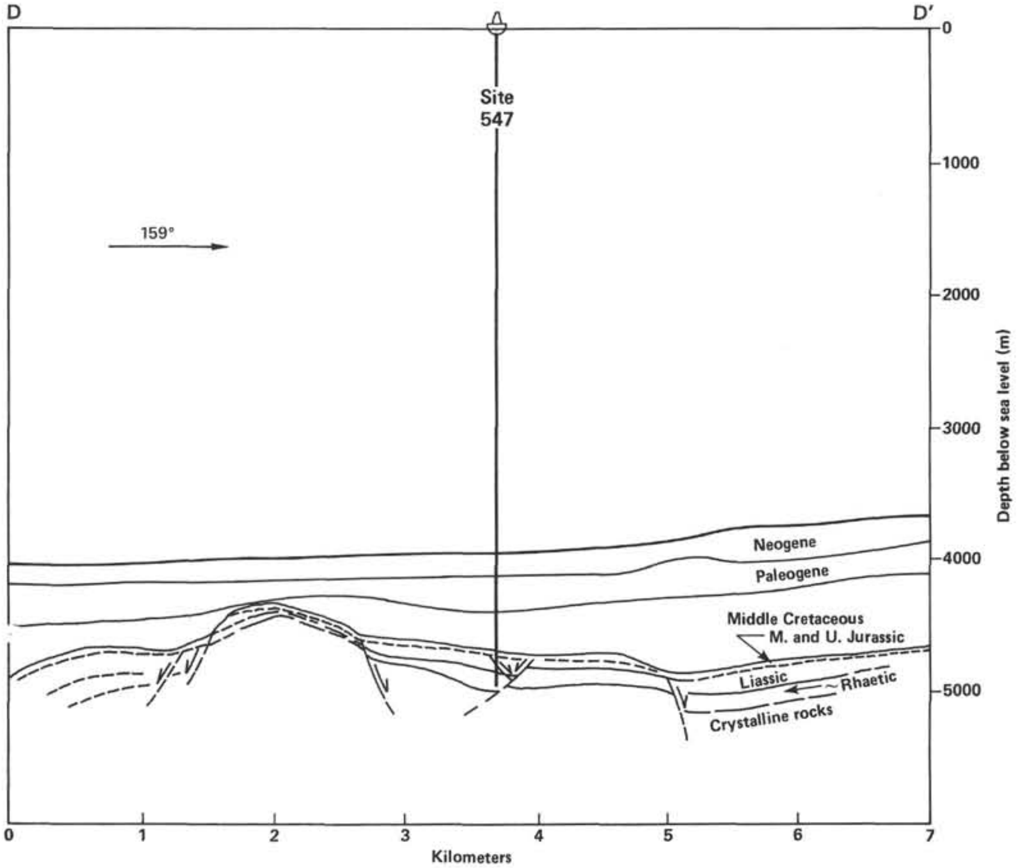

Figure 34. Geologic cross section along *Meteor* seismic profile 53-07, through Site 547 (line B–B′ on Fig. 4).

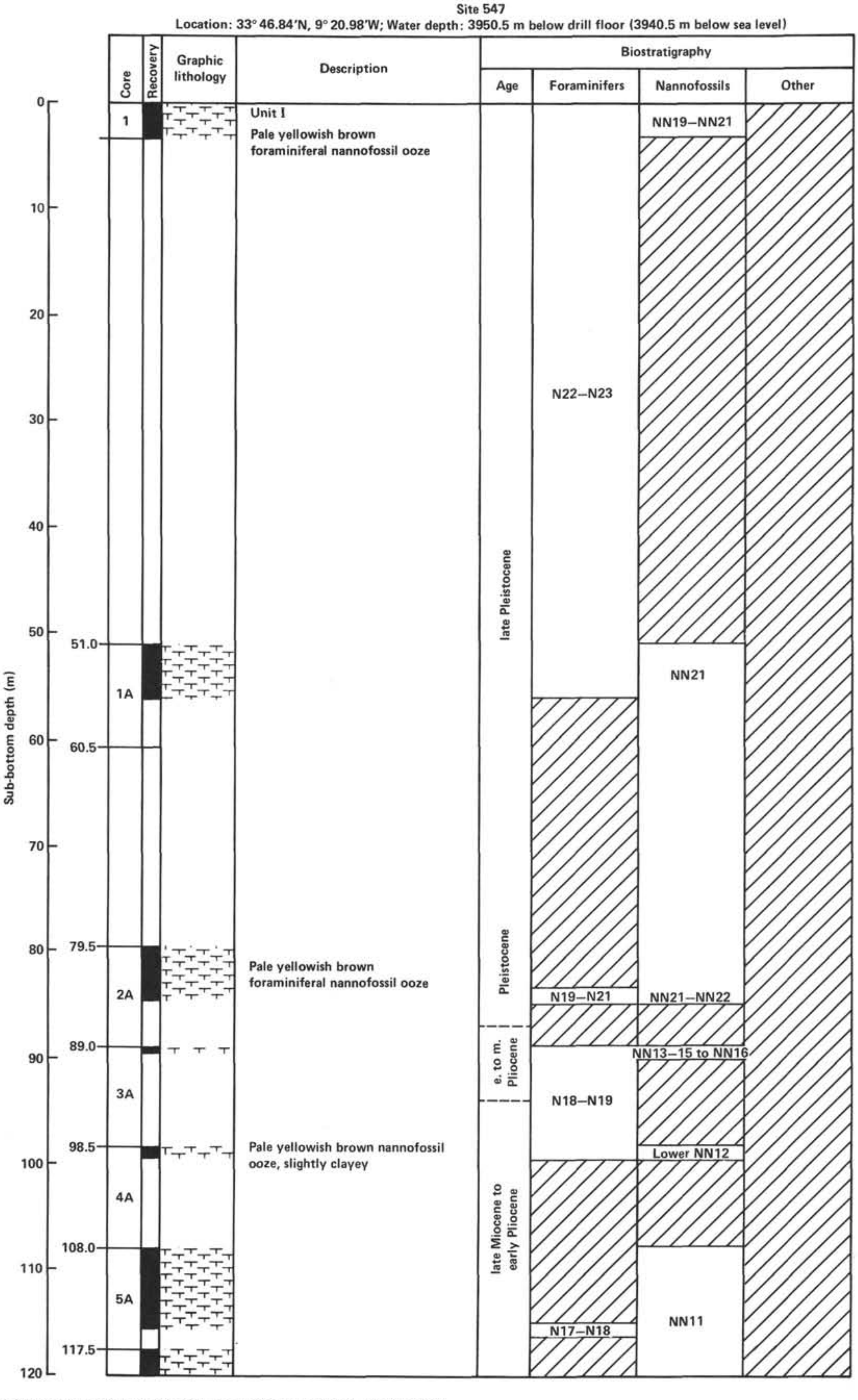

Figure 35. Detailed graphic log of holes drilled at Site 547.

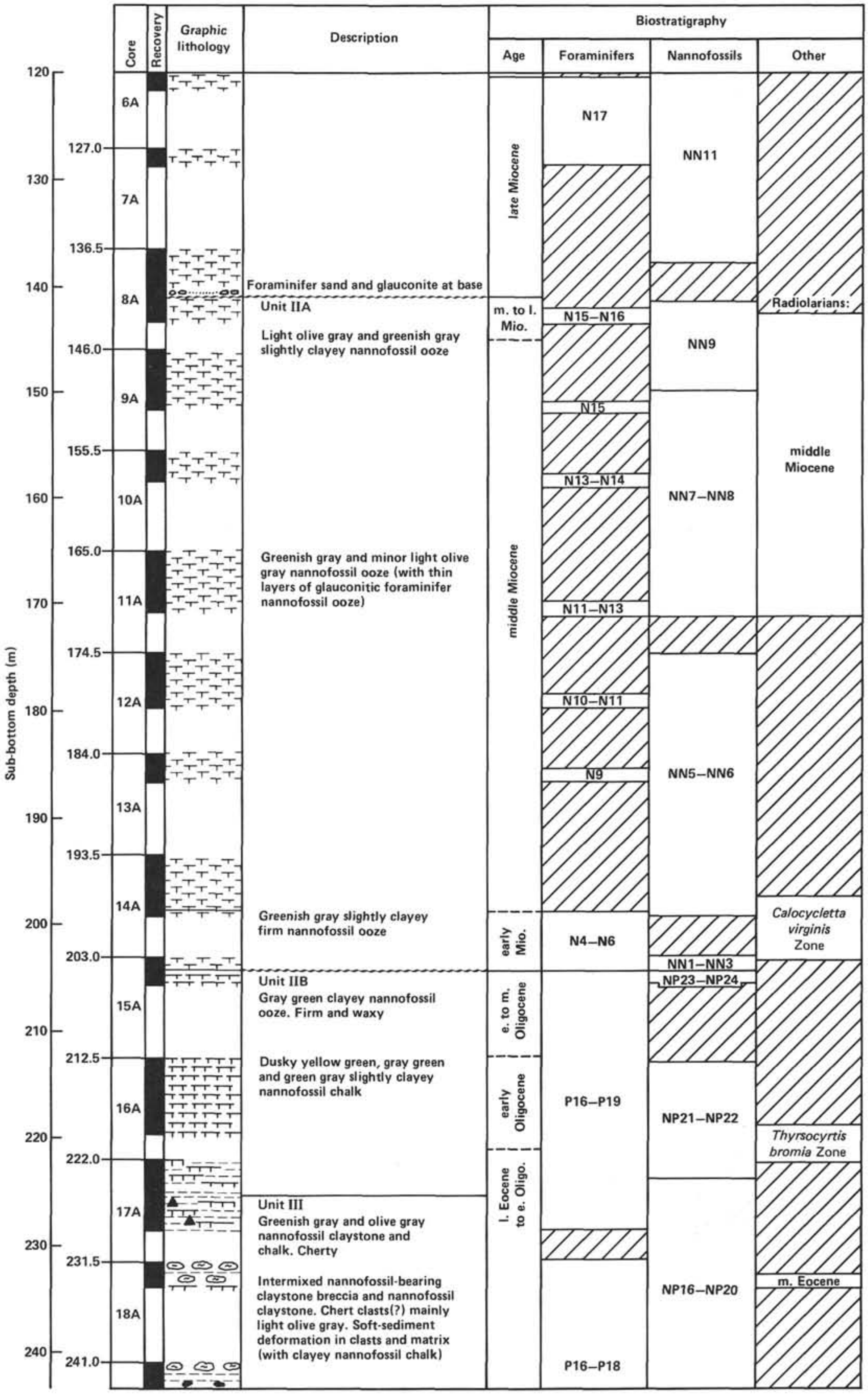

Figure 35. (Continued).

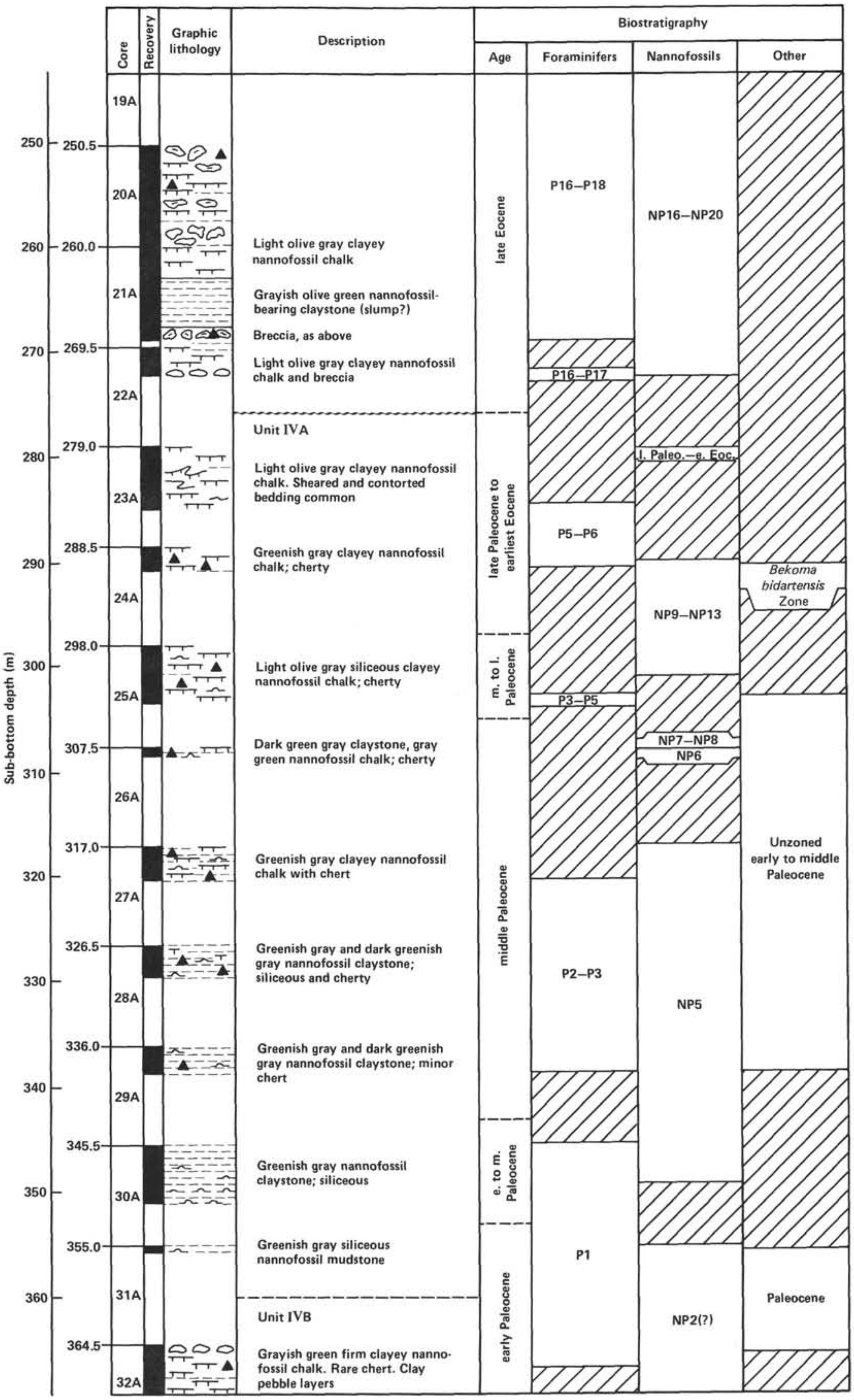

Figure 35. (Continued).

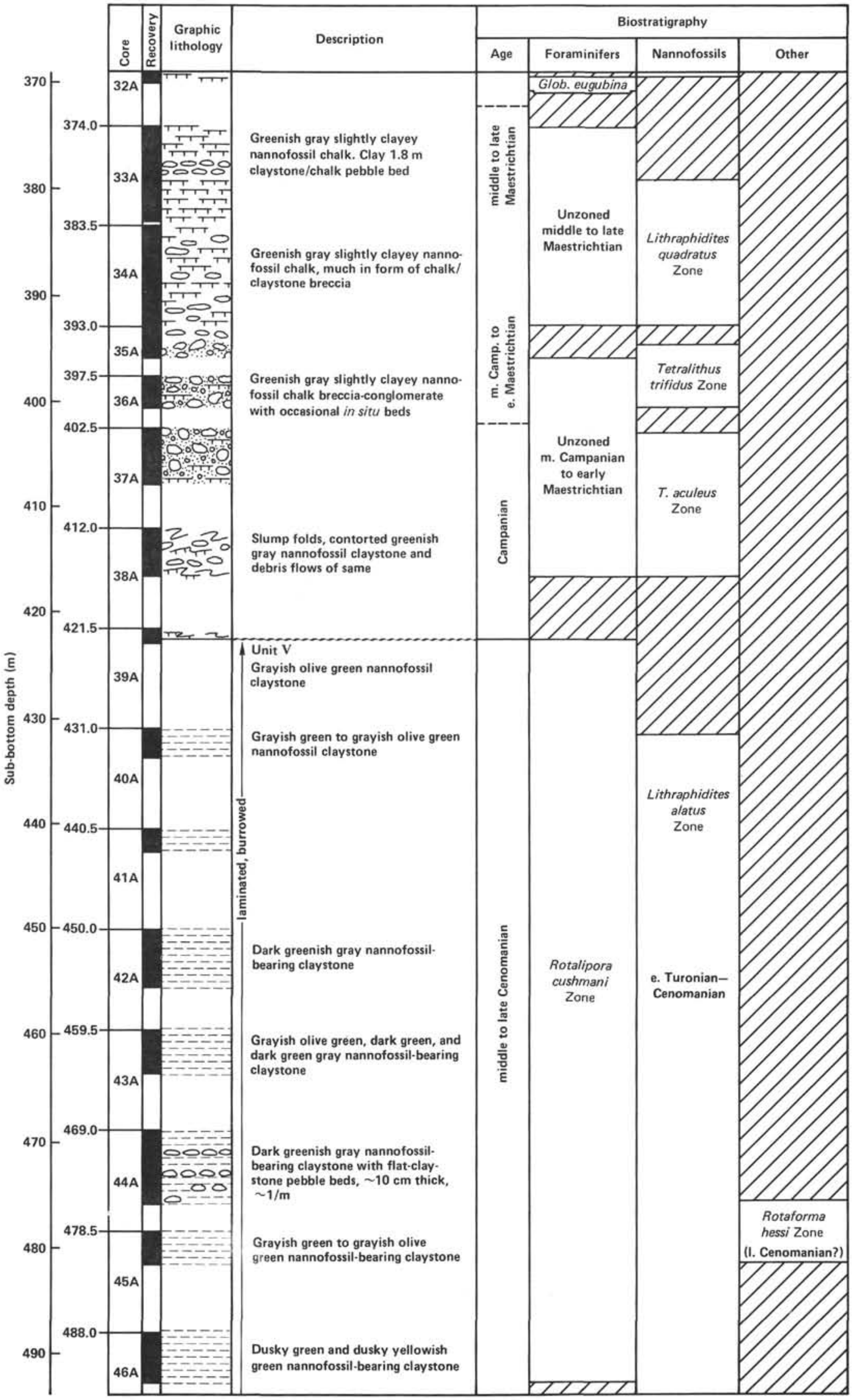

Figure 35. (Continued).

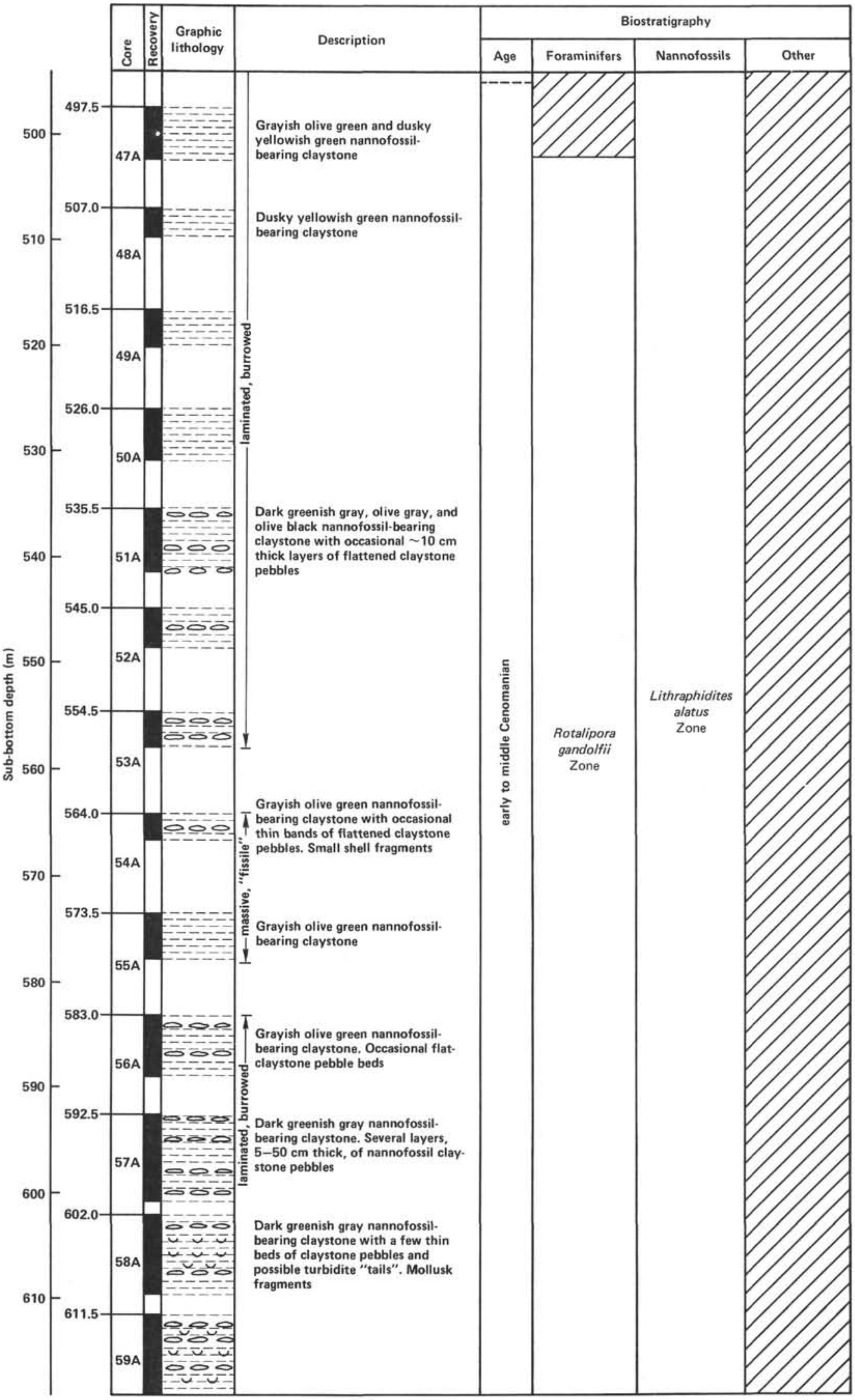

Grayish olive green and dusky yellowish green nannofossil-bearing claystone

Dusky yellowish green nannofossil-bearing claystone

Dark greenish gray, olive gray, and olive black nannofossil-bearing claystone with occasional ~10 cm thick layers of flattened claystone pebbles

Grayish olive green nannofossil-bearing claystone with occasional thin bands of flattened claystone pebbles. Small shell fragments

Grayish olive green nannofossil-bearing claystone

Grayish olive green nannofossil-bearing claystone. Occasional flat-claystone pebble beds

Dark greenish gray nannofossil-bearing claystone. Several layers, 5–50 cm thick, of nannofossil claystone pebbles

Dark greenish gray nannofossil-bearing claystone with a few thin beds of claystone pebbles and possible turbidite "tails". Mollusk fragments

Figure 35. (Continued).

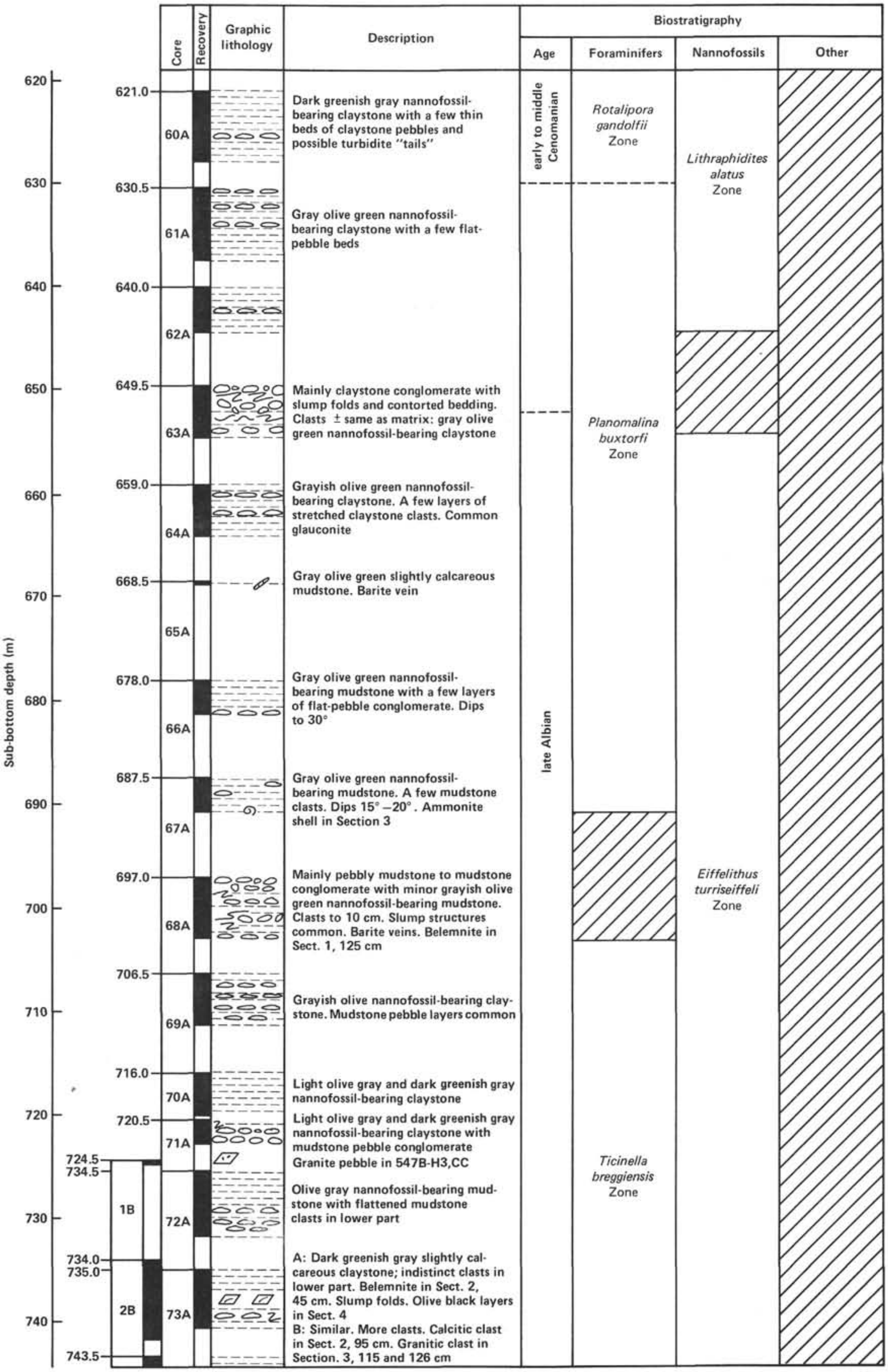

Dark greenish gray nannofossil-bearing claystone with a few thin beds of claystone pebbles and possible turbidite "tails"

Gray olive green nannofossil-bearing claystone with a few flat-pebble beds

Mainly claystone conglomerate with slump folds and contorted bedding. Clasts ± same as matrix: gray olive green nannofossil-bearing claystone

Grayish olive green nannofossil-bearing claystone. A few layers of stretched claystone clasts. Common glauconite

Gray olive green slightly calcareous mudstone. Barite vein

Gray olive green nannofossil-bearing mudstone with a few layers of flat-pebble conglomerate. Dips to 30°

Gray olive green nannofossil-bearing mudstone. A few mudstone clasts. Dips 15° –20°. Ammonite shell in Section 3

Mainly pebbly mudstone to mudstone conglomerate with minor grayish olive green nannofossil-bearing mudstone. Clasts to 10 cm. Slump structures common. Barite veins. Belemnite in Sect. 1, 125 cm

Grayish olive nannofossil-bearing claystone. Mudstone pebble layers common

Light olive gray and dark greenish gray nannofossil-bearing claystone

Light olive gray and dark greenish gray nannofossil-bearing claystone with mudstone pebble conglomerate Granite pebble in 547B-H3,CC

Olive gray nannofossil-bearing mudstone with flattened mudstone clasts in lower part

A: Dark greenish gray slightly calcareous claystone; indistinct clasts in lower part. Belemnite in Sect. 2, 45 cm. Slump folds. Olive black layers in Sect. 4
B: Similar. More clasts. Calcitic clast in Sect. 2, 95 cm. Granitic clast in Section. 3, 115 and 126 cm

Figure 35. (Continued).

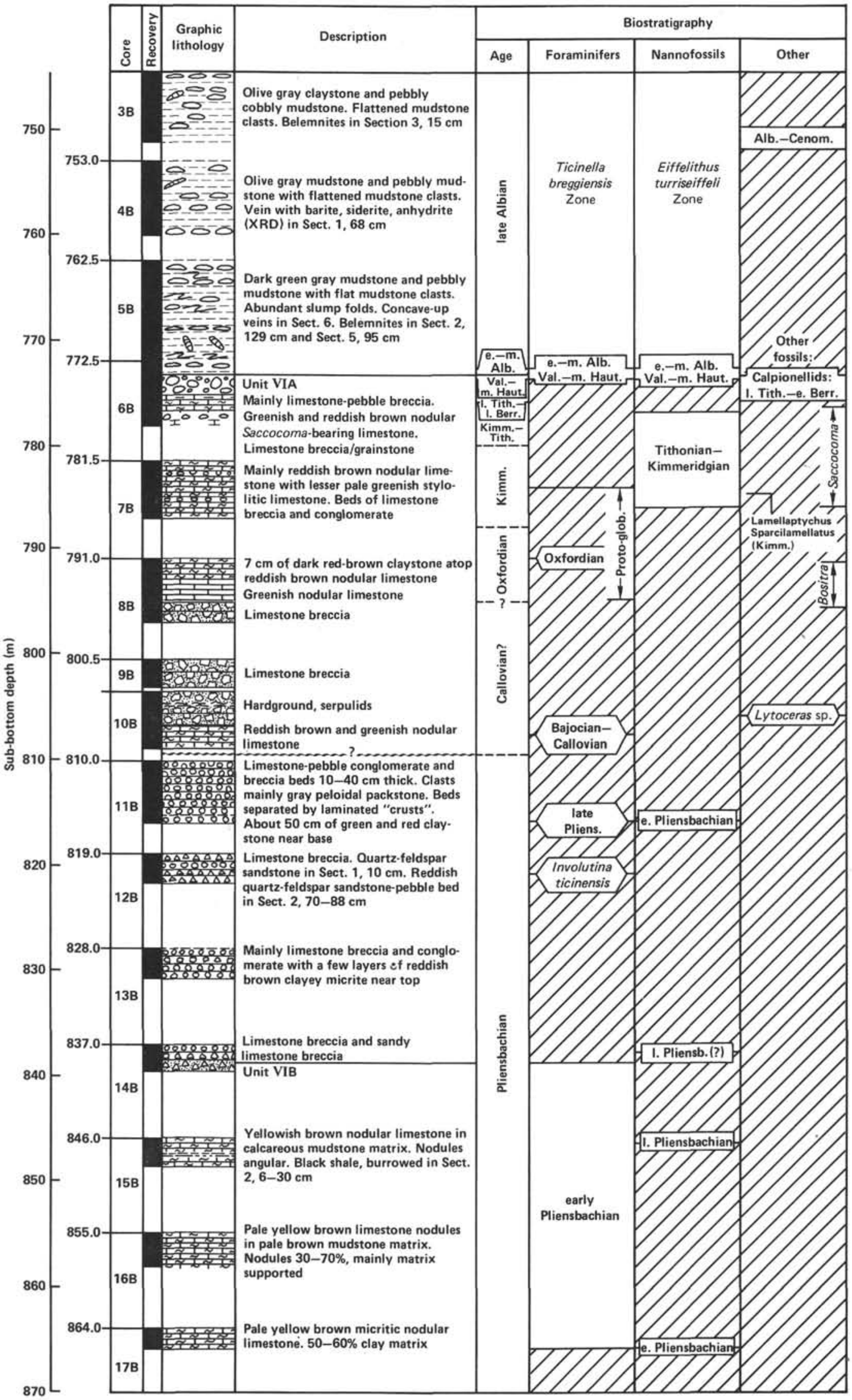

Olive gray claystone and pebbly cobbly mudstone. Flattened mudstone clasts. Belemnites in Section 3, 15 cm

Olive gray mudstone and pebbly mudstone with flattened mudstone clasts. Vein with barite, siderite, anhydrite (XRD) in Sect. 1, 68 cm

Dark green gray mudstone and pebbly mudstone with flat mudstone clasts. Abundant slump folds. Concave-up veins in Sect. 6. Belemnites in Sect. 2, 129 cm and Sect. 5, 95 cm

Unit VIA
Mainly limestone-pebble breccia.
Greenish and reddish brown nodular *Saccocoma*-bearing limestone.
Limestone breccia/grainstone

Mainly reddish brown nodular limestone with lesser pale greenish stylolitic limestone. Beds of limestone breccia and conglomerate

7 cm of dark red-brown claystone atop reddish brown nodular limestone
Greenish nodular limestone
Limestone breccia

Limestone breccia

Hardground, serpulids

Reddish brown and greenish nodular limestone
?

Limestone-pebble conglomerate and breccia beds 10–40 cm thick. Clasts mainly gray peloidal packstone. Beds separated by laminated "crusts". About 50 cm of green and red claystone near base

Limestone breccia. Quartz-feldspar sandstone in Sect. 1, 10 cm. Reddish quartz-feldspar sandstone-pebble bed in Sect. 2, 70–88 cm

Mainly limestone breccia and conglomerate with a few layers of reddish brown clayey micrite near top

Limestone breccia and sandy limestone breccia
Unit VIB

Yellowish brown nodular limestone in calcareous mudstone matrix. Nodules angular. Black shale, burrowed in Sect. 2, 6–30 cm

Pale yellow brown limestone nodules in pale brown mudstone matrix. Nodules 30–70%, mainly matrix supported

Pale yellow brown micritic nodular limestone. 50–60% clay matrix

Figure 35. (Continued).

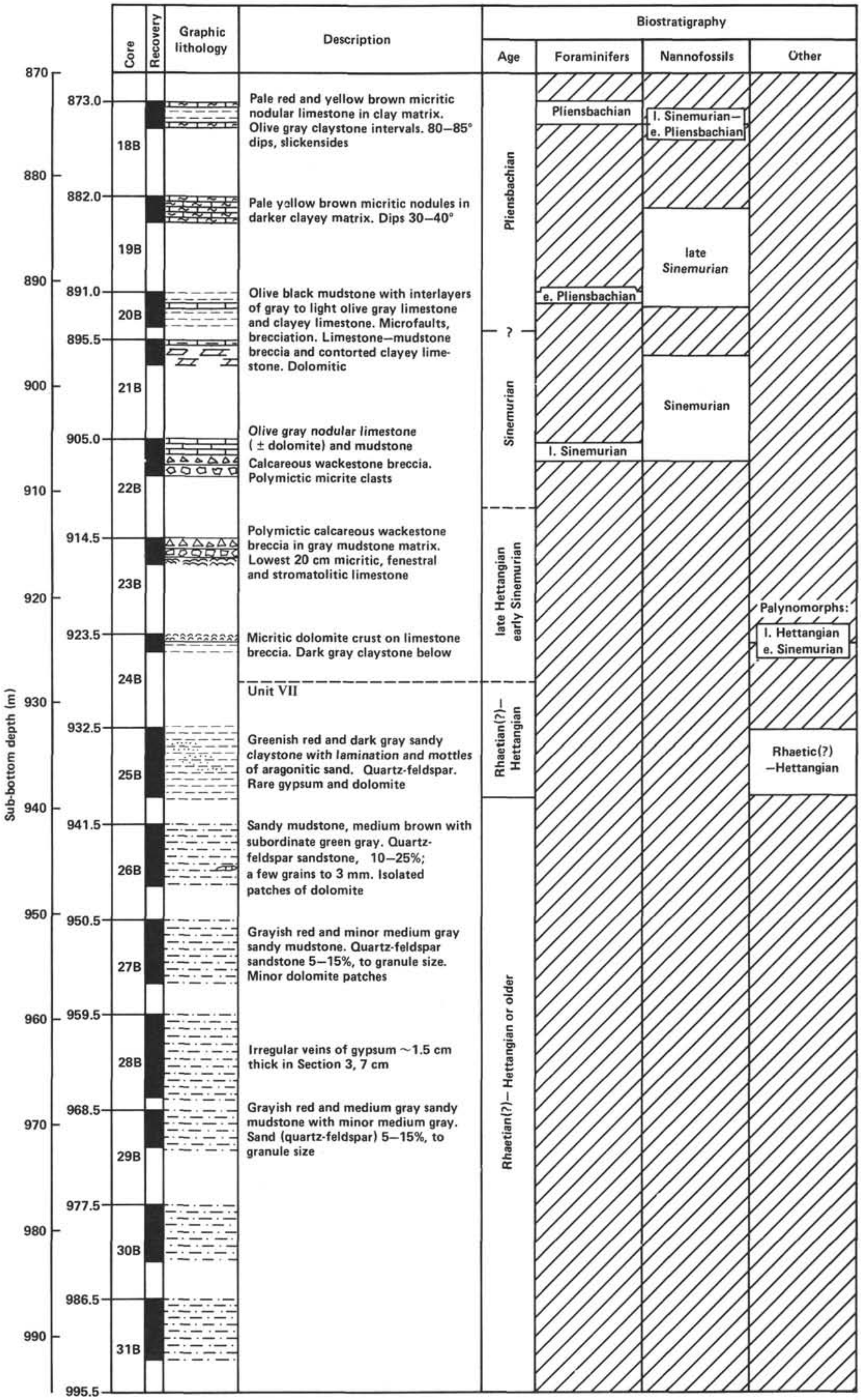

Pale red and yellow brown micritic nodular limestone in clay matrix. Olive gray claystone intervals. 80–85° dips, slickensides

Pale yellow brown micritic nodules in darker clayey matrix. Dips 30–40°

Olive black mudstone with interlayers of gray to light olive gray limestone and clayey limestone. Microfaults, brecciation. Limestone–mudstone breccia and contorted clayey limestone. Dolomitic

Olive gray nodular limestone (± dolomite) and mudstone Calcareous wackestone breccia. Polymictic micrite clasts

Polymictic calcareous wackestone breccia in gray mudstone matrix. Lowest 20 cm micritic, fenestral and stromatolitic limestone

Micritic dolomite crust on limestone breccia. Dark gray claystone below

Unit VII

Greenish red and dark gray sandy *claystone with lamination and mottles* of aragonitic sand. Quartz-feldspar. Rare gypsum and dolomite

Sandy mudstone, medium brown with subordinate green gray. Quartz-feldspar sandstone, 10–25%; a few grains to 3 mm. Isolated patches of dolomite

Grayish red and minor medium gray sandy mudstone. Quartz-feldspar sandstone 5–15%, to granule size. Minor dolomite patches

Irregular veins of gypsum ~1.5 cm thick in Section 3, 7 cm

Grayish red and medium gray sandy mudstone with minor medium gray. Sand (quartz-feldspar) 5–15%, to granule size

Figure 35. (Continued).

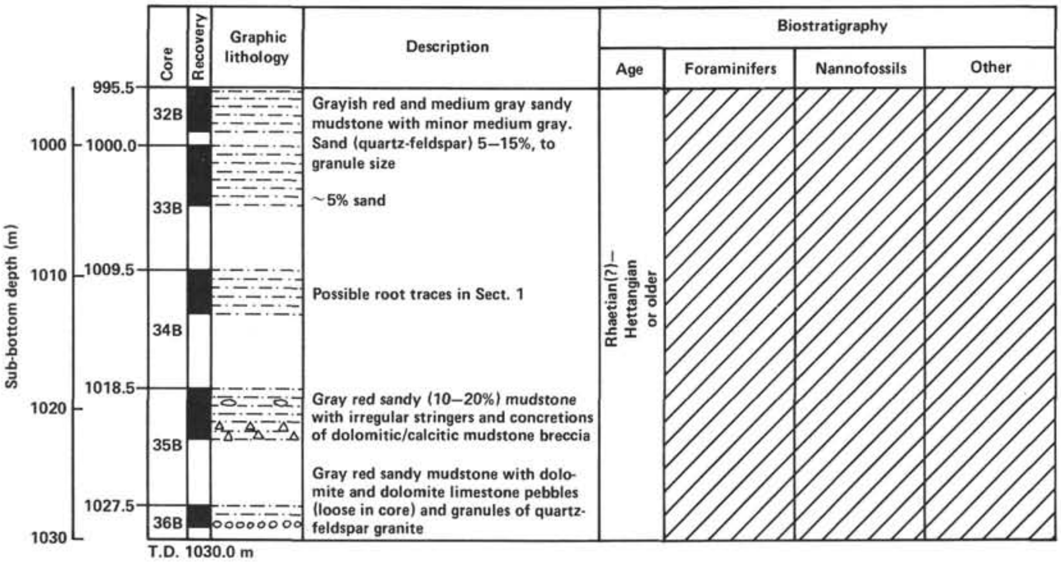

Grayish red and medium gray sandy mudstone with minor medium gray. Sand (quartz-feldspar) 5–15%, to granule size

~5% sand

Possible root traces in Sect. 1

Gray red sandy (10–20%) mudstone with irregular stringers and concretions of dolomitic/calcitic mudstone breccia

Gray red sandy mudstone with dolomite and dolomite limestone pebbles (loose in core) and granules of quartz-feldspar granite

Figure 35. (Continued).

SITE 547 HOLE CORE 1 CORED INTERVAL 0.0–3.5 m sub-bottom

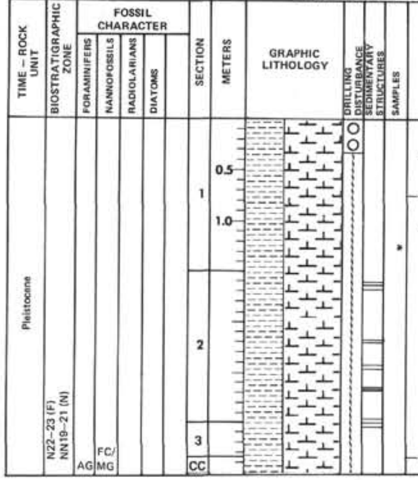

LITHOLOGIC DESCRIPTION

5YR 4/4

10YR 6/2

Highly deformed, mostly pale yellowish brown VERY CLAYEY NANNOFOSSIL OOZE with grayish olive green (5GY 3/2) patches and minor olive black laminae.

SMEAR SLIDE SUMMARY (%):

	1, 125 D
Texture:	
Silt	20
Clay	80
Composition:	
Quartz	4
Clay	25
Dolomite	2
Foraminifers	2
Calc. nannofossils	65
Sponge spicules	Tr

SITE 547 HOLE A CORE 1 CORED INTERVAL 51.0–60.5 m sub-bottom

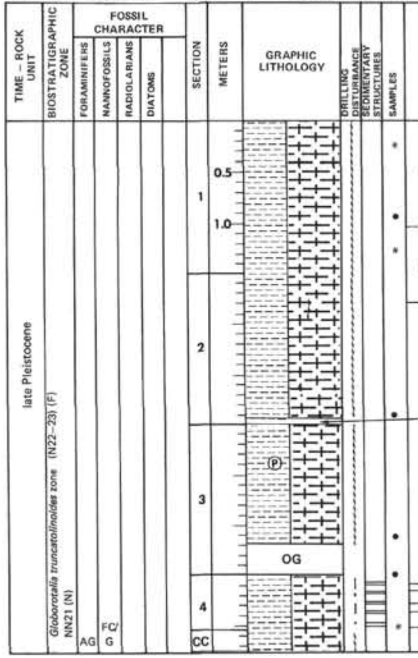

LITHOLOGIC DESCRIPTION

10YR 6/2

5Y 6/1

IW

Layers of 5YR 5/2 to 10YR 6/2

Highly disturbed, dominantly pale yellowish brown (10YR 6/2) VERY CLAYEY FORAMINIFERAL NANNOFOSSIL OOZE with minor layers of pale brown (5YR 5/2) and a light olive gray interval from Section 1, 105 to Section 2, 30 cm.

Rare pyrite throughout, one pyrite nodule in Section 3, 40–50 cm.

SMEAR SLIDE SUMMARY (%):

	1, 23 D	1, 120 D	4, 54 D
Texture:			
Sand	40	15	5
Silt	20	10	15
Clay	40	75	80
Composition:			
Quartz	1	5	2
Mica	–	2	–
Clay	25	10	20
Pyrite	1	Tr	1
Dolomite	–	–	3
Foraminifers	50	20	5
Calc. nannofossils	20	60	70
Sponge spicules	Tr	–	–

ORGANIC CARBON AND CARBONATE (%):

	1, 96–97	2, 144–150	3, 118–120	4, 0–2
Carbonate	62.7	–	–	49.4
$CaCO_3$	–	50.9	49.4	–

SITE 547 HOLE A CORE 2 CORED INTERVAL 79.5–89.0 m sub-bottom

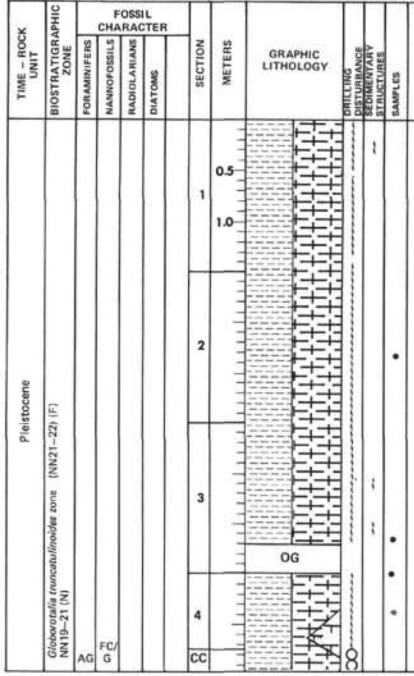

LITHOLOGIC DESCRIPTION

Highly disturbed, pale yellowish brown (10YR 6/2) VERY CLAYEY FORAMINIFERAL NANNOFOSSIL OOZE with occasional pyrite burrows and an interval of FORAMINIFERAL OOZE at Section 4, 66–72 cm.

SMEAR SLIDE SUMMARY (%):

	4, 40 D
Texture:	
Sand	5
Silt	10
Clay	85
Composition:	
Quartz	1
Mica	1
Clay	20
Pyrite	Tr
Dolomite	1
Foraminifers	5
Calc. nannofossils	70

ORGANIC CARBON AND CARBONATE (%):

	2, 86–87	3, 118–120	4, 0–2
Carbonate	58.2	–	–
$CaCO_3$	–	52.9	55.0

SITE 547 HOLE A CORE 3 CORED INTERVAL 89.0–98.5 m sub-bottom

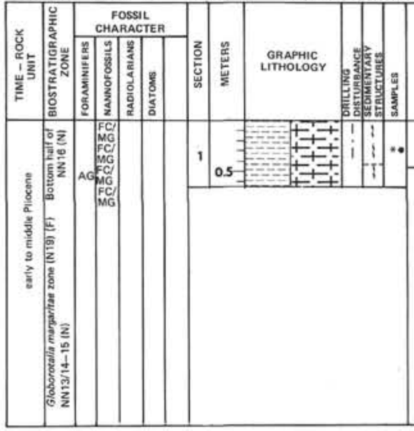

LITHOLOGIC DESCRIPTION

10YR 6/2

5YR 5/2

Moderately disturbed, pale yellowish brown (10YR 6/2) and grayish orange pink (5YR 5/2) VERY CLAYEY FORAMINIFERAL NANNOFOSSIL OOZE. In lower part faint color banding.

SMEAR SLIDE SUMMARY (%):

	1, 30 D
Composition:	
Quartz	1
Clay	15
Foraminifers	10
Calc. nannofossils	74

ORGANIC CARBON AND CARBONATE (%):

	1, 30–31
Carbonate	55.7

SITE 547 HOLE A CORE 4 CORED INTERVAL 98.5–108.0 m sub-bottom

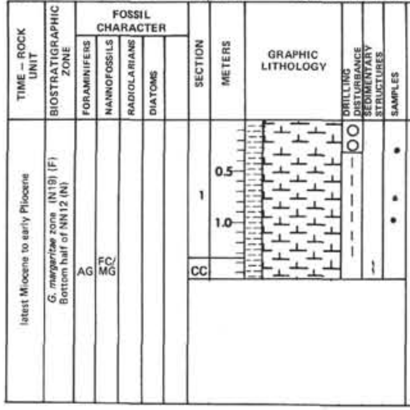

LITHOLOGIC DESCRIPTION

Mostly slightly disturbed, grayish orange pink (5YR 5/2) CLAYEY NANNOFOSSIL OOZE with faint color banding of yellowish gray (5Y 7/2).

SMEAR SLIDE SUMMARY (%):

	1, 80
	D
Composition:	
Quartz	1
Clay	15
Dolomite	1
Foraminifers	7
Calc. nannofossils	75

ORGANIC CARBON AND CARBONATE (%):

	1, 30–31	1, 100–116
Carbonate	76.6	80.4

SITE 547 HOLE A CORE 5 CORED INTERVAL 108.0–117.5 m sub-bottom

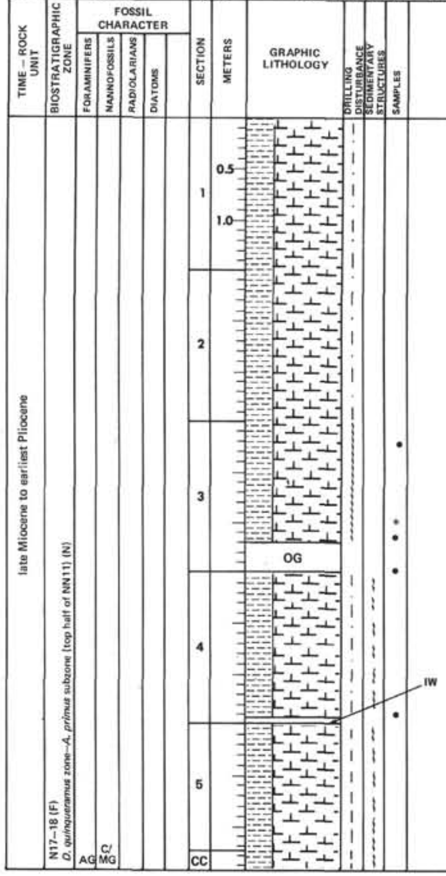

LITHOLOGIC DESCRIPTION

Moderately disturbed, pale yellowish brown (10YR 6/2) CLAYEY NANNOFOSSIL OOZE with few dark colored smeared laminae and burrows rich in iron sulfide.

SMEAR SLIDE SUMMARY (%):

	3, 100
	D
Composition:	
Quartz	Tr
Mica	15
Dolomite	1
Calc. nannofossils	85

ORGANIC CARBON AND CARBONATE (%):

	3, 28–29	3, 118–120	4, 0–2	4, 144–150
Carbonate	71.2	–	65.7	–
$CaCO_3$	–	61.6	–	63.1

SITE 547 HOLE A CORE 6 CORED INTERVAL 117.5–127.0 m sub-bottom

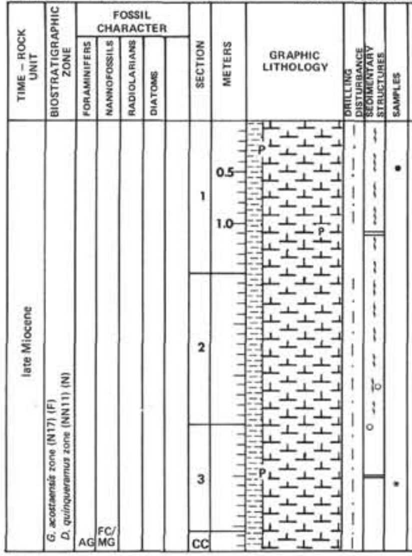

LITHOLOGIC DESCRIPTION

Moderately disturbed, pale yellowish brown (10YR 6/2) CLAYEY NANNOFOSSIL OOZE with common dark colored pyrite rich spots and laminae.

SMEAR SLIDE SUMMARY (%):

	3, 60
	D
Composition:	
Quartz	Tr
Feldspar	Tr
Clay	10
Dolomite	2
Foraminifers	2
Calc. nannofossils	85

ORGANIC CARBON AND CARBONATE (%):

	1, 49–50
Carbonate	74.2

SITE 547 HOLE A CORE 7 CORED INTERVAL 127.0–136.5 m sub-bottom

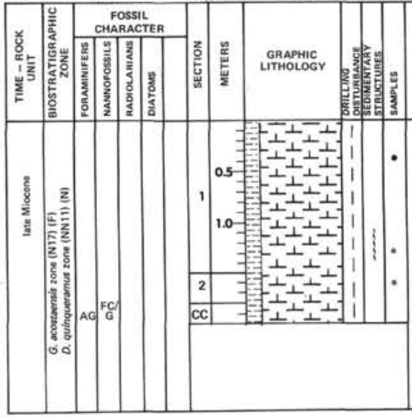

LITHOLOGIC DESCRIPTION

Slightly disturbed, pale yellowish brown (10YR 6/2) CLAYEY NANNOFOSSIL OOZE, with some bioturbation at Section 1, 120–130 cm and faint color mottling throughout.

SMEAR SLIDE SUMMARY (%):

	1, 130	2, 12
	D	D
Composition:		
Quartz	Tr	–
Feldspar	1	Tr
Mica	Tr	–
Clay	15	25
Glauconite	–	Tr
Calc. nannofossils	85	75

ORGANIC CARBON AND CARBONATE (%):

	1, 40–41
Carbonate	75.7

SITE 547 HOLE A CORE 8 CORED INTERVAL 136.5–146.0 m sub-bottom

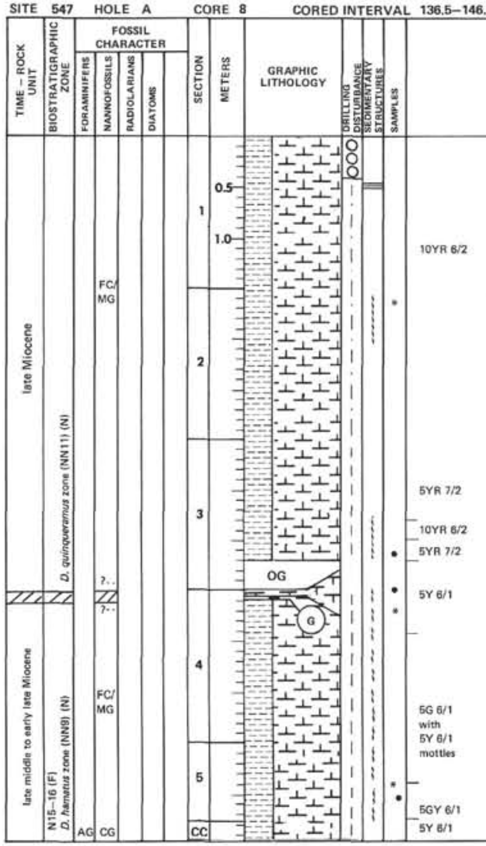

LITHOLOGIC DESCRIPTION

Sections 1 through 3: moderately disturbed, pale yellowish brown and grayish orange pink CLAYEY NANNOFOSSIL OOZE with blackish mottling due to pyrite rich burrow-fillings.

Section 4, 0–7 cm: grayish orange pink (5YR 7/2) FORAMINIFERAL SAND underlain by 1 cm of GLAUCONITIC SAND.

Section 4, 7 cm through Core-Catcher: light olive gray to greenish gray CLAYEY NANNOFOSSIL OOZE, with traces of glauconite.

SMEAR SLIDE SUMMARY (%):

	2, 20	4, 20	5, 40
	D	D	D
Composition:			
Quartz	Tr	Tr	Tr
Feldspar	1	Tr	–
Clay	10	15	15
Glauconite	–	–	1–2
Dolomite	1	1	1
Calc. nannofossils	85	85	83

ORGANIC CARBON AND CARBONATE (%):

	3, 118–120	4, 0–2	5, 53–54
Carbonate	–	78.4	64.7
$CaCO_3$	56.0	–	–

SITE 547 HOLE A CORE 9 CORED INTERVAL 146.0–155.5 m sub-bottom

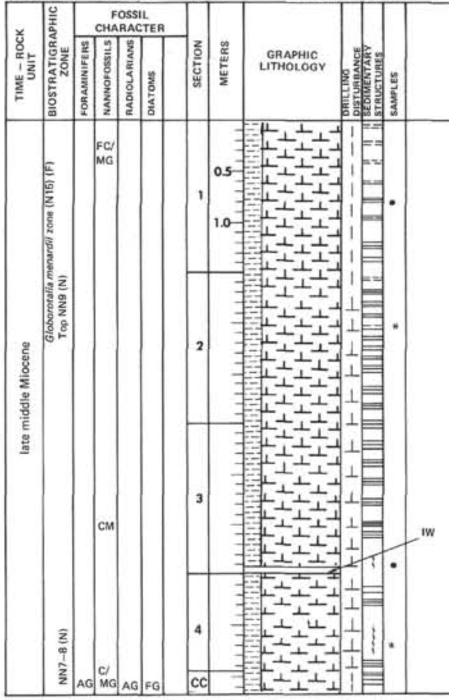

LITHOLOGIC DESCRIPTION

Mostly drilling cakes of greenish gray (5GY 6/1) and minor light olive gray (5Y 5/2) CLAYEY NANNOFOSSIL OOZE. Even, indistinct, slightly darker lamination, few dark iron sulfide blebs.

SMEAR SLIDE SUMMARY (%):

	2, 50	4, 70
	D	D
Composition:		
Quartz	Tr	1
Feldspar	Tr	Tr
Clay	15	15
Glauconite	Tr	2
Dolomite	1	2
Foraminifers	1	–
Calc. nannofossils	80	80

ORGANIC CARBON AND CARBONATE (%):

	1, 81–82	3, 144–150
Carbonate	74.2	78.4

SITE 547 HOLE A CORE 10 CORED INTERVAL 155.5–165.0 m sub-bottom

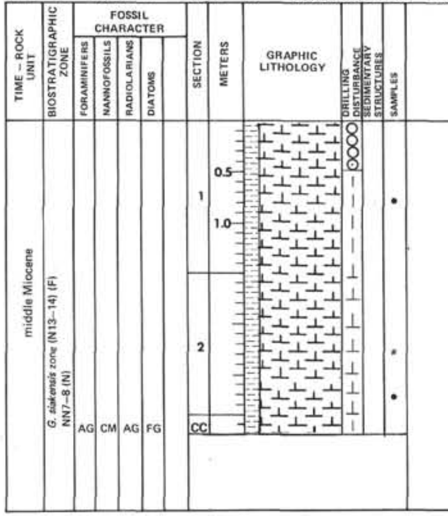

LITHOLOGIC DESCRIPTION

Slightly disturbed and drilling cakes of greenish gray (5GY 6/1) and gray yellowish brown (5GY 7/2) CLAYEY NANNOFOSSIL OOZE.

In Section 1 color banding visible plus finer indistinct laminae within each color.

Minor medium gray (N5) laminae of pyrite.

SMEAR SLIDE SUMMARY (%):

	2, 80
	D
Texture:	
Sand	1
Silt	1
Clay	98
Composition:	
Quartz	Tr
Clay	5
Pyrite	Tr
Dolomite	Tr
Foraminifers	1
Calc. nannofossils	94

ORGANIC CARBON AND CARBONATE (%):

	1, 81–82	2, 120–136
Carbonate	89.2	73.3

SITE 547 HOLE A CORE 11 CORED INTERVAL 165.0–174.5 m sub-bottom

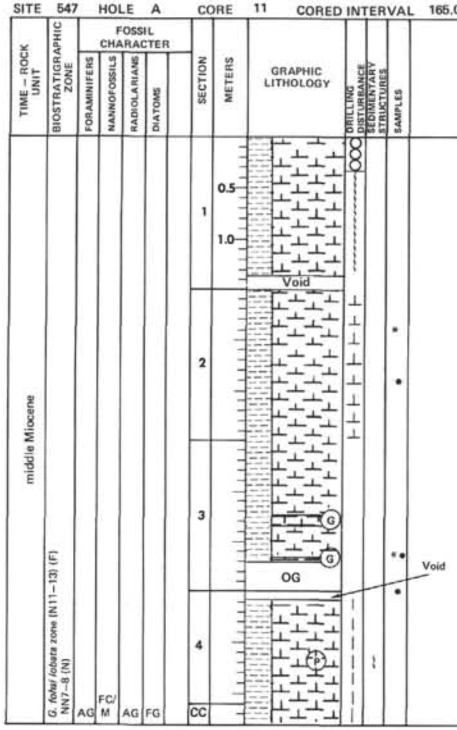

LITHOLOGIC DESCRIPTION

Highly disturbed, greenish gray (5GY 6/1) and light greenish gray (5G 8/1) CLAYEY NANNOFOSSIL OOZE.

At Section 3, 78–81 and 116–120 cm layers of GLAUCONITIC FORAMINIFERAL NANNOFOSSIL OOZE.

SMEAR SLIDE SUMMARY (%):

	2, 40 D	3, 118 M
Texture:		
Sand	–	15
Silt	10	15
Clay	90	70
Composition:		
Quartz	Tr	2
Clay	3	10
Glauconite	–	4
Pyrite	Tr	1
Dolomite	1	1
Foraminifers	Tr	20
Calc. nannofossils	95	60

ORGANIC CARBON AND CARBONATE (%):

	2, 90–91	3, 118–120	4, 0–2
Carbonate	70.2	–	–
$CaCO_3$	–	74.8	67.2

SITE 547 HOLE A CORE 12 CORED INTERVAL 174.5–184.0 m sub-bottom

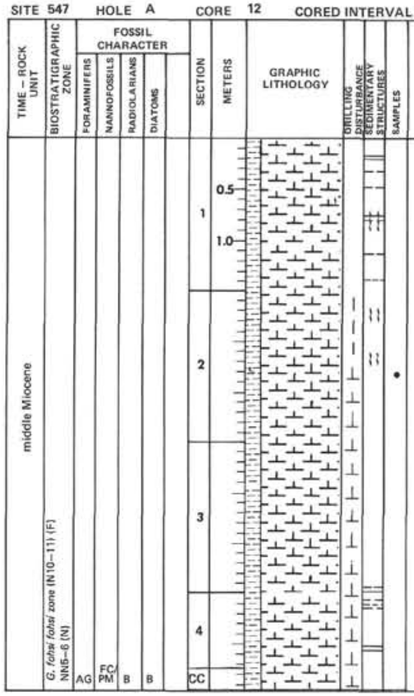

LITHOLOGIC DESCRIPTION

Mostly drilling cakes of greenish gray (5GY 6/1) and light olive gray (5Y 6/1) CLAYEY NANNOFOSSIL OOZE. Gradational, 10–40 cm thick color interlayers. Concentrations of medium gray (N5) or dark greenish gray (5GY 4/1) pyrite in layers and blebs throughout.

ORGANIC CARBON AND CARBONATE (%):

	2, 80–81
Carbonate	75.2

SITE 547 HOLE A CORE 13 CORED INTERVAL 184.0–193.5 m sub-bottom

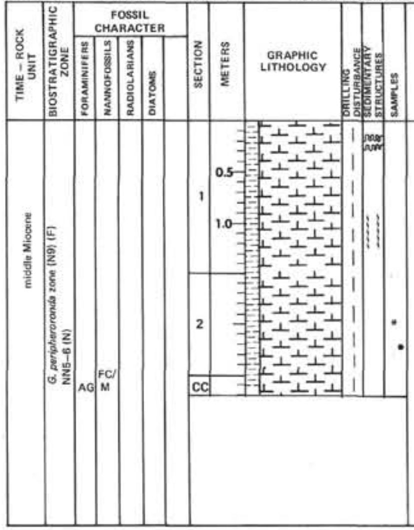

LITHOLOGIC DESCRIPTION

Slightly disturbed, light greenish gray (5GY 7/1) greenish gray (5G 6/1) and light olive gray (5Y 7/1) CLAYEY NANNOFOSSIL OOZE. Interlayers of 0.5–35 cm thick of all colors. Minor burrowing and convolute bedding and minor medium gray (N5) laminae and burrow linings.

SMEAR SLIDE SUMMARY (%):

	2, 50 D
Texture:	
Silt	10
Clay	90
Composition:	
Quartz	Tr
Heavy minerals	Tr
Clay	7
Glauconite	Tr
Pyrite	Tr
Dolomite	Tr
Foraminifers	5
Calc. nannofossils	85

ORGANIC CARBON AND CARBONATE (%):

	2, 74–75
Carbonate	79.1

SITE 547 HOLE A CORE 14 CORED INTERVAL 193.5–203.0 m sub-bottom

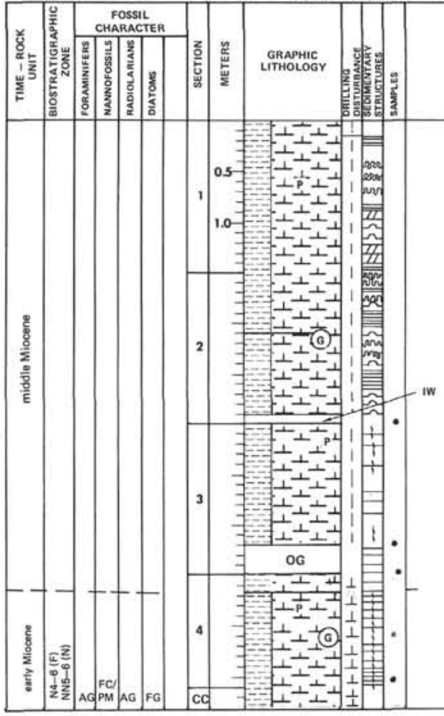

LITHOLOGIC DESCRIPTION

Mostly slightly disturbed light greenish gray (5GY 8/1) and greenish gray (5GY 6/1) CLAYEY NANNOFOSSIL OOZE. Fine color laminae of 0.5–5 mm thickness show abundant contorted bedding, and slump folds in Sections 1 and 2. Discordances and folds of 1–3 cm scale.

Lithological break at Section 4, 14 cm is associated with color change to light olive gray (5Y 5/2) Section 4, 14–59 and 74–110 cm and greenish gray (5G 8/1) 59–74 cm. Dark pyrite laminae and glauconite layers common.

SMEAR SLIDE SUMMARY (%):

	4, 55
	D
Texture:	
Sand	2
Silt	3
Clay	95
Composition:	
Quartz	1
Clay	15
Glauconite	Tr
Pyrite	1
Dolomite	1
Foraminifers	2
Calc. nannofossils	80
Radiolarians	Tr
Sponge spicules	Tr

ORGANIC CARBON AND CARBONATE (%):

	2, 144–150	3, 118–120	4, 0–2	4, 100–101
Carbonate	67.2	–	–	66.7
$CaCO_3$	–	69.2	72.8	–

SITE 547 HOLE A CORE 15 CORED INTERVAL 203.0–212.5 m sub-bottom

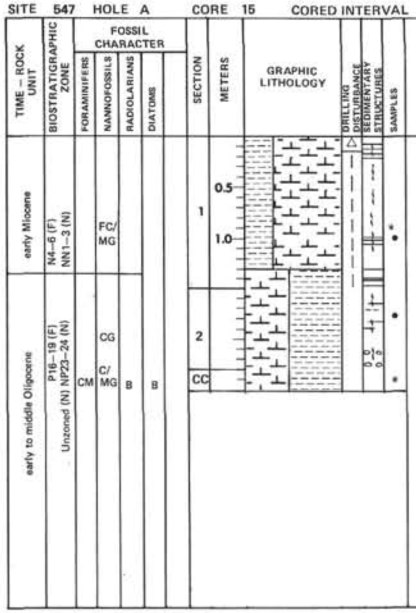

LITHOLOGIC DESCRIPTION

Section 1, 0–130 cm: slightly disturbed, firm, greenish gray (5GY 6/1) and medium greenish gray (5GY 4/1) VERY CLAYEY NANNOFOSSIL OOZE with common burrowing and dark greenish gray (5GY 4/1) or medium gray (N5) laminae.

Section 1, 130 cm to Core-Catcher: undisturbed, grayish green (10GY 5/2), very firm to waxy NANNOFOSSIL-RICH CLAY with indistinct layers of lighter and darker green shades.

At Section 2, 65 and 74 cm two layers of intraclasts.

SMEAR SLIDE SUMMARY (%):

	1, 90	CC
	D	D
Texture:		
Sand	1	–
Silt	5	2
Clay	94	98
Composition:		
Quartz	Tr	Tr
Mica	Tr	–
Clay	20	30
Pyrite	1	–
Dolomite	2	5
Foraminifers	Tr	–
Calc. nannofossils	75	65
Sponge spicules	–	Tr

ORGANIC CARBON AND CARBONATE (%):

	1, 100–101	2, 30–31
Carbonate	65.7	47.8

SITE 547 HOLE A CORE 16 CORED INTERVAL 212.5–222.0 m sub-bottom

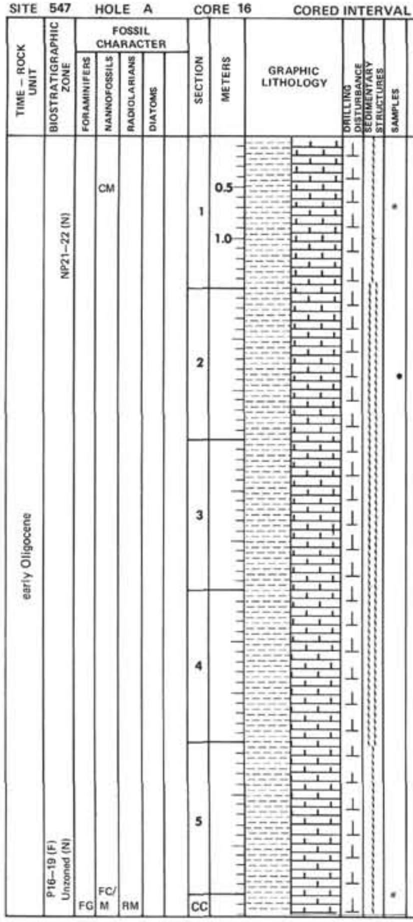

LITHOLOGIC DESCRIPTION

Mostly drilling cakes of grayish green (10GY 5/2) and greenish gray (5G 6/1) VERY CLAYEY NANNOFOSSIL CHALK with minor to moderate bioturbation marked by medium gray laminae blebs and burrow fillings generally rich in pyrite.

Core-Catcher shows dusky yellowish green (5GY 5/2) color.

SMEAR SLIDE SUMMARY (%):

	1, 70	CC, 5
	D	D
Texture:		
Silt	5	5
Clay	95	95
Composition:		
Quartz	Tr	1
Mica	Tr	Tr
Clay	10	10
Glauconite	–	Tr
Pyrite	2	1
Dolomite	2	1
Foraminifers	Tr	Tr
Calc. nannofossils	85	85

ORGANIC CARBON AND CARBONATE (%):

	2, 85–87
Carbonate	52.8

SITE 547 HOLE A CORE 17 CORED INTERVAL 222.0–231.5 m sub-bottom

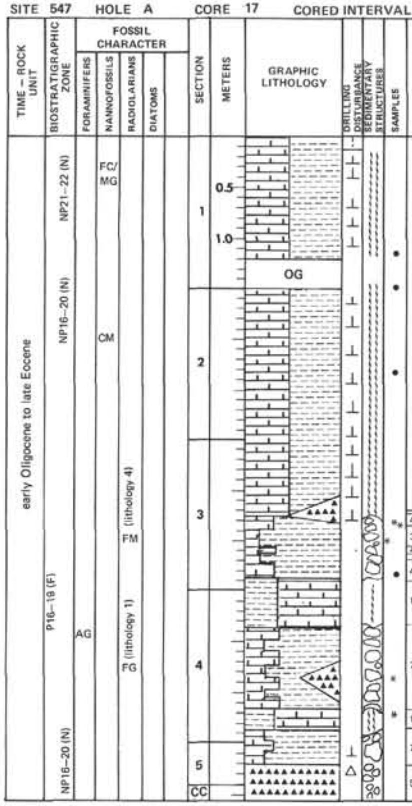

LITHOLOGIC DESCRIPTION

Section 1 through Section 3, 71 cm: drilling cakes of dark greenish gray (5G 4/1) NANNOFOSSIL-RICH CLAYSTONE with frequent bioturbation as frequent planolites and rare zoophycus and chondrites, rich in pyrite.

Section 3, 71 cm through Core-Catcher: CONGLOMERATE with mixed lithologies:

1. Light greenish gray (5GY 8/1) CLAYEY NANNOFOSSIL CHALK with abundant darker bioturbation.
2. Olive gray (5Y 3/2) and grayish olive (10Y 4/2) NANNOFOSSIL CLAYSTONE.
3. Grayish olive green (5GY 3/2) FORAMINIFERAL NANNOFOSSIL CLAYSTONE.
4. Olive brown (5Y/YR 3/2) NANNO CLAYSTONE.
5. Olive gray (5Y 4/1) to olive black (5Y 2/1) PORCELLANITE with darker traces of burrowing.

Reworked biostratigraphy: Paleogene and Cretaceous

1) Partly early to middle Paleocene
2) Partly early Eocene
3) Lower middle Cretaceous?
4) Partly late Paleocene/early Eocene

SMEAR SLIDE SUMMARY (%):

	3, 85 M	3, 87 M	3, 104 D	4, 88 D	4, 123 D
Texture:					
Sand	2	40	10	1	1
Silt	18	30	20	4	4
Clay	80	30	70	95	95
Composition:					
Quartz	4	5	10	1	1
Feldspar	–	–	2	–	–
Clay	65	30	50	85	40
Glauconite	–	40	–	–	–
Pyrite	Tr	2	4	2	Tr
Dolomite	10	1	1	1	1
Foraminifers	Tr	2	15	Tr	1
Calc. nannofossils	20	20	10	10	55

ORGANIC CARBON AND CARBONATE (%):

	1, 118–120	2, 0–2	2, 85–87	3, 137–139
Carbonate	–	–	45.8	66.7
$CaCO_3$	45.8	44.3	–	–

SITE 547 HOLE A CORE 18 CORED INTERVAL 231.5–241.0 m sub-bottom

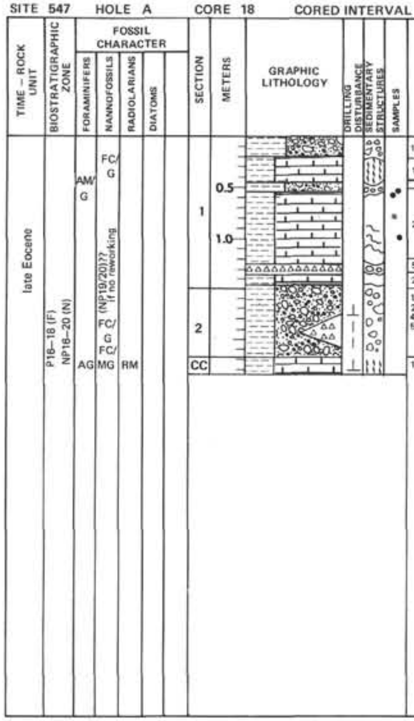

LITHOLOGIC DESCRIPTION

Mostly undisturbed, interlayered PEBBLY MUDSTONE CONGLOMERATE (Section 1, 0–20, 43–50, 145–150 cm; Section 2, 0–74 cm) and soft sediment deformed CLAYEY NANNOFOSSIL CHALK (big clast: Section 1, 23–45 cm, big clast or interlayer?: Section 1, 50–122 cm).

Clast lithologies (lithology numbers correspond to Core 17):

1. Light greenish gray (5GY 8/1) CLAYEY NANNOFOSSIL CHALK.
2. Dusky yellowish brown (10YR 2/2) CLAYEY NANNOFOSSIL CHALK.
4. Olive brown (5Y/YR 3/2) NANNOFOSSIL CLAY/MUDSTONE.
5. Dusky yellowish brown (10YR 2/2) PORCELLANITE CLASTS with fine granular texture, with mottling and occasional burrow structures.

SMEAR SLIDE SUMMARY (%):

	1, 80 D
Texture:	
Sand	5
Silt	20
Clay	75
Composition:	
Quartz	10
Feldspar	Tr
Mica	Tr
Heavy minerals	Tr
Clay	45
Volcanic glass	Tr
Glauconite	Tr
Pyrite	Tr
Foraminifers	5
Calc. nannofossils	35

ORGANIC CARBON AND CARBONATE (%):

	1, 55–56	1, 57–73	1, 99–100
Carbonate	71.2	–	64.6
$CaCO_3$	–	68.21	–

SITE 547 HOLE A CORE 19 CORED INTERVAL 241.0–250.5 m sub-bottom

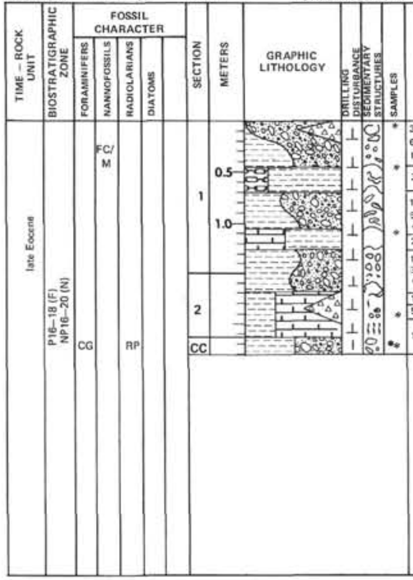

LITHOLOGIC DESCRIPTION

Faint drilling cakes of PEBBLY CLAYSTONE CONGLOMERATE interlayered with boulder sized clasts of NANNOFOSSIL CHALK.

M = "Matrix": light olive gray (5Y 5/2) CLAYEY NANNOFOSSIL CHALK.

Clast lithology (lithology numbers correspond through Cores 17–19):

1. Light greenish gray (5GY 8/1) CLAYEY NANNOFOSSIL CHALK.
2. Olive gray (5Y 3/2) NANNOFOSSIL CLAYSTONE.
3. Grayish olive green (5GY 3/2) CALCAREOUS CLAYSTONE.
5. Medium light gray (N6) PORCELLANITE.
6. Grayish yellow green (5GY 7/2) CLAYEY NANNOFOSSIL CHALK.

Soft sediment deformation overprinted by drilling disturbance.

SMEAR SLIDE SUMMARY (%):

	1, 3 D	1, 50 D	1, 110 D	2, 40 D	CC, 10 D
Composition:					
Quartz	2	3	1	1	Tr
Feldspar	–	Tr	3	–	–
Clay	85	60	57	20	15
Glauconite	–	–	1	–	–
Dolomite	3	3	3	3	–
Carbonate unspec.	–	27	–	10	30
Foraminifers	–	3	2	Tr	17
Calc. nannofossils	10	2	35	65	40

ORGANIC CARBON AND CARBONATE (%):

	CC, 3–4
Carbonate	67.2

SITE 547 HOLE A CORE 20 CORED INTERVAL 250.5–260.0 m sub-bottom

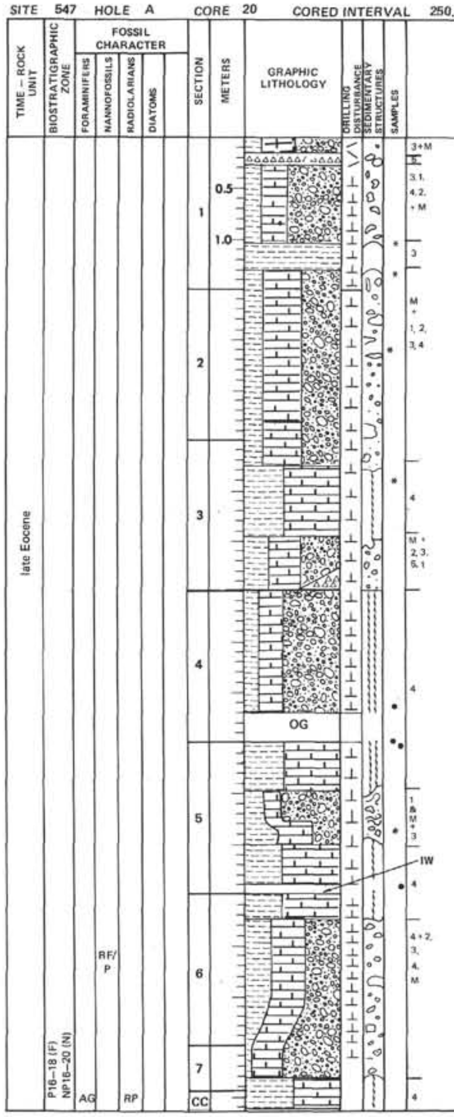

LITHOLOGIC DESCRIPTION

Drilling cakes of GRAVELLY MUDSTONE CONGLOMERATE with clast-free intervals (Section 3, 24–100 cm; Section 4, 0–5, 50 cm; Section 5, 95 cm–Section 6, 23 cm) of CLAYEY NANNOFOSSIL CHALK, moderate olive brown: 4.

M = "Matrix": light olive gray (5Y 5/2) CLAYEY NANNOFOSSIL CHALK.

Clast lithology (lithology numbers correlate through Cores 17–20):

1. Light greenish gray (5GY 8/1) CLAYEY NANNOFOSSIL CHALK.
2. Olive gray (5Y 3/2) NANNOFOSSIL CLAYSTONE.
3. Dusky yellow green (5GY 5/2) to grayish olive green (5GY 3/2) CALCAREOUS CLAYSTONE.
4. Moderate olive brown (5Y 4/4) CLAYEY NANNOFOSSIL CHALK.
5. Light gray (N5) PORCELLANITE.

Conglomerate mostly mud supported.

SMEAR SLIDE SUMMARY (%):

	1, 108 D	1, 135 D	2, 60 D	3, 40 D	5, 83 D
Composition:					
Quartz	–	5	3	1	1
Heavy minerals	–	–	–	–	Tr
Clay	88	20	25	40	15
Glauconite	–	4	–	–	–
Dolomite	–	3	5	1	2
Carbonate unspec.	2	15	10	5	15
Foraminifers	–	2	2	4	1
Calc. nannofossils	10	30	55	49	65

ORGANIC CARBON AND CARBONATE (%):

	4, 118–120	5, 0–2	5, 15–16	5, 140–150
Carbonate	–	–	57.7	59.0
$CaCO_3$	57.5	53.4	–	–

SITE 547 HOLE A CORE 21 CORED INTERVAL 260.0–269.5 m sub-bottom

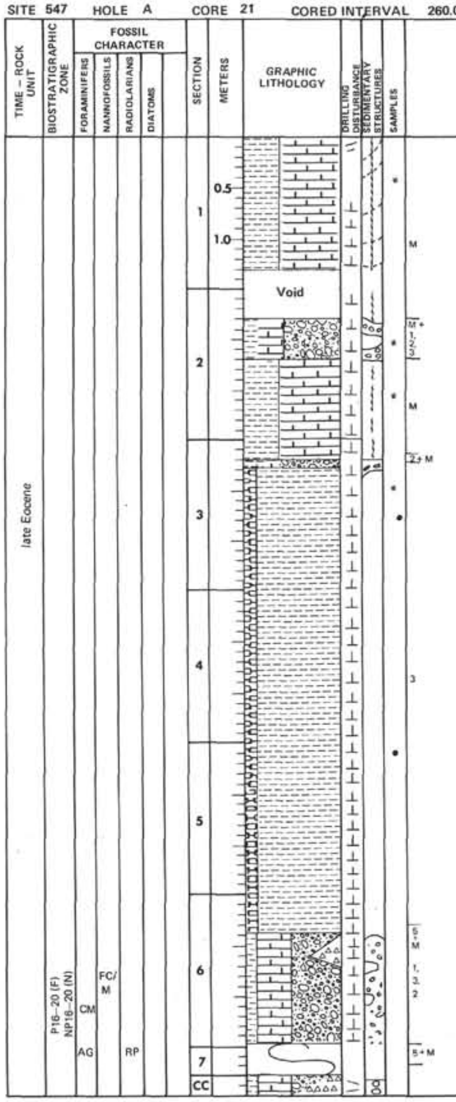

LITHOLOGIC DESCRIPTION

Section 1 through Section 3, 20 cm: drilling cakes of light olive gray (5Y 5/2) VERY CLAYEY NANNOFOSSIL CHALK (probably in situ lithology, M) with common burrowing.

At Section 2, 30–77 cm: an interval of GRAVELLY MUDSTONE CONGLOMERATE.

Section 3, 20 cm to Core-Catcher: interval of grayish olive green (5GY 3/2) *NANNOFOSSIL CLAYSTONE (Section 3, 28 cm–Section 6, 40 cm; 3, probably large clast of Cretaceous?)* bracketed by GRAVELLY MUDSTONE CONGLOMERATE.

Other clast lithologies (lithology numbers correlate through Cores 17–21):

1. White to light greenish gray (5GY 8/1) CLAYEY NANNOFOSSIL CHALK.
2. Olive gray (5Y 3/2) NANNOFOSSIL CLAYSTONE.
5. Light gray (N5–6) PORCELLANITE.

SMEAR SLIDE SUMMARY (%):

	1, 40 D	2, 50 D	2, 110 D	3, 50 D
Texture:				
Silt	–	–	–	15
Clay	–	–	–	85
Composition:				
Quartz	–	–	7	2
Feldspar	–	–	–	Tr
Mica	–	–	Tr	–
Clay	40	–	35	65
Pyrite	–	–	2	1
Dolomite	2	2	Tr	Tr
Carbonate unspec.	–	–	–	10
Foraminifers	8	–	5	2
Calc. nannofossils	50	98	50	20
Radiolarians	–	Tr	–	Tr
Fish remains	–	–	Tr	–

ORGANIC CARBON AND CARBONATE (%):

	3, 80–81	5, 10–11
Carbonate	16.9	10.6

SITE 547 HOLE A CORE 22 CORED INTERVAL 269.5–279.0 m sub-bottom

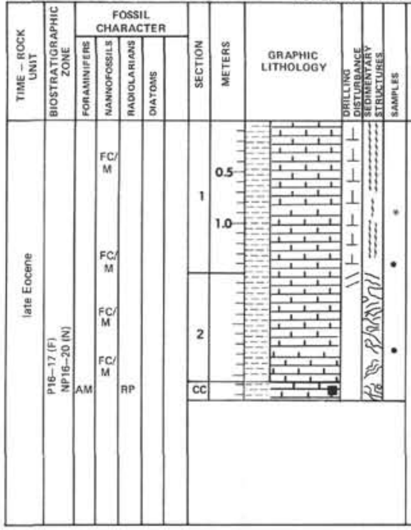

LITHOLOGIC DESCRIPTION

Partly drilling cakes and partly undisturbed, yellowish gray (5Y 7/2) and light olive gray (5Y 6/1) CLAYEY NANNOFOSSIL CHALK, with common, flattened and stretched bioturbation.

Section 2 and Core-Catcher show highly contorted and folded stratification with stretched and deformed clasts.

In Core-Catcher, top, a fragment of olive gray (5Y 4/1) to olive black (5Y 2/1) CHERT with traces of (prelithification) burrows.

SMEAR SLIDE SUMMARY (%):

	1, 90
Texture:	D
Silt	20
Clay	80
Composition:	
Quartz	2
Clay	30
Dolomite	1
Carbonate unspec.	5
Foraminifers	Tr
Calc. nannofossils	60
Radiolarians	Tr

ORGANIC CARBON AND CARBONATE (%):

	1, 149–150	2, 80–81
Carbonate	70.8	70.7

SITE 547 HOLE A CORE 23 CORED INTERVAL 279.0–288.5 m sub-bottom

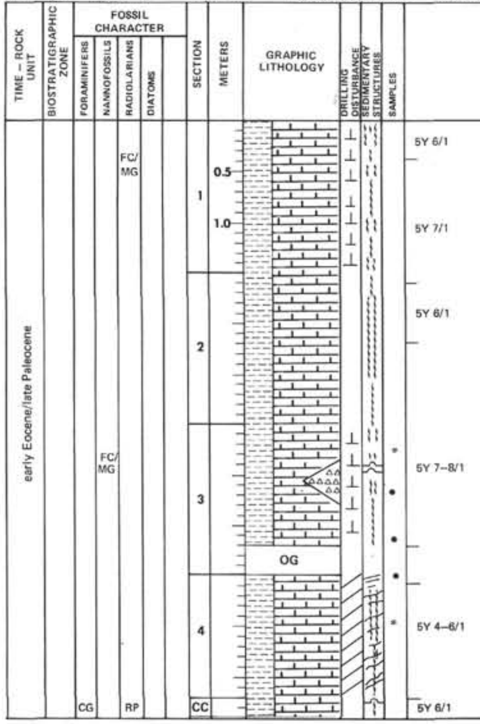

LITHOLOGIC DESCRIPTION

Drilling cakes of light yellowish gray (5Y 8/1) to olive gray (5Y 6/1) CLAYEY NANNOFOSSIL CHALK with moderate to abundant bioturbation, Burrows are stretched and flattened and partly sheared.

More massive clast(?) or layer of clay rich sediment at Section 3, 17–30 cm. In Section 4, irregular lamination, dip of approximately 10°.

Section 3, 53–56 cm light gray (N6) PORCELLANITE.

SMEAR SLIDE SUMMARY (%):

	3, 27	4, 45
	D	D
Texture:		
Silt	20	30
Clay	80	70
Composition:		
Quartz	2	2
Clay	40	30
Dolomite	Tr	Tr
Carbonate unspec.	10	7
Calc. nannofossils	45	50
Radiolarians	–	4

ORGANIC CARBON AND CARBONATE (%):

	3, 70–71	3, 118–120	4, 0–2
Carbonate	70.7	–	57.5
$CaCO_3$	–	73.8	–

SITE 547 HOLE A CORE 24 CORED INTERVAL 288.5–298.0 m sub-bottom

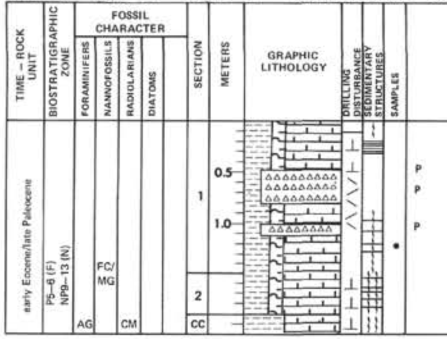

LITHOLOGIC DESCRIPTION

Moderately fragmented, light greenish gray (5GY 8/1) to light olive gray (5Y 6/1) SILICEOUS CLAYEY NANNOFOSSIL CHALK with gradations to PORCELLANITE (P). Moderate bioturbation shows flattening throughout; radiolarians common.

ORGANIC CARBON AND CARBONATE (%):

	1, 120–121
Carbonate	56.7

SITE 547 HOLE A CORE 25 CORED INTERVAL 298.0–307.5 m sub-bottom

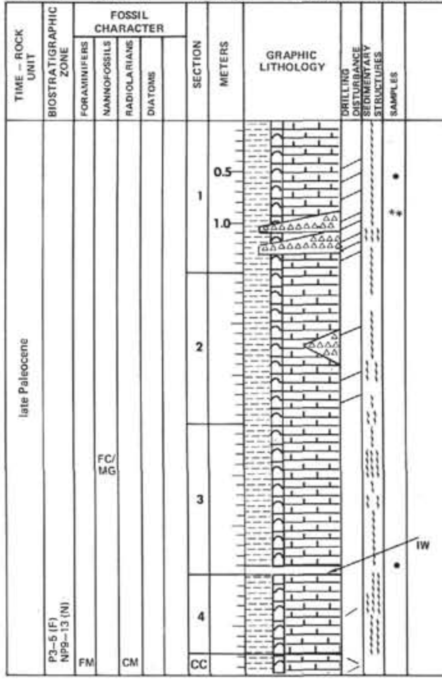

LITHOLOGIC DESCRIPTION

Slightly fragmented, light olive gray (5Y 6/1) SILICEOUS CLAYEY NANNOFOSSIL CHALK with common to abundant olive gray (5Y 4/1) burrows (mostly planolites and some chondrites and zoophycus).

Gradations to PORCELLANITE of same color and texture (P).

SMEAR SLIDE SUMMARY (%):

	1, 90	1, 92
	D	D
Texture:		
Silt	30	–
Clay	70	–
Composition:		
Quartz	2	2
Clay	30	40
Pyrite	–	Tr
Dolomite	Tr	Tr
Carbonate unspec.	10	12
Calc. nannofossils	55	45
Radiolarians	Tr	Tr

ORGANIC CARBON AND CARBONATE (%):

	1, 54–55	3, 140–150
Carbonate	62.2	59.5

SITE 547 HOLE A CORE 26 CORED INTERVAL 307.5–317.0 m sub-bottom

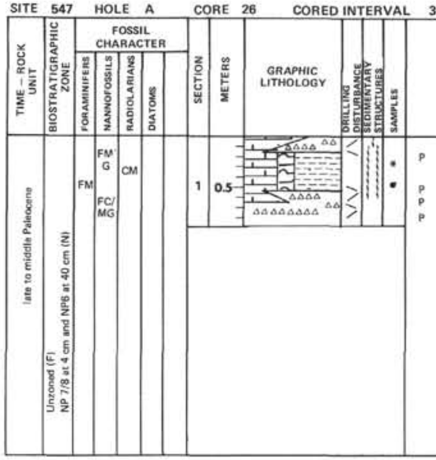

LITHOLOGIC DESCRIPTION

Highly fragmented, dark greenish gray (5GY 4/1) SILICEOUS NANNOFOSSIL-RICH CLAYSTONE with irregular layering grading to olive black (5Y 2/1) PORCELLANITE(?). P

Section 1, 0–10 cm: greenish gray (5GY 6/1) VERY CLAYEY NANNOFOSSIL CHALK with burrowing.

SMEAR SLIDE SUMMARY (%):

	1, 25
	D
Composition:	
Clay	55
Pyrite	1
Dolomite	1
Calc. nannofossils	42
Radiolarians	Tr

ORGANIC CARBON AND CARBONATE (%):

	1, 47–48
Carbonate	34.3

SITE 547 HOLE A CORE 27 CORED INTERVAL 317.0–326.5 m sub-bottom

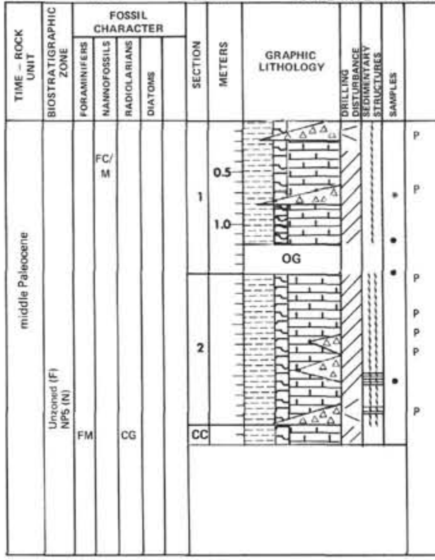

LITHOLOGIC DESCRIPTION

Slightly fragmented, greenish gray (5GY 6/1) SILICEOUS CLAYEY NANNOFOSSIL CHALK to CLAYSTONE, common bioturbation (predominantly zoophycus in Section 1 and planolites and zoophycus in Section 2).

Gradational contacts to olive black (5Y 2/1) PORCELLANITE/CHERT (P) with similar burrowing.

SMEAR SLIDE SUMMARY (%):

	1, 70
	D
Texture:	
Sand	Tr
Silt	5
Clay	95
Composition:	
Quartz	2
Clay	25
Volcanic glass	Tr
Dolomite	2
Carbonate unspec.	1
Foraminifers	3
Calc. nannofossils	60
Sponge spicules	Tr

ORGANIC CARBON AND CARBONATE (%):

	1, 118–120	2, 0–2	2, 104–105
Carbonate	–	–	35.8
$CaCO_3$	48.3	51.9	–

SITE 547 HOLE A CORE 28 CORED INTERVAL 326.5–336.0 m sub-bottom

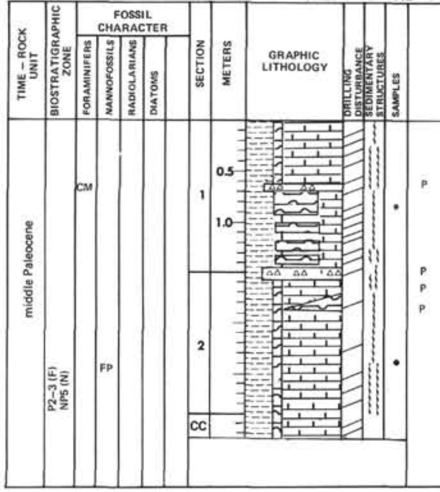

LITHOLOGIC DESCRIPTION

Slightly fragmented, greenish gray SILICEOUS CLAYEY NANNOFOSSIL CHALK with abundant, well preserved burrowing: planolites, zoophycus, and chondrites.

Siliceous intervals grade to light-colored PORCELLANITE (P) containing burrowing as above.

SMEAR SLIDE SUMMARY (%):

	1, 83
	D
Texture:	
Silt	25
Clay	75
Composition:	
Quartz	1
Clay	50
Pyrite	1
Dolomite	Tr
Carbonate unspec.	7
Foraminifers	40

ORGANIC CARBON AND CARBONATE (%):

	2, 83–84
Carbonate	56.7

SITE 547 HOLE A CORE 29 CORED INTERVAL 336.0–345.5 m sub-bottom

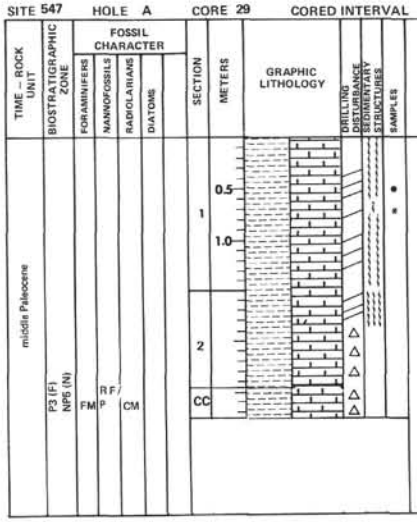

LITHOLOGIC DESCRIPTION

Slightly fractured and drilling breccia of greenish gray (5GY 4/1) VERY CLAYEY NANNOFOSSIL CHALK to CLAYSTONE with common to abundant burrowing: mostly flattened, common zoophycus, and some planolites. Many reburrowed burrows.

Minor siliceous levels.

SMEAR SLIDE SUMMARY (%):

	1, 68
	D
Texture:	
Silt	30
Clay	70
Composition:	
Quartz	2
Clay	55
Pyrite	1
Dolomite	Tr
Carbonate unspec.	10
Calc. nannofossils	30

ORGANIC CARBON AND CARBONATE (%):

	1, 48–50
Carbonate	55.7

SITE 547 HOLE A CORE 30 CORED INTERVAL 345.5–355.0 m sub-bottom

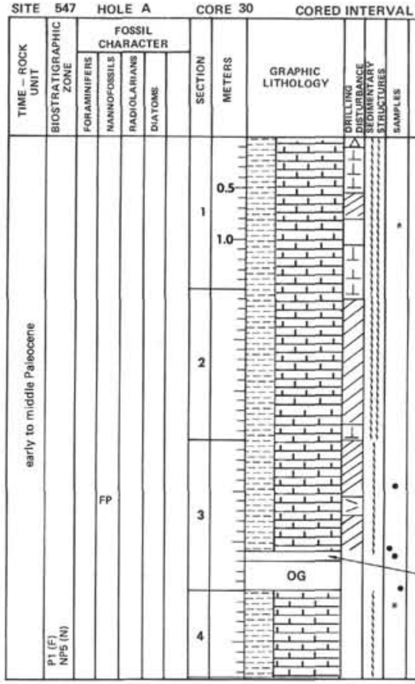

LITHOLOGIC DESCRIPTION

Mostly slightly fractured, greenish gray (5GY 6/1) SLIGHTLY SILICEOUS CLAYEY NANNOFOSSIL CHALK with common zoophycus and planolites in top of core; getting rare and indistinct towards base.

SMEAR SLIDE SUMMARY (%):

	1, 80	4, 10	CC
	D	D	D
Texture:			
Silt	30	20	25
Clay	70	80	75
Composition:			
Quartz	5	15	10
Mica	Tr	3	3
Heavy minerals	Tr	1	–
Clay	50	50	50
Volcanic glass	1	Tr	–
Dolomite	1	1	Tr
Carbonate unspec.	–	–	Tr
Calc. nannofossils	35	20	25
Diatoms	Tr	–	–
Radiolarians	4	7	4
Sponge spicules	Tr	Tr	1

ORGANIC CARBON AND CARBONATE (%):

	3, 40–43	3, 110–120	3, 118–120	4, 0–2
Carbonate	55.2	–	–	67.7
$CaCO_3$	–	66.2	64.6	–

SITE 547 HOLE A CORE 31 CORED INTERVAL 355.0–364.5 m sub-bottom

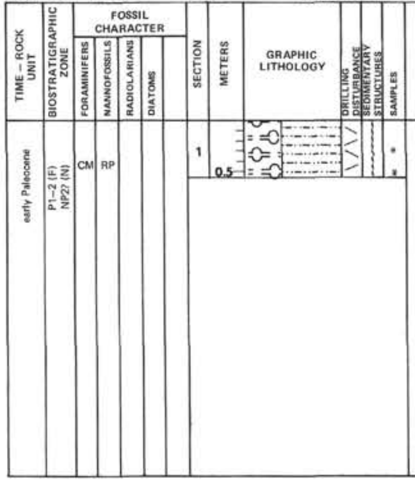

LITHOLOGIC DESCRIPTION

Highly fragmented, greenish gray (5GY 5–6/1) SILICEOUS NANNOFOSSIL-BEARING MUDSTONE.

SMEAR SLIDE SUMMARY (%):

	1, 30	1, 52
	D	D
Texture:		
Sand	Tr	-
Silt	20	–
Clay	80	–
Composition:		
Quartz	10	10
Mica	Tr?	–
Heavy minerals	Tr?	2?
Clay	50	35
Volcanic glass	5?	10
Dolomite	1	1
Carbonate unspec.	–	2
Calc. nannofossils	25	15
Radiolarians	8	20
Sponge spicules	1	5

SITE 547 HOLE A CORE 32 CORED INTERVAL 364.5–374.0 m sub-bottom

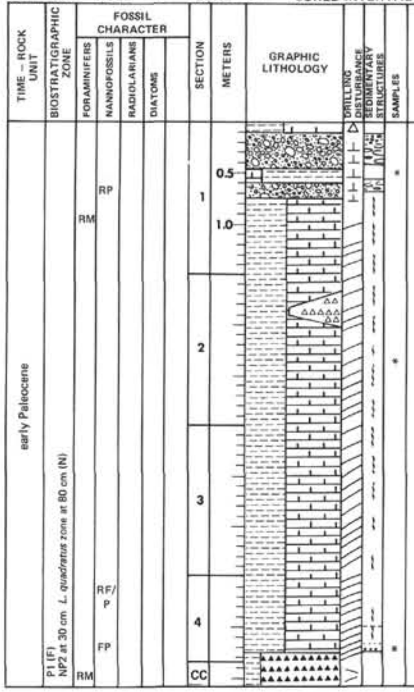

LITHOLOGIC DESCRIPTION

Major lithology: slightly fragmented, grayish green (10GY 5/2) to greenish gray (5G 4/1) VERY CLAYEY NANNOFOSSIL CHALK. At Section 1, 10–40 and 58–74 cm two beds of PEBBLY CONGLOMERATE, with densely packed, flattened pebbles of light gray (N6) NANNOFOSSIL CHALK, medium gray (N4) PORCELLANITE and variable green to dark gray (N3) CLAYEY NANNOFOSSIL CHALK. Upper bed shows indistinct grading from 4 cm to 5 mm at the top. At Section 4, 67–75 cm GRADED BED of foraminiferal sand with granule-sized clasts of nannofossil chalk grading upwards into dark greenish gray (5G 4/1) clayey nannofossil chalk.

SMEAR SLIDE SUMMARY (%):

	1, 45	2, 90	4, 73
	D	D	D
Composition:			
Quartz	4	3	3
Clay	82	30	35
Dolomite	2	3	1
Carbonate unspec.	–	–	24
Foraminifers	Tr	7	7
Calc. nannofossils	12	57	30
Sponge spicules	–	–	Tr

SITE 547 HOLE A CORE 33 CORED INTERVAL 374.0–383.5 m sub-bottom

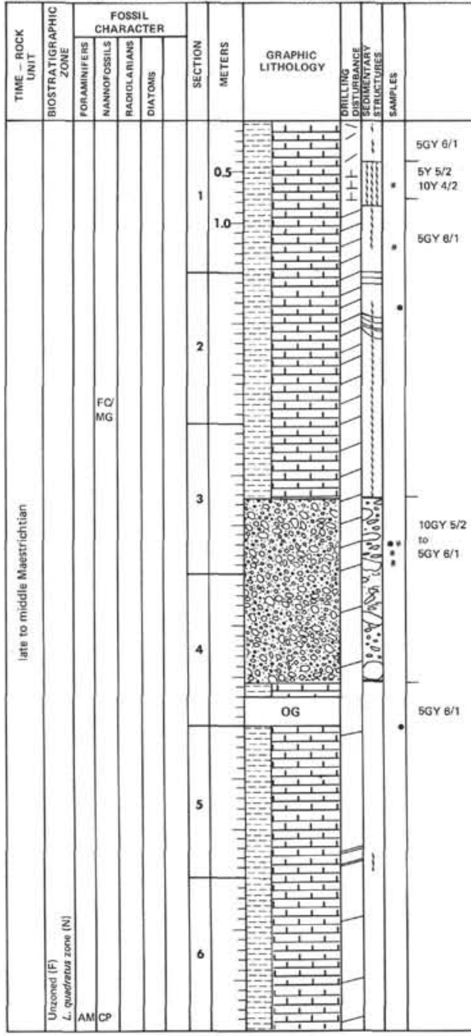

LITHOLOGIC DESCRIPTION

Major lithology: slightly fractured, greenish gray (5GY 6/1) CLAYEY NANNOFOSSIL CHALK with few grayish olive (10Y 4/2) bioturbation (planolites and chondrites-like).

Section 1, 40–81 cm, light olive gray (5Y 5/2) to grayish olive (10Y 4/2) CLAYEY NANNOFOSSIL CHALK with abundant, deformed bioturbation.

Section 3, 74 cm through Section 4, 106 cm GRAVELLY CONGLOMERATE with moderately to well rounded clasts of plates and darker colored CLAYEY NANNOFOSSIL CHALK and of dusky yellowish green (5GY 5/2) NANNOFOSSIL CLAYSTONE.

SMEAR SLIDE SUMMARY (%):

	1, 61	1, 125	3, 118	3, 127	3, 133
	D	D	D	M	M
Composition:					
Quartz	5	–	1	0.5	0.5
Clay	30	10	40	55	40
Pyrite	Tr	–	–	–	Tr
Dolomite	Tr	2	Tr	–	2
Foraminifers	5	2	3	–	2
Calc. nannofossils	55	85	57	45	55
Radiolarians	Tr	–	–	–	–
Plant debris	Tr	–	–	–	–
Very fine spicules	4	–	–	–	–

ORGANIC CARBON AND CARBONATE (%):

	2, 33–34	3, 118–120	5, 0–2
Carbonate	71.7	–	–
$CaCO_3$	–	53.9	73.3

SITE 547 HOLE A CORE 34 CORED INTERVAL 383.5–393.0 m sub-bottom

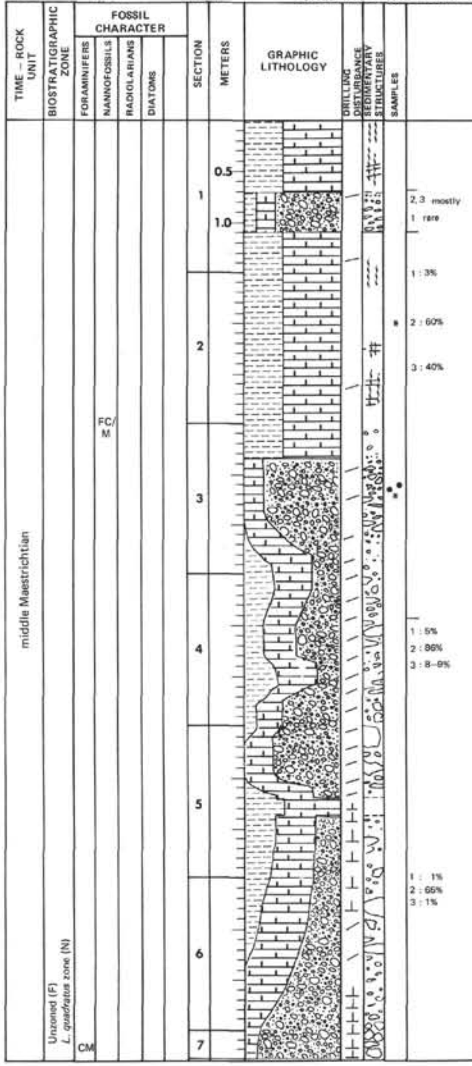

LITHOLOGIC DESCRIPTION

Section 1, 0–70 and 110 cm through Section 3, 35 cm, almost undisturbed greenish gray (5GY 6/1) VERY CLAYEY NANNOFOSSIL CHALK with common zoophycus, planolites and chondrites-type bioturbation.

Section 1, 70–110 and Section 3, 35 cm through Core-Catcher: variably disturbed mostly grayish green (10G 4/2) PEBBLY-COBBLY CONGLOMERATE.

Clast lithologies:

1. Grayish-green (10G 4/2), waxy NANNOFOSSIL-BEARING CLAYSTONE.
2. Variably grayish green CLAYEY NANNOFOSSIL CHALK.
3. Olive gray (5Y 4/1) NANNOFOSSIL CLAYSTONE.
4. Dark greenish gray (5GY 4/1) soft waxy CALCAREOUS CLAYSTONE.

SMEAR SLIDE SUMMARY (%):

	2, 50	3, 69
	D	D
Composition:		
Quartz	2	2
Clay	35	55
Pyrite	–	0.5
Dolomite	2	2
Foraminifers	3	1
Calc. nannofossils	58	43
Fish remains	–	Tr

ORGANIC CARBON AND CARBONATE (%):

	3, 54–55	3, 66–67
Carbonate	10.5	37.1

SITE 547 HOLE A CORE 35 CORED INTERVAL 393.0–397.5 m sub-bottom

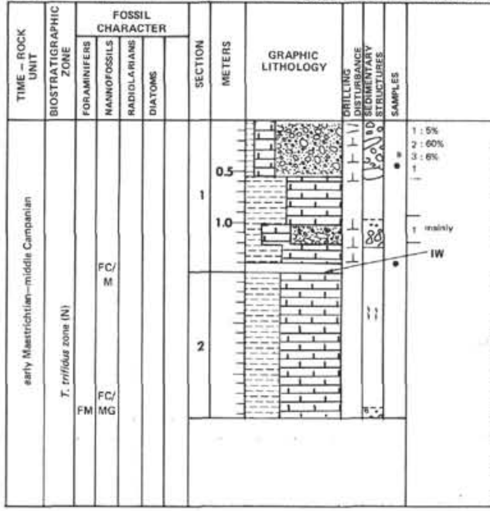

LITHOLOGIC DESCRIPTION

Section 1, 0–55 and 100–127 cm: PEBBLY MUDSTONE CONGLOMERATE with clast lithologies described in Core 34, Sections 1–3. Matrix: dusky yellowish green GLAUCONITE-BEARING VERY CLAYEY NANNOFOSSIL CHALK.

Section 1, 55–100, 127–140 cm and Section 2: greenish gray (5GY 6/1) VERY CLAYEY NANNOFOSSIL CHALK with rare bioturbation and occasional darker granules (base of Section 2).

SMEAR SLIDE SUMMARY (%):

	1, 34
	D
Composition:	
Quartz	1
Heavy minerals	Tr
Clay	40
Glauconite	3
Pyrite	Tr
Dolomite	5
Calc. nannofossils	45
Fish remains	Tr

ORGANIC CARBON AND CARBONATE (%):

	1, 42–43	1, 140–150
Carbonate	1.0	62.6

SITE 547 HOLE A CORE 36 CORED INTERVAL 397.5–402.5 m sub-bottom

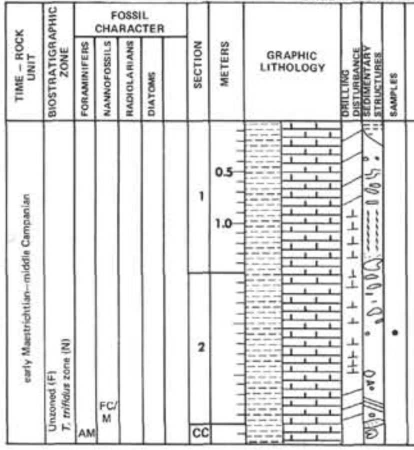

LITHOLOGIC DESCRIPTION

Major lithology: slightly fragmented, greenish gray (5GY 6/1) VERY CLAYEY NANNOFOSSIL CHALK.

In Section 1, 40–85 cm and 140 cm through Section 2, 55 and 100–112 cm and Section 3: scattered pebble to cobble sized rounded, clasts of the types described in Core 34.

ORGANIC CARBON AND CARBONATE (%):

	2, 58–60
Carbonate	66.2

SITE 547 HOLE A CORE 37 CORED INTERVAL 402.5–412.0 m sub-bottom

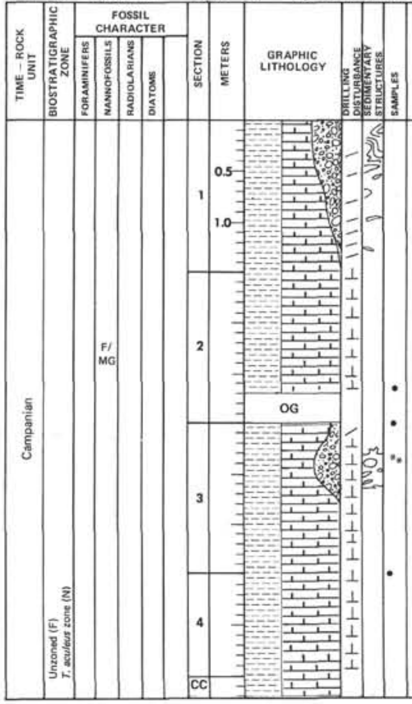

LITHOLOGIC DESCRIPTION

Major lithology: moderately fragmented grayish green (10GY 5/2) VERY CLAYEY NANNOFOSSIL CHALK.

Flattened and contorted mud pebbles of the lithologies described in Core 34, occur scattered throughout and are enriched in Section 1, 0–50 cm and Section 3, 25–50 cm.

SMEAR SLIDE SUMMARY (%):

	3, 36	3, 40
	D	D
Composition:		
Quartz	1	–
Clay	55	95
Dolomite	3	0.5
Foraminifers	1	–
Calc. nannofossils	40	5

ORGANIC CARBON AND CARBONATE (%):

	2, 118–120	3, 0–2	4, 1–2
Carbonate	–	–	59.7
$CaCO_3$	61.1	56.5	–

SITE 547 HOLE A CORE 38 CORED INTERVAL 412.0–421.5 m sub-bottom

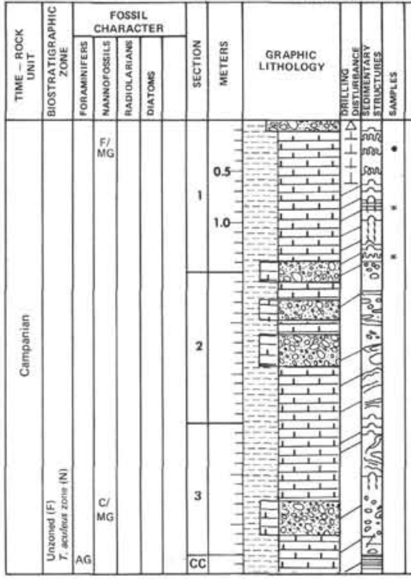

LITHOLOGIC DESCRIPTION

Mostly slightly fragmented, greenish gray (5GY 6/1) VERY CLAYEY NANNOFOSSIL CHALK with common bioturbation. Slump folded and contorted throughout. CONGLOMERATE layers occur at several levels. Clasts are matrix supported, strongly flattened and are of the types described in Core 34. Most lithologies have very sharp boundaries and suggest cobble to boulder sized clasts.

SMEAR SLIDE SUMMARY (%):

	1, 84	1, 133
	D	D
Texture:		
Sand	2	–
Silt	7	–
Clay	90	–
Composition:		
Quartz	2	2
Feldspar	Tr	–
Mica	Tr	–
Clay	70	50
Pyrite	2	Tr
Dolomite	1	2
Foraminifers	Tr	Tr
Calc. nannofossils	20	45
Radiolarians	–	Tr

ORGANIC CARBON AND CARBONATE (%):

	1, 26–27
Carbonate	59.7

SITE 547 HOLE A CORE 39 CORED INTERVAL 421.5–431.0 m sub-bottom

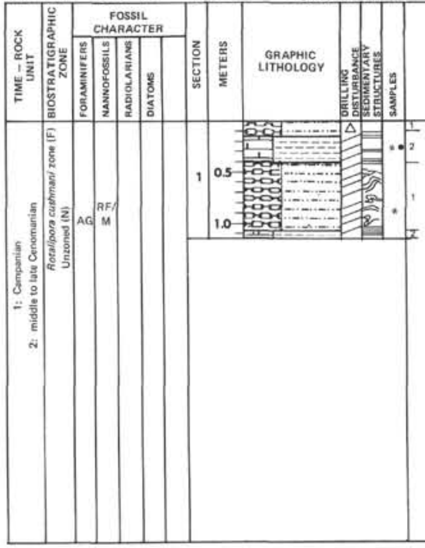

LITHOLOGIC DESCRIPTION

1. Greenish gray (5G 6/1) CALCAREOUS MUDSTONE, slump folded burrows.
2. Grayish olive green (5GY 3/2) NANNOFOSSIL-RICH CLAYSTONE with indistinct, very flattened laminae, abundant pyrite as nodules and burrow fillings. Clays swell quickly after splitting the core.

SMEAR SLIDE SUMMARY (%):

	1, 25	1, 90
	D	D
Texture:		
Silt	20	45
Clay	80	55
Composition:		
Quartz	5	10
Feldspar	Tr	–
Mica	–	Tr
Clay	65	40
Pyrite	–	1
Dolomite	2	2
Carbonate unspec.	2	30
Foraminifers	Tr	–
Calc. nannofossils	20	15
Radiolarians	Tr	–

ORGANIC CARBON AND CARBONATE (%):

	1, 25–26
Carbonate	27.9

SITE 547 HOLE A CORE 40 CORED INTERVAL 431.0–440.5 m sub-bottom

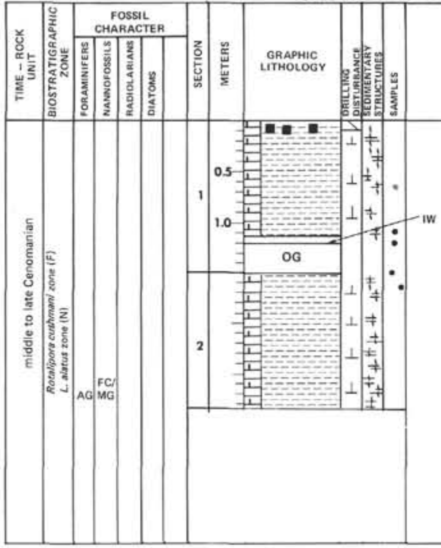

LITHOLOGIC DESCRIPTION

Section 1, 0–15 cm: highly fragmented grayish green (10GY 5/2) to grayish olive green (5GY 3/2) NANNOFOSSIL CLAYSTONE with greenish gray (5GY 6/1) fragments of CALCAREOUS MUDSTONE.

Section 1, 15 cm to base of core: incipient drilling cake disturbance, grayish green (10GY 5/2) to grayish olive green (5GY 3/2) NANNOFOSSIL CLAYSTONE with some pyritic burrow fillings.

XRD shows illite, mixed layered smectite-illite(?) kaolinite.

SMEAR SLIDE SUMMARY (%):

	1, 66
	D
Texture:	
Silt	10
Clay	90
Composition:	
Quartz	2
Mica	1
Clay	50
Pyrite	1
Dolomite	2
Calc. nannofossils	45

ORGANIC CARBON AND CARBONATE (%):

	1, 110–120	1, 118–120	2, 0–2	2, 20–21
Carbonate	–	–	20.3	21.9
$CaCO_3$	17.8	23.9	–	–

SITE 547 HOLE A CORE 41 CORED INTERVAL 440.5–450.0 m sub-bottom

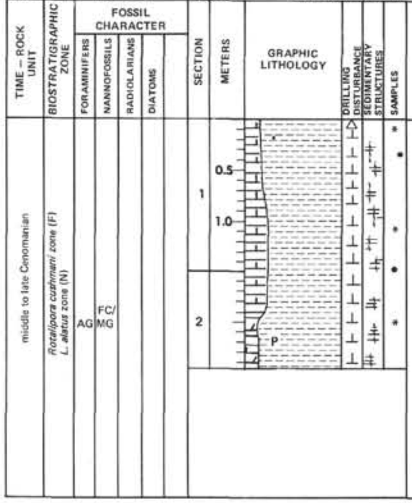

LITHOLOGIC DESCRIPTION

Incipient drilling disturbance, grayish olive green (5GY 3/2) NANNOFOSSIL CLAYSTONE with pyrite filled burrows.

In Section 2, 47–65 and 80–95 cm: SLIGHTLY DOLOMITIC CLAYSTONE rich in pyrite, about 10% dolomite and 3% pyrite.

SMEAR SLIDE SUMMARY (%):

	1, 10	1, 105	2, 50
	M	D	D
Texture:			
Silt	20	10	20
Clay	80	90	80
Composition:			
Quartz	1	–	2
Mica	–	Tr	Tr
Clay	40	90	80
Pyrite	–	–	3
Dolomite	2	5	10
Carbonate unspec.	1	–	–
Foraminifers	Tr	–	–
Calc. nannofossils	55	5	5

ORGANIC CARBON AND CARBONATE (%):

	1, 34–50	1, 149–150
Carbonate	15.7	22.3

SITE 547 HOLE A CORE 42 CORED INTERVAL 450.0–459.5 m sub-bottom

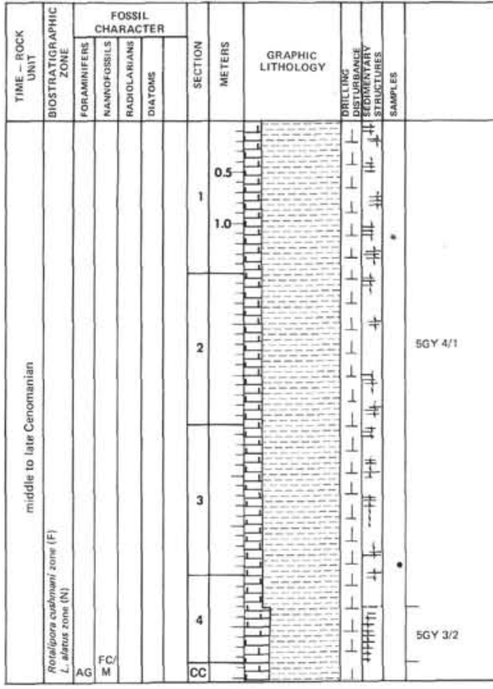

LITHOLOGIC DESCRIPTION

Drilling cakes of dark greenish gray (5GY 4/1) to grayish olive green (5GY 3/2) NANNOFOSSIL CLAYSTONE with very indistinct laminae of olive gray (5Y 3/2) which represent mostly flattened burrows. Burrows are rich in pyrite, most are 0.5–3 mm in diameter. Swelling clays disrupt cut surface towards base of core.

Color change to grayish olive green (5GY 3/2), slightly more calcareous lithology with better preserved burrowing.

SMEAR SLIDE SUMMARY (%):

	1, 114 D
Texture:	
Silt	20
Clay	80
Composition:	
Quartz	5
Clay	70
Gypsum?	1
Pyrite	1
Dolomite	2
Calc. nannofossils	20

ORGANIC CARBON AND CARBONATE (%):

	3, 140–142
Carbonate	21.9

SITE 547 HOLE A CORE 43 CORED INTERVAL 459.5–469.0 m sub-bottom

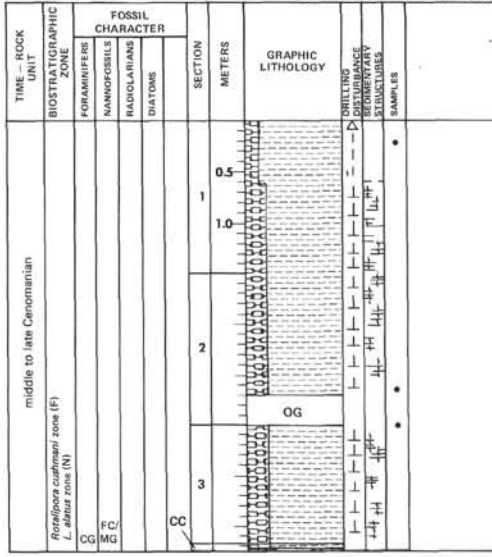

LITHOLOGIC DESCRIPTION

Mostly drilling cakes of grayish olive green (5GY 3/2) CALCAREOUS CLAYSTONE with thin layers and laminae of dark greenish gray (5G 4/1).

Pyrite is common throughout and sometimes concentrated in layers of 0.5 cm thickness and nodules of 2–4 mm. Swelling clays. A variably developed thin lamination represents flattened burrows.

Section 1, 0–60 cm: very waxy, not swelling, structureless, no burrowing.

ORGANIC CARBON AND CARBONATE (%):

	1, 23–24	2, 118–120	3, 0–2
Carbonate	21.4	–	18.3
$CaCO_3$	–	13.7	–

SITE 547 HOLE A CORE 44 CORED INTERVAL 469.0–478.5 m sub-bottom

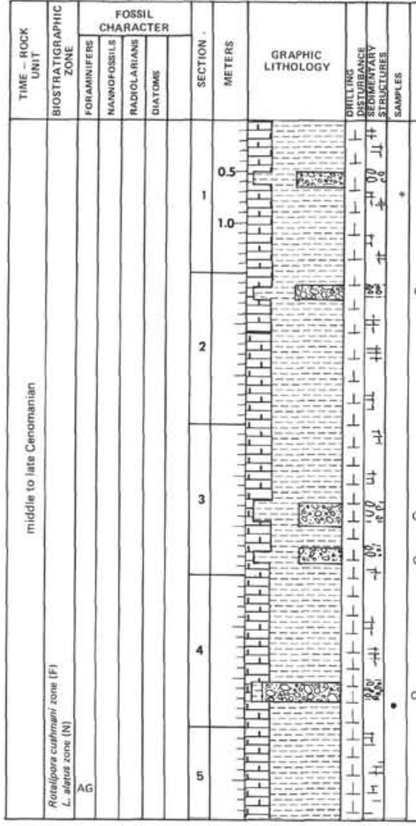

LITHOLOGIC DESCRIPTION

Major lithology: drilling cakes of dark greenish gray (5GY 4/1) NANNOFOSSIL CLAYSTONE with faint lamination and in places common bioturbation. Pyrite common throughout.

C = at several levels PEBBLY CLAYSTONES with throughly flattened (length to thickness 5:1) claystone pebbles of same lithology as matrix.

At Section 4, 100–120 cm, roughly graded turbidite.

SMEAR SLIDE SUMMARY (%):

	1, 72 D
Composition:	
Quartz	1
Clay	78
Pyrite	1
Barite	Tr
Dolomite	Tr
Foraminifers	1
Calc. nannofossils	20

ORGANIC CARBON AND CARBONATE (%):

	4, 127–128
Carbonate	25.9

SITE 547 HOLE A CORE 45 CORED INTERVAL 478.5–488.0 m sub-bottom

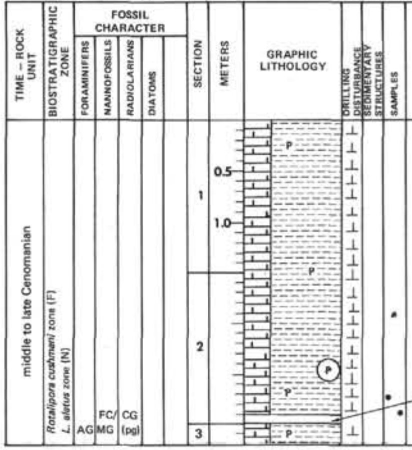

LITHOLOGIC DESCRIPTION

Drilling cakes of grayish green (10G 4/2) to grayish olive green (5GY 3/2) NANNOFOSSIL CLAYSTONE with olive gray (5Y 4/1) burrows and wisps rich in pyrite.

SMEAR SLIDE SUMMARY (%):

	2, 40
	D
Composition:	
Quartz	Tr
Clay	82
Dolomite	Tr
Foraminifers	4
Calc. nannofossils	12
Radiolarians	Tr
Sponge spicules	1

ORGANIC CARBON AND CARBONATE (%):

	1, 121–122	2, 140–150
Carbonate	25.9	22.3

SITE 547 HOLE A CORE 46 CORED INTERVAL 488.0–497.5 m sub-bottom

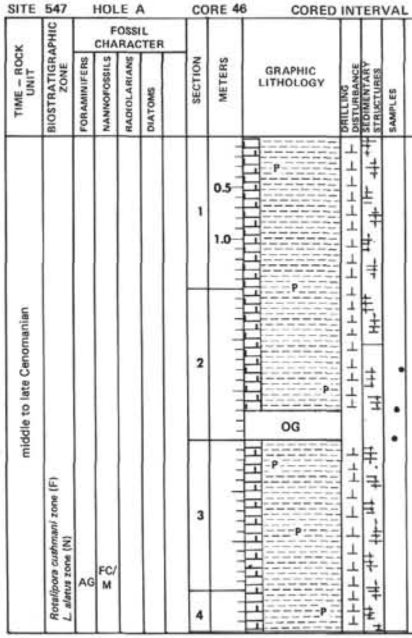

LITHOLOGIC DESCRIPTION

Drilling cakes of dusky green (5G 3/2) to dusky yellowish green (10GY 3/2) NANNOFOSSIL CLAYSTONE with olive gray (5Y 4/1), very flattened burrow traces rich in pyrite.

ORGANIC CARBON AND CARBONATE (%):

	2, 79–80	2, 118–120	3, 0–2
Carbonate	20.4	–	–
$CaCO_3$	–	13.7	29.0

SITE 547 HOLE A CORE 47 CORED INTERVAL 497.5–507.0 m sub-bottom

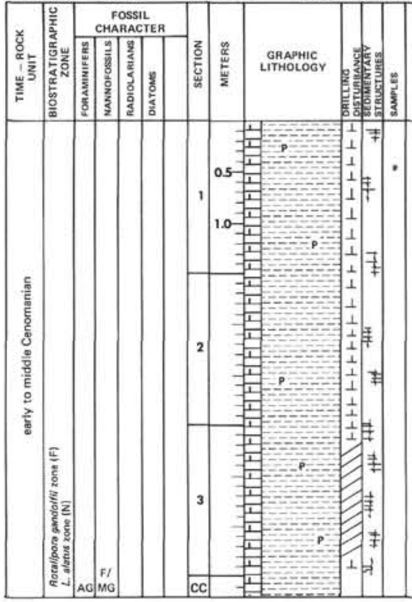

LITHOLOGIC DESCRIPTION

Mostly drilling cakes of grayish olive-green (5GY 3/2) and dusky yellowish-green (10GY 3/2) NANNOFOSSIL CLAYSTONE with olive gray (5Y 4/1), flattened burrows. Rich in pyrite throughout.

SMEAR SLIDE SUMMARY (%):

	1, 50
	D
Composition:	
Quartz	Tr
Clay	62
Dolomite	1
Carbonate unspec.	2
Foraminifers	5
Calc. nannofossils	30
Sponge spicules	Tr

SITE 547 HOLE A CORE 48 CORED INTERVAL 507.0–516.5 m sub-bottom

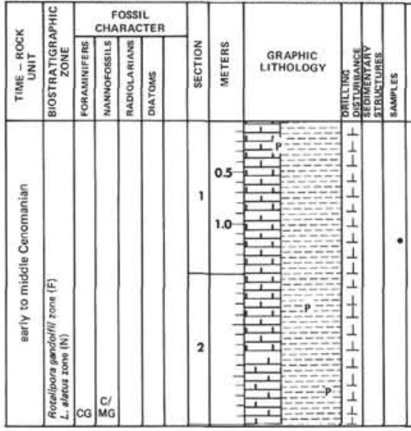

LITHOLOGIC DESCRIPTION

Drilling cakes of dusky yellowish-green (10GY 3/2) NANNOFOSSIL CLAYSTONE with dusky green burrow mottling. Pyrite present throughout.

ORGANIC CARBON AND CARBONATE (%):

	1, 119–120
Carbonate	28.9

SITE 547 HOLE A CORE 49 CORED INTERVAL 516.5–526.0 m sub-bottom

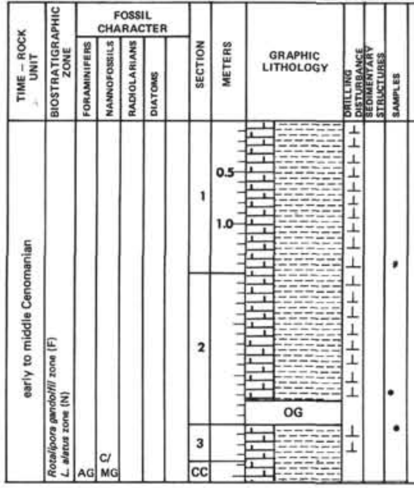

LITHOLOGIC DESCRIPTION

Drilling cakes of dark greenish gray (5GY 4/1) NANNOFSSIL CLAYSTONE, firm, structureless.

SMEAR SLIDE SUMMARY (%):

	1, 140
	D
Composition:	
Quartz	1
Clay	75
Dolomite	2
Pyrite	2
Barite	1
Zeolite	Tr
Carbonate unspec.	3
Foraminifers	2
Calc. nannofossils	15

ORGANIC CARBON AND CARBONATE (%):

	2, 118–120	3, 0–2
Carbonate	14.2	24.4

SITE 547 HOLE A CORE 50 CORED INTERVAL 526.0–535.5 m sub-bottom

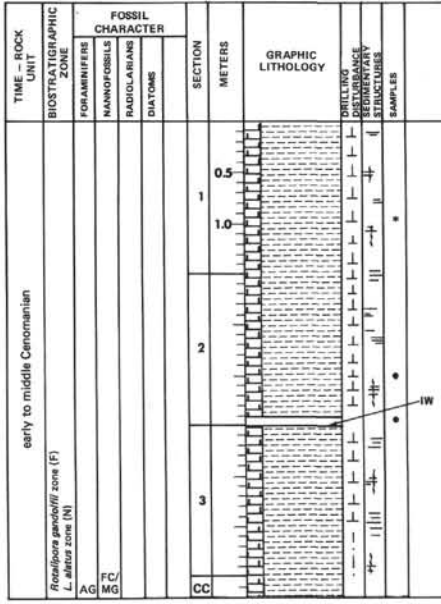

LITHOLOGIC DESCRIPTION

Drilling cakes of dark greenish gray (5G 4/1) NANNOFOSSIL CLAYSTONE with faint lamination and rare burrowing.

SMEAR SLIDE SUMMARY (%):

	1, 95
	M
Texture:	
Silt	10
Clay	90
Composition:	
Quartz	2
Clay	75
Pyrite	2
Barite	Tr
Dolomite	Tr
Foraminifers	Tr
Calc. nannofossils	20

ORGANIC CARBON AND CARBONATE (%):

	2, 99–100	2, 140–150
Carbonate	17.9	18.3

SITE 547 HOLE A CORE 51 CORED INTERVAL 535.5–545.0 m sub-bottom

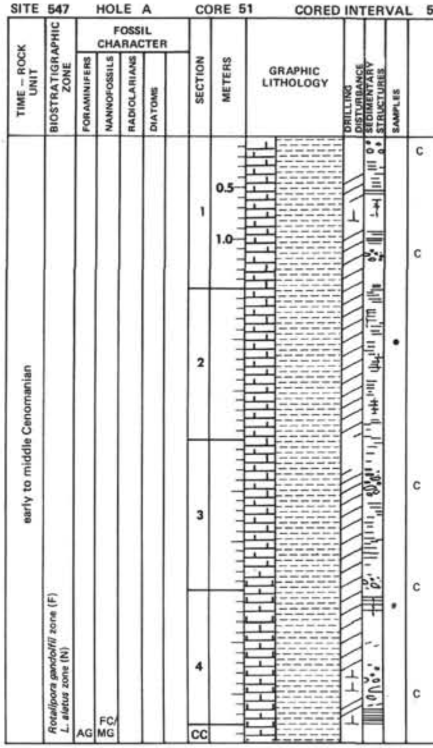

LITHOLOGIC DESCRIPTION

Major lithology: slightly fractured, dark greenish gray (5GY 4/1) NANNOFOSSIL CLAYSTONE with faint, thin lamination of some mm thickness of greenish black (5Y 2/1). Intermixed layers of waxy and swelling claystones. Swelling layers contain a mixed layer illite-smectite component (XRD), waxy, non-swelling.

C = several intervals of PEBBLY CLAYSTONE, dark greenish gray and olive gray (5Y 4/1) clasts are rounded, elongate, parallel to bedding.

SMEAR SLIDE SUMMARY (%):

	4, 17
	D
Texture:	
Silt	10
Clay	90
Composition:	
Quartz	2
Clay	75
Volcanic glass	Tr
Pyrite	1
Dolomite	Tr
Carbonate unspec.	1
Foraminifers	Tr
Calc. nannofossils	20

ORGANIC CARBON AND CARBONATE (%):

	2, 53–54
Carbonate	30.5

SITE 547 HOLE A CORE 52 CORED INTERVAL 545.0–554.5 m sub-bottom

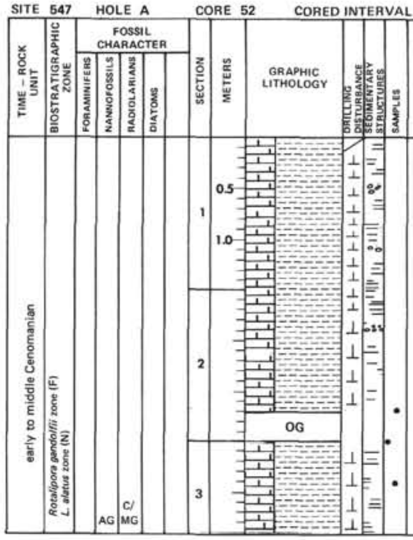

LITHOLOGIC DESCRIPTION

Moderately fragmented and drilling cakes of dark greenish gray (5GY 4/1) NANNOFOSSIL CLAYSTONE with indistinct laminae and occasional flattened burrows. Minor stretched clasts at Section 1, 45–49, 108–110 cm and Section 2, 38–40 cm.

Alternating waxy and swelling layers of claystone, about 60% waxy, 40% swelling.

ORGANIC CARBON AND CARBONATE (%):

	2, 118–120	3, 0–2	3, 44–45
Carbonate	–	–	30.0
$CaCO_3$	23.9	27.9	–

SITE 547 HOLE A CORE 53 CORED INTERVAL 554.5–564.0 m sub-bottom

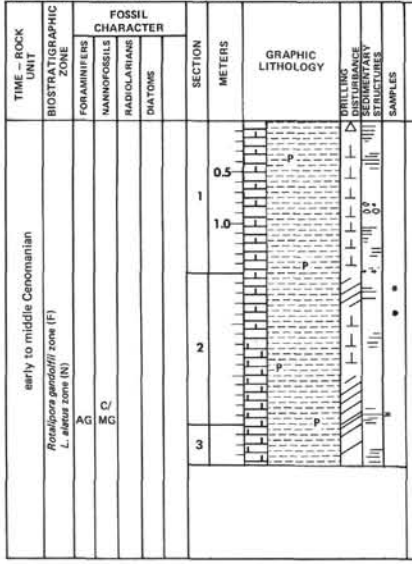

LITHOLOGIC DESCRIPTION

Slightly fragmented and drilling cakes of dark greenish gray (5G 4/1) NANNOFOSSIL CLAYSTONE indistinct laminae probably are flattened burrows. Pyrite in burrow-fillings throughout, alternating, 0.5 m thick, waxy and cm thick swelling layers.

Minor clast layers in Section 1, 82–93 and 144–150 cm.

Also some pyrite nodules up to 4 mm across.

SMEAR SLIDE SUMMARY (%):

	2, 20 D	2, 140 D
Texture:		
Sand	–	Tr
Silt	20	10
Clay	80	90
Composition:		
Quartz	2	2
Mica	–	Tr
Clay	80	85
Volcanic glass	Tr?	–
Glauconite	Tr	Tr
Pyrite	Tr	Tr
Carbonate unspec.	5	3
Foraminifers	2	Tr
Calc. nannofossils	8	10

ORGANIC CARBON AND CARBONATE (%):

	2, 41–42
Carbonate	24.1

SITE 547 HOLE A CORE 54 CORED INTERVAL 564.0–573.5 m sub-bottom

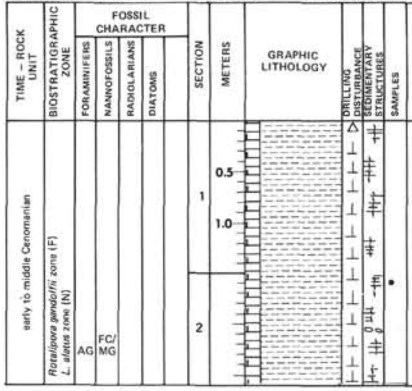

LITHOLOGIC DESCRIPTION

Drilling cakes of grayish olive green (5GY 3/2) NANNOFOSSIL CLAYSTONE with indistinct laminae and pyrite-rich specks and burrow-fills throughout.

Minor flattened clasts at Section 2, 56–59 cm.

ORGANIC CARBON AND CARBONATE (%);

	2, 10–11
Carbonate	16.1

SITE 547 HOLE A CORE 55 CORED INTERVAL 573.5–583.0 m sub-bottom

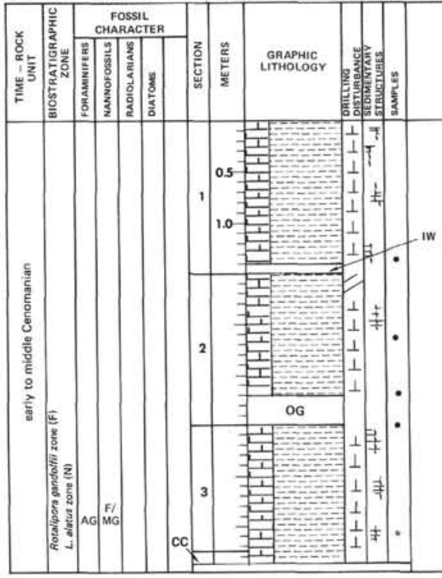

LITHOLOGIC DESCRIPTION

Drilling cakes of grayish olive green (5GY 3/2) NANNOFOSSIL CLAYSTONE with indistinct fine lamination, flattened burrows and interlayering of swelling and non-swelling waxy layers. Base of core is fissile and shows slickensides on broken surfaces.

SMEAR SLIDE SUMMARY (%):

	3, 110 D
Texture:	
Silt	20
Clay	80
Composition:	
Quartz	5
Mica	Tr
Heavy minerals	Tr
Clay	80
Volcanic glass	Tr?
Glauconite	Tr
Pyrite	1
Dolomite	2
Carbonate unspec.	4
Foraminifers	Tr
Calc. nannofossils	5

ORGANIC CARBON AND CARBONATE (%):

	1, 140–150	2, 63–64	2, 118–120	3, 0–2
Carbonate	–	36.0	–	21.8
$CaCO_3$	20.8	–	29.5	–

SITE 547 HOLE A CORE 56 CORED INTERVAL 583.0–592.5 m sub-bottom

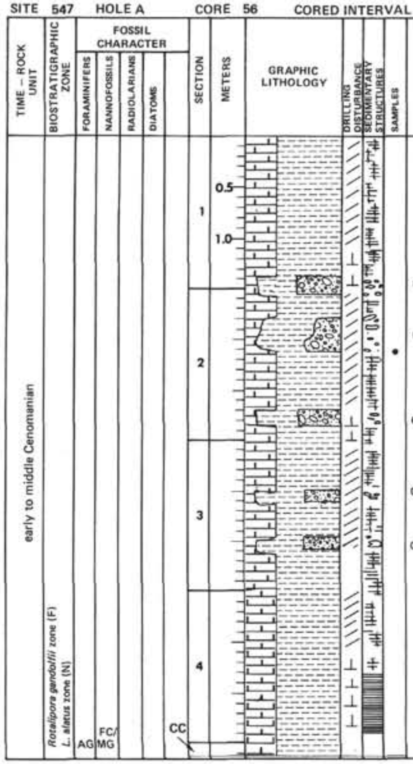

LITHOLOGIC DESCRIPTION

Slightly fragmented and some drilling cakes of grayish olive green (5GY 3/2) NANNOFOSSIL-RICH CLAYSTONE with indistinct lamination produced by flattened burrows. Better laminated than the more "massive" fissile previous two cores. Minor interlayers of swelling claystone.

C = Several layers of PEBBLY CLAYSTONE. Clasts are flattened, matrix supported and of very similar lithology as matrix.

ORGANIC CARBON AND CARBONATE (%):

	2, 62–63
Carbonate	36.5

SITE 547 HOLE A CORE 57 CORED INTERVAL 592.5–602.0 m sub-bottom

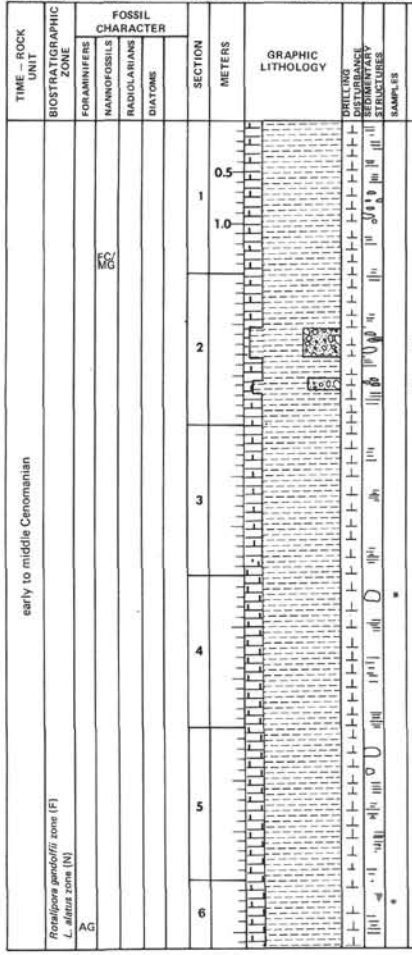

LITHOLOGIC DESCRIPTION

Drilling cakes of dark greenish gray (5G 4/1) NANNOFOSSIL CLAYSTONE with thin faint lamination.

C = Some horizons of PEBBLY CLAYSTONE with lengthened clasts of same lithology, matrix supported.

At Section 4, 17–24 cm and Section 5, 20–27 and 40–45 cm, claystone intraclasts with white speckles of fine skeletal debris.

SMEAR SLIDE SUMMARY (%):

	4, 20 M	6, 20 M
Composition:		
Quartz	Tr	–
Clay	75	75
Barite	1	–
Pyrite	–	1
Micronodules	2	–
Dolomite	2	1
Foraminifers	4	2
Calc. nannofossils	15	20
Fish remains	–	Tr
Plant debris	–	Tr

SITE 547 HOLE A CORE 58 CORED INTERVAL 602.0–611.5 m sub-bottom

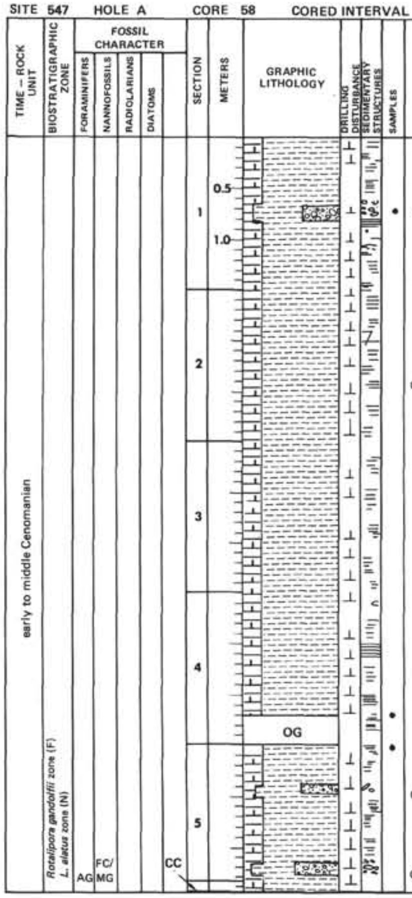

LITHOLOGIC DESCRIPTION

Mostly drilling cakes of dark greenish gray (5G 4/1) NANNOFOSSIL CLAYSTONE with flattened burrowing, rare shell fragments of thin shelled molluscs.

Some of the fine horizontal lamination may represent fine tails of turbidites.

C = Several horizons of PEBBLY CLAYSTONE occur throughout matrix supported flattened clasts of similar lithology.

ORGANIC CARBON AND CARBONATE (%):

	1, 74–75	4, 118–120	5, 0–2
Carbonate	34.5	–	–
$CaCO_3$	–	25.9	15.7

SITE 547 HOLE A CORE 59 CORED INTERVAL 611.5–621.0 m sub-bottom

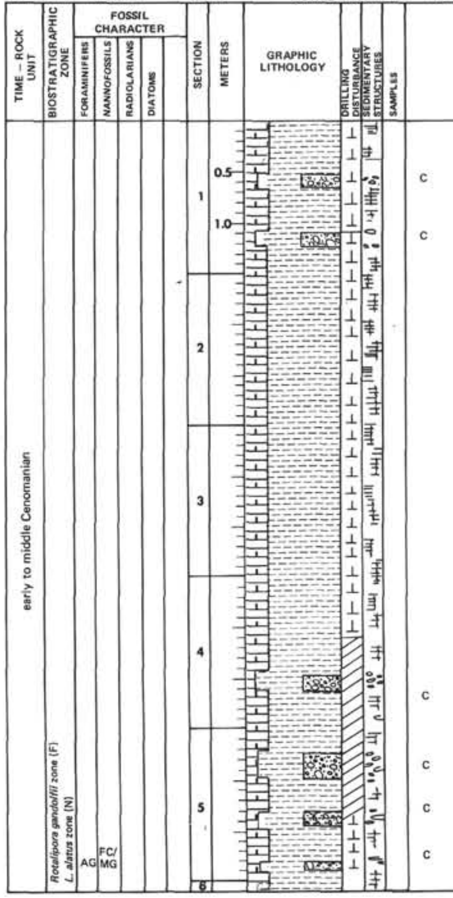

LITHOLOGIC DESCRIPTION

Mostly drilling cakes of dark greenish gray (5G 4/1) NANNOFOSSIL-CLAYSTONE with faint irregular lamination probably representing flattened burrows.

C = Some PEBBLY CLAYSTONE layers occur throughout.

SITE 547 HOLE A CORE 60 CORED INTERVAL 621.5–630.5 m sub-bottom

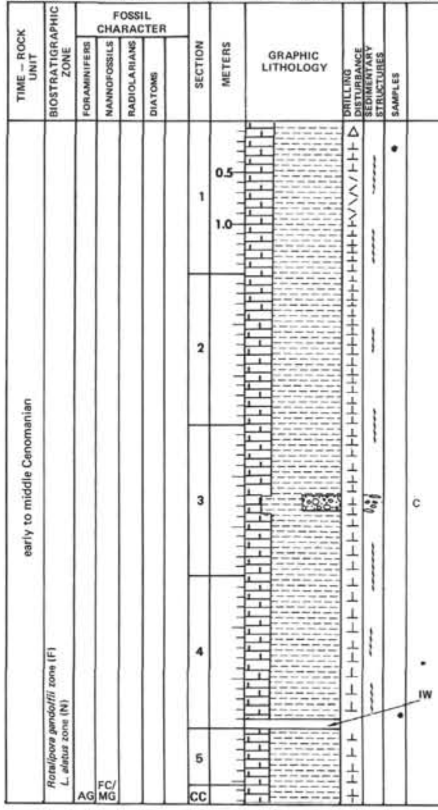

LITHOLOGIC DESCRIPTION

Drilling cakes of grayish olive green (5GY 3/2) and grayish olive (10Y 4/2) NANNOFOSSIL CLAYSTONE with compacted burrows often rich in pyrite. Dip up to 18° to core axis.

C = One layer of PEBBLY CLAYSTONE with flattened clasts of same lithology.

ORGANIC CARBON AND CARBONATE (%):

	1, 25–27	4, 140–150
Carbonate	34.5	25.9

SITE 547 HOLE A CORE 61 CORED INTERVAL 630.5–640.0 m sub-bottom

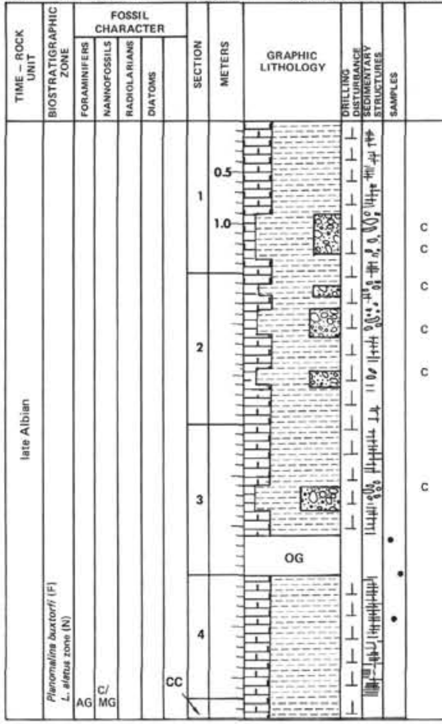

LITHOLOGIC DESCRIPTION

Drilling cakes of grayish olive green (5GY 3/2) NANNOFOSSIL CLAYSTONE with indistinct lamination throughout, flattened burrows common. Minor pyrite nodules and burrows.

C = Several thin layers of PEBBLY CLAYSTONE with very flattened stretched and deformed.

ORGANIC CARBON AND CARBONATE (%):

	3, 118–120	4, 0–2	4, 40–42
Carbonate	–	–	49.4
$CaCO_3$	24.9	27.4	–

SITE 547 HOLE A CORE 62 CORED INTERVAL 640.0–649.5 m sub-bottom

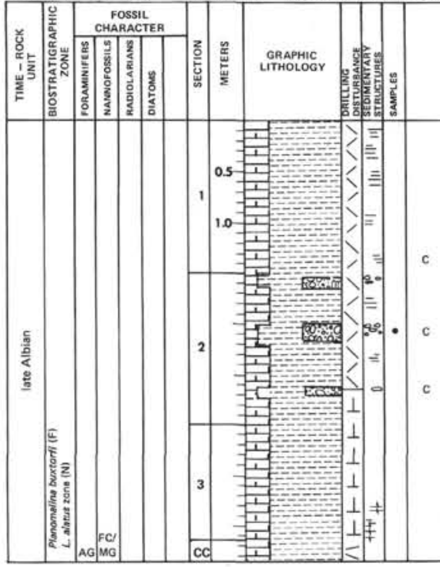

LITHOLOGIC DESCRIPTION

Highly fragmented grayish olive green (5GY 3/2) NANNOFOSSIL CLAYSTONE with indistinct laminae probably representing flattend burrows.

C = Several thin layers of PEBBLY CLAYSTONE with matrix supported strongly flattened small clasts of darker DOLOMITIC MUDSTONE.

ORGANIC CARBON AND CARBONATE (%):

	2, 53–54
Carbonate	23.1

SITE 547 HOLE A CORE 63 CORED INTERVAL 649.5–659.0 m sub-bottom

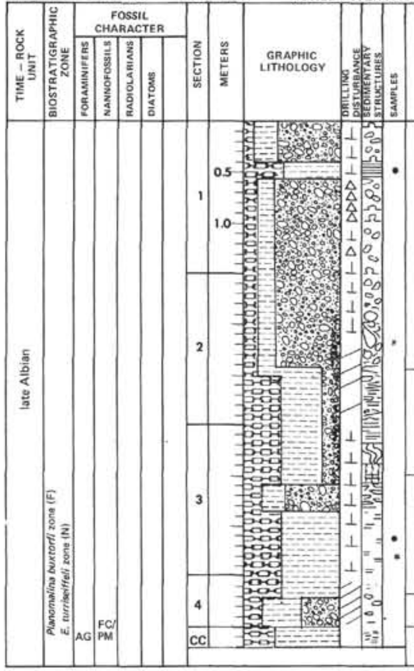

LITHOLOGIC DESCRIPTION

Major lithology: moderately to highly disturbed grayish olive green (5GY 3/2), olive gray (5Y 3/2) and light olive gray (5Y 5/2) CLAYSTONE CONGLOMERATE with slump folds and contorted bedding. Both compact, rigid and highly elongate and deformed clasts occur. Clasts oriented at all angles to bedding.

5GY 3/2–
5Y 3–5/2–
10GY 5/2

In Section 1, 37–55 cm and Section 2, 90 cm to Section 3, 60 cm intervals with few flattened clasts, some burrowing (Section 3, 40–52 cm) mainly CALCAREOUS MUDSTONE.

In Section 3, 80 cm to Section 4, 22 cm CALCAREOUS MUDSTONE with very indistinct lamination more silty than above.

SMEAR SLIDE SUMMARY (%):

	2, 69 M	3, 130 D
Texture:		
Sand	–	Tr
Silt	20	30
Clay	80	70
Composition:		
Quartz	6	5
Feldspar	–	Tr
Mica	–	Tr
Clay	70	85
Volcanic glass	–	Tr?
Glauconite	Tr	Tr
Pyrite	2	1
Dolomite	7	1
Carbonate unspec.	–	3
Foraminifers	–	2
Calc. nannofossils	15	5
Diatoms	–	Tr

5GY 3/2–
10GY 3/2

5GY 3–4/1–2

5GY 3/2

ORGANIC CARBON AND CARBONATE (%):

	2, 48–50	3, 110–126
Carbonate	36.0	32.5

SITE 547 HOLE A CORE 64 CORED INTERVAL 659.0–668.5 m sub-bottom

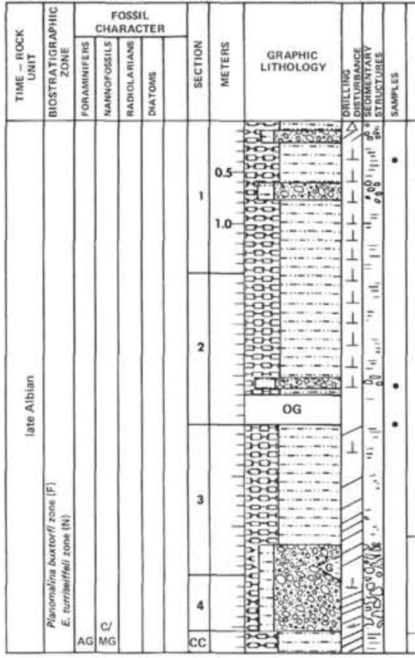

LITHOLOGIC DESCRIPTION

C

C

Drilling cakes and more slightly fragmented zones of grayish olive green (5GY 3/2) VERY CALCAREOUS MUDSTONE with a very indistinct lamination in most of the core probably mainly flattened burrows.

C = Several layers of MUDSTONE CONGLOMERATE with very flattened clasts of similar lithology as matrix. At Section 3, 140–145 cm pebble of gray yellowish brown (5GY 7/2) GLAUCONITE-BEARING CLAYSTONE.

ORGANIC CARBON AND CARBONATE (%):

	1, 40–42	2, 118–120	3, 0–2
Carbonate	36.0	–	34.1
$CaCO_3$	–	34.1	–

C

C

SITE 547 HOLE A CORE 65 CORED INTERVAL 668.5–678.0 m sub-bottom

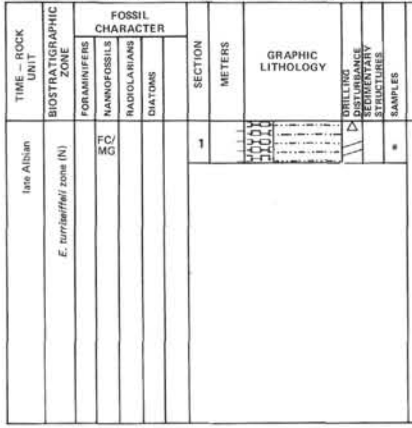

LITHOLOGIC DESCRIPTION

Lightly fractured, grayish olive green (5GY 3/2) CALCAREOUS MUDSTONE with indistinct lamination and flattened burrows at 25° to core axis.

SMEAR SLIDE SUMMARY (%):

	1, 30 D
Texture:	
Sand	8
Silt	12
Clay	80
Composition:	
Quartz	5
Clay	80
Glauconite	1
Pyrite	Tr
Dolomite	2
Foraminifers	1
Calc. nannofossils	9

SITE 547 HOLE A CORE 66 CORED INTERVAL 678.0–687.5 m sub-bottom

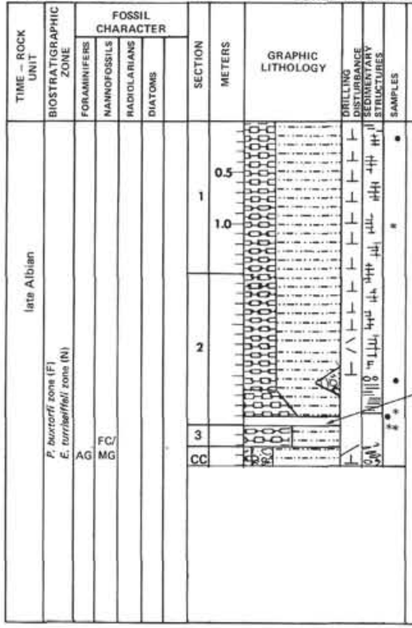

LITHOLOGIC DESCRIPTION

Drilling cakes of grayish olive green (5GY 3/2) NANNOFOSSIL MUDSTONE indistinct laminae probably representing flattened burrows.

At Section 2, 105–107 cm some dusky yellow green (5GY 5/2) clasts.

Section 2, 107–139 cm dusky yellow green (5GY 5/2) undeformed VERY CALCAREOUS MUDSTONE with distinct laminae and flattened burrows at a 30° angle to core horizontal.

Core-Catcher: grayish olive green (5GY 3/2) and greenish gray (5GY 5/1) PEBBLY MUDSTONE with flattened and stretched and some folded clasts.

SMEAR SLIDE SUMMARY (%):

	1, 105 D	2, 137 M	3, 6 D	3, 7 D
Texture:				
Sand	5	–	5	5
Silt	20	15	20	15
Clay	75	85	75	80
Composition:				
Quartz	2	6	2	2
Mica	–	–	1	2
Clay	70	80	75	80
Pyrite	2	1	Tr	1
Dolomite	3	3	10	5
Foraminifers	Tr	Tr	4	1
Calc. nannofossils	10	7	5	5
Sponge spicules	–	–	Tr	–
Clasts (fec. pellets?)	15	–	–	5

ORGANIC CARBON AND CARBONATE (%):

	1, 29–30	2, 109–110	2, 140–150
Carbonate	29.5	32.0	–
$CaCO_3$	–	–	48.8

SITE 547 HOLE A CORE 67 CORED INTERVAL 687.5–697.0 m sub-bottom

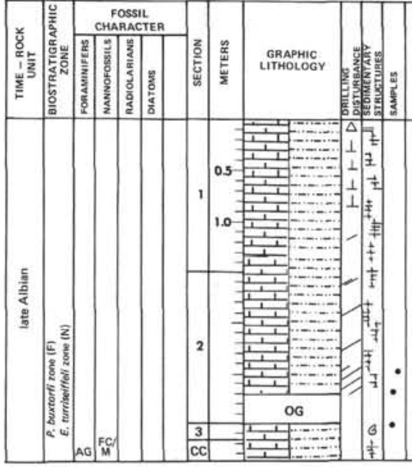

LITHOLOGIC DESCRIPTION

Top highly and below slightly deformed, grayish olive green (5GY 3/2) and grayish olive (10Y 4/2) NANNOFOSSIL-RICH MUDSTONE with indistinct laminae and flattened burrows throughout. Dips variable, up to 20° to core horizontal.

ORGANIC CARBON AND CARBONATE (%):

	2, 98–100	2, 118–120	3, 0–2
Carbonate	45.9	–	41.2
$CaCO_3$	–	49.9	–

SITE 547 HOLE A CORE 68 CORED INTERVAL 697.0–706.5 m sub-bottom

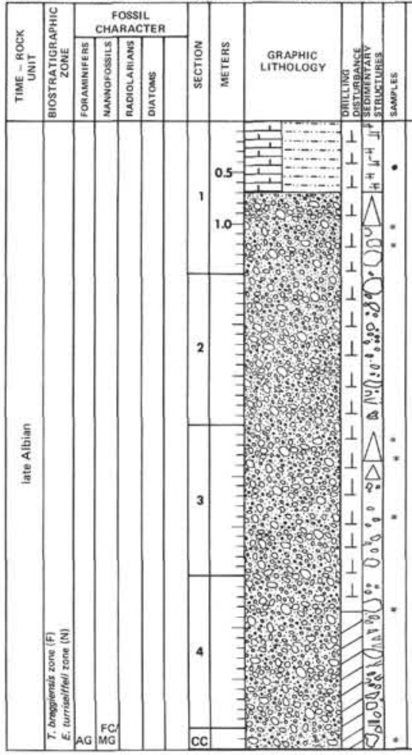

LITHOLOGIC DESCRIPTION

Section 1, 0–70 cm: drilling cakes of dark greenish gray (5GY 4/1) NANNOFOSSIL-RICH MUDSTONE with flattened burrows.

Section 1, 70 cm–Core-Catcher: moderately fragmented multicolored PEBBLY MUDSTONE to MUDSTONE CONGLOMERATE. Most clasts are heavily deformed and slumped. In some levels matrix nearly absent, others are matrix supported.

Clasts consist of light olive gray (5Y 5/2) DOLOMITIC MUDSTONE greenish gray (5GY 6/1), olive gray (5Y 3/2) to grayish yellow green (5GY 7/2) NANNOFOSSIL CLAYSTONE.

SMEAR SLIDE SUMMARY (%):

	1, 106 D	1, 126 D	3, 15 D	3, 32 D	3, 94 D	4, 37 M	CC,13 D
Texture:							
Sand	2	5	2	2	5	–	3
Silt	3	30	7	13	15	100	7
Clay	95	65	90	85	80	–	90
Composition:							
Quartz	1	5	2	1	3	Tr	3
Feldspar	–	2	–	–	–	–	–
Mica	1	2	1	1	2	–	1
Clay	90	60	80	80	80	–	60
Pyrite	Tr	–	Tr	2	Tr	–	Tr
Dolomite	2	25	4	10	5	99	2
Foraminifers	2	Tr	2	Tr	5	–	1
Calc. nannofossils	5	5	10	5	3	–	30

ORGANIC CARBON AND CARBONATE (%):

	1, 48–50
Carbonate	38.0

SITE 547 HOLE A CORE 69 CORED INTERVAL 706.5–716.0 m sub-bottom

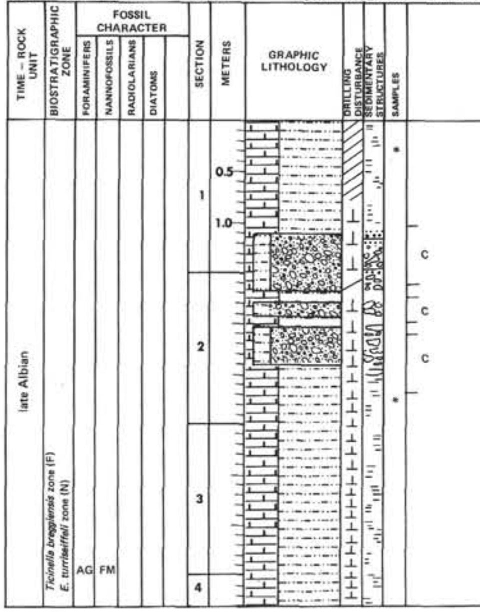

LITHOLOGIC DESCRIPTION

Mostly drilling cakes of light olive gray (5Y 5/2) and grayish olive (10Y 4/2) NANNOFOSSIL-RICH CLAYSTONE with irregular lamination.

C = Three layers of PEBBLY to COBBLY CONGLOMERATE with clasts similar to those in Core 68. Topmost layer (Section 1, 112 cm to Section 2, 15 cm) shows three distinctly graded cycles. Clasts are strongly flattened and wedging out into slump folds clast supported.

Section 3, 54–78 cm thin fracture filled with calcite.

SMEAR SLIDE SUMMARY (%):

	1, 30	2, 126
	D	D
Composition:		
Quartz	2	3
Clay	60	51
Pyrite	–	Tr
Barite	–	1
Dolomite	–	8
Carbonate unspec.	15	25
Foraminifers	3	2
Calc. nannofossils	20	10

SITE 547 HOLE A CORE 70 CORED INTERVAL 716.0–720.5 m sub-bottom

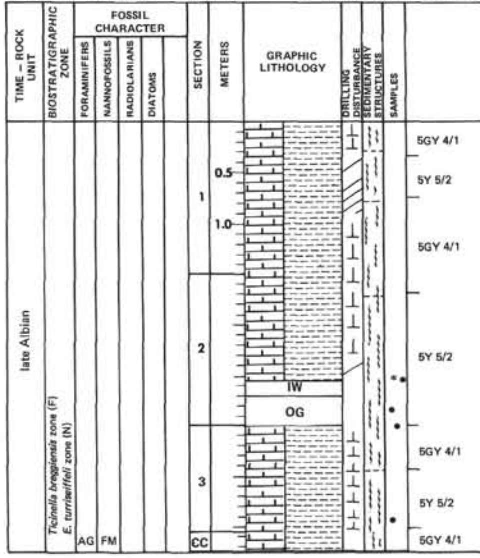

LITHOLOGIC DESCRIPTION

Mostly moderately fragmented dark greenish gray (5GY 4/1) and light olive gray (5Y 5/2) NANNOFOSSIL-RICH CLAYSTONE with common bioturbation.

SMEAR SLIDE SUMMARY (%):

	2, 102
	M
Composition:	
Clay	60
Carbonate unspec.	30
Foraminifers	Tr
Calc. nannofossils	10

ORGANIC CARBON AND CARBONATE (%):

	2, 104–106	2, 136–150	3, 0–2	3, 93–94
Carbonate	–	–	39.3	42.9
$CaCO_3$	54.5	39.7	–	–

SITE 547 HOLE A CORE 71 CORED INTERVAL 720.5–725.5 m sub-bottom

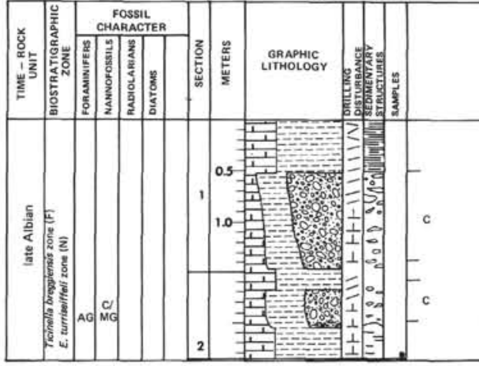

LITHOLOGIC DESCRIPTION

Slightly to moderately deformed, dark greenish gray (5G 4/1) and light olive gray (5Y 5/2) NANNOFOSSIL-RICH CLAYSTONE with very fine lamination.

C = Two layers of PEBBLY CONGLOMERATE flattened, matrix supported pebbles of lithologies described in Core 68.

ORGANIC CARBON AND CARBONATE (%):

	2, 82–83
Carbonate	32.0

SITE 547 HOLE A CORE 72 CORED INTERVAL 725.5–735.0 m sub-bottom

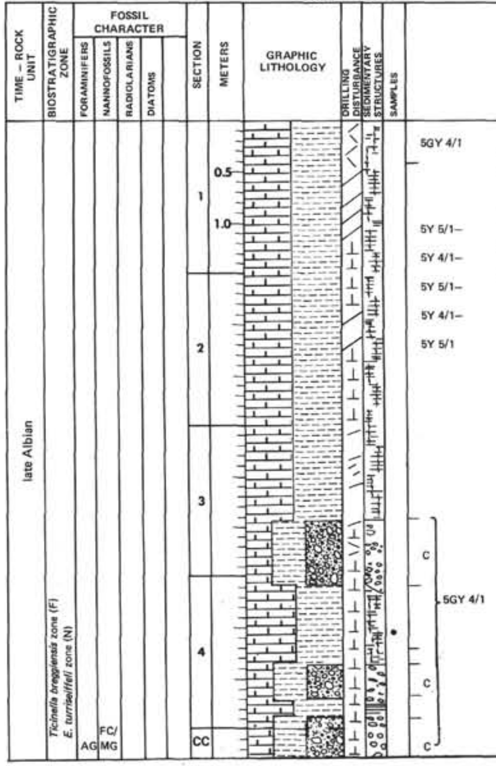

LITHOLOGIC DESCRIPTION

Slightly to highly fragmented dark greenish gray (5GY 4/1) and moderate olive gray (5Y 5/1) NANNOFOSSIL-RICH CLAYSTONE with indistinct lamination and flattened burrows throughout.

C = Three layers of PEBBLY CLAYSTONES with sparse stretched and flattened clasts supported by claystone matrix.

ORGANIC CARBON AND CARBONATE (%):

	4, 56–57
Carbonate	49.4

SITE 547 HOLE A CORE 73 CORED INTERVAL 735.0–744.5 m sub-bottom

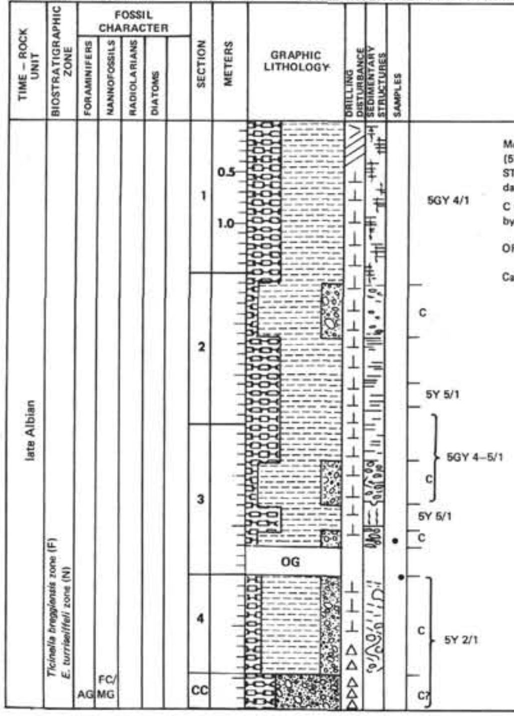

LITHOLOGIC DESCRIPTION

Moderately fragmented dark greenish gray (5GY 4/1) to dark olive gray (5Y 3/1) to olive black (5YR 2/1) VERY CALCAREOUS CLAYSTONE with indistinct lamination and faint color variation towards darker colors at base of section.

C = several intervals contaning very flattened sparse clasts accompanied by slump folds.

ORGANIC CARBON AND CARBONATE (%):

	3, 118–120	4, 0–2
Carbonate	33.6	34.6

SITE 547 HOLE B CORE H1 CORED INTERVAL 28.0–211.5 m sub-bottom

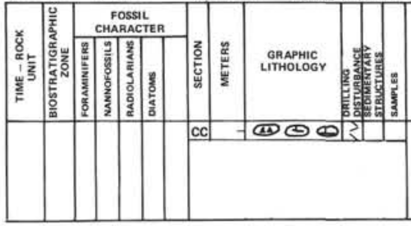

LITHOLOGIC DESCRIPTION

Core-Catcher: one piece of dusky brown (5YR 2/2) CHERT.

One piece of light brown (5YR 6/4) NANNOFOSSIL OOZE.

One piece of pale green (5G 7/2) NANNOFOSSIL OOZE.

SITE 547 HOLE B CORE H2 CORED INTERVAL 211.5–354.0 m sub-bottom

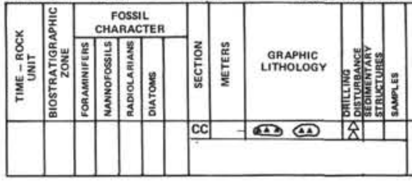

LITHOLOGIC DESCRIPTION

Core-Catcher: several broken chunks of dusky brown (5YR 2/2) CHERT.

SITE 547 HOLE B CORE H3 CORED INTERVAL 354.0–724.5 m sub-bottom

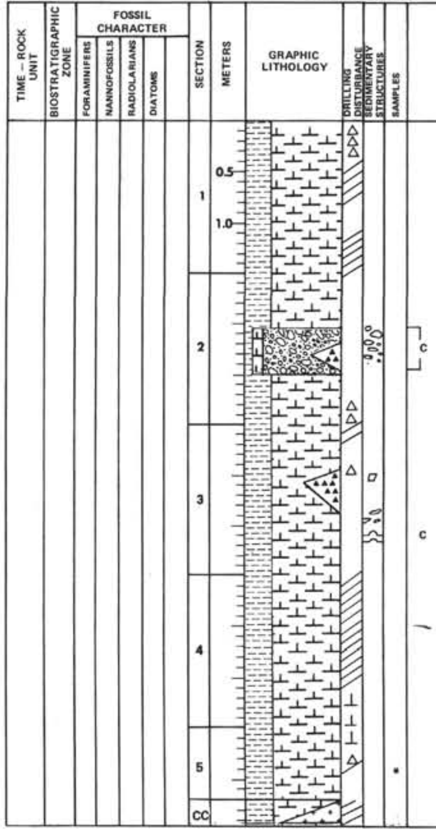

LITHOLOGIC DESCRIPTION

Variably disturbed, greenish gray (5GY 6/1) to dark greenish gray (5GY 4/1) CLAYEY NANNOFOSSIL OOZE with indistinct lamination and minor burrowing. Zoophycus common.

C = 2 layers of PEBBLY CONGLOMERATE with flattened pebbles including some angular chert fragment.

Minor slump folds (drilling disturbance?) in Section 3.

Section 4, 120–150 cm: grayish yellow green (5GY 7/2 to 10GY 5/2) CALCAREOUS CLAYSTONE with swelling clays.

Core-Catcher contains one cobble of coarse crystalline K-feldspar, plagioclase, quartz, biotite-GRANITE.

SMEAR SLIDE SUMMARY (%):

	5, 40	CC, 29
	D	D
Composition:		
Quartz	1	Tr
Clay	25	74
Pyrite	–	Tr
Dolomite	3	5
Foraminifers	3	–
Calc. nannofossils	68	20

SITE 547 HOLE B CORE H4 CORED INTERVAL 0.0–160.5 m sub-bottom

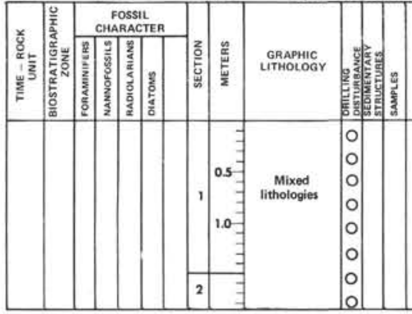

LITHOLOGIC DESCRIPTION

Washed core: drilling slurry of mixed lithologies.

SITE 547 HOLE B CORE H5 CORED INTERVAL 160.5–803.5 m sub-bottom

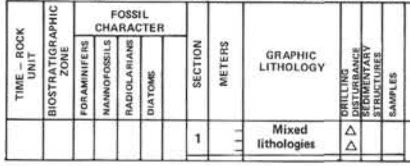

LITHOLOGIC DESCRIPTION

Washed core: drilling breccia of mixed lithologies.

SITE 547 HOLE B CORE 1 CORED INTERVAL 724.5–734.0 m sub-bottom

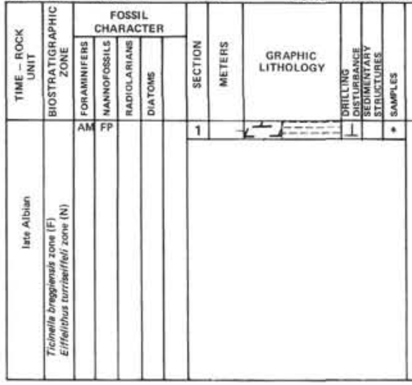

LITHOLOGIC DESCRIPTION

Moderately fragmented, greenish gray (5GY 6/1) VERY DOLOMITIC CLAYSTONE with olive gray laminae and some burrowing.

SMEAR SLIDE SUMMARY (%):

	1, 10 D
Texture:	
Sand	10
Silt	20
Clay	70
Composition:	
Quartz	5
Clay	70
Dolomite	10
Carbonate unspec.	15
Calc. nannofossils	1

SITE 547 HOLE B CORE 2 CORED INTERVAL 734.0–743.5 m sub-bottom

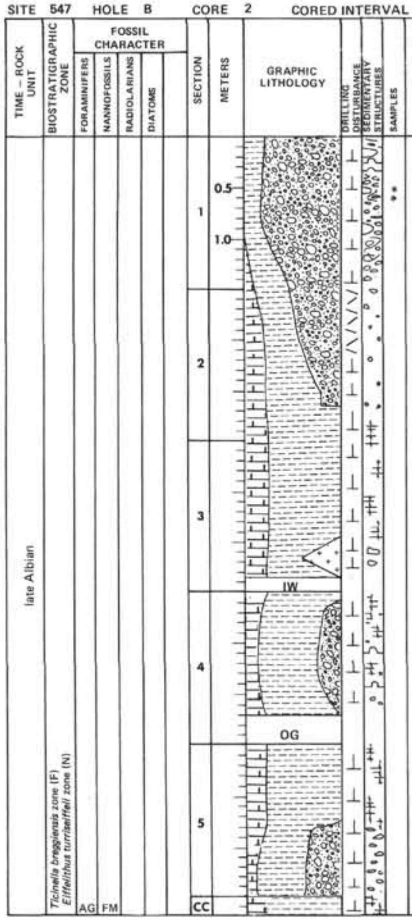

LITHOLOGIC DESCRIPTION

Drilling cakes and highly fractured, olive gray (5Y 3/2) NANNOFOSSIL MUDSTONE with intervals of MUDSTONE CONGLOMERATE and PEBBLY/COBBLY MUDSTONE.

Most clasts are highly flattened and associated with slump folds, and of light olive gray (5Y 5/2), grayish olive (10Y 4/2), and olive gray (5Y 3/2) color.

At Section 3, 115 and 126 cm two GRANITE CLASTS containing chlorite and abundant clays, weathered surface.

SMEAR SLIDE SUMMARY (%):

	1, 52 M	1, 60 D
Texture:		
Sand	5	5
Silt	15	10
Clay	80	85
Composition:		
Quartz	18	5
Feldspar	2	–
Mica	Tr	Tr
Heavy minerals	Tr	–
Clay	60	85
Glauconite	Tr	–
Pyrite	Tr	Tr
Dolomite	5	1
Carbonate unspec.	5	–
Foraminifers	–	3
Calc. nannofossils	5	5
Radiolarians	Tr	–
Palynmorphs	Tr	–

SITE 547 HOLE B CORE 3 CORED INTERVAL 743.5–753.0 m sub-bottom

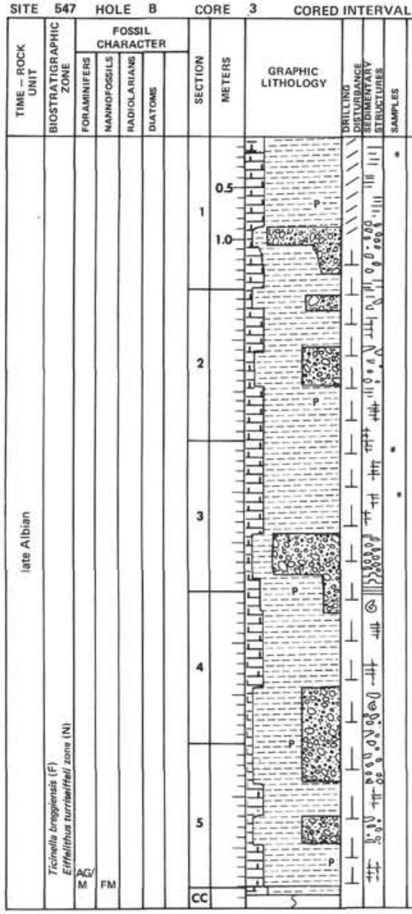

LITHOLOGIC DESCRIPTION

Mostly drilling cakes of olive gray (5Y 3/2) and grayish olive. CALCAREOUS CLAYSTONE with several intervals of MUDSTONE CONGLOMERATE and PEBBLY/COBBLY MUDSTONE.

Pyrite is very common in burrows.

Clasts dominantly of light olive gray (5Y 5/2) color, flattened, mud supported.

SMEAR SLIDE SUMMARY (%):

	1, 20	3, 10	3, 50
	D	D	D
Texture:			
Sand	–	–	10
Silt	10	10	20
Clay	90	90	70
Composition:			
Quartz	3	6	10
Feldspar	–	Tr	Tr
Mica	–	Tr	–
Heavy minerals	–	Tr	Tr?
Clay	90	75	60
Pyrite	1	2	1
Dolomite	2	2	4
Carbonate unspec.	–	5	10
Foraminifers	Tr	–	5
Calc. nannofossils	5	5	10

SITE 547 HOLE B CORE 4 CORED INTERVAL 753.0–762.5 m sub-bottom

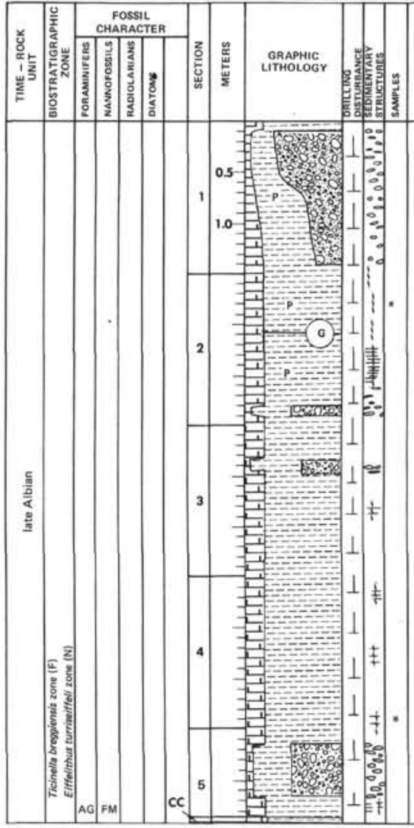

LITHOLOGIC DESCRIPTION

Drilling cakes of grayish olive (10Y 4/2) and grayish olive green (5GY 3/2) CALCAREOUS MUDSTONE/CLAYSTONE with several layers of MUDSTONE CONGLOMERATE TO PEBBLY MUDSTONE.

Pyrite very common throughout.

Clasts of some lithology as matrix, flattened, stretched, mostly matrix supported except in Section 1, 20–60 cm. Grains of glauconite locally.

SMEAR SLIDE SUMMARY (%):

	2, 30	4, 140
	D	D
Texture:		
Sand	Tr	2
Silt	15	10
Clay	85	88
Composition:		
Quartz	5	4
Mica	Tr	–
Clay	75	68
Pyrite	1	1
Dolomite	3	5
Carbonate unspec.	10	10
Foraminifers	–	1
Calc. nannofossils	10	10
Sponge spicules	–	1

SITE 547 HOLE B CORE 5 CORED INTERVAL 762.5–772.0 m sub-bottom

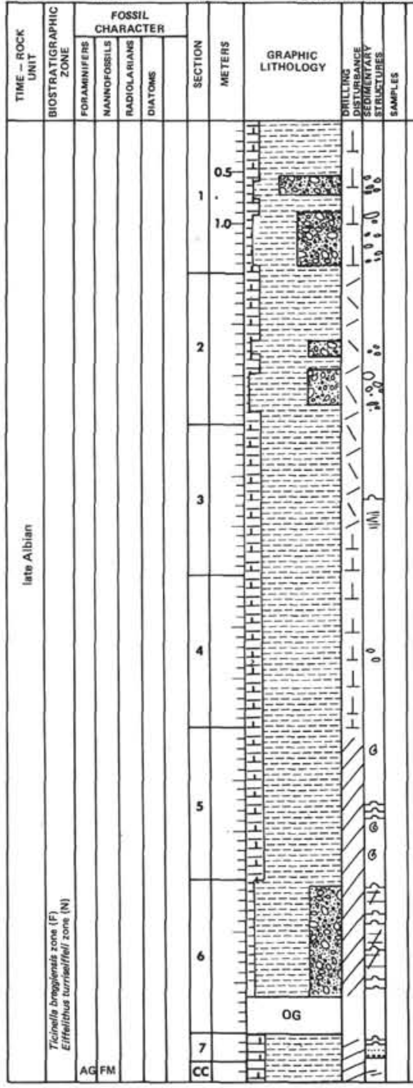

LITHOLOGIC DESCRIPTION

Drilling cakes and slightly disturbed, olive gray (5Y 3/2) NANNOFOSSIL CLAYSTONE with several layers of PEBBLY CLAYSTONE. Claystones show common bioturbation and faint lamination.

Towards the base of core (Section 5, 75 cm to Section 6 at base) increased slumping and fracturing of slumped conglomerate.

Clasts are of same lithology and color as matrix, lengthened and associated with contorted bedding.

SITE 547 HOLE B CORE 6 CORED INTERVAL 772.0–781.5 m sub-bottom

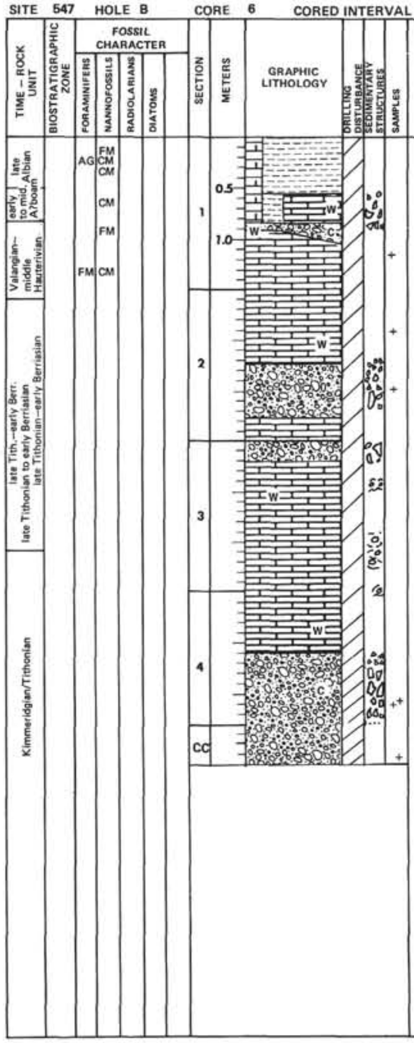

LITHOLOGIC DESCRIPTION

Section 1, 0–53 cm: slightly fractured dark greenish gray (5GY 4/1) to grayish olive green (5GY 3/2) NANNOFOSSIL CLAYSTONE.

Section 1, 53–84 cm: slightly fractured dusky brown (5YR 2/2) to olive gray (5Y 3/2) laminated, slump folded NANNO-BEARING CLAYSTONE with angular clasts of LIMESTONE (bioclastic wackestone).

Section 1, 84 cm–Core-Catcher: slightly fractured alternation of olive gray (5Y 4/1), grayish green (5G 5/2), pale green (5G 7/2) BIOCLASTIC WACKESTONE and LIMESTONE CONGLOMERATE of sand to pebble grain size.

From Section 3, 140 cm–Section 4, 43 cm: colors are dark reddish brown (10R 3/4) and pale reddish brown (10R 5/4).

THIN SECTION/PEEL SUMMARY (%):

	1, 118–120	*2, 40–44*	*2, 97–100*
	D	D	D
Texture:			
Rudite	35	–	60
Arentie	65	20	35
Silt	–	80	5
Composition:			
Micrite	–	80	5
Sparite	30	–	35
Intraclasts	20	–	45
Oncoids	35	–	10
Ooids	1	–	–
Skeletal grains:			
Crinoids	2	1	2
Bivalves	–	–	Tr
Gastropods	–	–	Tr
Ammonites	Tr	–	–
Brachiopods	Tr	–	–
Forams	Tr	–	Tr
Aptychi	–	3	–
Calpionellids	–	5	–
Radiolarians calc.	–	10	–
Siliceous sponge fragments	–	–	Tr
Structure:			
Pyrite	5	–	–

	4, 108–112	4, 108–112	CC, 31–33
	D	M	M
Texture:			
Rudite	–	–	60
Arenite	35	25	35
Silt	65	75	5
Composition:			
Micrite	65	75	–
Sparite	–	–	20
Intraclasts	10	–	40
Oncoids	20	–	–
Peloids	–	20	–
Skeletal grains:			
Crinoids	Tr	1	20
Ammonites	Tr	–	–
Brachiopods	Tr	–	–
Forams	Tr	Tr	–
Quartz grains	–	4	–
Aptychi	Tr	–	Tr
Radiolarians calc.	5	–	–
Structure:			
Veins	–	Tr	–
Porosity	–	–	20

SITE 547 HOLE B CORE 7 CORED INTERVAL 781.5–791.0 m sub-bottom

TIME – ROCK UNIT: Kimmeridgian

BIOSTRATIGRAPHIC ZONE: *Protoglobigerina* (F) *Saccocoma*

FOSSIL CHARACTER: FORAMINIFERS CM; NANNOFOSSILS RM; RADIOLARIANS; DIATOMS

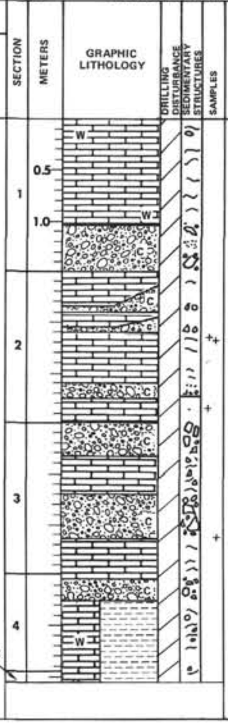

LITHOLOGIC DESCRIPTION

5G 7/1
5YR 3/4
5G 7/1
5G 8/1
5YR 3/4
5G 7/1
5YR 3/4
5YR 7/2
5G 7/1
5G 8/1
5G 7/1

5R 6/2
5YR 4/4
5G 6/1

5R 6/2
5YR 7/2
(10R 4/2)

5R 6/2
5G 7/2

5G 7/2
10YR 6/2
5YR 8/1
5YR 7/2
5YR 3/4
5G 7/2
5YR 3/4

10YR 8/2
5G 7/1
5G 8/1
10YR 6/2
5YR 8/1
10YR 6/2
5YR 3/4

Slightly fractured WACKESTONE containing few bioclasts (ammonite fragments, aptychi, echinoderms, calcified radiolarians, foaminifers, tintinnids). These micritic limestones alternate with graded calcareous gravity flows occurring as GRAINSTONES, CONGLOMERATES, and BRECCIAS.

In Section 1, 103–150 cm; Section 2, 37–40, 55–58, and 112–124 cm; and Section 4, 5–24 cm the gravity flows contain rock fragments of wackestones with superficial ooids and micrites with calcified radiolarians.

In Section 3, 0–32 and 70–115 cm increasing shallow water influence: hyrozoans, bryozoans, litholid foraminifers.

Biostratigraphy: *Saccocoma, Protoglobigerina, Bositra* (Section 2, 69–72 and 136–139 cm), *Protopeneroplis* (Section 3, 112–115 cm): Late Jurassic.

THIN SECTION/PEEL SUMMARY (%):

	2, 69–72 D	2, 69–72 M	2, 136–139 D	3, 112–115 D
Texture:				
Rudite	–	–	–	20
Arenite	45	25	10	80
Silt	55	75	90	–
Composition:				
Micrite	55	75	90	–
Sparite	–	–	–	35
Intraclasts	–	–	–	30
Oncoids	–	–	Tr	5
Peloids	25	–	–	
Skeletal grains:				
Crinoids (+ saccocoma)	15	3	2	20
Bivalves (+ filaments)	5	10	5	Tr
Ammonites	Tr	Tr	–	–
Forams	–	2	–	Tr
Aptychi	–	–	Tr	–
Radiolarians (calcif.)	Tr	7	–	–
Quartz grains	–	–	3	–
Hydrozoans	–	–	–	Tr
Structure:				
Veins	–	–	Tr	–

SITE 547 HOLE B CORE 8 CORED INTERVAL 791.0–800.5 m sub-bottom

TIME – ROCK UNIT: Oxfordian-

BIOSTRATIGRAPHIC ZONE: *Lamellaptychus sparcieamellosus* (Section 3, 75 cm)

FOSSIL CHARACTER: FORAMINIFERS FM; NANNOFOSSILS B, RP, RP; RADIOLARIANS; DIATOMS

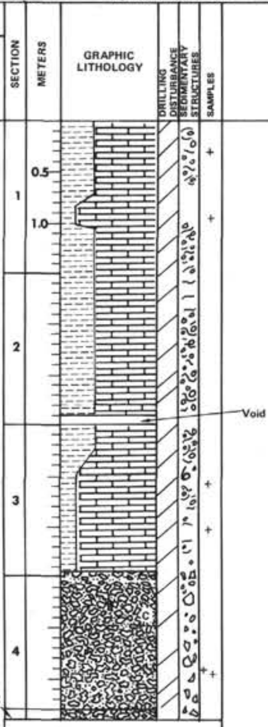

LITHOLOGIC DESCRIPTION

Section 1, 0 cm through Section 3, 145 cm slightly fractured NODULAR LIMESTONE. Wackestone composed of pelmicritic nodules in a matrix of clayey micrite. In Section 3 nodules are densely packed grading into less clayey massive limestones with indistinct nodularity. At Section 3, 14–22, 37–41, 47–52, 55–62, and 90–96 cm layers of a "filament" lumachelle: FILAMENT-PACKSTONE.

Below Section 3, 145 cm beginning with a hard ground, stromatolitic crusts, glauconitic material, and stylolites. Slightly fractured polymictic LIMESTONE BRECCIA with subangular clasts of different micritic bioclastic limestones.

Matrix of the breccia is a slightly recrystallized micrite deposited with geopetal fabric.

THIN SECTION/PEEL SUMMARY (%):

	1, 30–33 D	1, 95–100 D	3, 57–61 D
Texture:			
Rudite	–	–	20
Arenite	60	10	40
Silt	40	90	40
Composition:			
Micrite	40	90	35
Sparite	–	–	5
Skeletal grains:			
Crinoids	5	2	–
Bivalves	5	2	60
Gastropods	–	Tr	–
Ammonites	–	Tr	–
Brachiopods	–	Tr	–
Forams	Tr	Tr	–
Calcified components unspec.	50	5	–
Quartz grains	1	1	–
Structure:			
Geopetal fab.	–	–	Tr

	3, 101–106 D	4, 91–95 D	4, 95–100 D
Texture:			
Rudite	–	20	40
Arenite	10	50	40
Silt	90	30	20
Composition:			
Micrite	90	30	20
Sparite	–	–	10
Intraclasts	–	20	40
Oncoids	–	10	20
Peloids	Tr	–	–
Skeletal grains:			
Crinoids	5	40	10
Bivalves	5	Tr	–
Gastropods	Tr	–	–
Ammonites	Tr	–	Tr
Forams	Tr	Tr	Tr
Quartz grains	Tr	–	–

SITE 547 HOLE B CORE 9 CORED INTERVAL 800.5–803.5 m sub-bottom

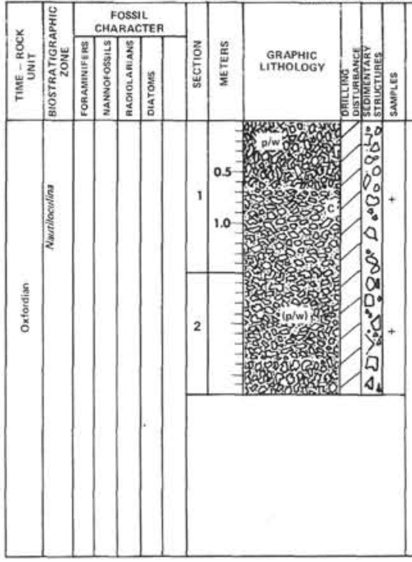

LITHOLOGIC DESCRIPTION

Slightly fractured LIMESTONE BRECCIA similar to Core 8 Section 3, 145 cm through Section 4 with grayish red (10R 4/2), greenish gray (5G 6/1), and yellowish gray (5Y 7/2) angular or rounded limestone fragments in a light brown (5YR 6/4) micritic matrix. Lithology of the clasts: mudstone, echinoderm-molluscan shell-packstone, ammonite-foraminiferal-wackestone, sponge spicule-radiolarian-wackestone, crust fragments including relicts of sponge skeletons and serpulids, echinoderm packstone, foraminiferal superficial ooid grainstone. Grainsize of the breccia: sand to 12 cm.

THIN SECTION/PEEL SUMMARY (%):

	1, 78–82 D	2, 56–60 D
Texture:		
Rudite	10	80
Arenite	70	20
Silt	20	–
Composition:		
Micrite	30	35
Sparite	5	5
Intraclasts	15	40
Oncoids	40	10
Skeletal grains:		
Crinoids	10	Tr
Bivalves	Tr	10
Gastropods	Tr	–
Ammonites	Tr	Tr
Serpulids	Tr	–
Forams	Tr	–
Quartz grains	Tr	–
Sil. sponge fragments	Tr	Tr

SITE 547 HOLE B CORE 10 CORED INTERVAL 803.5–810.0 m sub-bottom

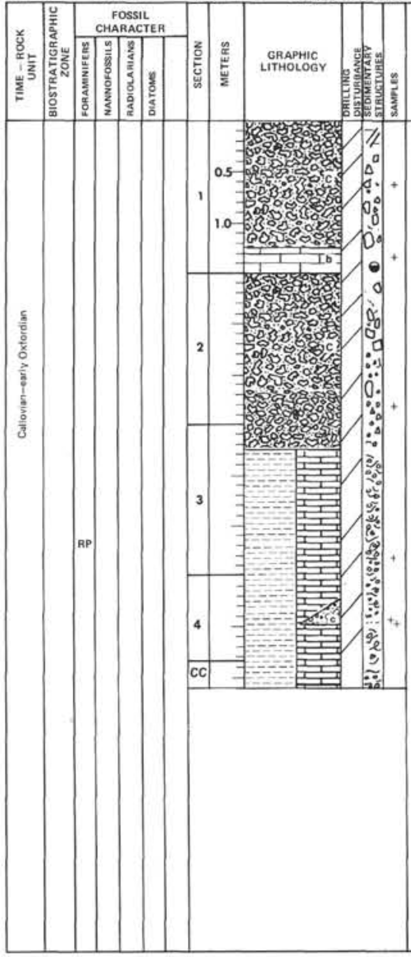

LITHOLOGIC DESCRIPTION

Section 1, 0–124 cm: slightly fractured LIMESTONE BRECCIA similar to Core 9.

From 51–67 cm: pale olive (10Y 6/2) to pale red (10R 6/2) INTRACLAST WACKESTONE with 2–8 cm sized fragments of ammonites, filament packstone, echinoderms, peloids and quartz grains in a pelmicritic matrix.

From 124–150 cm: greenish gray (5GY 6/1) to pale green (5G 7/2) pelmicritic crusts: BOUNDSTONE (BINDSTONE) overgrown by serpulids.

Section 2 through Section 3, 25 cm: LIMESTONE BRECCIA similar to Section 1, 0–124 cm grading finally into SKELETAL INTRACLASTIC GRAINSTONES.

Section 3, 25 cm through Section 4: pale green (10GY 7/2) to very pale green (10G 8/2) NODULAR LIMESTONE: wackestone of pelmicritic nodules in a matrix of clayey micrite. Gravity flows.

THIN SECTION/PEEL SUMMARY (%):

	1, 62–66 D	1, 133–137 D	2, 130–134 D
Texture:			
Rudite	15	–	20
Arenite	45	–	50
Silt	40	–	30
Composition:			
Micrite	40	80	–
Sparite	–	–	40
Intraclasts	–	–	45
Oncoids	5	5	5
Skeletal grains:			
Crinoids	30	5	10
Bivalves	25	Tr	–
Ammonites	Tr	–	–
Serpulids	–	10	–
Forams	1	Tr	Tr
Dasyclads	–	Tr	–
Ostracods	–	Tr	–
Quartz grains	1	Tr	–
Structure:			
Geopetal fab.	–	Tr	–

	3, 133–135 D	4, 46–48 D	4, 48–50 D
Texture:			
Rudite	40	–	10
Arenite	–	40	90
Silt	60	60	–
Composition:			
Micrite	60	60	–
Sparite	–	–	35
Intraclasts	40	40	5
Oncoids	–	–	55
Skeletal grains:			
Crinoids	–	Tr	3
Bivalves	Tr	1	–
Ammonites	–	Tr	1
Forams	–	Tr	1
Ostracods	Tr	–	–
Calcified radiolarians	Tr	–	–

SITE 547 HOLE B CORE 11 CORED INTERVAL 810.0–819.0 m sub-bottom

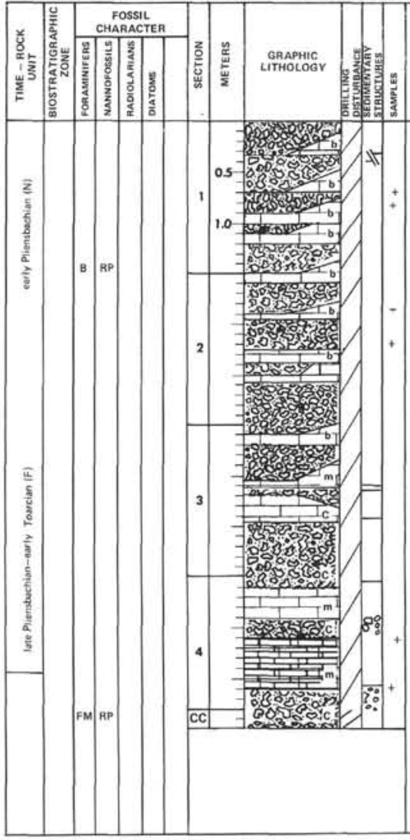

LITHOLOGIC DESCRIPTION

Section 1 through Section 3, 56 cm: slightly fractured alternation of grayish green (5G 5/2) to pale green (5G 7/2) BOUNDSTONE (BINDSTONE): pelmicritic crusts (10–23 cm thick) and LIMESTONE BRECCIA in 12 cycles of 20–40 cm thickness. Cavities within the crusts as well as the interspaces between the clasts of the breccia show internal sediment with geopetal fabric.

Section 3, 65 cm–Section 4, 108 cm: alternation of light olive gray (5Y 5/2) slightly laminated and bioturbated MICRITE and light greenish gray (5GY 8/1) BOUNDSTONE-BRECCIA facies similar to Section 1–Section 3, 56 cm. In Core 4 predominance of micrite with a thin breccia layer at 40–58 cm.

Section 4, 108 cm: beginning of a LIMESTONE BRECCIA described in Core 12.

THIN SECTION/PEEL SUMMARY (%):

	1, 71–74	1, 82–86	3, 36–39
	D	D	D
Composition:			
Micrite	40	90	99
Sparite	50	1	1
Oncoids	–	4	–
Coated grains	–		–
Skeletal grains:			
Crinoids	1	3	–
Bivalves	Tr	–	Tr
Ammonites	Tr	–	Tr
Forams	Tr	–	–
Calcif. radiolarians + spicules	3	2	Tr
Quartz grains	Tr	–	–
Structure:			
Geopetal fab.	Tr	Tr	–

	3, 71–75	4, 65–68	4, 110–115
	D	D	D
Texture:			
Arenite	5	–	–
Silt	95	–	–
Composition:			
Micrite	95	99	50
Sparite	5	–	25
Intraclasts	–	–	5
Skeletal grains:			
Crinoids	–	–	5
Bivalves	–	1	–
Serpulids	–	–	Tr
Ostracods	–	–	Tr
Calcif. radiolarians + spicules	–	–	2
Calcite crystals	Tr	–	–
Structure:			
Geopetal fab.	–	–	Tr

SITE 547 HOLE B CORE 12 CORED INTERVAL 819.0–828.0 m sub-bottom

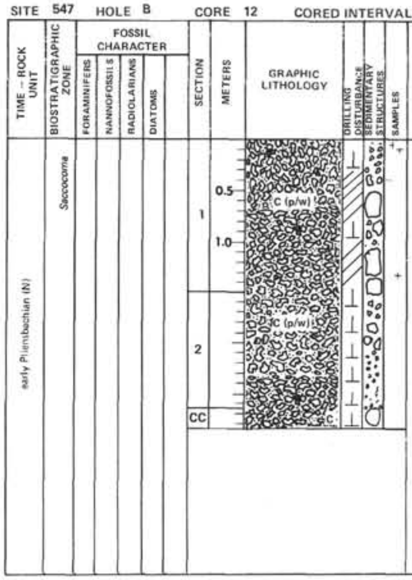

LITHOLOGIC DESCRIPTION

5YR 7/2
5YR 6/4
5G 6/1
5GY 6/1

5R 6/2
10R 6/2
10YR 7/4

5YR 7/2
5Y 6/4
10R 4/2
10G 6/2
5Y 8/1
10R 4/2

Moderately to slightly fractured LIMESTONE BRECCIA with mainly greenish gray (5G 6/1, 5GY 6/1), pale red (10R 6/2), grayish orange (10YR 7/4), grayish orange pink (5YR 7/2), dusky yellow (5Y 6/4) angular limestone clasts and grayish red (10R 4/2) rounded claystone fragments in a pale red (5R 6/2) or pale green (10G 6/2) micritic matrix partly with geopetal fabric. Grain size: coarse sand to boulder size. *Components: pelmicritic limestone with fragments of* calcified siliceous sponges, pelmicritic crusts, micrite with quartz grains, wackestone with pelmicritic nodules, clasts of micrite, coarse sandstone and single quartz grains, molluscan shell fragments, echinoderm remains.

THIN SECTION/PEEL SUMMARY (%):

	1, 4–8	1, 12–14	1, 40–44	1, 134–137
	D	D	D	D
Texture:				
Rudite	90	–	50	–
Arenite	10	35	20	–
Silt	40	65	30	–
Composition:				
Micrite	40	65	40	95
Sparite	5	–	7	4
Intraclasts	55	–	50	–
Skeletal grains:				
Crinoids	Tr	–	1	–
Gastropods	–	–	–	Tr
Quartz grains	Tr	35	2	–
Calc. sponge spicules	–	–	–	Tr
Ostracods	–	–	–	Tr
Structure:				
Geopetal fab.	–	–	–	Tr

SITE 547 HOLE B CORE 13 CORED INTERVAL 828.0–837.0 m sub-bottom

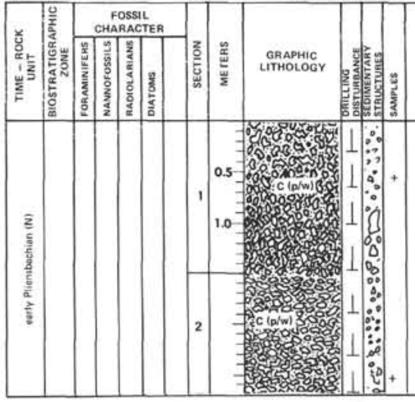

LITHOLOGIC DESCRIPTION

10R 4/4
5G 5/2
10R 4/4
10YR 5/4
5G 5/2
10YR 5/4
5G 5/2

10R 6/2
10R 4/2
10R 4/4
5R 4/2
5G 6/2
5YR 5/2
5G 8/1
5G 6/1

Moderately fractured LIMESTONE BRECCIA with varying colors and sizes (cm to several cm) of the angular and rounded limestone, sandstone, and claystone clasts. Lithology of the clasts similar to Core 12. Matrix composed of micrite intercalated of thin layers of quartz grains.

THIN SECTION/PEEL SUMMARY (%):

	1, 59–60	2, 105–108
Texture:		
Rudite	25	50
Arenite	25	10
Silt	50	40
Composition:		
Micrite	70	40
Intraclasts	25	55
Skeletal grains:		
Crinoids	–	1
Quartz grains	5	4

SITE 547 HOLE B CORE 14 CORED INTERVAL 837.0–846.0 m sub-bottom

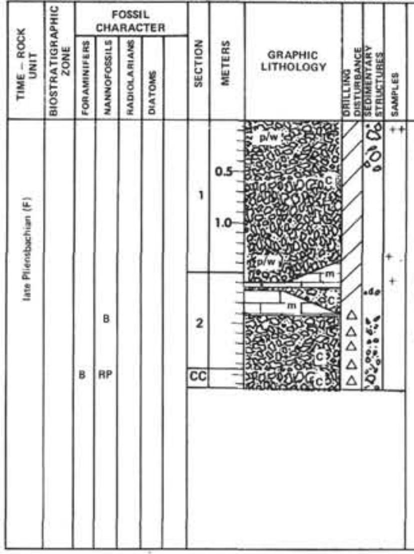

LITHOLOGIC DESCRIPTION

10R 4/2
5R 6/2
10YR 6/2
5Y 6/1
N4/N7
5Y 6/1
10YR 6/2
N3–5

Section 1 through Section 2, 10 cm: slightly fragmented LIMESTONE BRECCIA with densely packed angular to rounded clasts of limestone, sandstone, and claystone varying in color, Matrix partly infilled (geopetal fabric) showing high content of terrigenous quartz.

Section 2, 10–38 cm: slightly disturbed pale yellowish brown SANDY MUDSTONE interlayered by beds of PELOID PACKSTONE at 10–11 and 19–21 cm and LIMESTONE BRECCIA at 12–15 cm.

Section 2, 38–94 cm: drilling breccia of a LIMESTONE BRECCIA composed of angular limestone, and mudstone clasts in a terrigenous matrix. Grain size 1–5 cm.

THIN SECTION/PEEL SUMMARY (%):

	1, 13–16	1, 13–16	1, 134–136	2, 10–12
	D	M	D	D
Texture:				
Rudite	–	–	30	–
Arenite	5	50	35	100
Silt	95	50	35	–
Composition:				
Micrite	95	50	35	–
Sparite	–	–	–	30
Intraclasts	–	5	20	–
Peloids	–	–	–	70
Skeletal grains:				
Crinoids	–	5	–	–
Gastropods	1	–	–	–
Ammonites	3	–	–	Tr
Serpulids	Tr	–	–	–
Quartz grains	Tr	40	45	Tr

SITE 547 HOLE B CORE 15 CORED INTERVAL 846.0–855.0 m sub-bottom

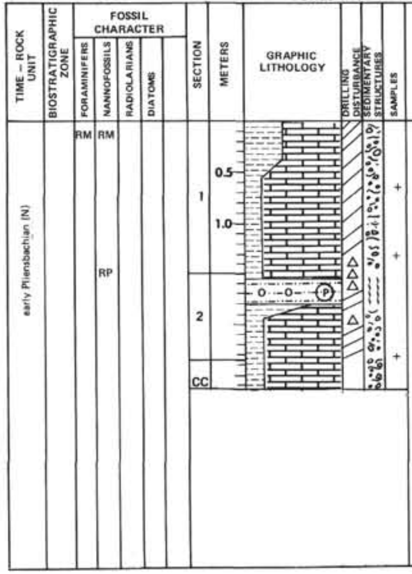

LITHOLOGIC DESCRIPTION

Slightly and minor drilling brecciated NODULAR LIMESTONE: pale yellowish brown (10YR 6/2) and pale brown (5YR 5/2) pelmicritic nodules in a matrix of dark yellowish brown (10YR 4/2) calcareous mudstone.

Section 1, 0–42 cm: nodules floating in matrix.

Section 1, 42–150 cm: nodules densely packed to merged.

Section 2, 6–30 cm: dark gray (N3) to olive black (5Y 2/1) highly burrowed PYRITE-BEARING MUDSTONE.

Section 2, 30 cm–Core-Catcher: pale yellowish brown (10YR 6/2) and pale brown (5YR 5/2) NODULAR LIMESTONE similar to Section 1 with wackestone texture.

THIN SECTION/PEEL SUMMARY (%):

	1, 77–82	1, 136–140	2, 82–87
	D	D	D
Texture:			
Rudite	30	–	35
Arenite	–	1	–
Silt	70	99	65
Composition:			
Micrite	70	95	65
Sparite	–	2	–
Intraclasts	30	–	35
Skeletal grains:			
Quartz grains	Tr	–	–
Calcified radiolarians	1	–	–
Calcified spicules	2	–	–
Structure:			
Geopetal fab.	Tr	–	–

SITE 547 HOLE B CORE 16 CORED INTERVAL 855.0–864.0 m sub-bottom

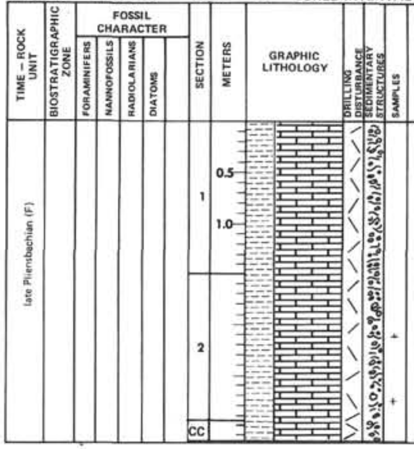

LITHOLOGIC DESCRIPTION

Highly fragmented NODULAR LIMESTONE, pale yellowish brown (10YR 6/2) pelmicritic nodules in a pale brown (5YR 5/2) mudstone matrix. The shape of the nodules is angular: they are densely packed (packstone texture).

THIN SECTION/PEEL SUMMARY (%):

	2, 61–66	2, 126–130
	D	D
Texture:		
Rudite	40	–
Arentie	–	1
Silt	60	99
Composition:		
Micrite	60	50
Intraclasts	30	50
Peloids	Tr	–
Skeletal grains:		
Calcified radiolarians	5	–
Structure:		
Geopetal fab.	–	Tr
Veins	–	Tr
Porosity	5	–

SITE 547 HOLE B CORE 17 CORED INTERVAL 864.0–873.0 m sub-bottom

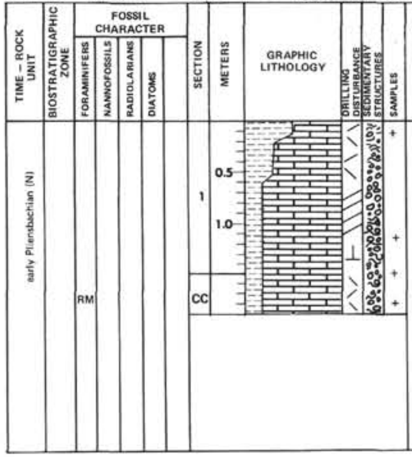

LITHOLOGIC DESCRIPTION

Highly to slightly fragmented LIMESTONE BRECCIA, pale yellowish brown (10YR 6/2) and pale red (10R 6/2) pelmicritic nodules in pale brown (5YR 5/2) and light olive gray (5Y 5/2) mudstone matrix.

Section 1, 55–150 cm: limestone massive with densely packed nodules and a matrix of stylolitization clay seams.

THIN SECTION/PEEL SUMMARY (%):

	1, 11–15	1, 114–118	CC, 0–4	CC, 31–35
	D	D	D	D
Texture:				
Rudite	90	–	30	25
Arenite	10	1	–	40
Silt	–	99	70	35
Composition:				
Micrite	–	99	70	35
Sparite	5	–	–	–
Intraclasts	95	–	30	65
Skeletal grains:				
Crinoids	–	Tr	–	–
Bivalves	–	Tr	–	–
Quartz grains	Tr	Tr	Tr	–
Sponge spicules	–	1	–	–
Structure:				
Veins	–	–	Tr	Tr

SITE 547 HOLE B CORE 18 CORED INTERVAL 873.0–882.0 m sub-bottom

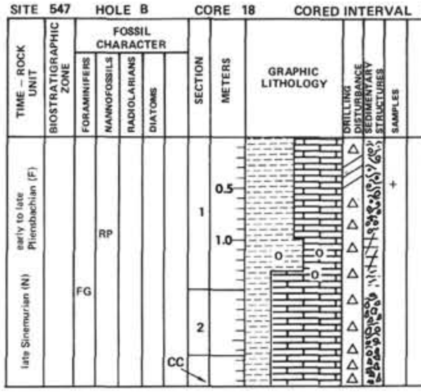

LITHOLOGIC DESCRIPTION

Drilling brecciated to highly fragmented NODULAR LIMESTONE, pale red (10R 6/2) to pale yellowish brown (10YR 6/2) pelmicritic nodules floating in a grayish olive (10Y 4/2) and dark yellowish brown (10YR 4/2) matrix of calcareous mudstone.

At Section 1, 80–120 cm: tectonic contact (dip 80°) between nodular limestone underlain by olive gray (5Y 4/1) bioturbated MUDSTONE and MICRITE without nodules. Reappearance of nodules at the beginning of Section 2.

THIN SECTION/PEEL SUMMARY (%):

	1, 49–50
Composition:	
Micrite	70
Intraclasts	30
Structure:	
Geopetal fab.	Tr

SITE 547 HOLE B CORE 19 CORED INTERVAL 882.0–891.0 m sub-bottom

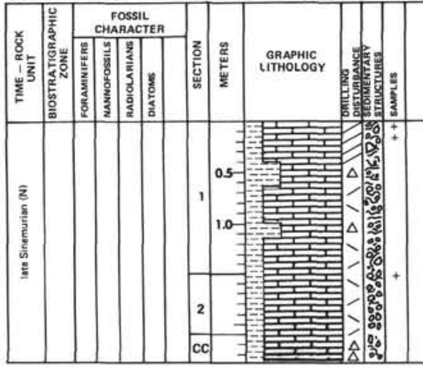

LITHOLOGIC DESCRIPTION

Drilling brecciated, highly and slightly fragmented NODULAR LIMESTONE, pale yellowish brown (10YR 6/2) pelmicritic nodules in a pale brown (5YR 5/2) matrix of calcareous sandstone. Massive limestones are mostly brecciated with stylolitic clay seams between the nodules of frequently angular shape.

THIN SECTION/PEEL SUMMARY (%):

	1, 3–8 D	1, 22–26 D	2, 1–5 D
Texture:			
Rudite	50	50	60
Silt	50	50	40
Composition:			
Micrite	50	50	40
Intraclasts	50	50	60

SITE 547 HOLE B CORE 20 CORED INTERVAL 891.0–895.5 m sub-bottom

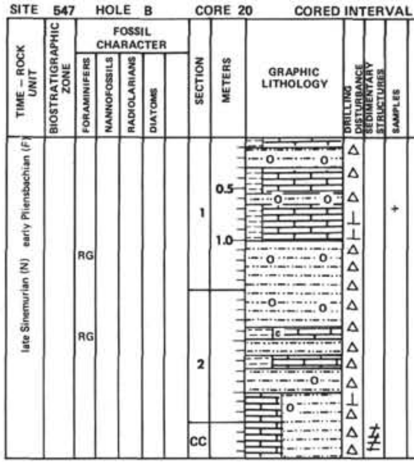

LITHOLOGIC DESCRIPTION

Drilling brecciated to moderately fragmented olive black (5Y 2/1) MUDSTONE with interlayers of medium gray (N5) to light olive gray (5Y 6/1) SLIGHTLY CLAYEY MICRITIC LIMESTONES.

Section 2, 35–46 and 65–75 cm: intervals of light olive gray (5Y 5/2) NODULAR LIMESTONE.

In the Core-Catcher medium dark gray (N4) to light gray (N6) microfractured CALCAREOUS MUDSTONE.

THIN SECTION/PEEL SUMMARY (%):

	1, 71–74 D
Texture:	
Arenite	1
Silt	99
Composition:	
Micrite	99
Skeletal grains:	
Quartz grains	1
Ostracods	Tr

SITE 547 HOLE B CORE 21 CORED INTERVAL 895.5–905.0 m sub-bottom

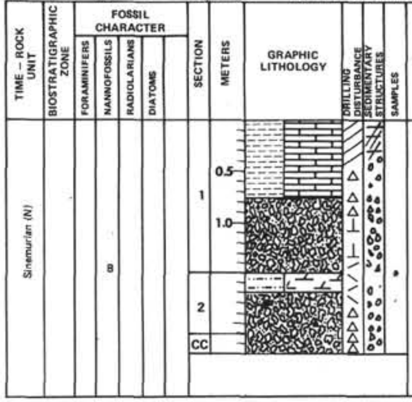

LITHOLOGIC DESCRIPTION

Section 1, 0–75 cm: slightly fragmented light olive gray (5Y 6/1) light gray (N7) to dark gray (N5) layered CLAYEY LIMESTONE and drilling brecciated CALCAREOUS CLAYSTONE.

Section 1, 75 cm–Section 2, 60 cm: moderately fragmented brown gray (5YR 4/1) to light olive gray (5Y 6/1) and olive black (5Y 2/1) LIMESTONE BRECCIA interlayered by olive black (5Y 2/1) MUDDY DOLOMITE.

SMEAR SLIDE SUMMARY (%):

	2, 3 D
Texture:	
Silt	90
Clay	10
Composition:	
Quartz	5
Clay	10
Pyrite	20
Dolomite	65

SITE 547 HOLE B CORE 22 CORED INTERVAL 905.0–914.5 m sub-bottom

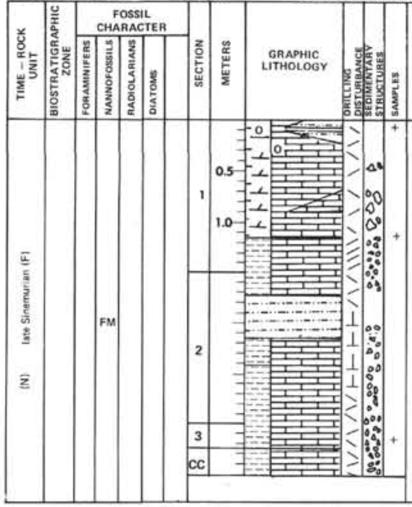

LITHOLOGIC DESCRIPTION

Section 1, 0–117 cm: highly fragmented heterogenous sequence of dark greenish gray (5GY 4/1) and greenish gray (5GY 6/1) DOLOMITIC MICRITIC LIMESTONE, olive gray (5Y 4/1), greenish gray (5GY 6/1) to dark yellowish brown (10YR 4/2) MUDSTONE (partly calcareous) and greenish gray (5GY 6/1) NODULAR LIMESTONE.

Section 1, 117 cm–Core-Catcher: highly fragmented NODULAR LIMESTONE: grayish pink (5R 8/2), pale red (5R 6/2), light gray (N7) light brownish gray (5YR 6/1) clasts in a pale brown (5YR 5/2) and medium light gray (N6) matrix.

Section 2, 23–64 cm: layer of olive gray (5Y 4/1) bioturbated NANNO-BEARING CLAYSTONE.

THIN SECTION/PEEL SUMMARY (%):

	1, 9–13 D	1, 116–120 D	3, 19–23 D
Texture:			
Rudite	–	30	70
Arenite	–	30	15
Silt	–	40	15
Composition:			
Micrite	99	40	15
Intraclasts	–	60	85
Skeletal grains:			
Quartz grains	1	–	–
Structure:			
Veins	–	Tr	–

SITE 547 HOLE B CORE 23 CORED INTERVAL 914.5–923.5 m sub-bottom

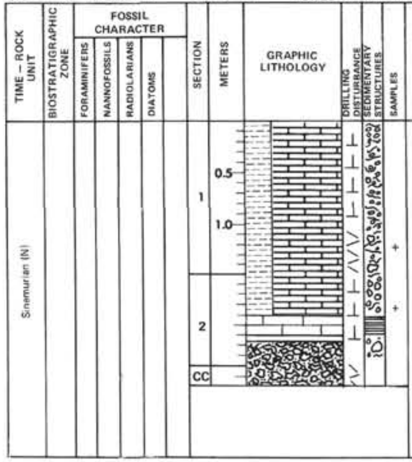

LITHOLOGIC DESCRIPTION

Section 1 through Section 2, 40 cm: highly to moderately fragmented NODULAR LIMESTONE wackestone with pale yellowish brown (10YR 6/2) pelmicritic nodules in a pale brown (5YR 5/2) matrix of calcareous mudstone. Section 1, 89–150 cm polymictic composition of pale pink, light gray, and bluish gray limestone and mudstone clasts.

Section 2, 40–62 cm: sequence of light olive gray (5Y 5/2) STROMATOLITE (BOUNDSTONE-BINDSTONE).

From Section 2, 62 cm–Core-Catcher grayish olive (10Y 4/2) and olive black (5Y 2/1) monomictic LIMESTONE BRECCIA composed of microsparitic angular clasts of reworked stromatolites.

THIN SECTION/PEEL SUMMARY (%):

	1, 121–125 D	2, 39–47 D
Texture:		
Arenite	–	100
Silt	100	–
Composition:		
Micrite	100	–
Peloids	–	99
Skeletal grains:		
Calcified radiolarians	–	1

SITE 547 HOLE B CORE 24 CORED INTERVAL 923.5–932.5 m sub-bottom

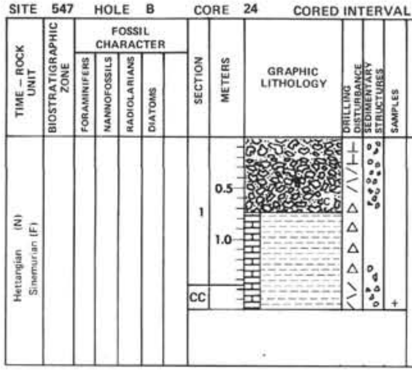

LITHOLOGIC DESCRIPTION

0–73 cm: drilling brecciated to highly fragmented medium gray (N5) LIMESTONE BRECCIA.

73 cm–Core-Catcher: medium dark gray (N4), grayish red (10R 4/2), medium gray (N5) to dark greenish gray (5G 4/1) SLIGHTLY CALCAREOUS CLAYSTONE.

THIN SECTION/PEEL SUMMARY (%):

	CC, 19–23
Texture:	
Rudite	25
Arenite	40
Silt	35
Composition:	
Micrite	35
Intraclasts	65

SITE 547 HOLE B CORE 25 CORED INTERVAL 932.5–941.5 m sub-bottom

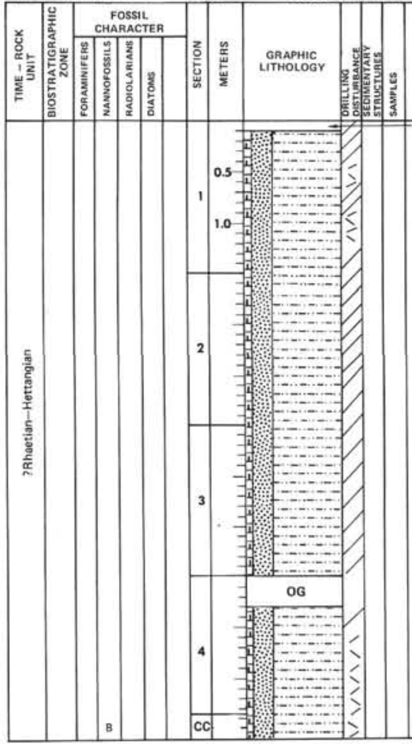

LITHOLOGIC DESCRIPTION

IW

Mostly slightly disturbed, grayish red (10R 4/2) to medium gray (N5) to dusky brown (5YR 2/2) CALCAREOUS/DOLOMITIC SANDY CLAYSTONE to MUDSTONE.

SITE 547 HOLE B CORE 26 CORED INTERVAL 941.5–950.5 m sub-bottom

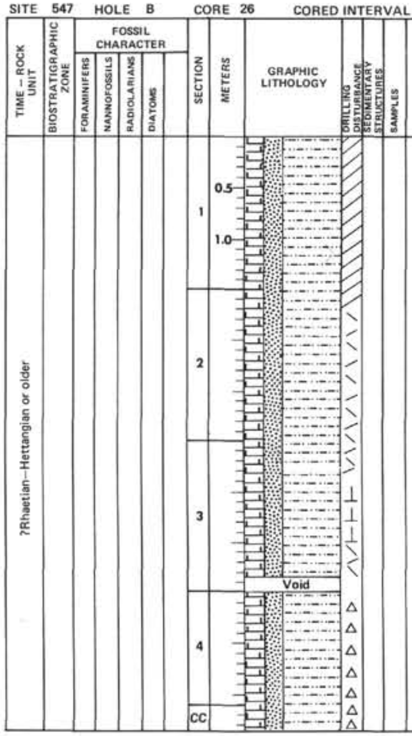

LITHOLOGIC DESCRIPTION

Mostly highly fragmented, medium gray (N5) to medium dark gray (N4) and moderate brown (5YR 3/4) to grayish red (5R 4/2) CALCAREOUS SANDY MUDSTONE.

SITE 547 HOLE B CORE 27 CORED INTERVAL 950.5–959.5 m sub-bottom

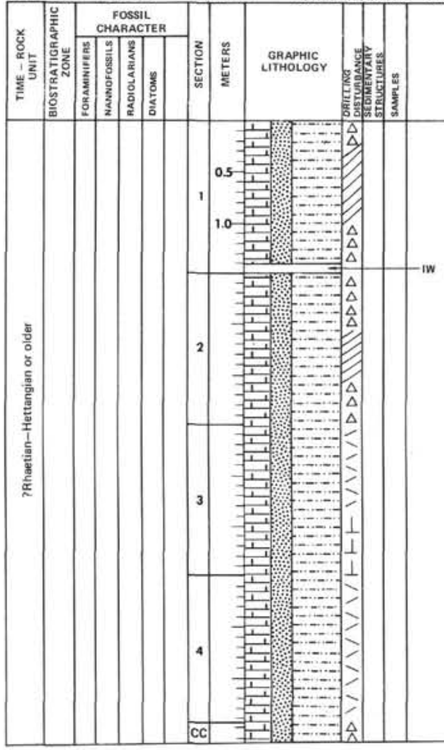

LITHOLOGIC DESCRIPTION

Mostly highly fragmented and deformed, grayish red (5R 4/2) moderate brown (5YR 3/4) and bluish gray (5B 6/1) CALCAREOUS SANDY MUDSTONE with common dolomite nodules, feldspath and quartz and minor feldspatch-quartz (granite) grains.

SITE 547 HOLE B CORE 28 CORED INTERVAL 959.5–968.5 m sub-bottom

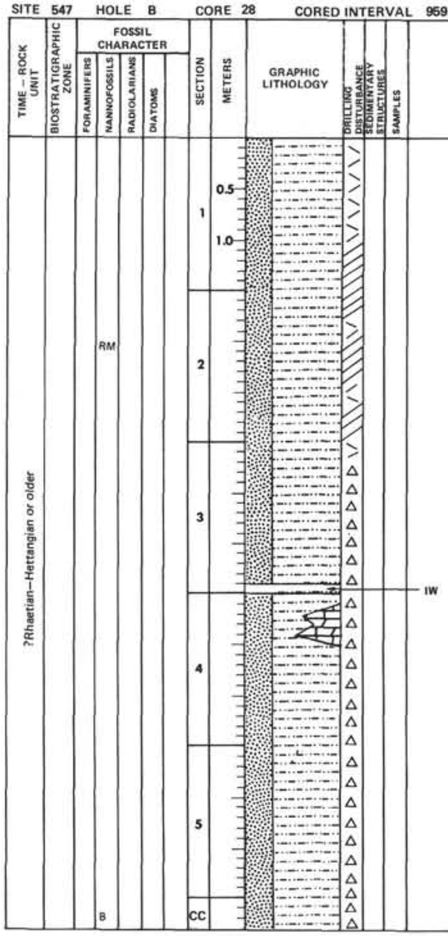

LITHOLOGIC DESCRIPTION

Mostly highly fragmented to brecciated, medium dark gray (N4), moderate brown (5YR 3/4) and grayish brown (5YR 3/2) MUDSTONE and SANDY MUDSTONE.

Fragments of GYPSUM at Section 4, 6–8, 20–25, and 52–55 cm.

SITE 547 HOLE B CORE 29 CORED INTERVAL 968.5–977.5 m sub-bottom

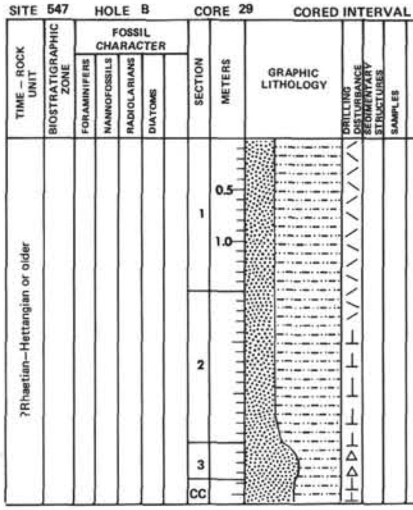

LITHOLOGIC DESCRIPTION

Moderately to highly fragmented grayish red (10R 4/2) and medium dark gray (N5) SANDY MUDSTONE and minor MUDDY SANDSTONE at base.

Quartz-feldspathic sands.

SITE 547 HOLE B CORE 30 CORED INTERVAL 977.5–986.5 m sub-bottom

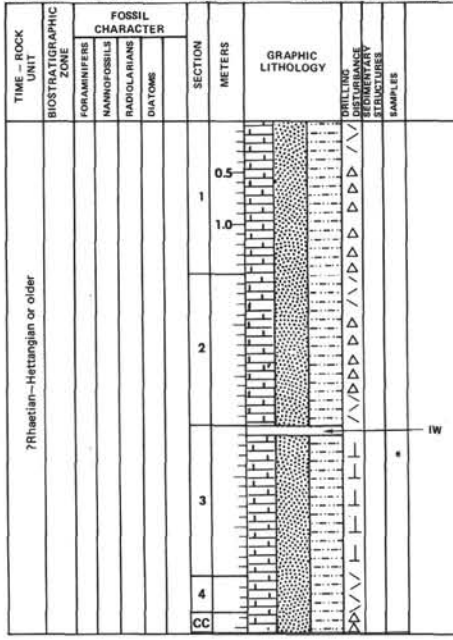

LITHOLOGIC DESCRIPTION

Mostly highly brecciated, grayish red (10R 4/2) and medium dark gray (N5) CALCAREOUS SANDY MUDSTONES and PEBBLY MUDSTONES – mud pebbles.

SMEAR SLIDE SUMMARY (%):

	2, 30
Composition:	
Quartz	8
Feldspar	2
Clay	80
Gypsum	8
Dolomite	2

SITE 547 HOLE B CORE 31 CORED INTERVAL 986.5–995.5 m sub-bottom

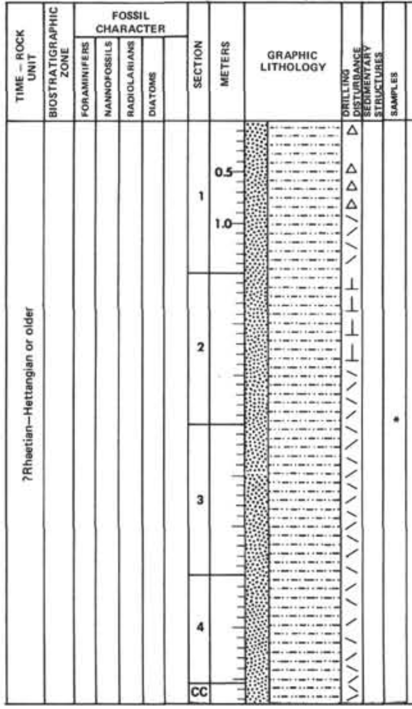

LITHOLOGIC DESCRIPTION

Mostly highly fragmented grayish red (10R 4/2) SANDY MUDSTONE. Scattered cm sized fragments of gypsum(?) throughout Section 2.

SMEAR SLIDE SUMMARY (%):

	2, 142
	M
Texture:	
Sand	100
Composition:	
Gypsum	100

SITE 547 HOLE B CORE 32 CORED INTERVAL 995.5–1000.0 m sub-bottom

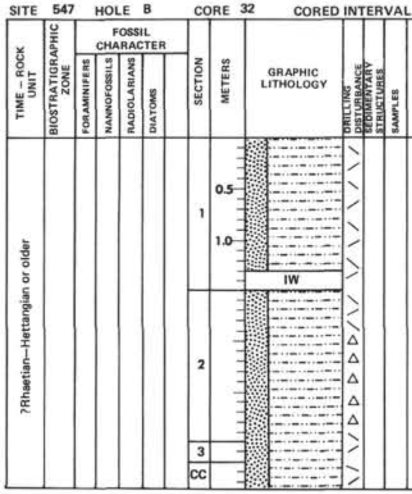

LITHOLOGIC DESCRIPTION

Highly fragmented to brecciated, grayish red (10R 4/2) SANDY MUDSTONE with minor amounts of dolomite, quartz, and feldspath granules and gypsum.

SITE 547 HOLE B CORE 33 CORED INTERVAL 1000.0–1009.5 m sub-bottom

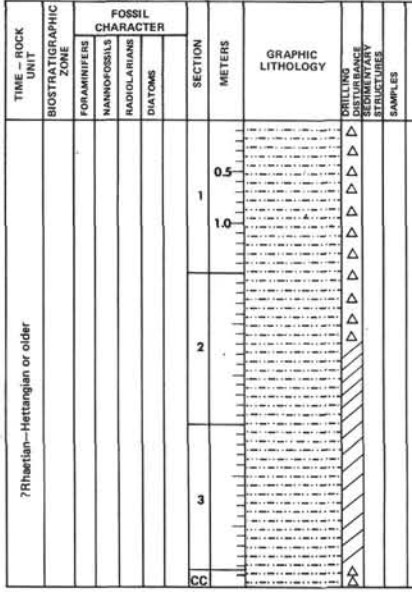

LITHOLOGIC DESCRIPTION

Highly fragmented and brecciated, grayish red (10R 4/2) MUDSTONE with scattered sand grains and granules of quartz, feldspath and composite (granitic) grains.

SITE 547 HOLE B CORE 34 CORED INTERVAL 1009.5–1018.5 m sub-bottom

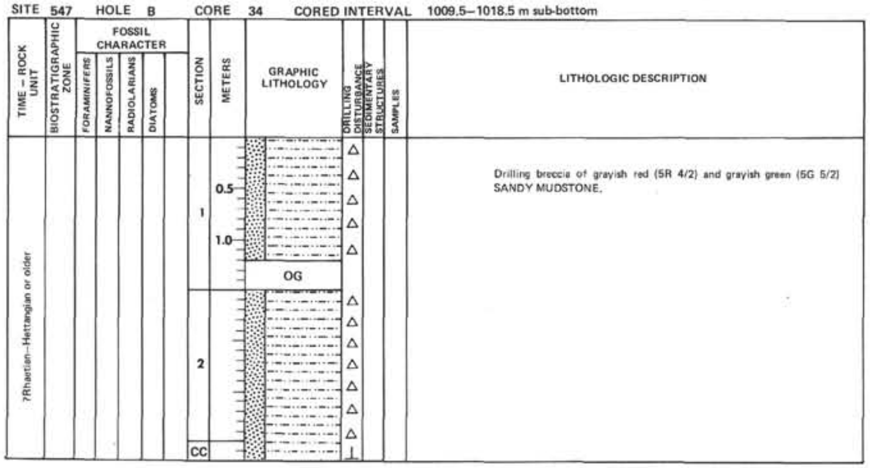

Drilling breccia of grayish red (5R 4/2) and grayish green (5G 5/2) SANDY MUDSTONE.

SITE 547 HOLE B CORE 35 CORED INTERVAL 1018.5–1027.5 m sub-bottom

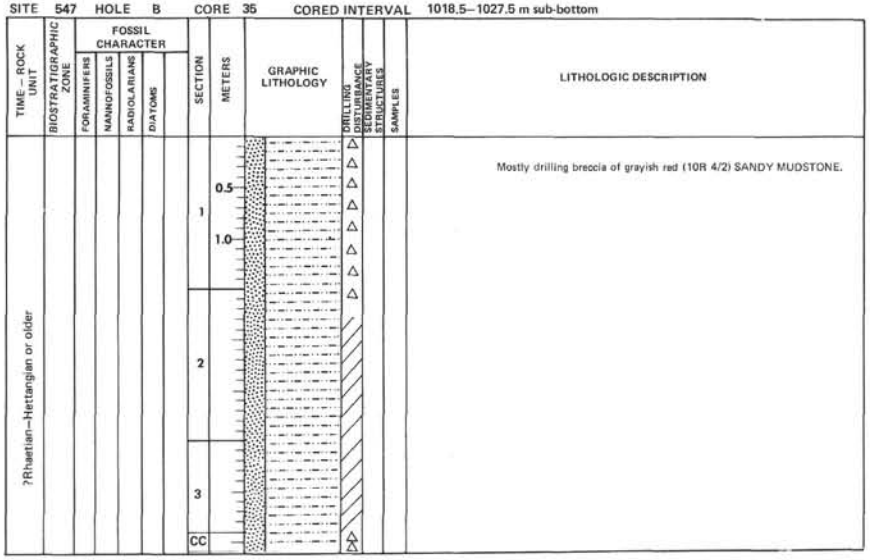

Mostly drilling breccia of grayish red (10R 4/2) SANDY MUDSTONE.

SITE 547 HOLE B CORE 36 CORED INTERVAL 1027.5–1030.0 m sub-bottom

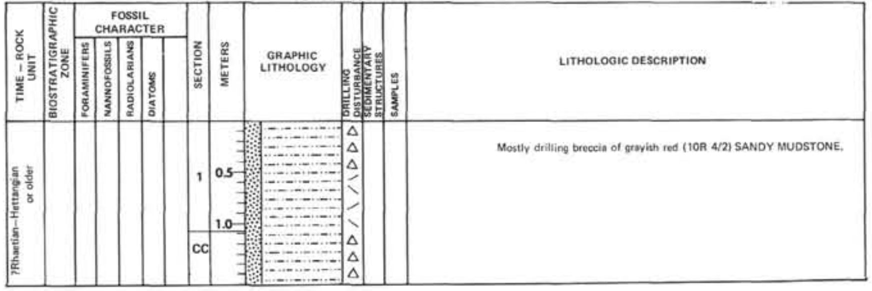

Mostly drilling breccia of grayish red (10R 4/2) SANDY MUDSTONE.

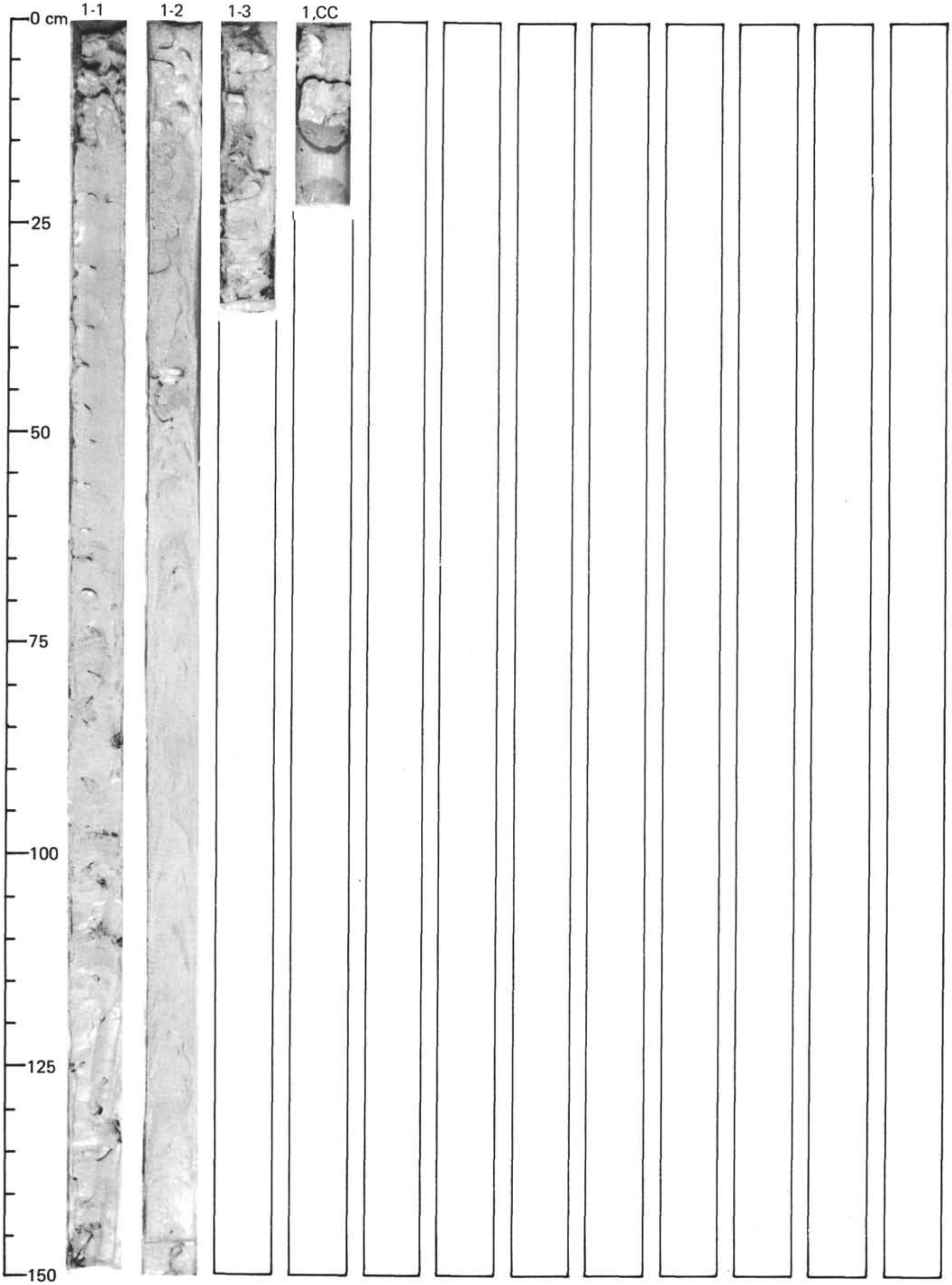
0 cm
25
50
75
100
125
150
1-1
1-2
1-3
1,CC

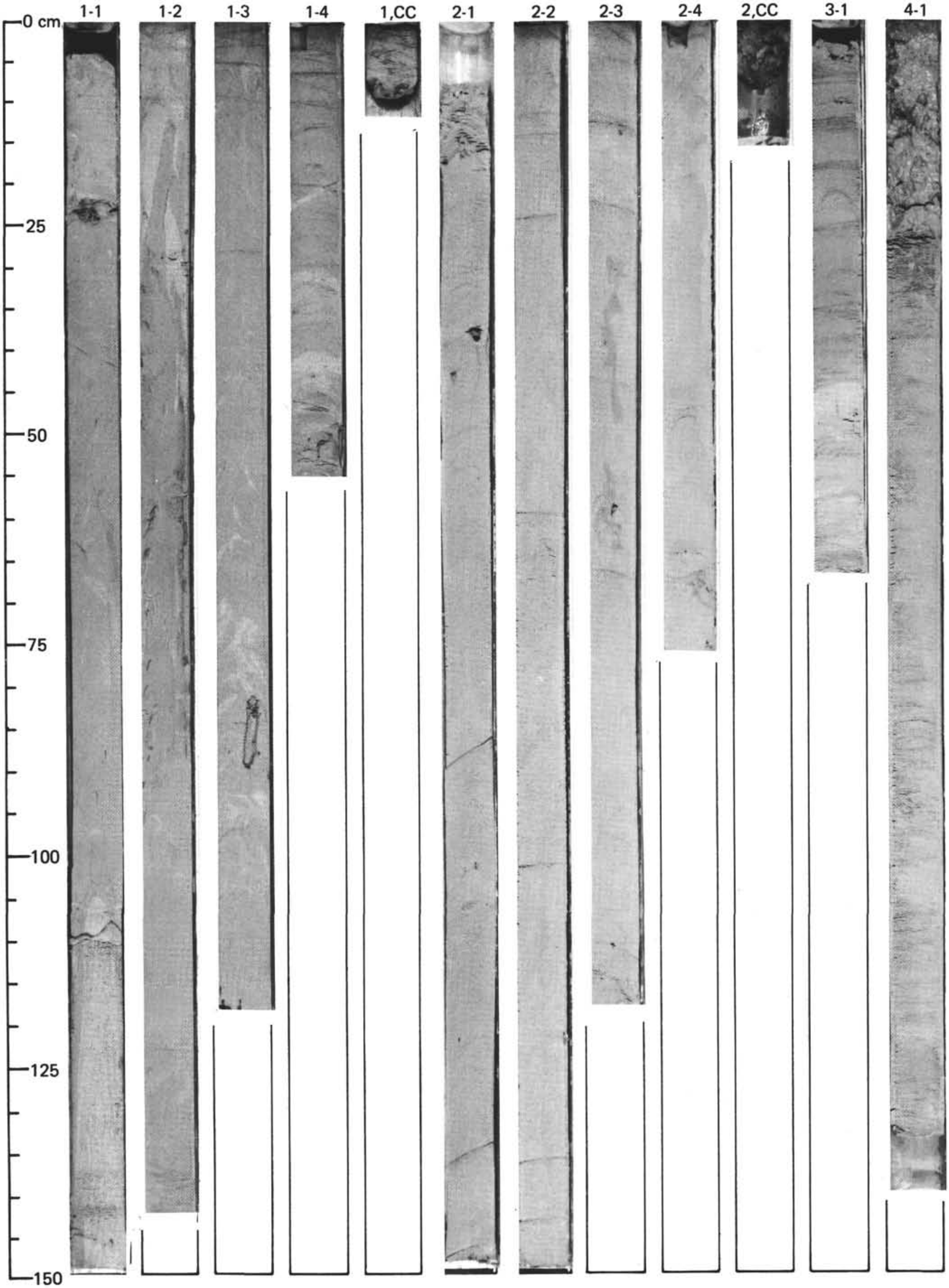

1-1
1-2
1-3
1-4
1,CC
2-1
2-2
2-3
2-4
2,CC
3-1
4-1
0 cm
25
50
75
100
125
150

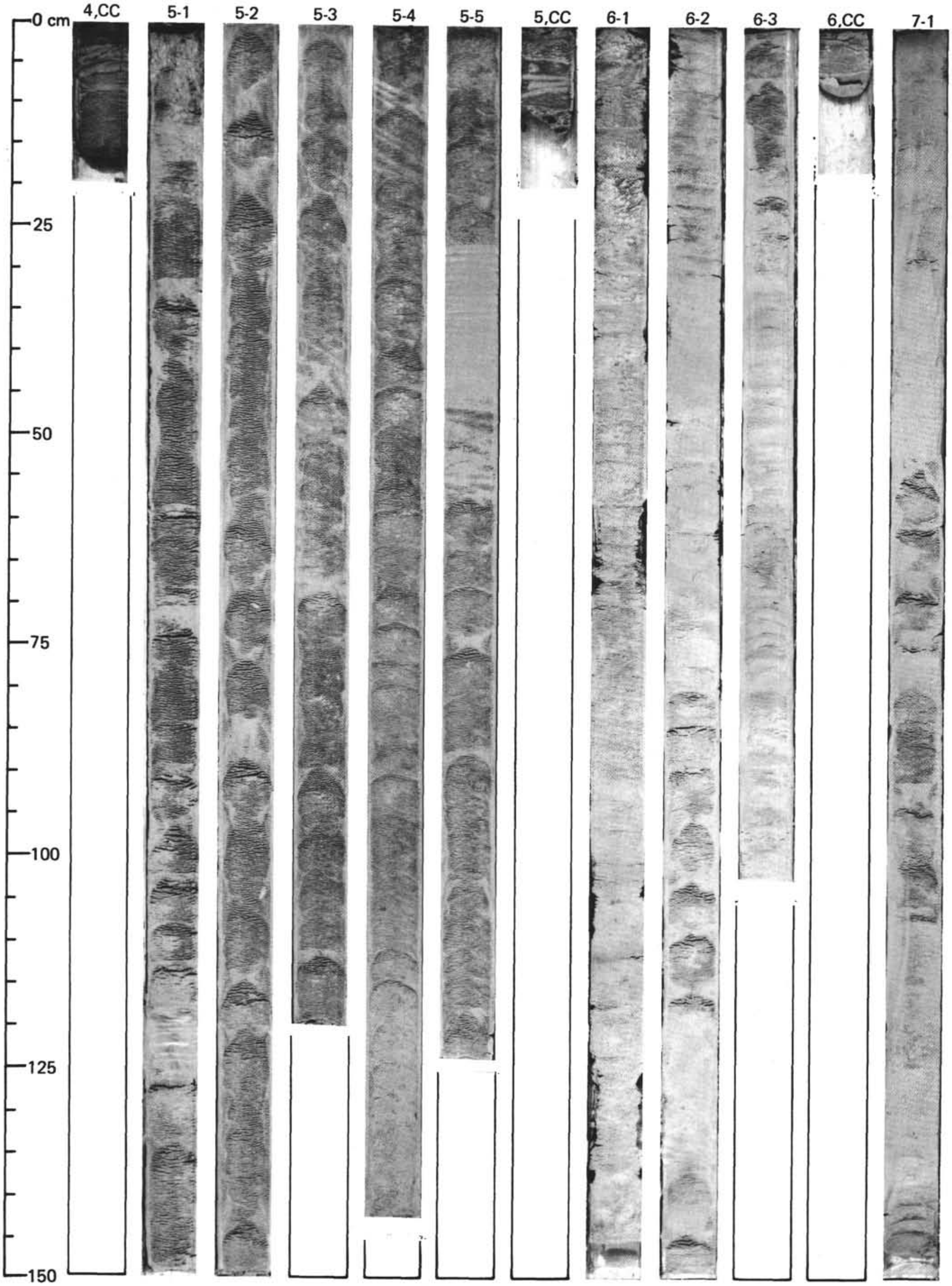
0 cm
25
50
75
100
125
150
4,CC
5-1
5-2
5-3
5-4
5-5
5,CC
6-1
6-2
6-3
6,CC
7-1

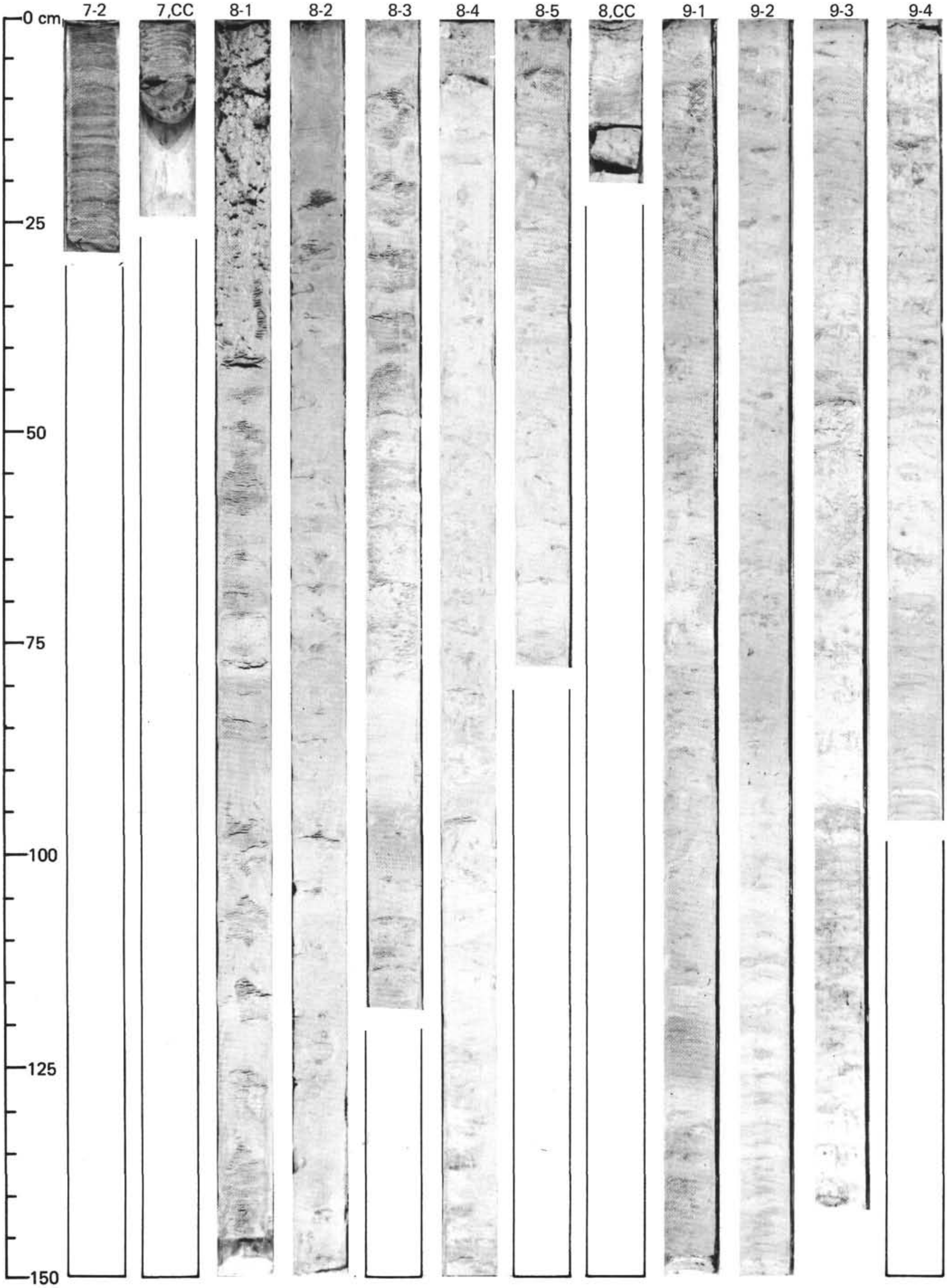
7-2
7,CC
8-1
8-2
8-3
8-4
8-5
8,CC
9-1
9-2
9-3
9-4
0 cm
25
50
75
100
125
150

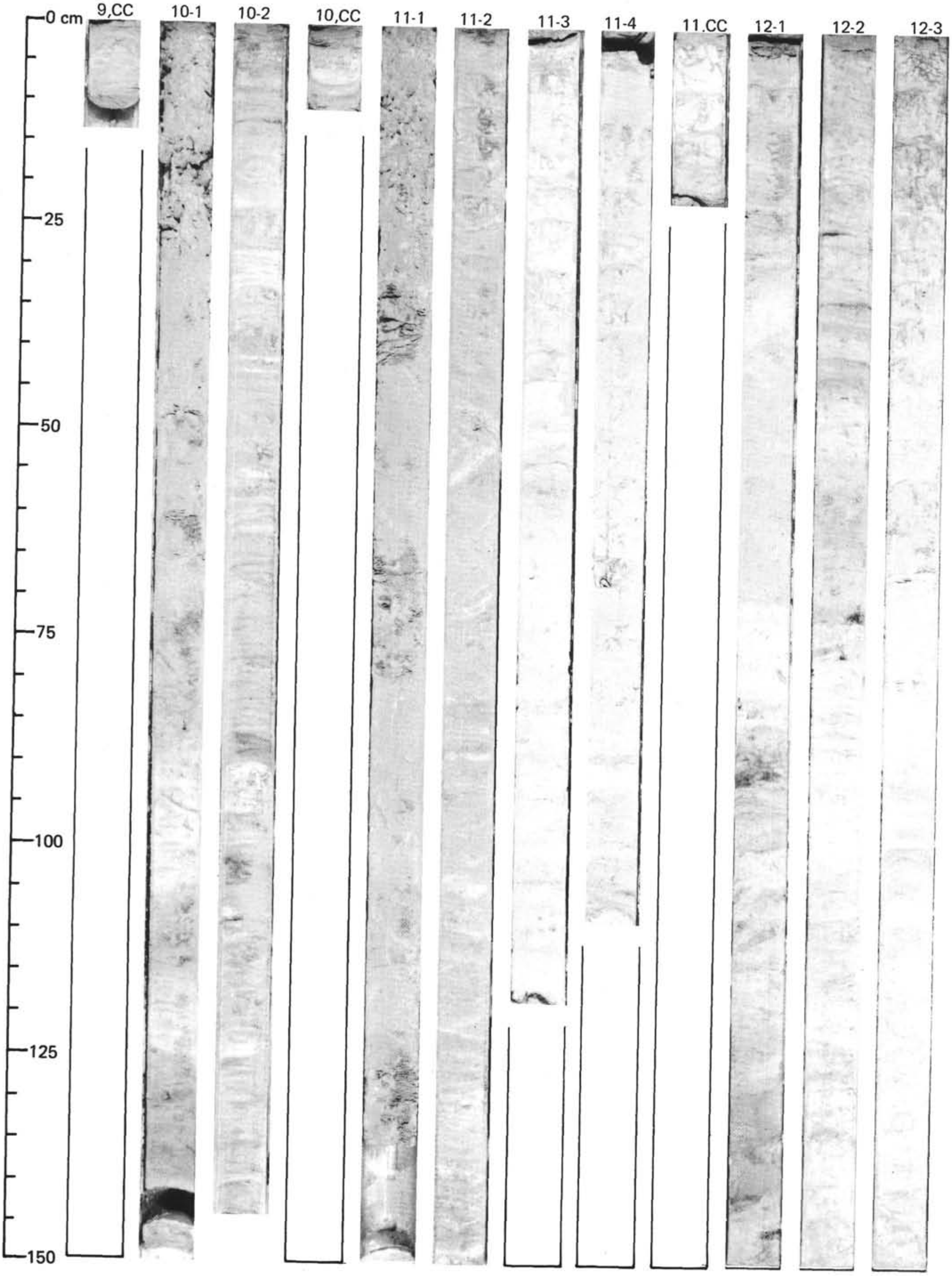
0 cm
25
50
75
100
125
150
9,CC
10-1
10-2
10,CC
11-1
11-2
11-3
11-4
11,CC
12-1
12-2
12-3

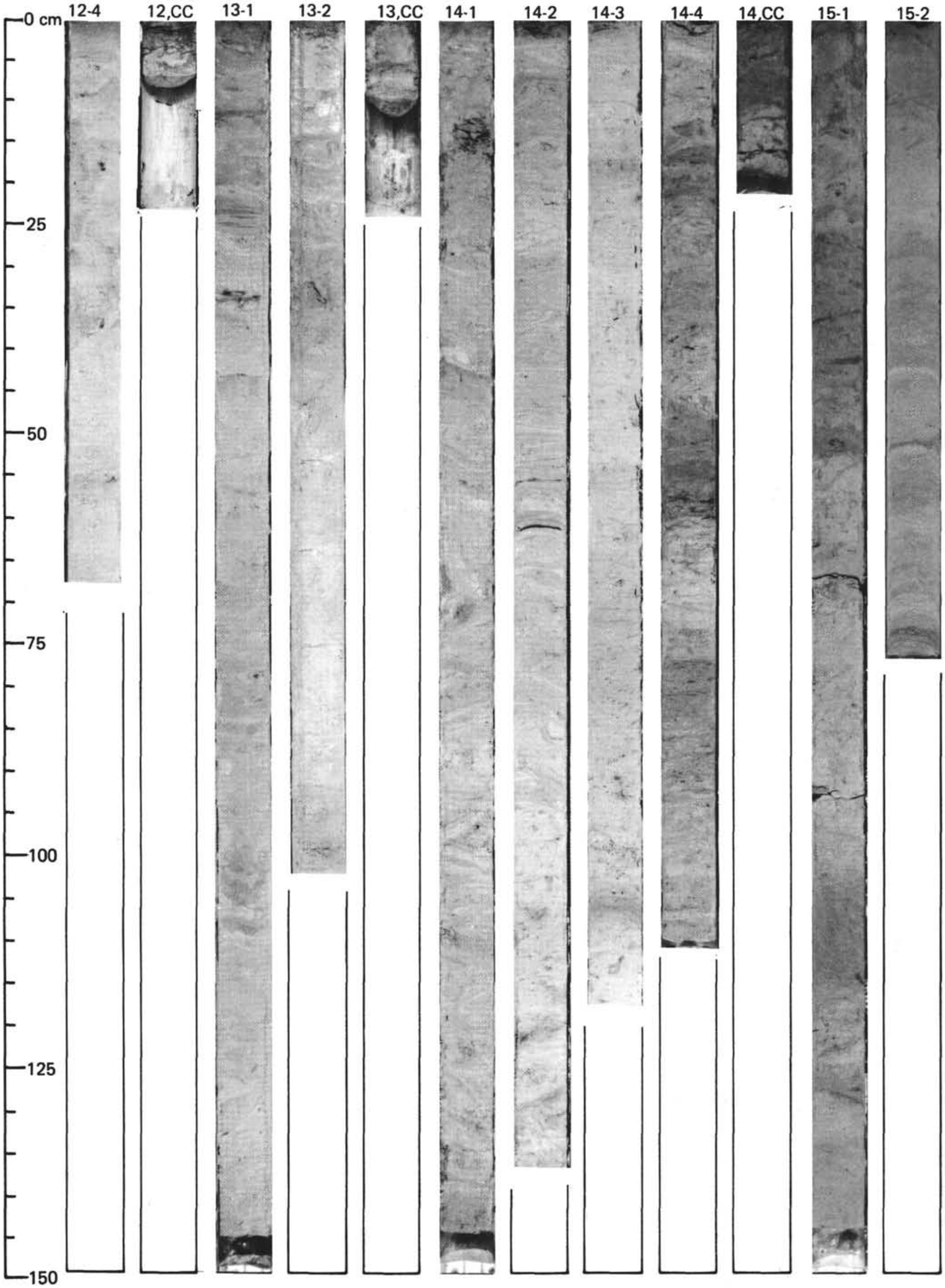
0 cm
25
50
75
100
125
150
12-4
12,CC
13-1
13-2
13,CC
14-1
14-2
14-3
14-4
14,CC
15-1
15-2

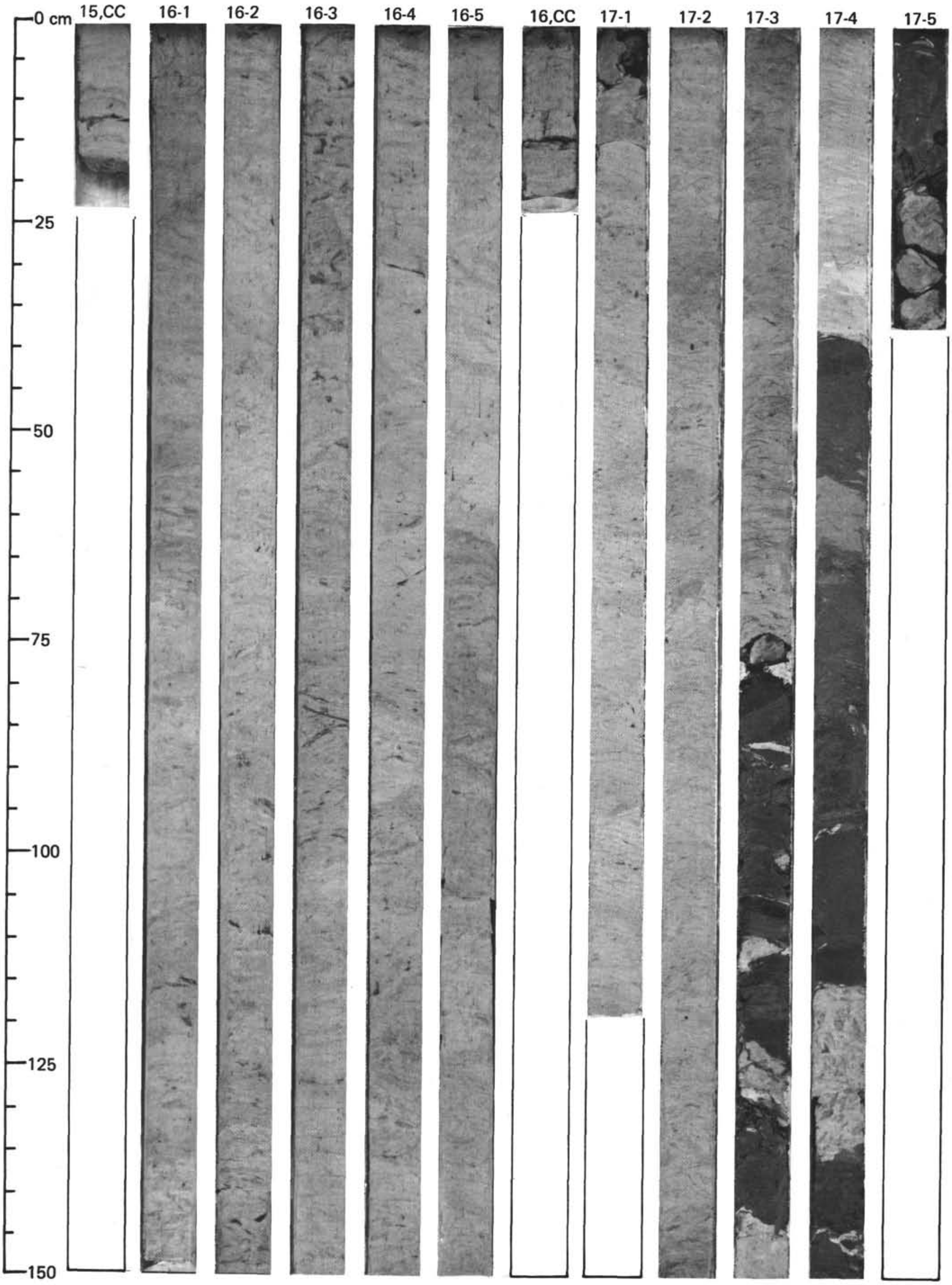
0 cm
25
50
75
100
125
150
15,CC
16-1
16-2
16-3
16-4
16-5
16,CC
17-1
17-2
17-3
17-4
17-5

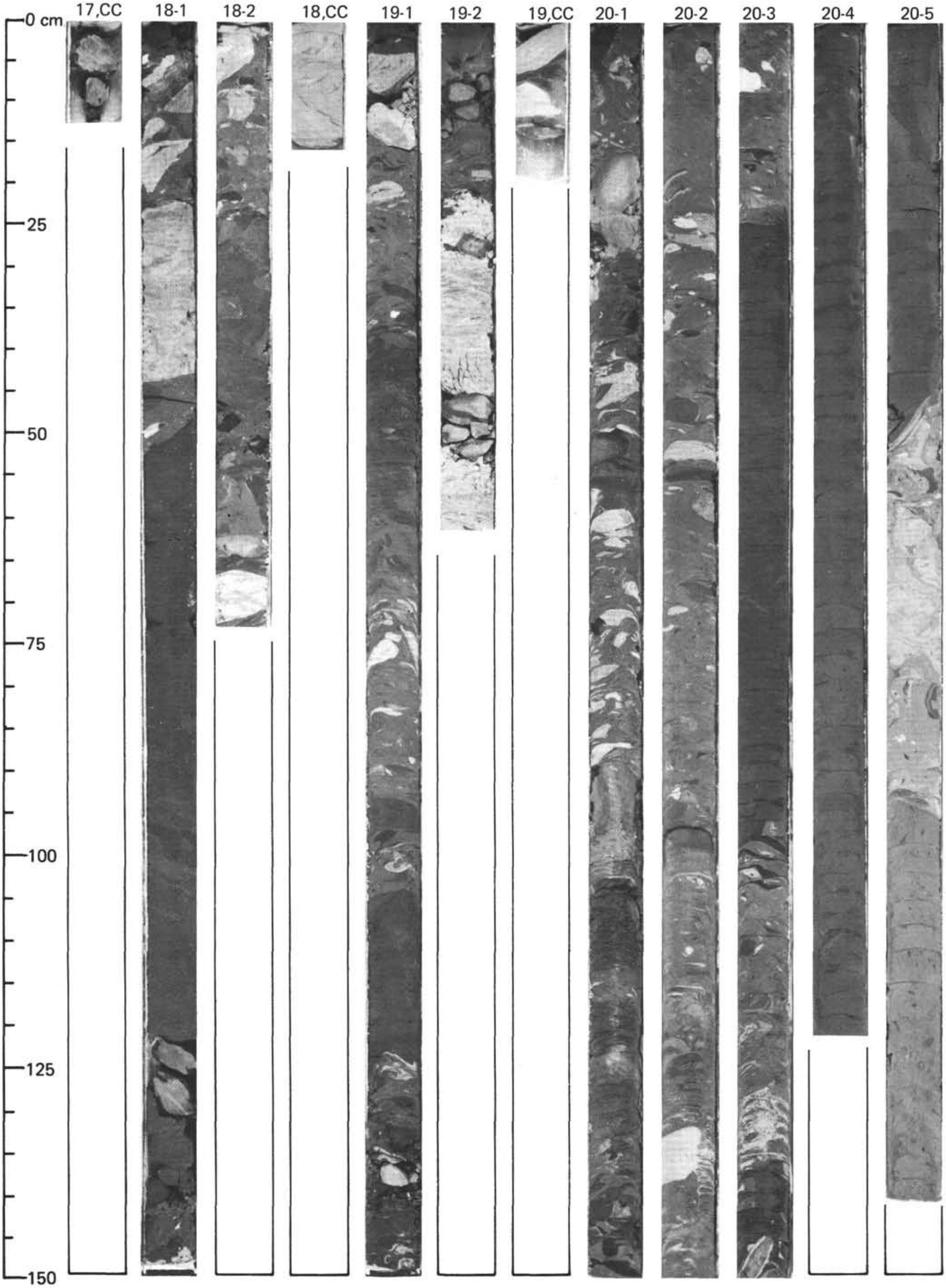
17,CC
18-1
18-2
18,CC
19-1
19-2
19,CC
20-1
20-2
20-3
20-4
20-5
0 cm
25
50
75
100
125
150

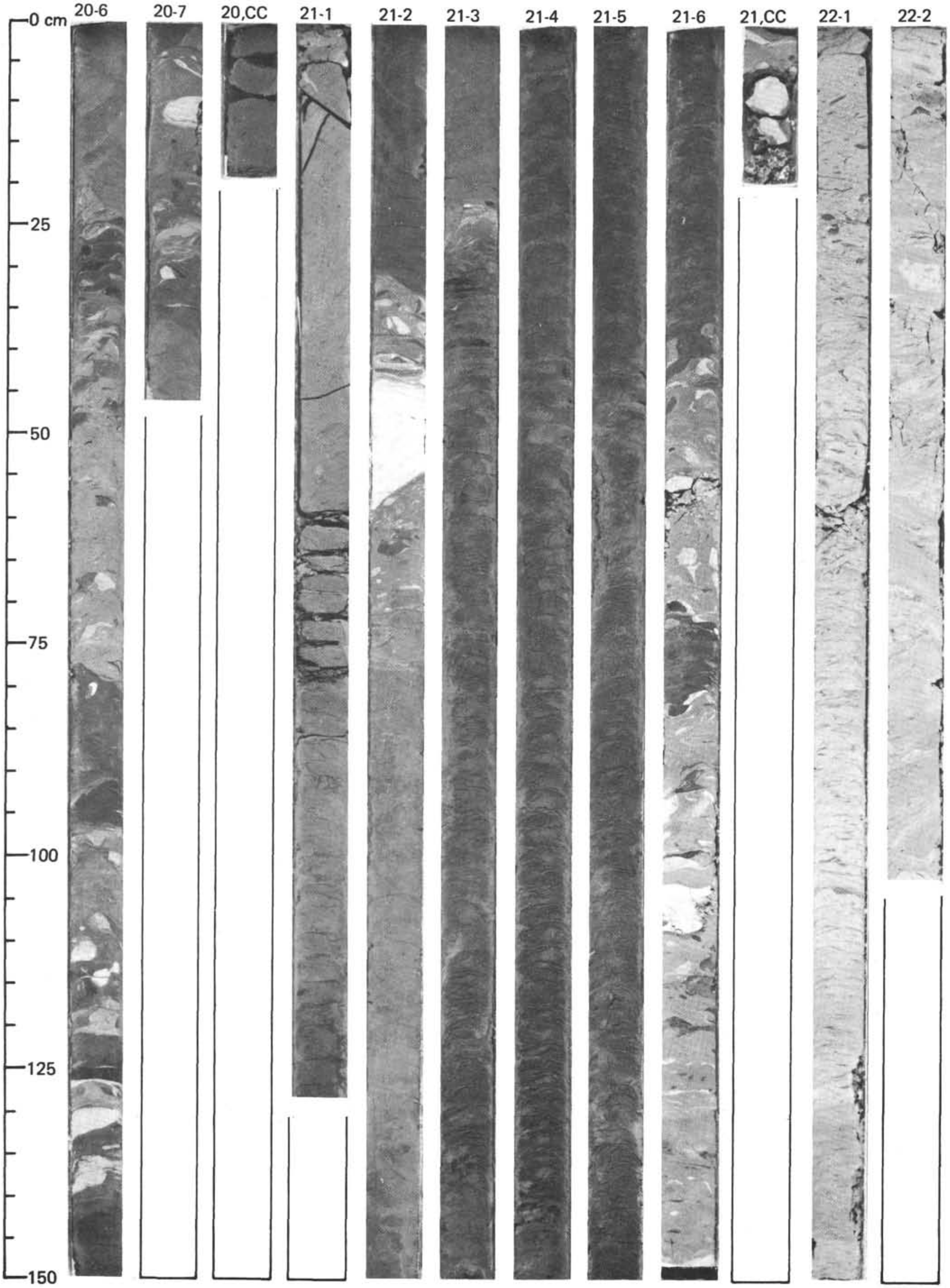
0 cm
25
50
75
100
125
150
20-6
20-7
20,CC
21-1
21-2
21-3
21-4
21-5
21-6
21,CC
22-1
22-2

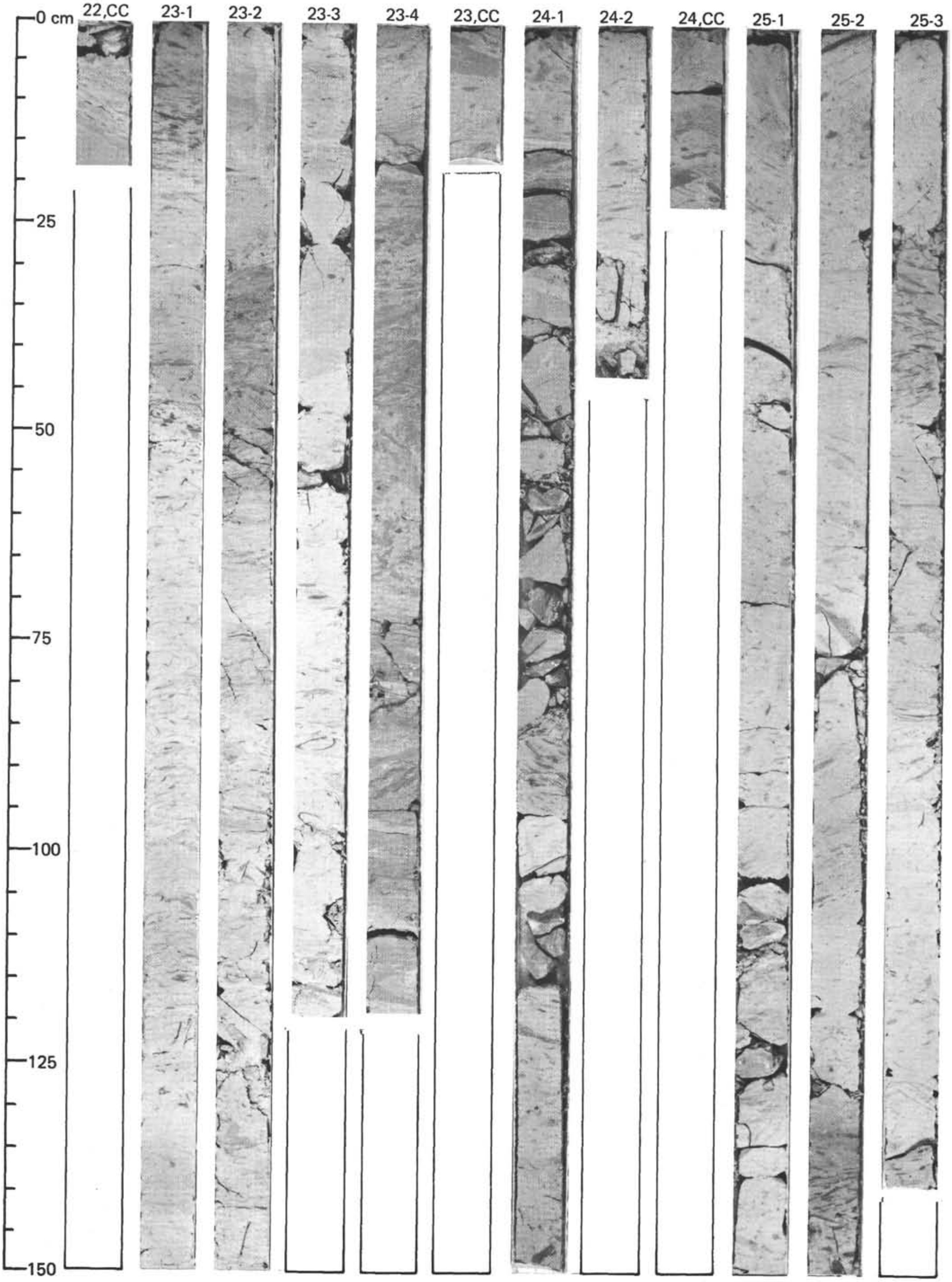
0 cm
25
50
75
100
125
150
22,CC
23-1
23-2
23-3
23-4
23,CC
24-1
24-2
24,CC
25-1
25-2
25-3

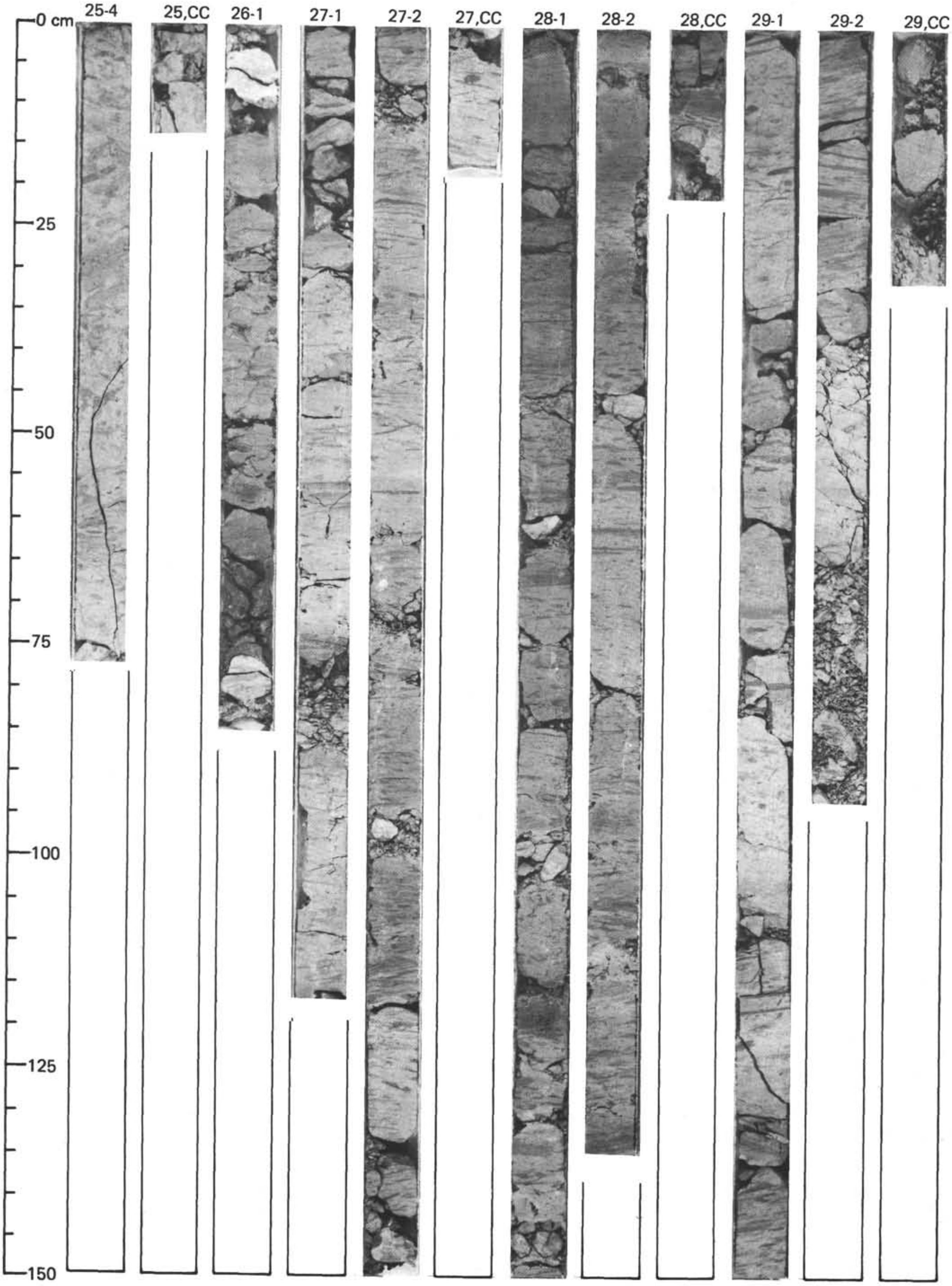
0 cm
25
50
75
100
125
150
25-4
25,CC
26-1
27-1
27-2
27,CC
28-1
28-2
28,CC
29-1
29-2
29,CC

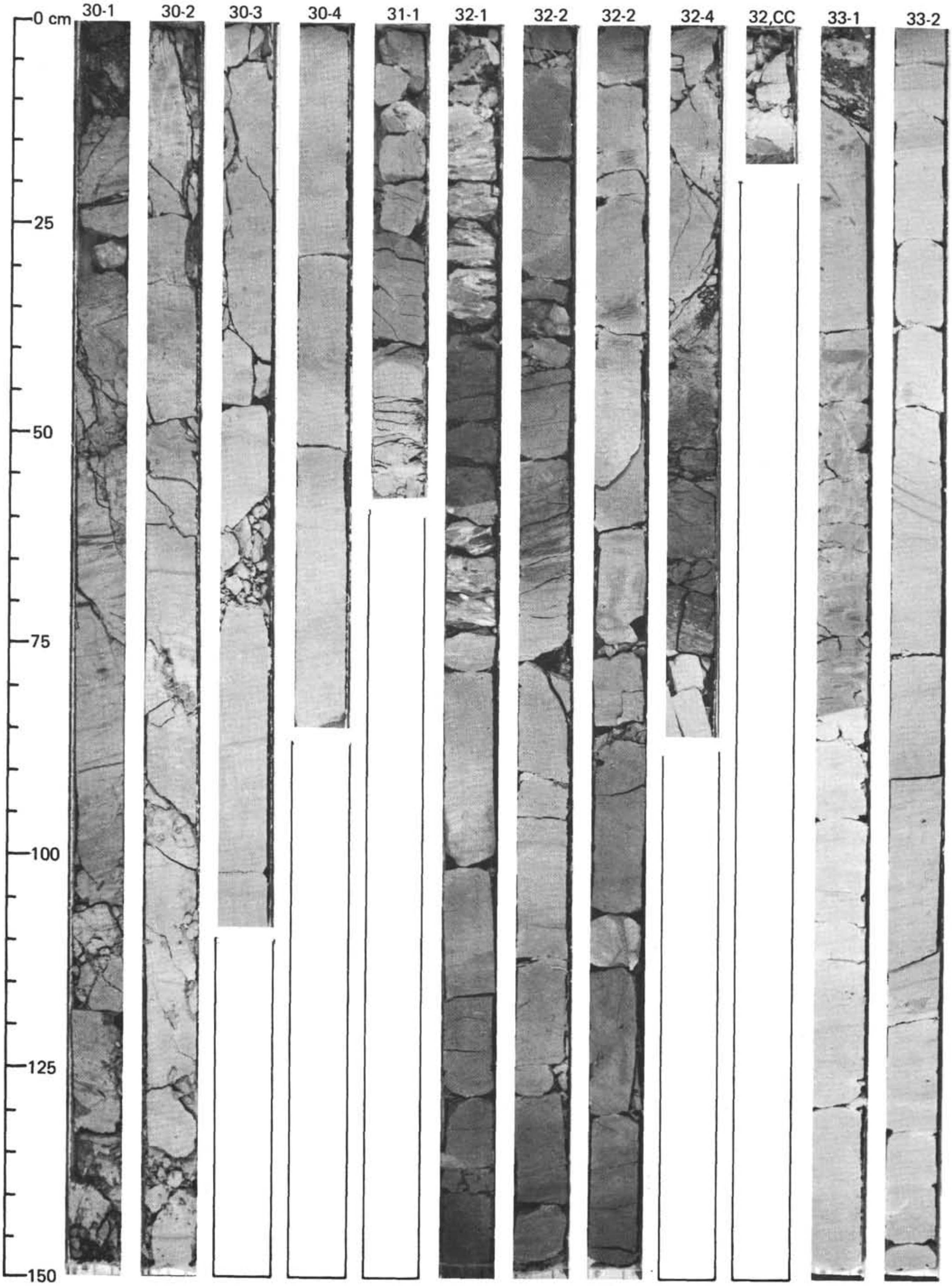
0 cm
25
50
75
100
125
150
30-1
30-2
30-3
30-4
31-1
32-1
32-2
32-2
32-4
32,CC
33-1
33-2

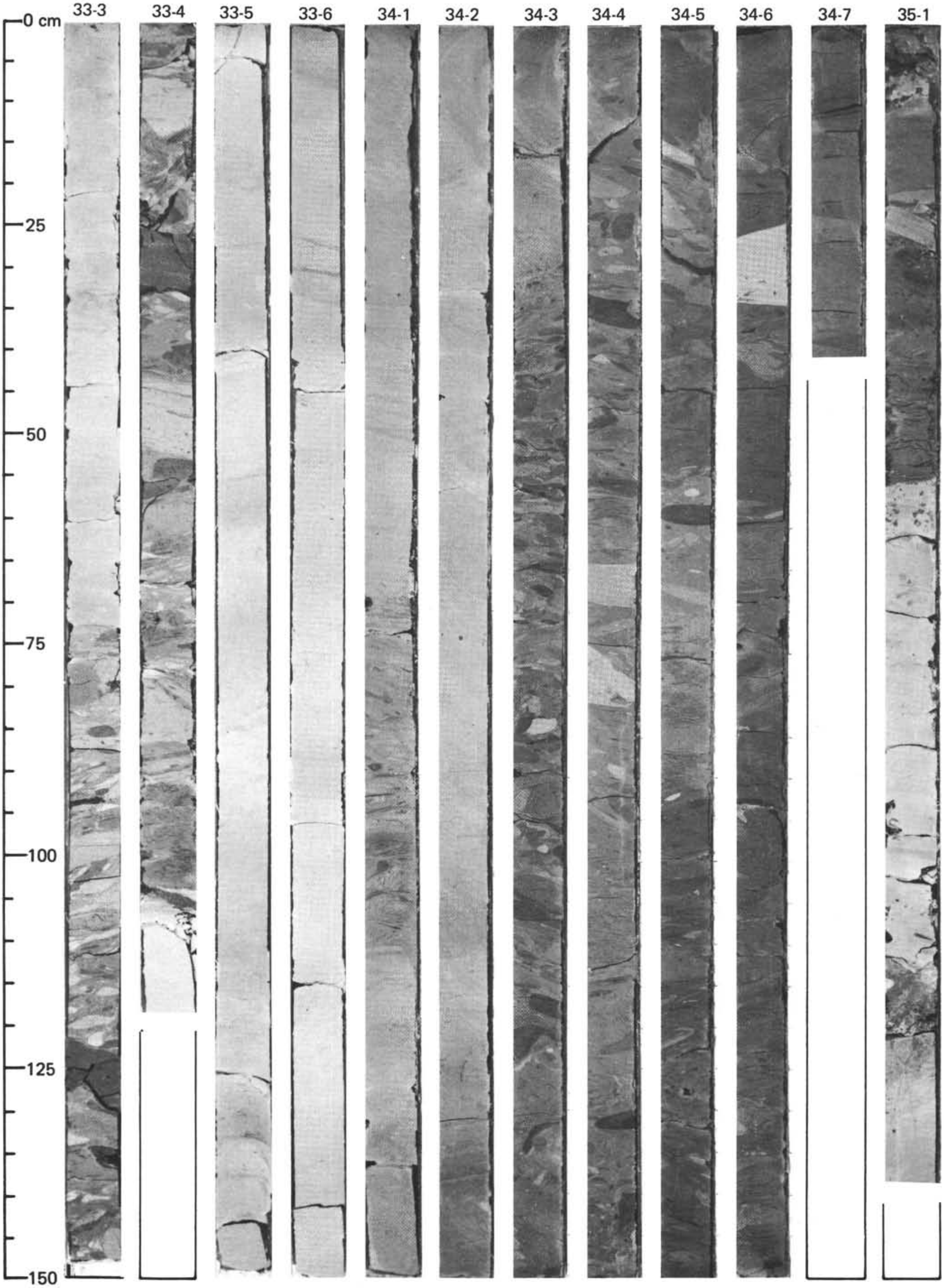
33-3
33-4
33-5
33-6
34-1
34-2
34-3
34-4
34-5
34-6
34-7
35-1
0 cm
25
50
75
100
125
150

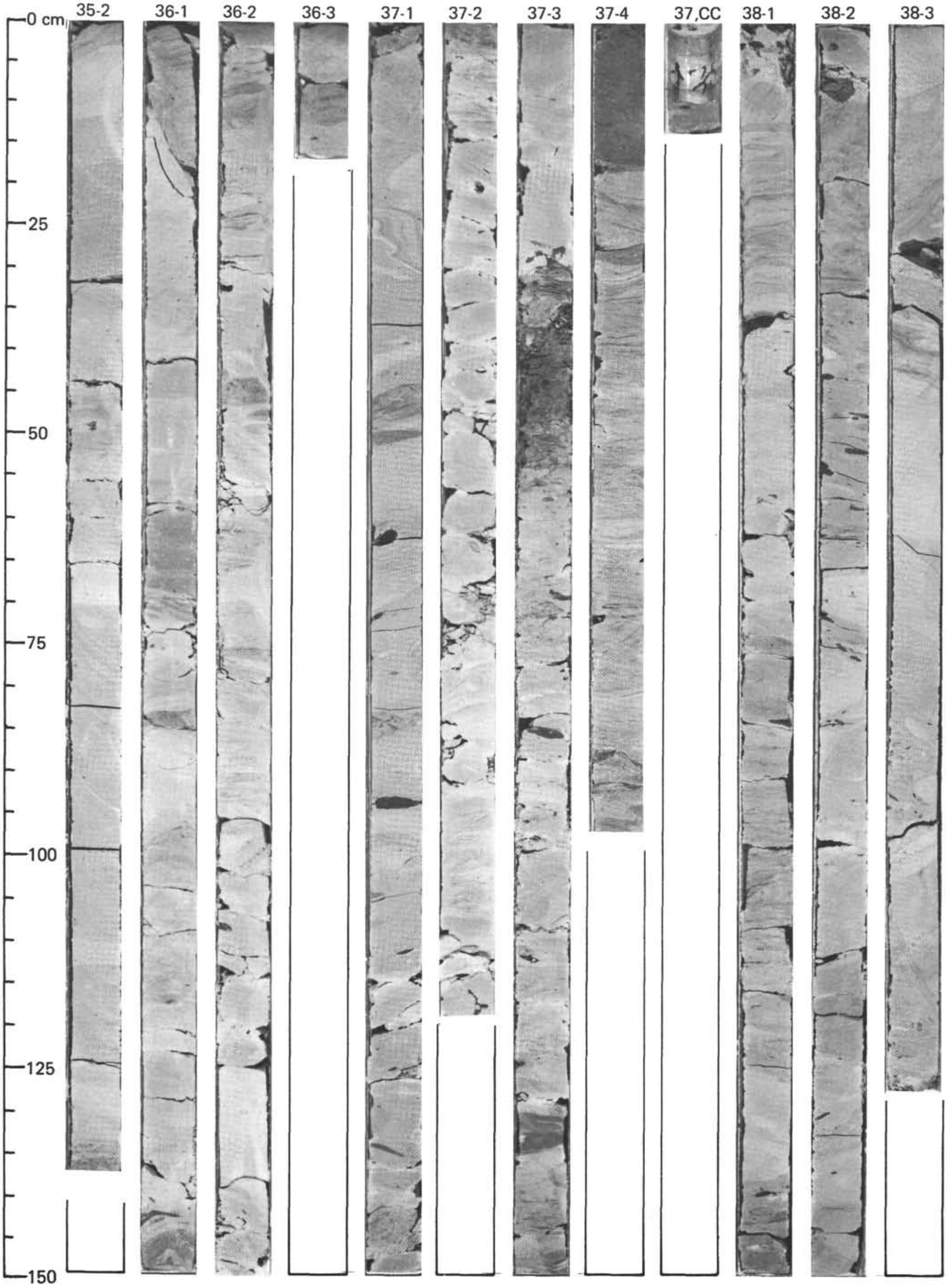
35-2
36-1
36-2
36-3
37-1
37-2
37-3
37-4
37,CC
38-1
38-2
38-3
0 cm
25
50
75
100
125
150

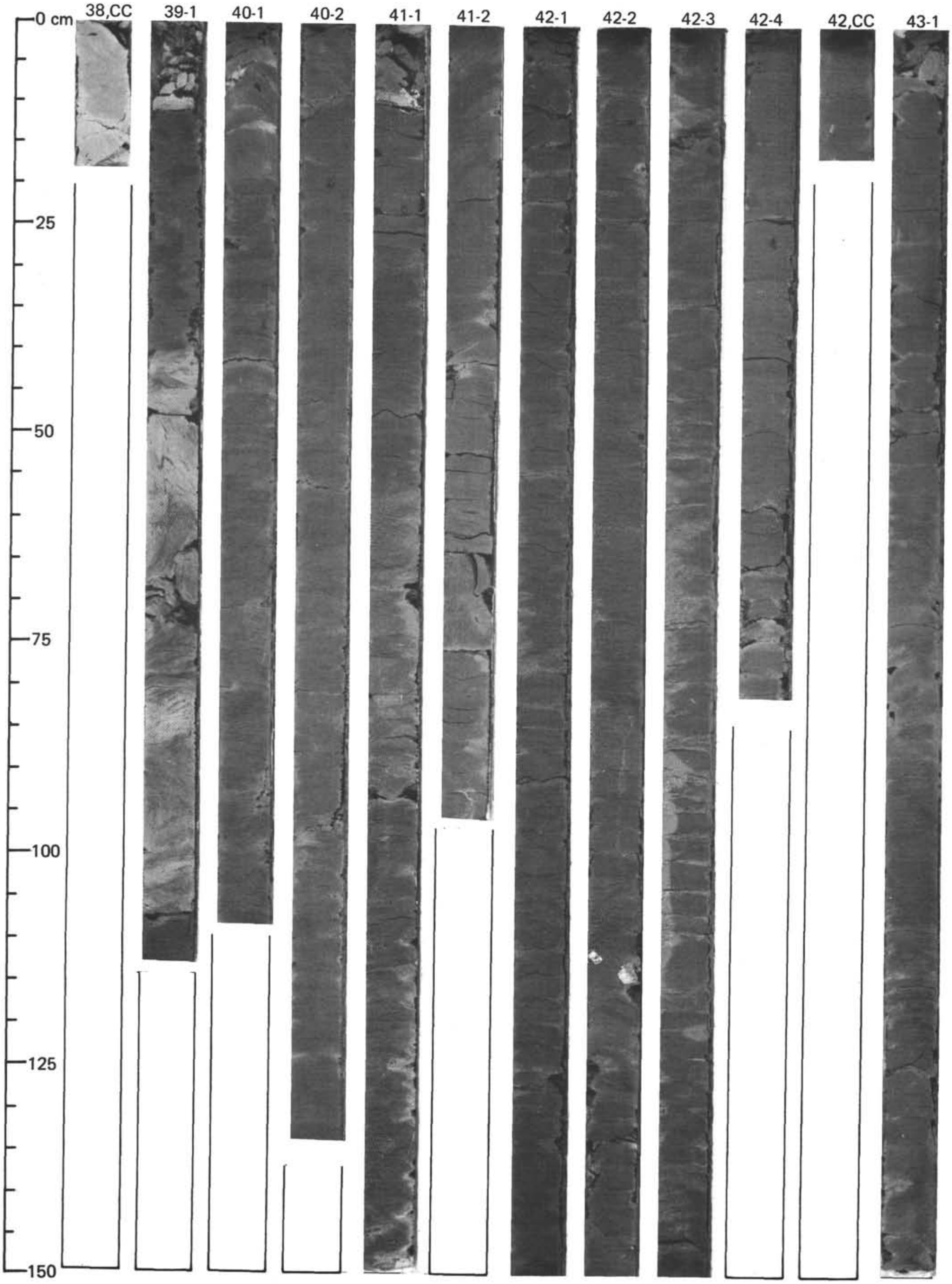
0 cm
25
50
75
100
125
150
38,CC
39-1
40-1
40-2
41-1
41-2
42-1
42-2
42-3
42-4
42,CC
43-1

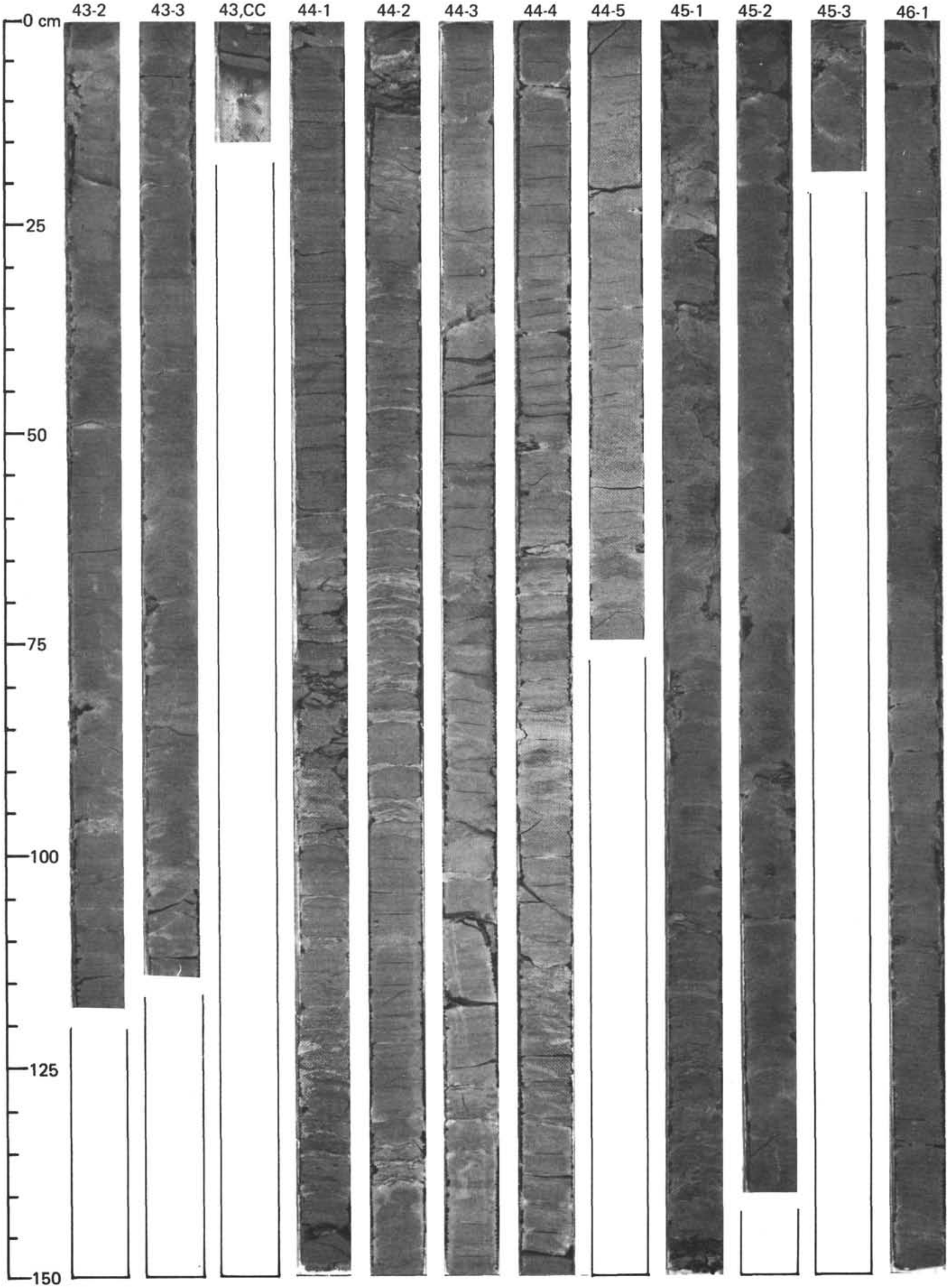
43-2
43-3
43,CC
44-1
44-2
44-3
44-4
44-5
45-1
45-2
45-3
46-1
0 cm
25
50
75
100
125
150

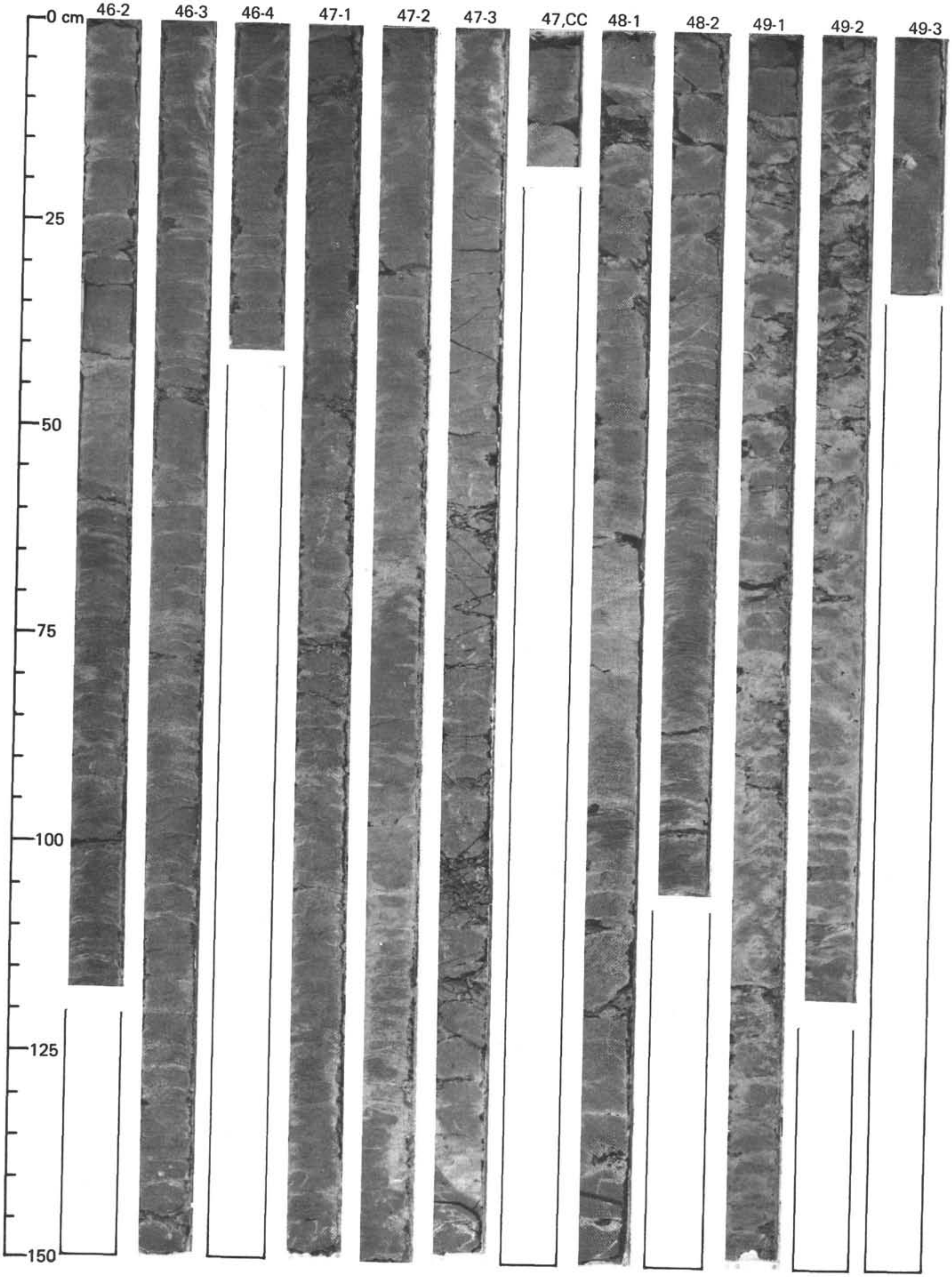
0 cm
25
50
75
100
125
150
46-2
46-3
46-4
47-1
47-2
47-3
47,CC
48-1
48-2
49-1
49-2
49-3

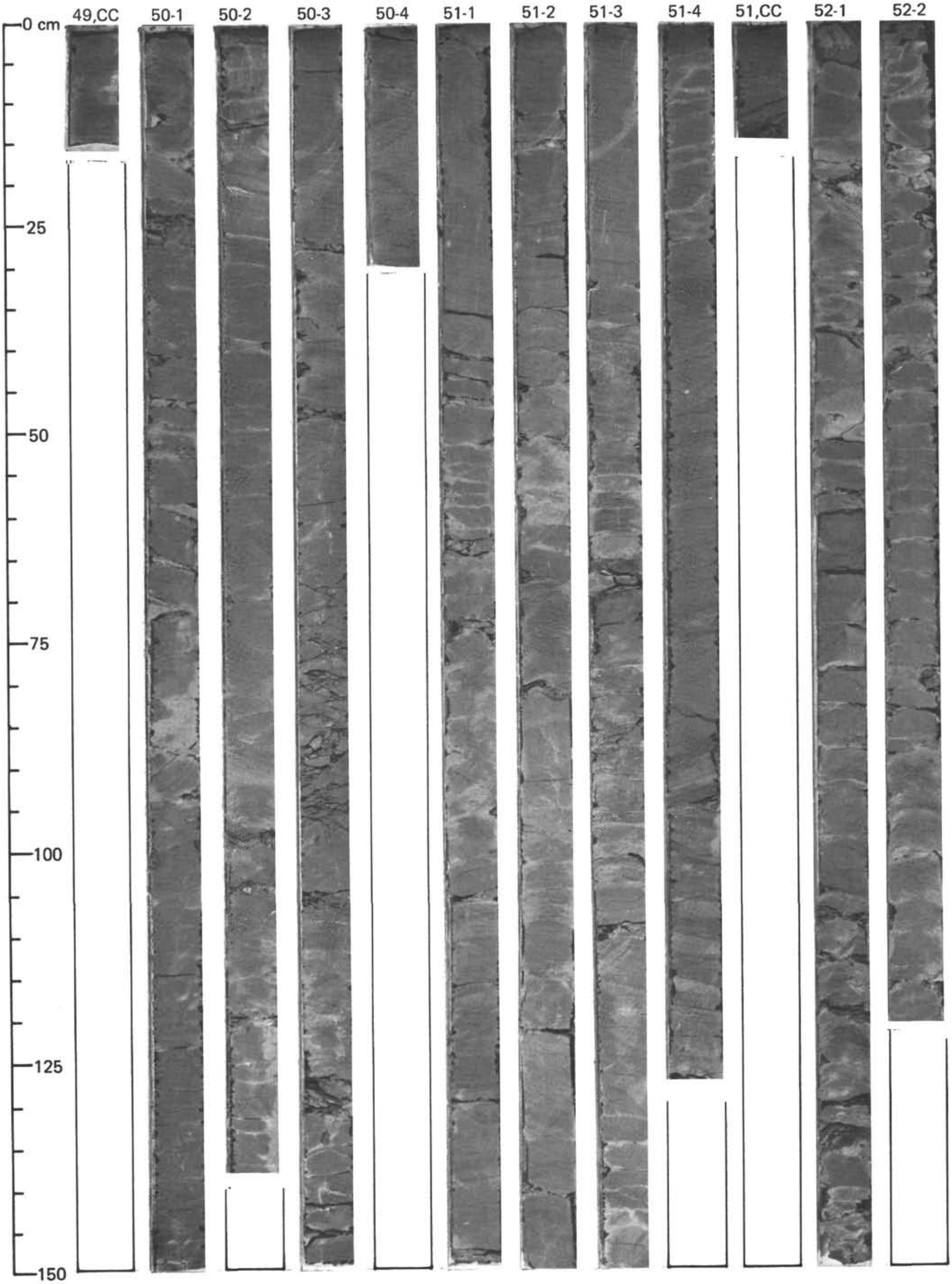
49,CC
50-1
50-2
50-3
50-4
51-1
51-2
51-3
51-4
51,CC
52-1
52-2
0 cm
25
50
75
100
125
150

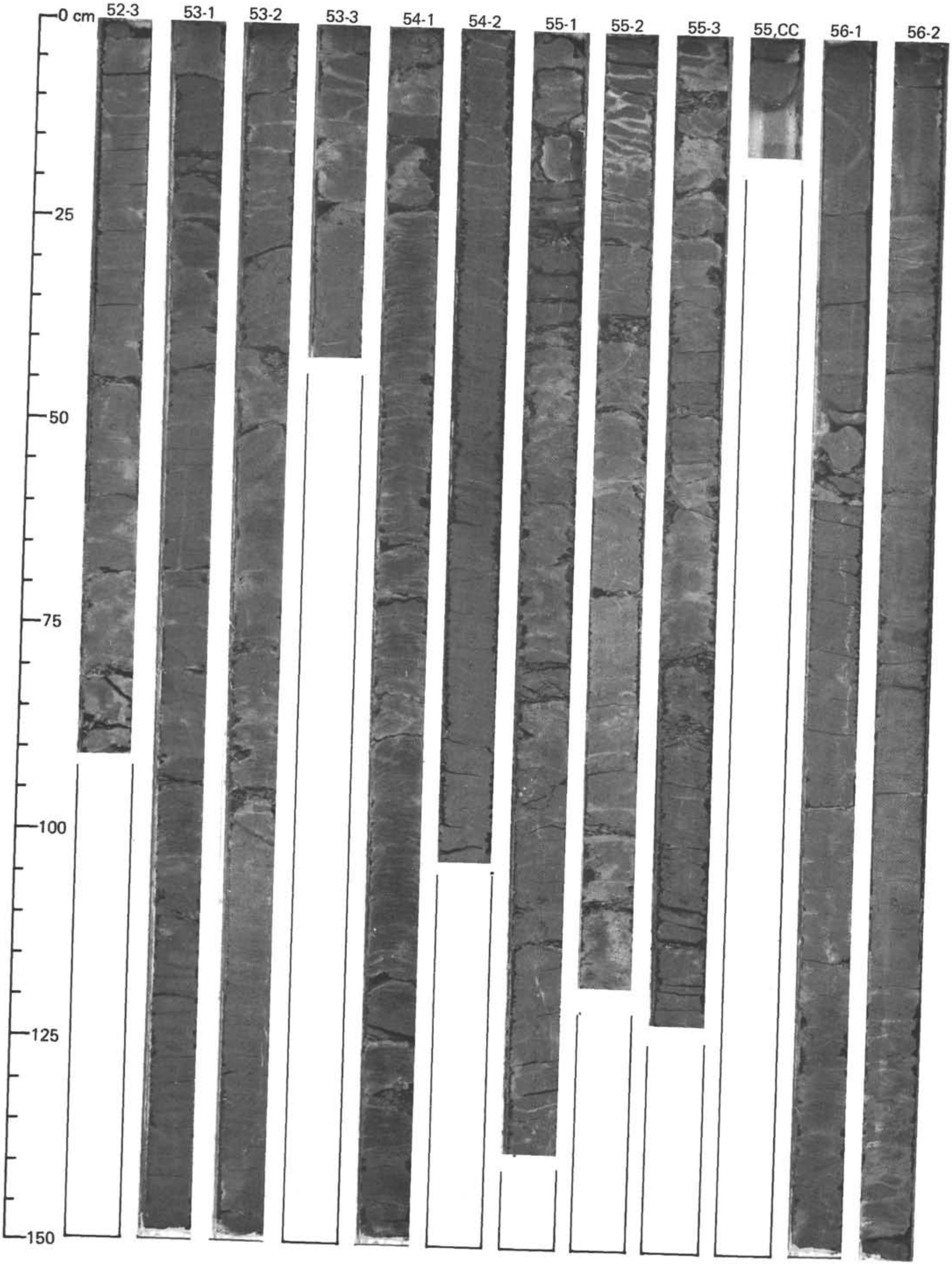
0 cm
25
50
75
100
125
150
52-3
53-1
53-2
53-3
54-1
54-2
55-1
55-2
55-3
55,CC
56-1
56-2

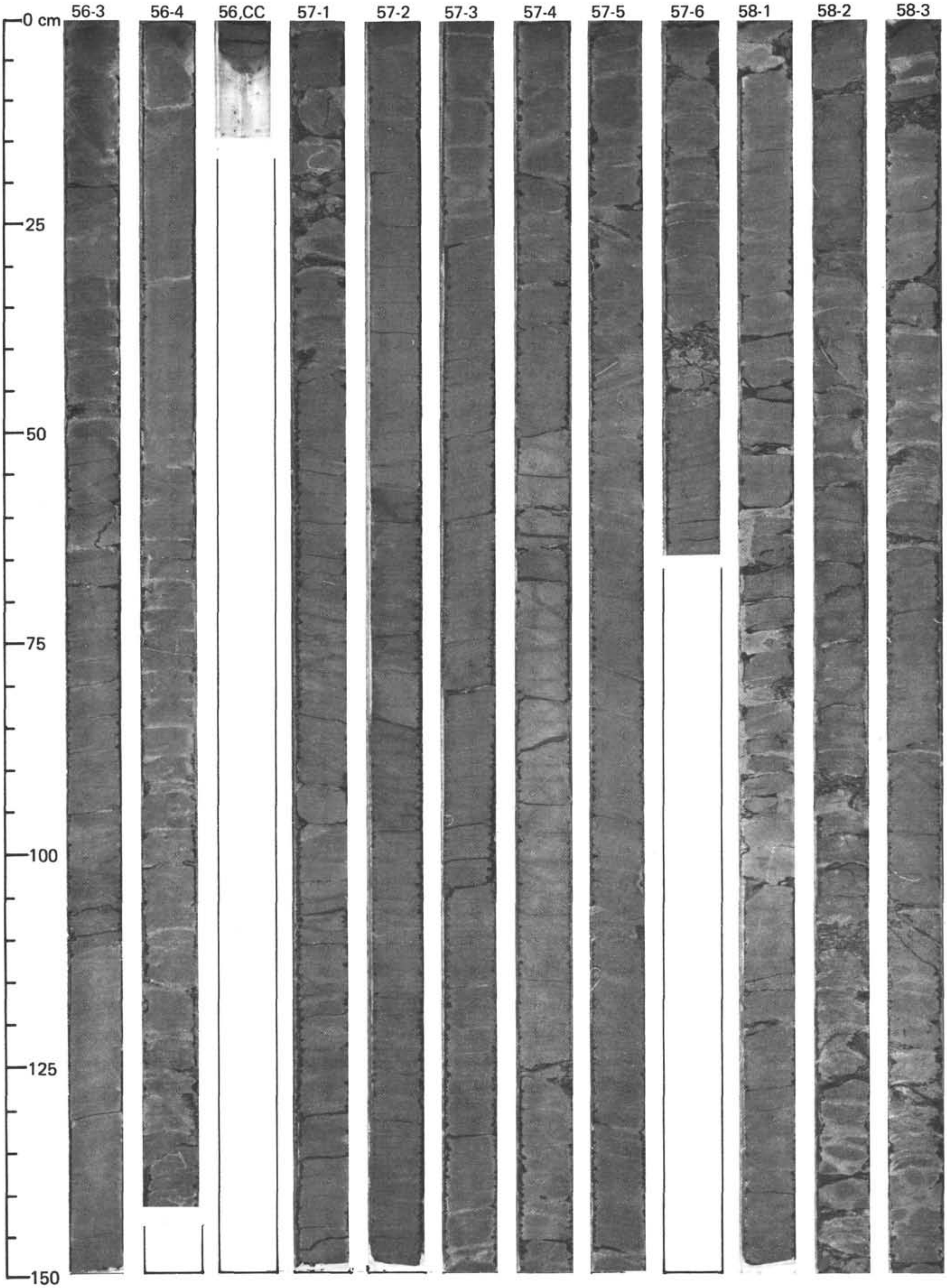
56-3
56-4
56,CC
57-1
57-2
57-3
57-4
57-5
57-6
58-1
58-2
58-3
0 cm
25
50
75
100
125
150

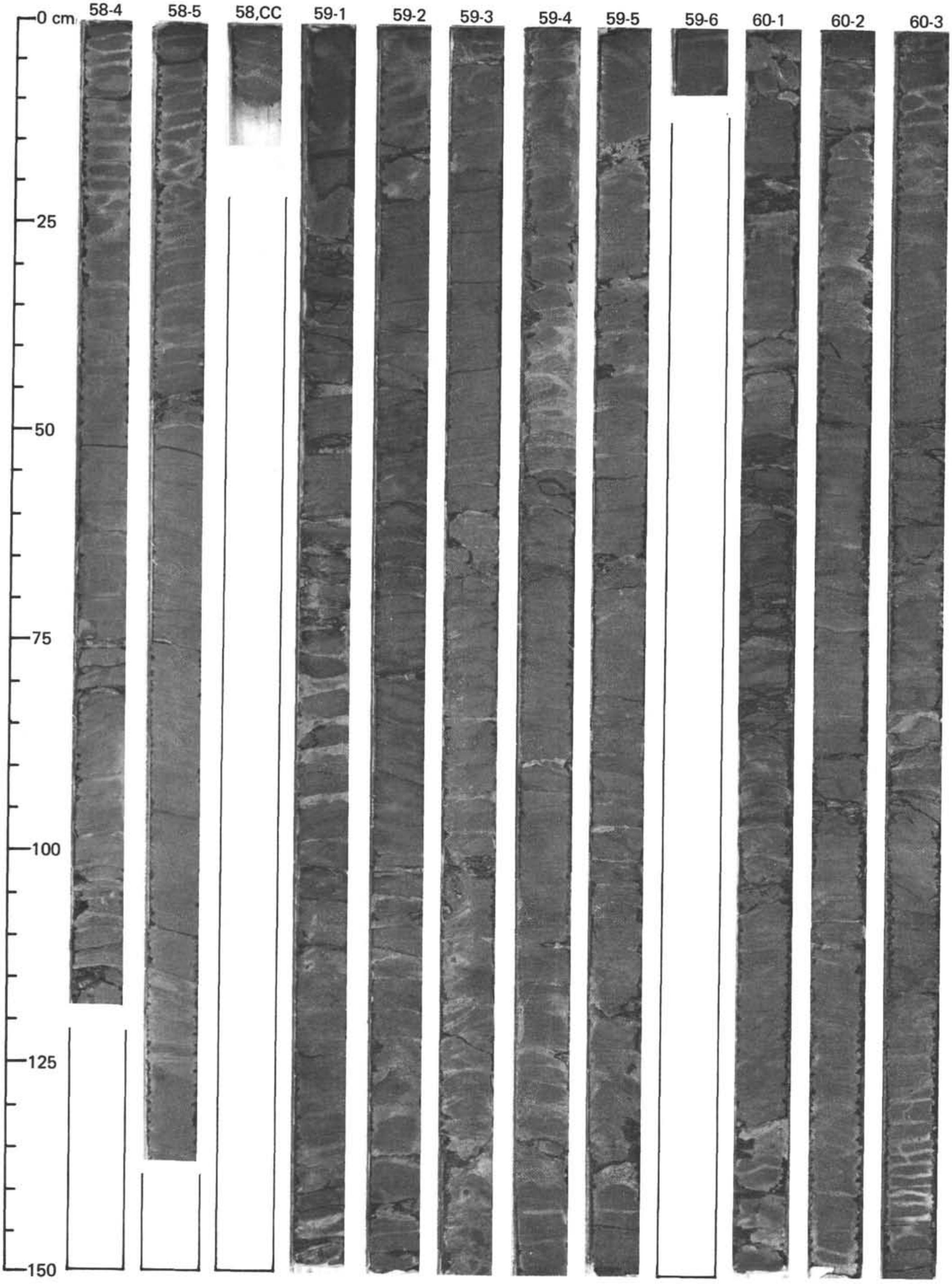
0 cm
25
50
75
100
125
150
58-4
58-5
58,CC
59-1
59-2
59-3
59-4
59-5
59-6
60-1
60-2
60-3

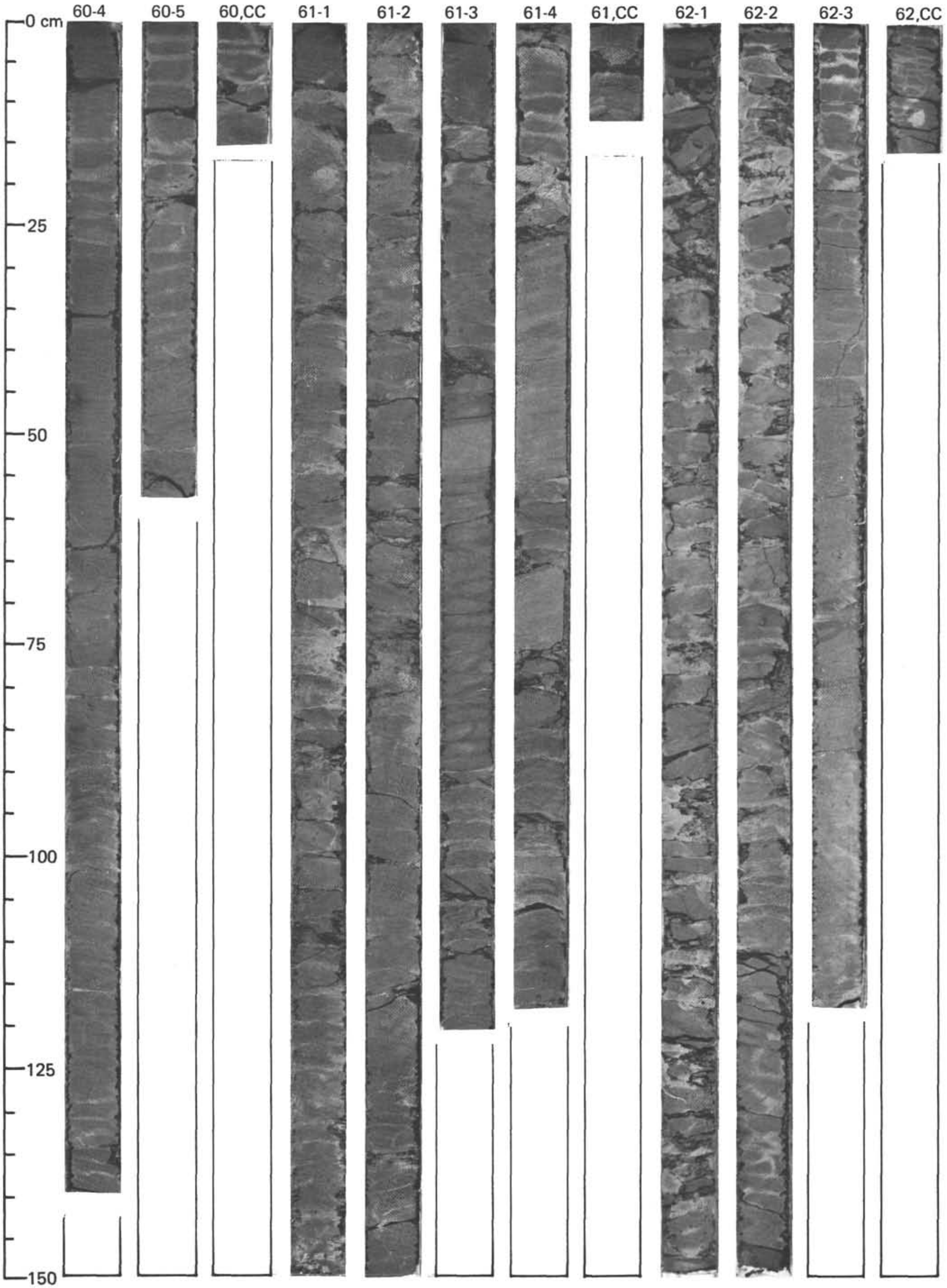
60-4
60-5
60,CC
61-1
61-2
61-3
61-4
61,CC
62-1
62-2
62-3
62,CC
0 cm
25
50
75
100
125
150

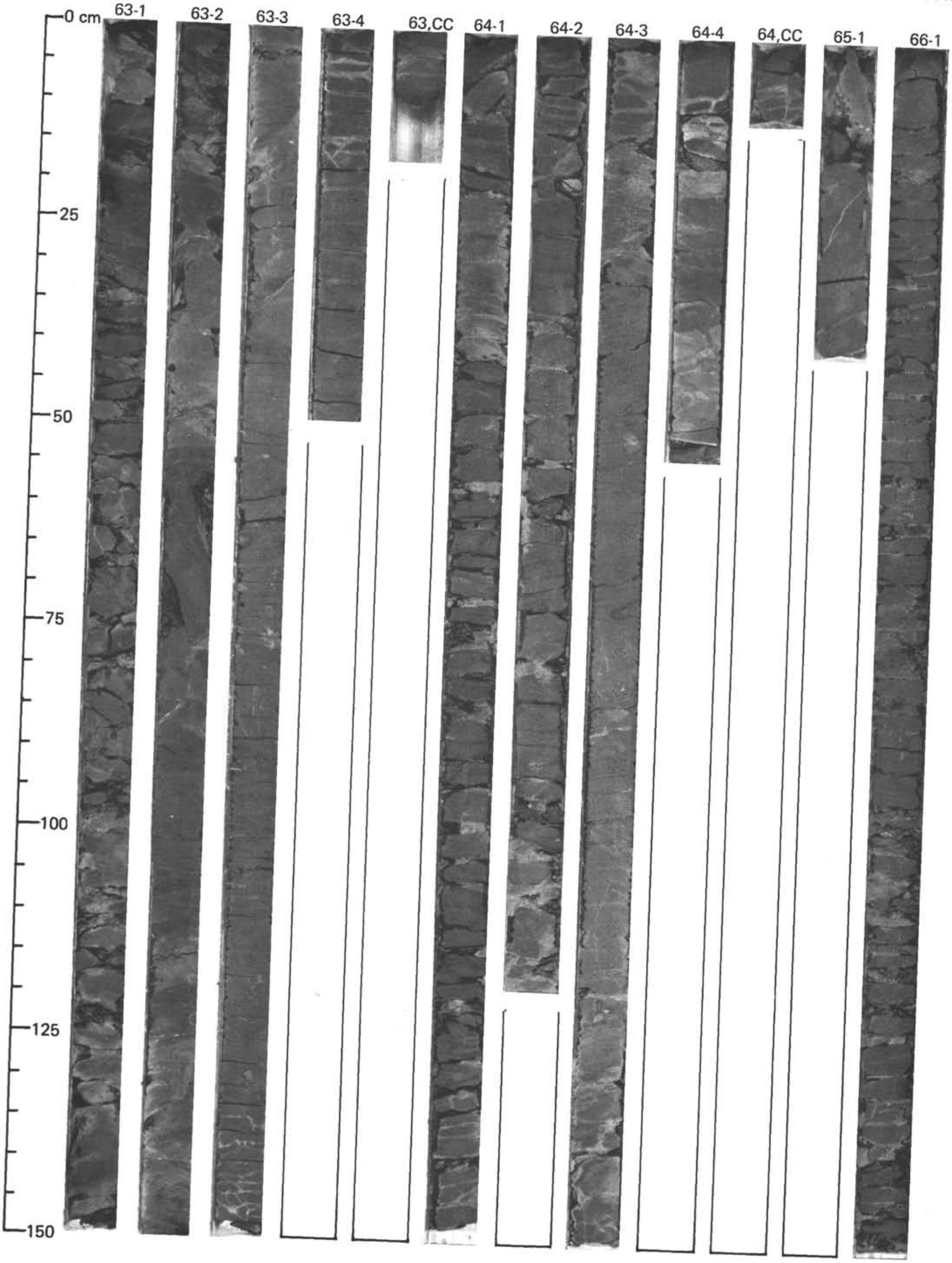
0 cm
25
50
75
100
125
150
63-1
63-2
63-3
63-4
63,CC
64-1
64-2
64-3
64-4
64,CC
65-1
66-1

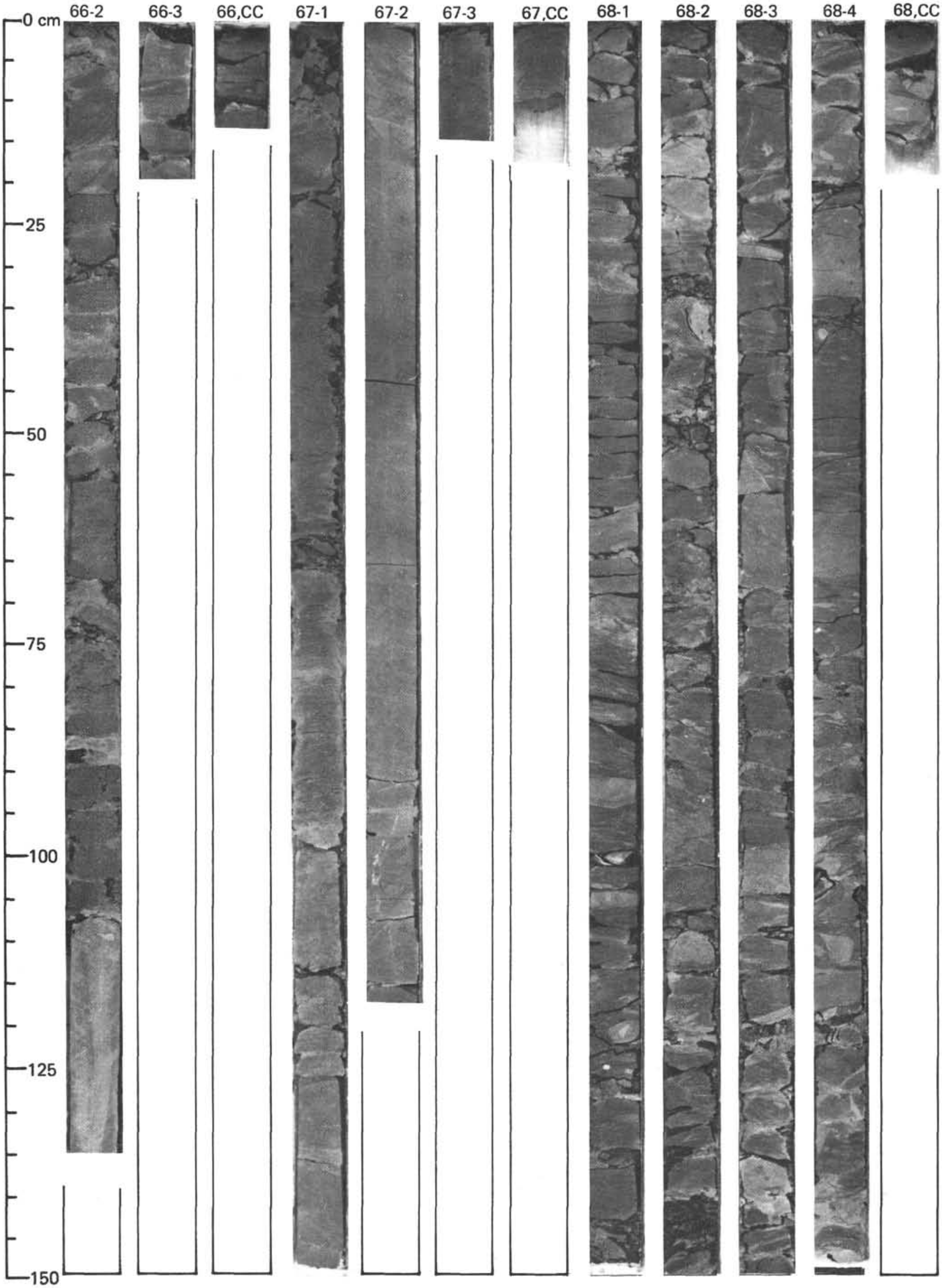
66-2
66-3
66,CC
67-1
67-2
67-3
67,CC
68-1
68-2
68-3
68-4
68,CC
0 cm
25
50
75
100
125
150

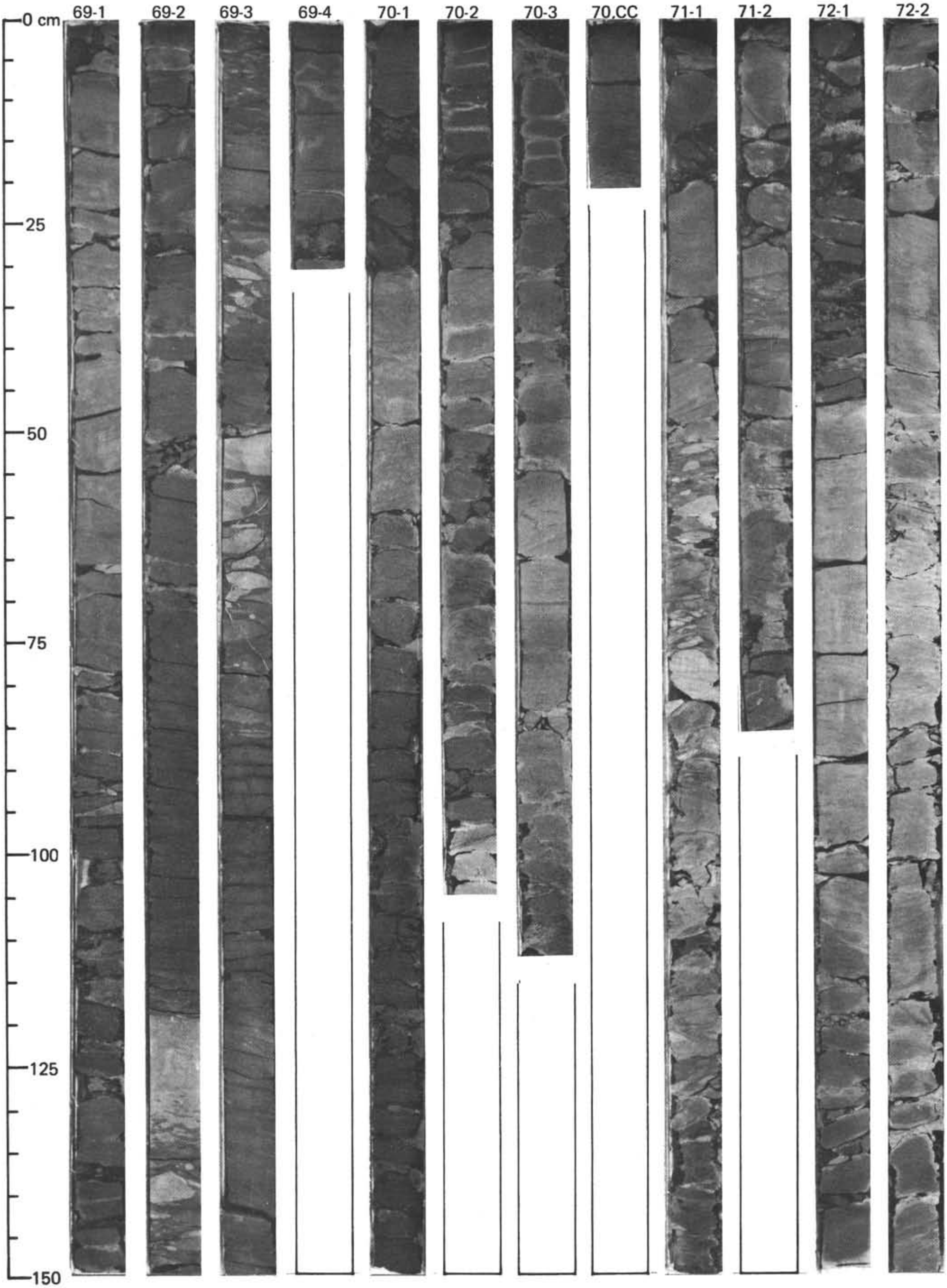
0 cm
25
50
75
100
125
150
69-1
69-2
69-3
69-4
70-1
70-2
70-3
70,CC
71-1
71-2
72-1
72-2

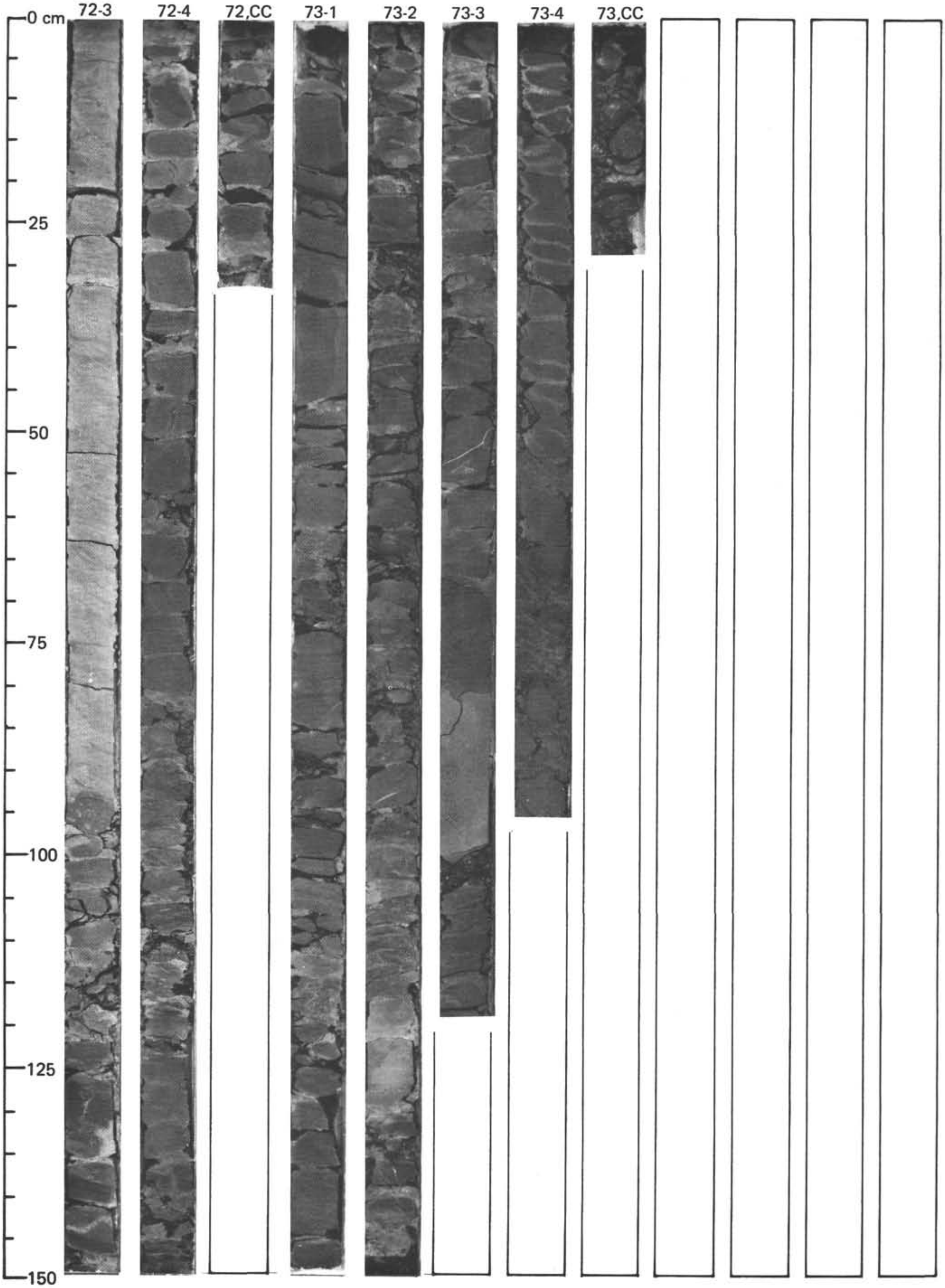
0 cm
25
50
75
100
125
150
72-3
72-4
72,CC
73-1
73-2
73-3
73-4
73,CC

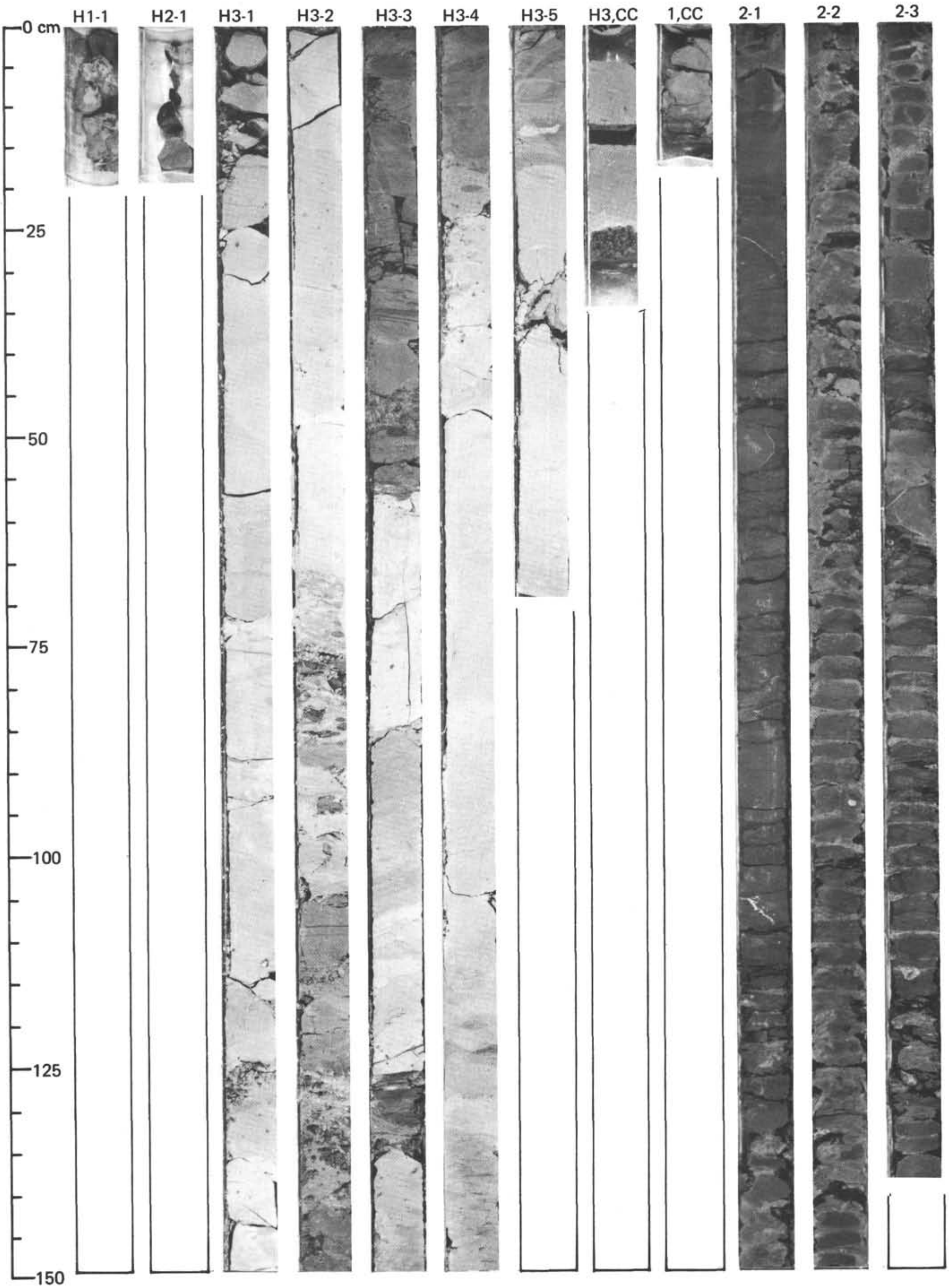
0 cm
25
50
75
100
125
150
H1-1
H2-1
H3-1
H3-2
H3-3
H3-4
H3-5
H3,CC
1,CC
2-1
2-2
2-3

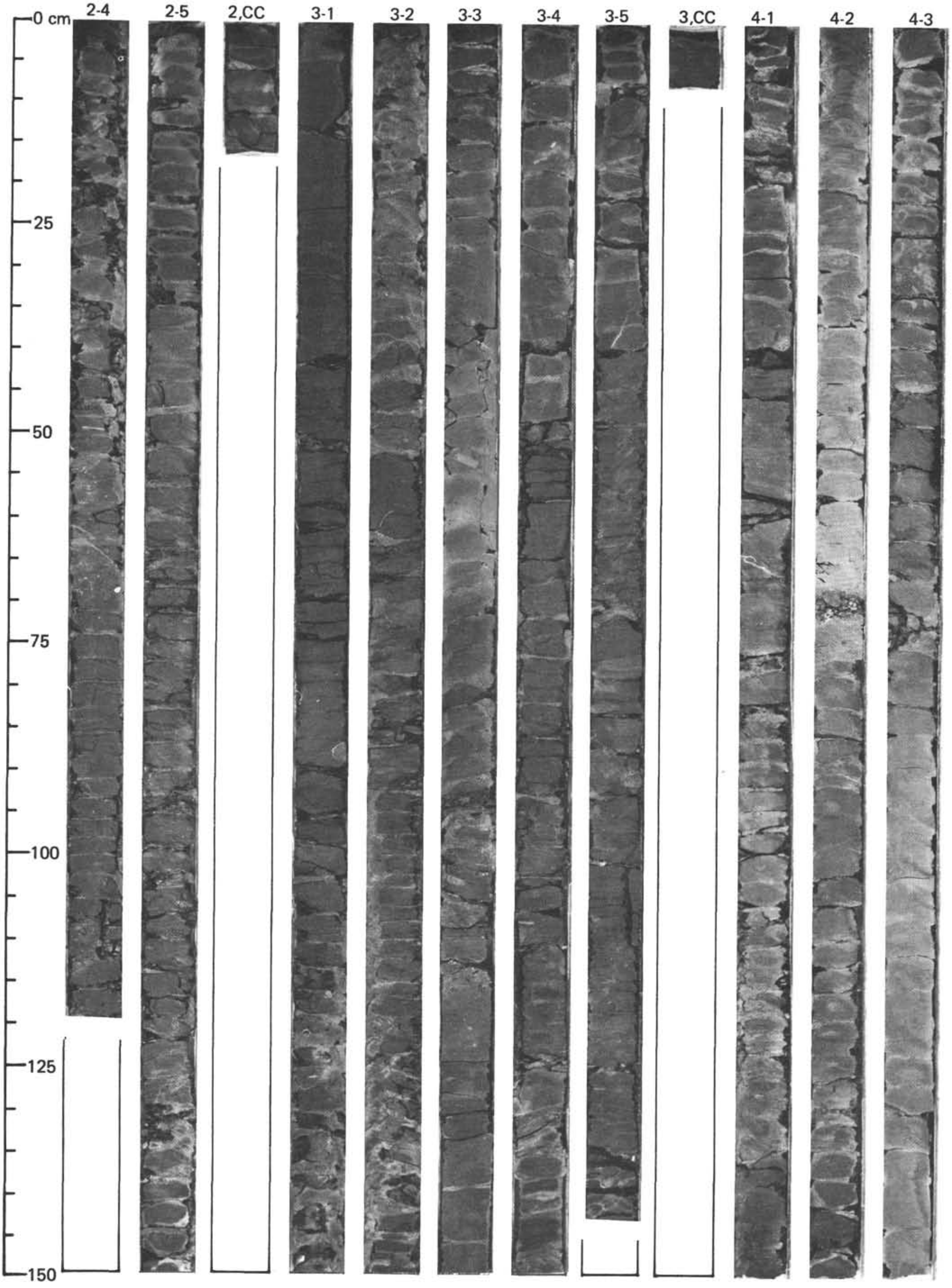
0 cm
25
50
75
100
125
150
2-4
2-5
2,CC
3-1
3-2
3-3
3-4
3-5
3,CC
4-1
4-2
4-3

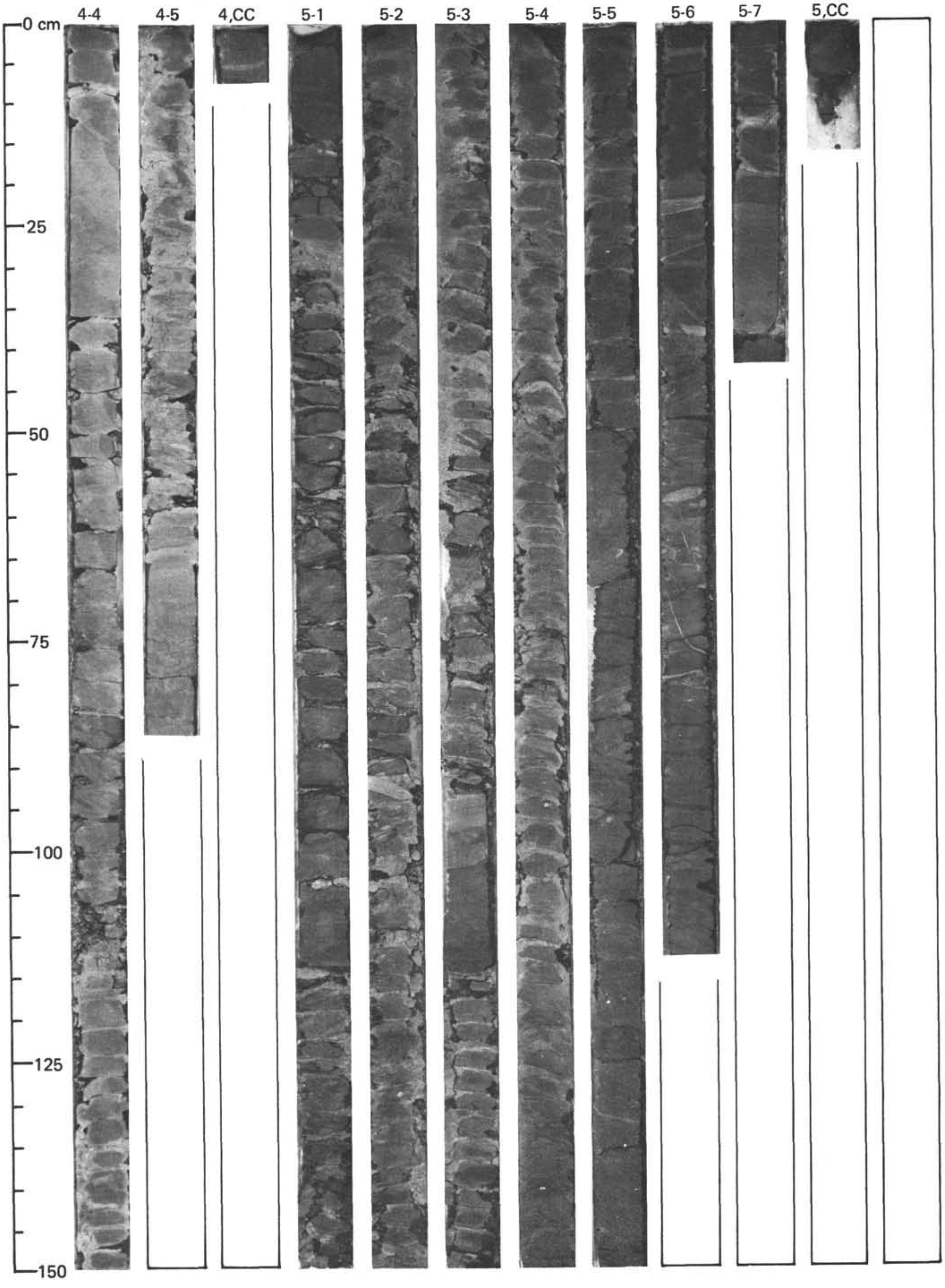

0 cm
25
50
75
100
125
150
4-4
4-5
4,CC
5-1
5-2
5-3
5-4
5-5
5-6
5-7
5,CC

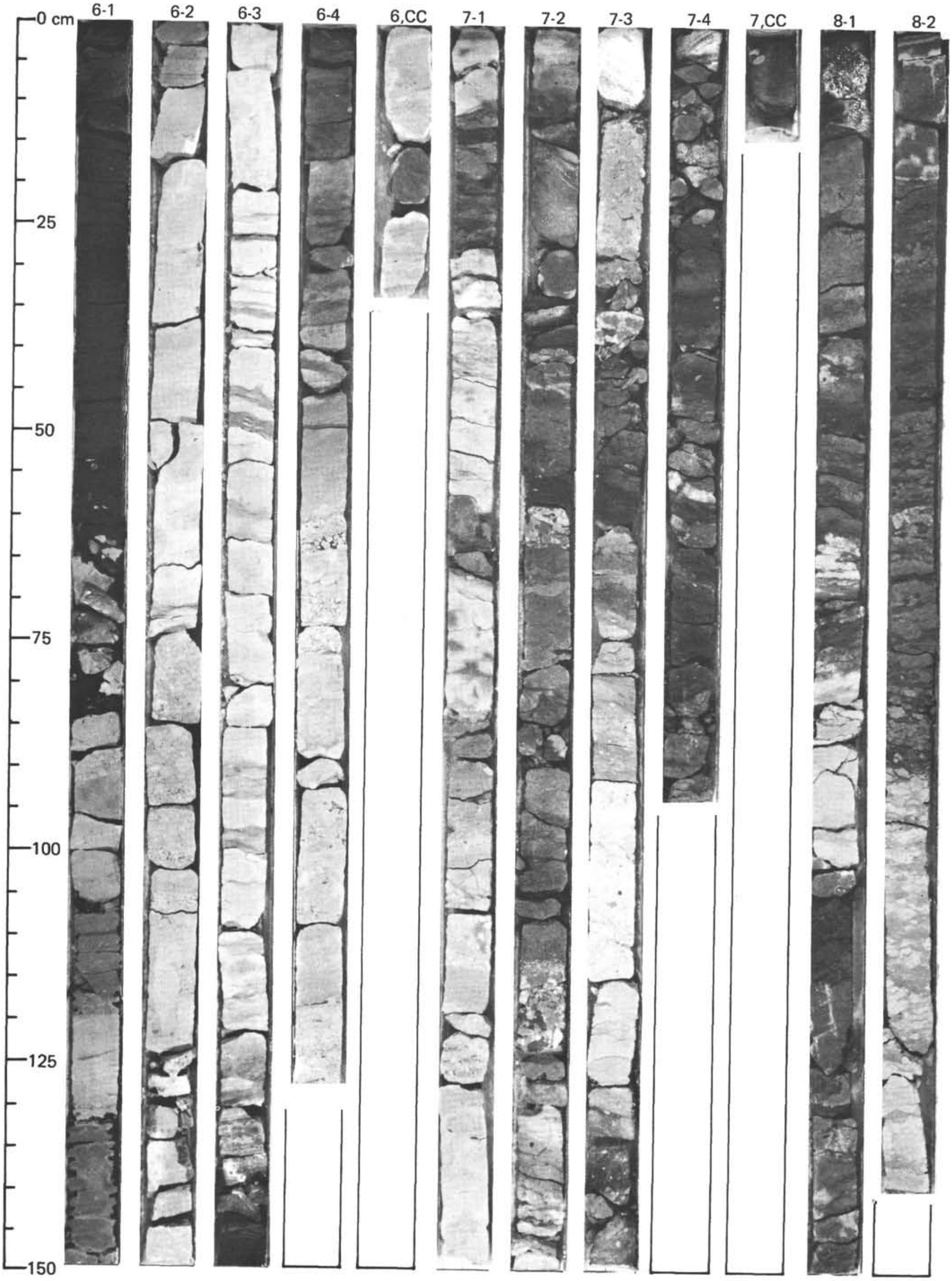
0 cm
25
50
75
100
125
150
6-1
6-2
6-3
6-4
6,CC
7-1
7-2
7-3
7-4
7,CC
8-1
8-2

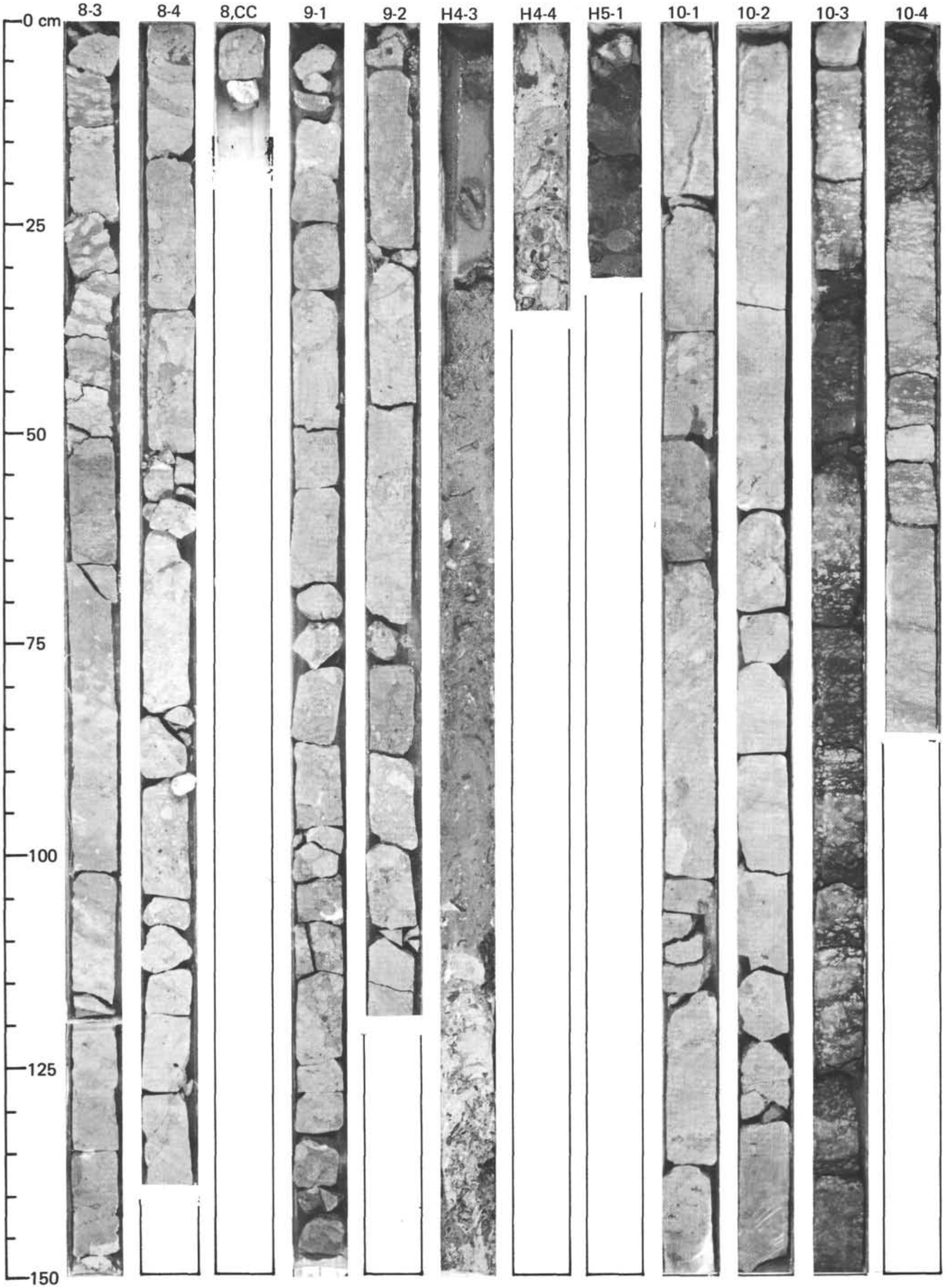
8-3
8-4
8,CC
9-1
9-2
H4-3
H4-4
H5-1
10-1
10-2
10-3
10-4
0 cm
25
50
75
100
125
150

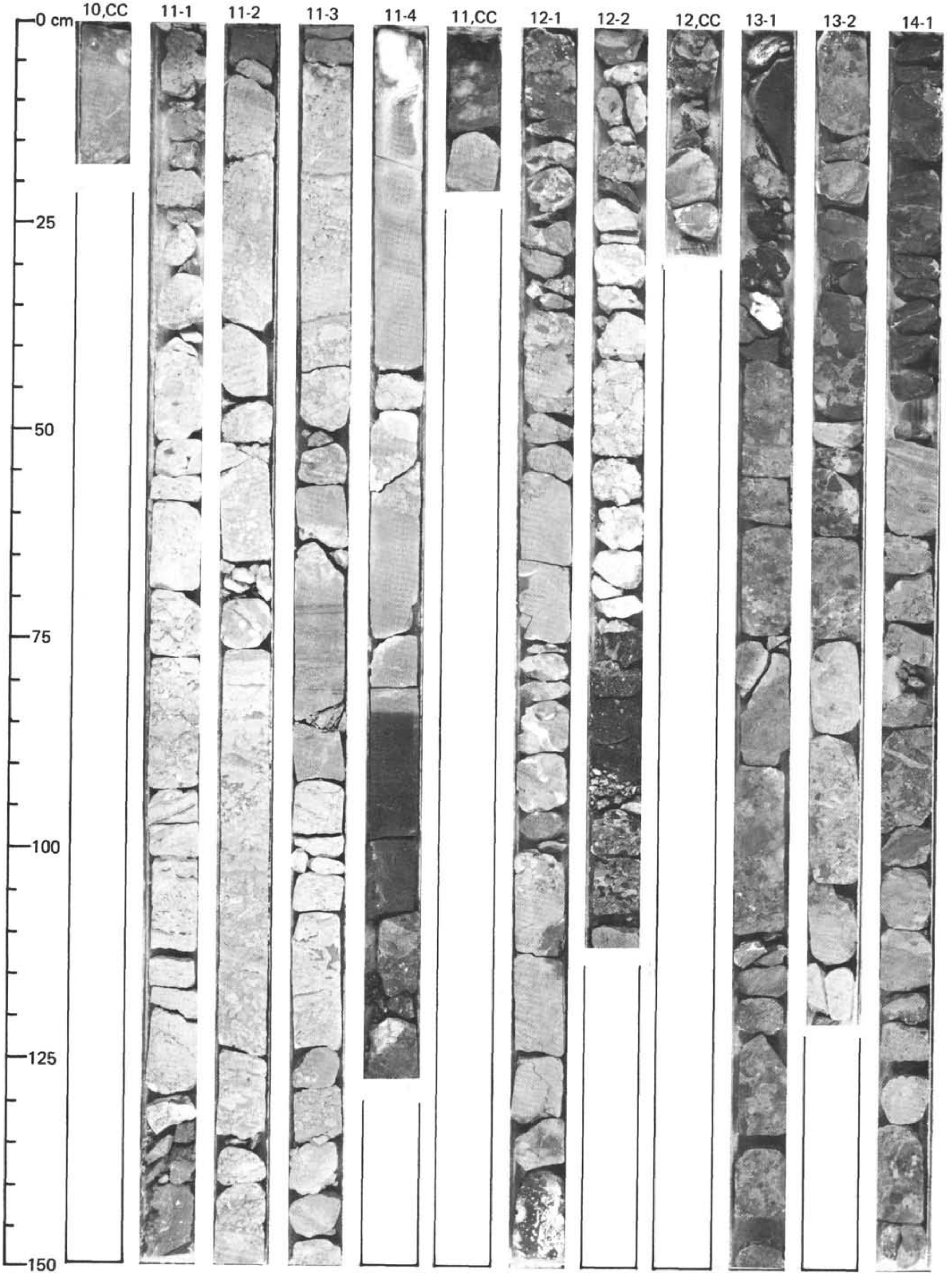
0 cm
25
50
75
100
125
150
10,CC
11-1
11-2
11-3
11-4
11,CC
12-1
12-2
12,CC
13-1
13-2
14-1

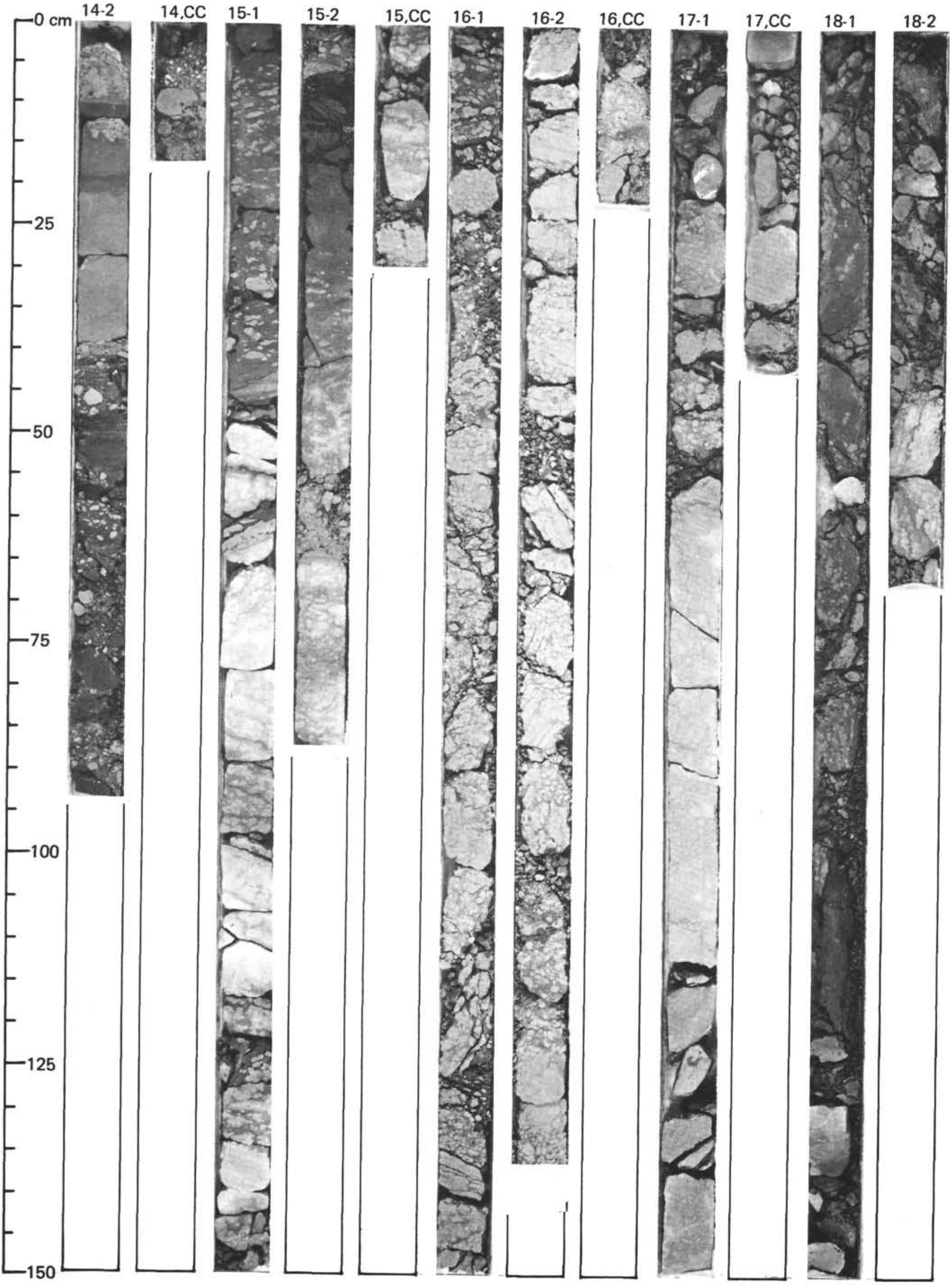

0 cm
25
50
75
100
125
150
14-2
14,CC
15-1
15-2
15,CC
16-1
16-2
16,CC
17-1
17,CC
18-1
18-2

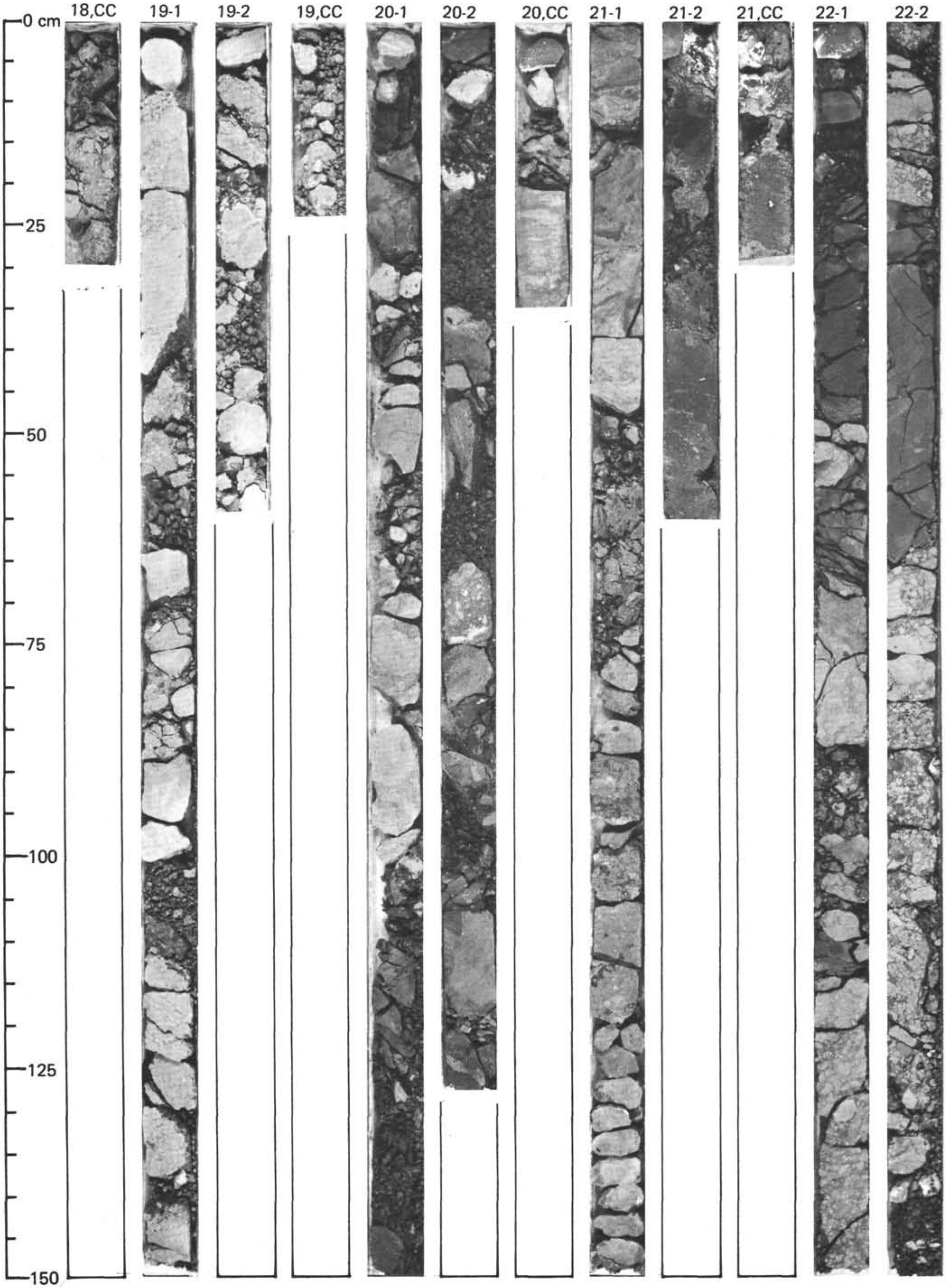
0 cm
25
50
75
100
125
150
18,CC
19-1
19-2
19,CC
20-1
20-2
20,CC
21-1
21-2
21,CC
22-1
22-2

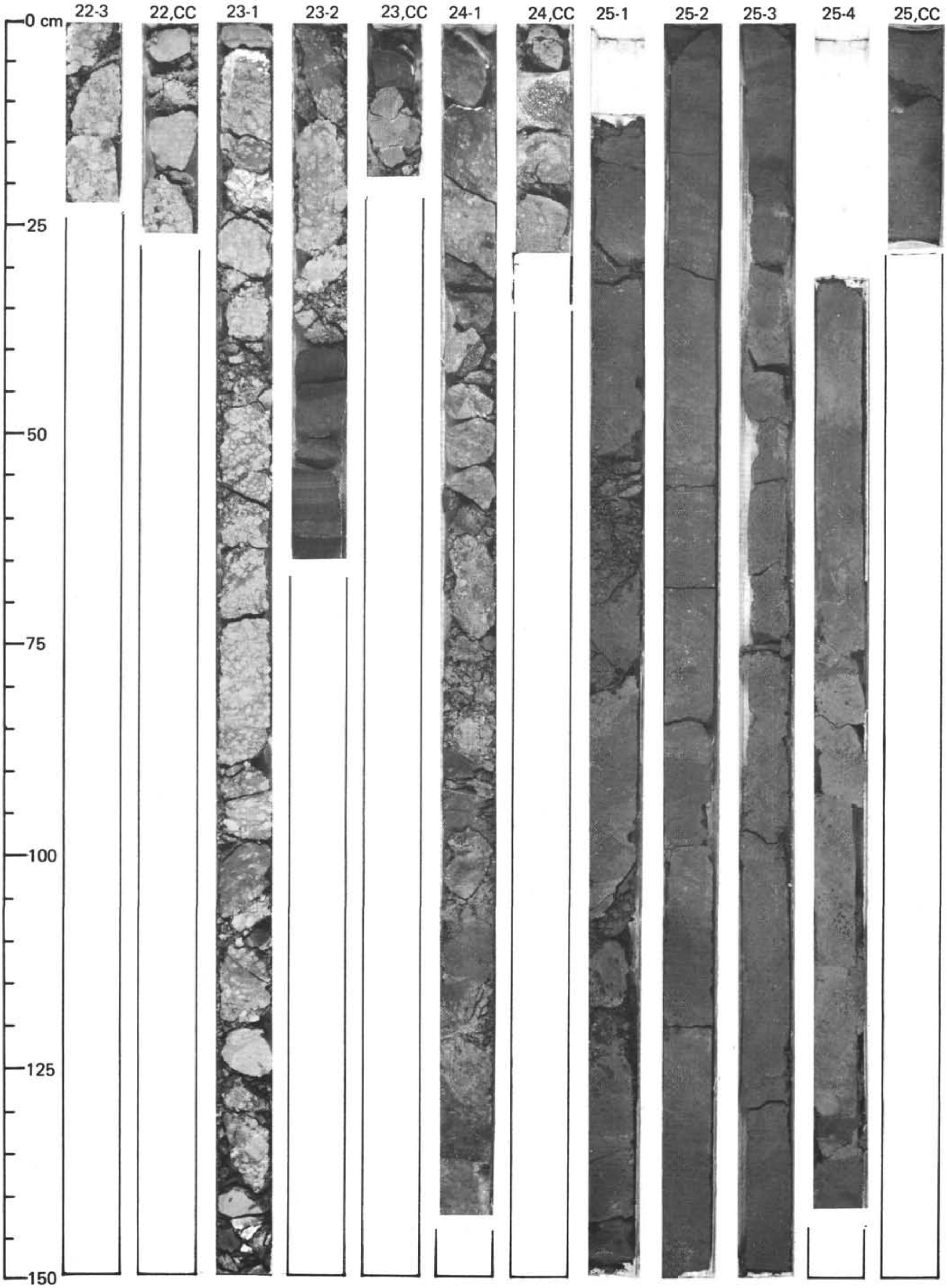
22-3
22,CC
23-1
23-2
23,CC
24-1
24,CC
25-1
25-2
25-3
25-4
25,CC
0 cm
25
50
75
100
125
150

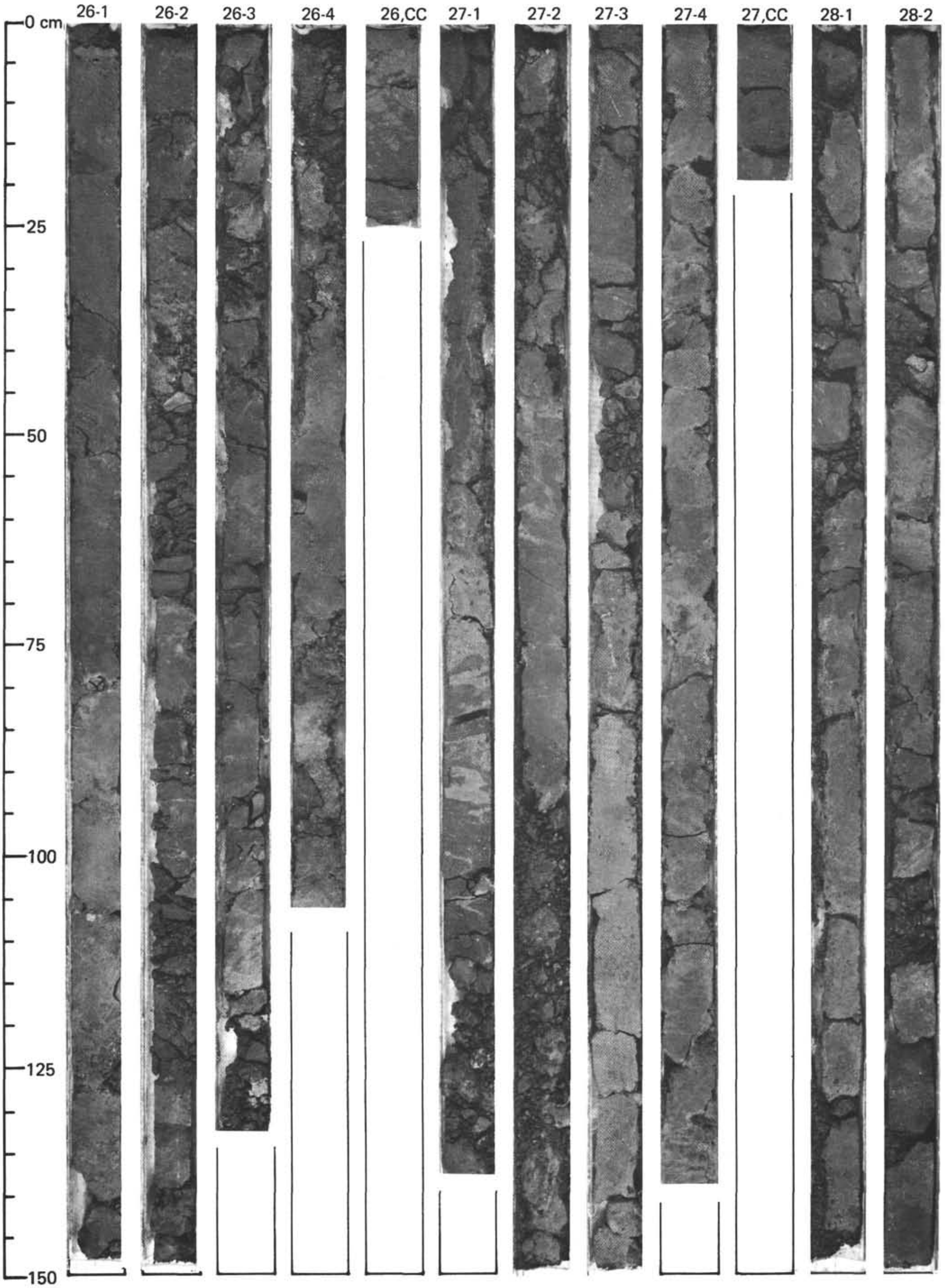
26-1
26-2
26-3
26-4
26,CC
27-1
27-2
27-3
27-4
27,CC
28-1
28-2
0 cm
25
50
75
100
125
150

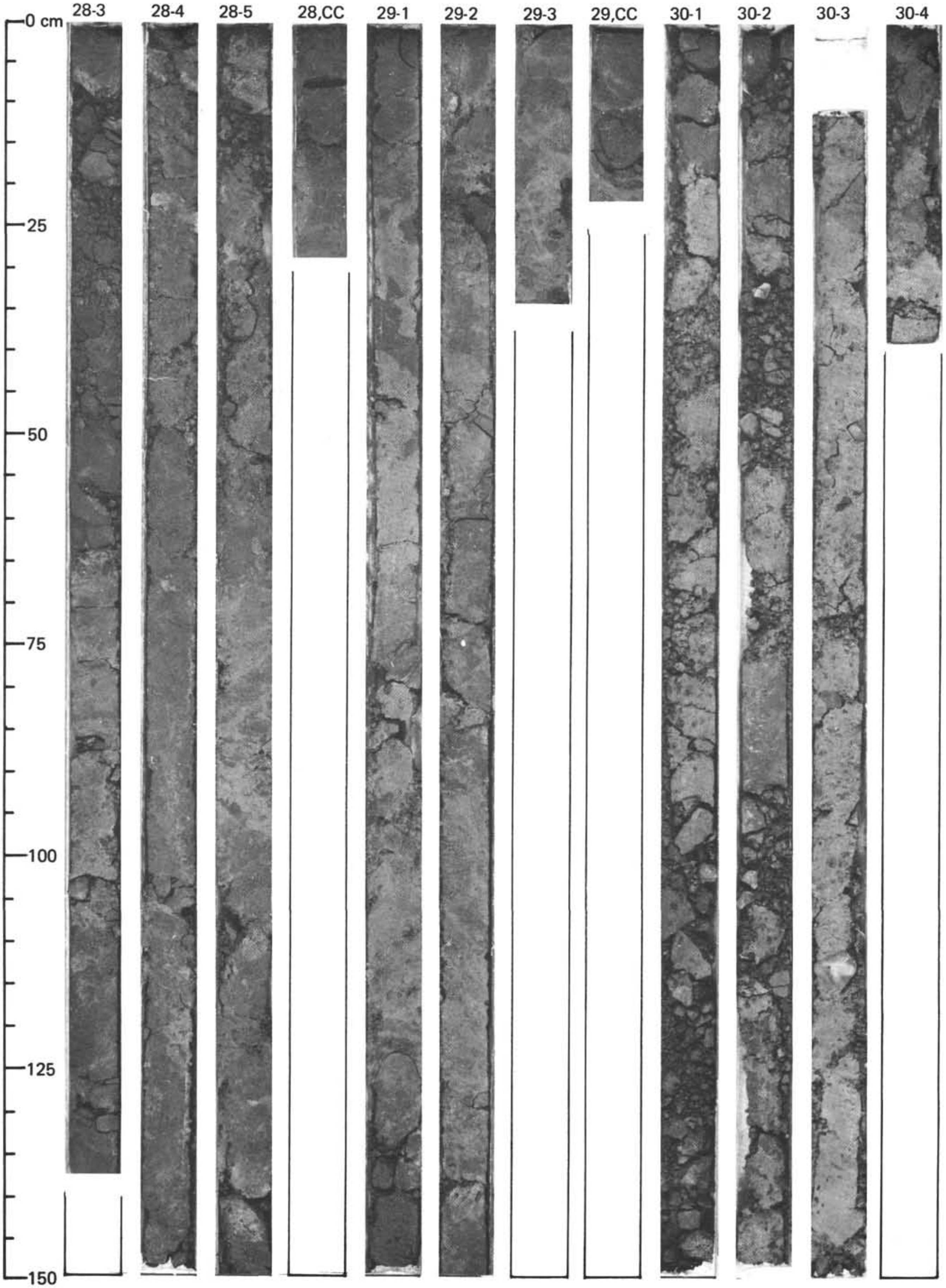
28-3
28-4
28-5
28,CC
29-1
29-2
29-3
29,CC
30-1
30-2
30-3
30-4
0 cm
25
50
75
100
125
150

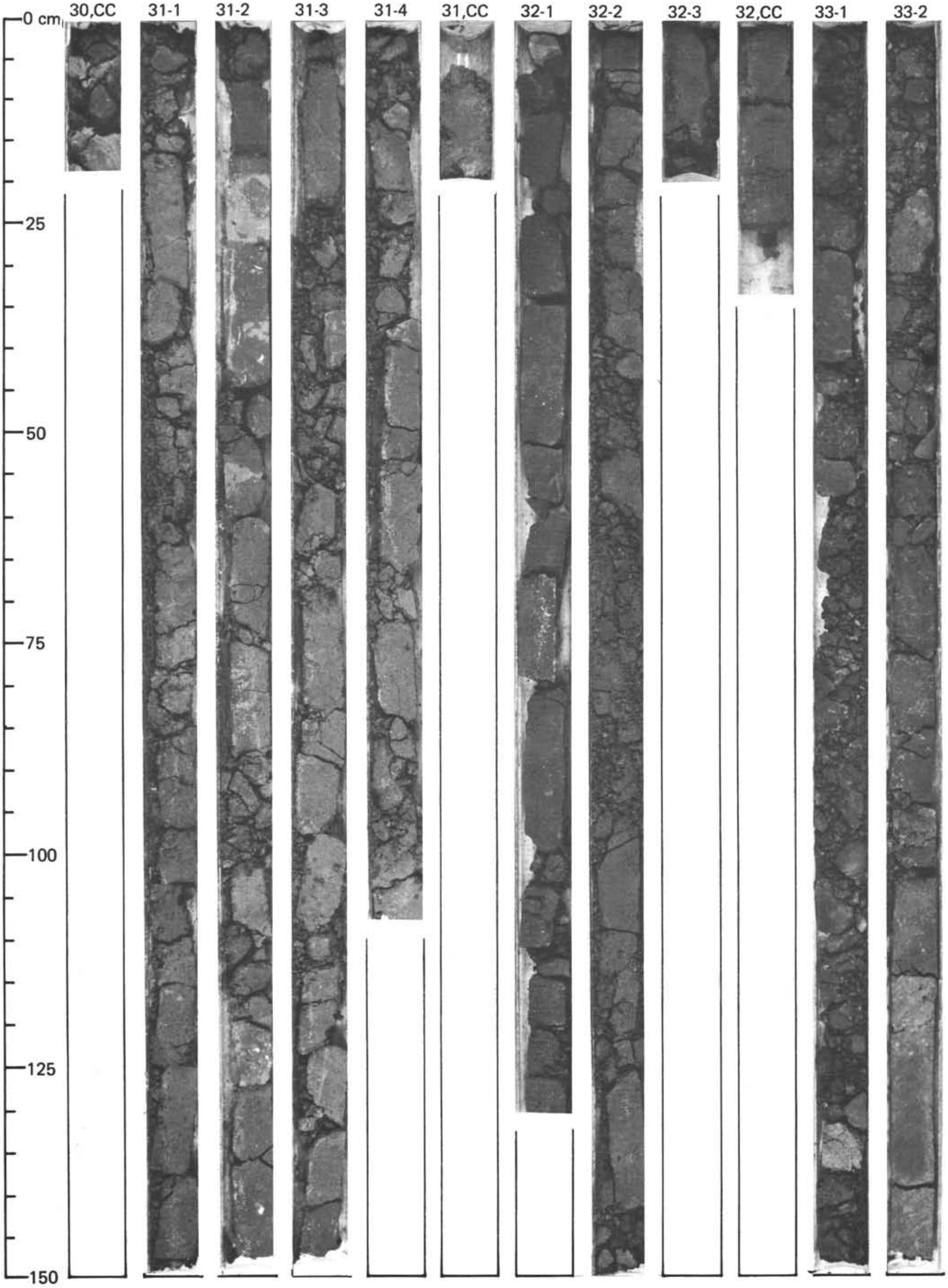
30,CC
31-1
31-2
31-3
31-4
31,CC
32-1
32-2
32-3
32,CC
33-1
33-2
0 cm
25
50
75
100
125
150

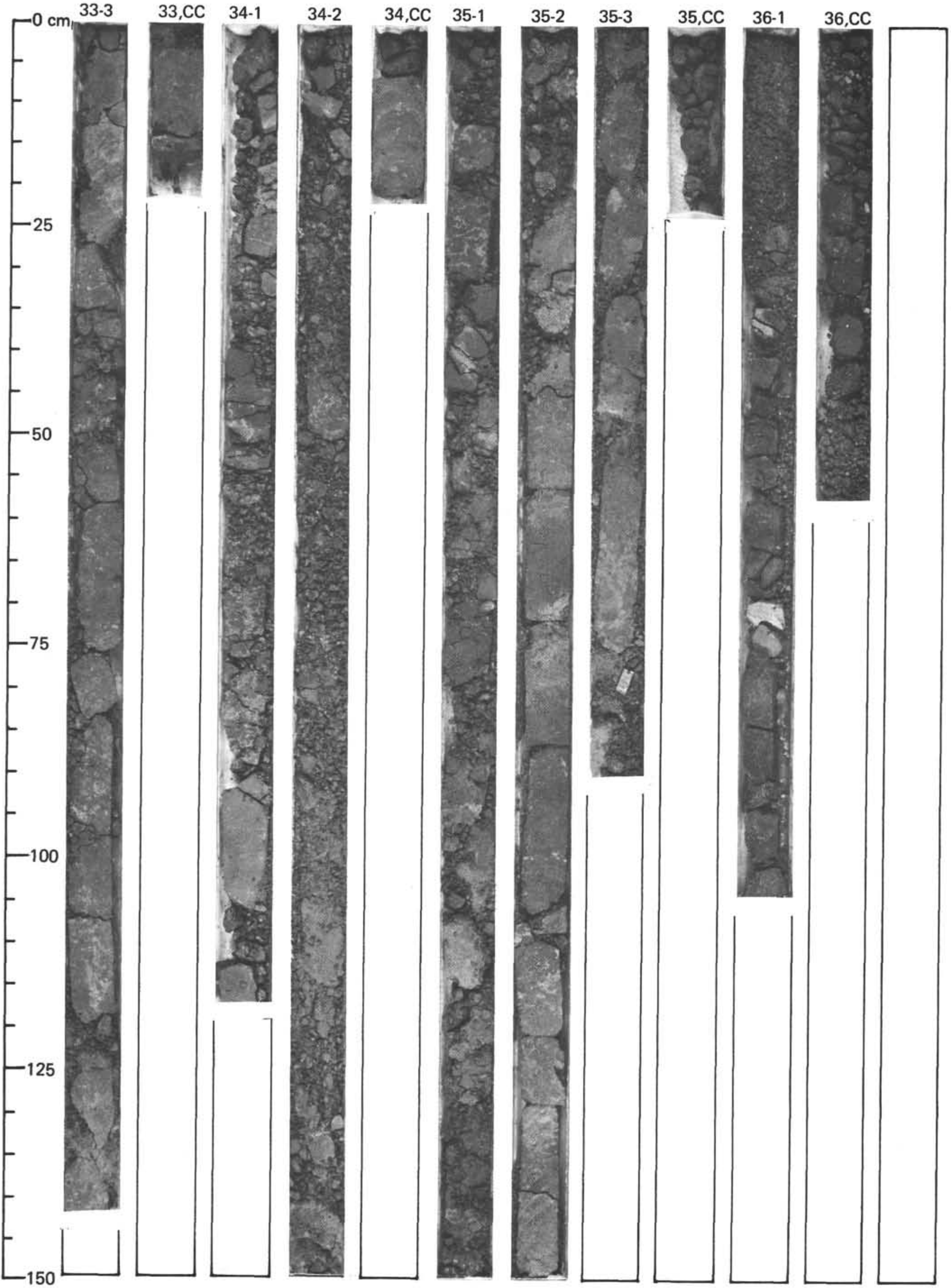
0 cm
25
50
75
100
125
150
33-3
33,CC
34-1
34-2
34,CC
35-1
35-2
35-3
35,CC
36-1
36,CC